



HAL
open science

Function of the histone variant H3.3 and its chaperone DAXX on heterochromatin organization in pluripotent cells

Antoine Canat

► **To cite this version:**

Antoine Canat. Function of the histone variant H3.3 and its chaperone DAXX on heterochromatin organization in pluripotent cells. Molecular biology. Université Paris Cité, 2020. English. NNT : 2020UNIP7245 . tel-03832812

HAL Id: tel-03832812

<https://theses.hal.science/tel-03832812>

Submitted on 28 Oct 2022

HAL is a multi-disciplinary open access archive for the deposit and dissemination of scientific research documents, whether they are published or not. The documents may come from teaching and research institutions in France or abroad, or from public or private research centers.

L'archive ouverte pluridisciplinaire **HAL**, est destinée au dépôt et à la diffusion de documents scientifiques de niveau recherche, publiés ou non, émanant des établissements d'enseignement et de recherche français ou étrangers, des laboratoires publics ou privés.



Thèse de doctorat

En vue de l'obtention du titre de docteur

Université de Paris

Ecole doctorale HOB (Hématologie, Oncogenèse, Biothérapies) - ED 561

Spécialité : Oncogenèse

Laboratoire UMR INSERM 944 / CNRS 7212 – IRSL

Function of the histone variant H3.3 and its chaperone DAXX on heterochromatin organization in pluripotent cells

Par **Antoine CANAT**

Thèse dirigée par **Emmanuelle FABRE**, Directrice de recherche, CNRS

Thèse co-encadrée par **Pierre THERIZOLS**, Chargé de recherche, CNRS

Soutenue publiquement le mardi 27 octobre 2020

Devant un jury composé de :

Alice JOUINEAU, Chargée de recherche, INRAE - Université Paris Saclay

Rapporteur

Daan NOORDERMEER, Chargé de recherche, CNRS –
I2BC, Université Paris Saclay

Rapporteur

Sophie POLO, Directrice de recherche, CNRS – Université de Paris

Présidente

Michele GOODHARDT, Directrice de recherche, CNRS – IRSL, Université de Paris

Examinatrice

Christophe ESCUDE, Chargé de recherche, CNRS – MNHN, Sorbonne Université

Examinateur

Valérie LALLEMAND-BREITENBACH, Directrice de recherche, INSERM
– Collège de France, Université PSL

Examinatrice

“ *Omnis cellula e cellula* ”

Cellularpathologie, Rudolf Virchow, 1858

“ - *La science, mon garçon, est faite d'erreurs, mais d'erreurs qu'il est bon de commettre,*
car elles mènent peu à peu à la vérité. ”

Voyage au centre de la terre, Jules Verne, 1864

“ [...] *a genome may react to conditions for which it is unprepared but to which it responds*
in a totally unexpected manner. ”

Nobel Prize lecture, Barbara McClintock, 1983

Acknowledgments

Acknowledgments

En premier lieu, je tiens à remercier chaleureusement les membres du jury pour avoir accepté d'évaluer ce travail : Alice Jouneau et Daan Noordermeer pour l'évaluation de ce manuscrit, ainsi qu'à Michele Goodhardt, Sophie Polo, Valérie Lallemand-Breitenbach et Christophe Escudé pour juger mon travail de thèse.

Je remercie également les membres de mon comité de suivi de thèse, qui ont suivi l'évolution de mon travail année après année : Michele Goodhardt, Daan Noordermeer, Jean-François Ouimette et David Garrick.

Je remercie grandement Emmanuelle pour m'avoir accepté dans son laboratoire lors de mon stage de M2 puis pour la thèse. Plus de quatre ans ont passé, et j'ai eu grand plaisir à venir tous les jours au labo ! Je n'ai jamais perdu ma motivation et ma passion pour la science, et je te remercie d'y avoir contribué.

Mes plus forts remerciements vont naturellement vers Pierre. Un très grand merci pour avoir accepté de diriger ce travail lors de ces quatre années. Tu m'as tout appris sur la chromatine et sur les cellules ES, et tu m'as transmis ta passion et ton énergie. Ces longues discussions ont, je le crois, été essentielles à ma construction en tant que jeune scientifique – même si elles m'auront mises en retard plus d'une fois ! Tu m'as toujours soutenu, même dans des expériences auxquelles tu ne croyais pas au début, et qu'elles aient été succès ou échecs, cela m'a permis de grandir intellectuellement. Je repenserai également à toutes nos discussions non-scientifiques et à toutes tes blagues, notamment lors des repas, qui ont égayées mes journées.

Je pense bien sûr à Adeline, sans qui j'aurais été complètement perdu. Merci de m'avoir montré à peu près toutes les techniques que je sais utiliser aujourd'hui ! Tu as été bien plus qu'une collègue à mes yeux, tu as été une amie. Nos discussions dans le labo, mais aussi la musique (Barbara continue même depuis ton départ) et nos moments de rigolades ont été très importants.

Merci à Etienne et à Zack, mes compagnons de discussions politiques qui n'en finissaient plus ! Nous avons beaucoup échangés, et bu quelques bières (et quelques Coca pour Zack ;), des moments que je n'oublierai pas.

Je remercie Fabiola, collègue et amie avec qui j'ai eu le plaisir de partager les moments intenses en parallèle : projet de quatrième année, écriture et préparation de la soutenance de thèse... Merci pour tous ces moments ici à Paris, et bien sûr merci à ta famille pour l'accueil exceptionnel au Pérou !

Je remercie également tous les membres de l'équipe (la nouvelle, GeBi bien sûr). Merci à Pascale, pour son attention, sa bonne humeur et sa passion des éléments transposables. Merci à Anastasia, pour avoir été ma voisine durant ces dernières années et avoir partagé des discussions sur tout et rien ainsi que des discussions scientifiques. Merci à Renaud, bien qu'arrivé plus tardivement dans notre équipe, avec qui j'ai partagé un nombre inimaginable de café, de repas, et de discussions sur beaucoup de chose. Merci à Amandine, pour ses remarques toujours avisées ; à Amna, pour ses pauses café partagées ; à Arthur bien sûr pour nos longues heures en salle de culture à discuter tout en écoutant ouiFM ; à Joëlle, pour ses histoires et sa profonde gentillesse ; à Alessia, pour sa bonne humeur ; à Noé, pour ses fameuses pizzas du jeudi. Je remercie également Anna, pour ses (très) longues discussions, mais aussi ses conseils sur l'après thèse ; et Laura, pour nos (trop rares) discussions. Merci aux anciens membres naturellement, à Yasmine, pour être elle-même, et nous faire voyager dans son monde à elle, et aussi pour l'élaboration des scripts que je continue à utiliser ; à Julie, pour son dynamisme ; à Alice, pour sa gentillesse ; à Charlotte, pour son caractère bien trempé ; ainsi que toutes les personnes passées par notre équipe au fil des ans.

Parce que l'équipe n'était pas seule dans ce bâtiment Jean Bernard, je remercie nos voisins de palier, l'équipe Amara : Alexis, pour toutes ses anecdotes ; Sarah, pour nos manifestations partagées ; Laurent, pour tes blagues, mais aussi Ali, Athéna, Estelle, Lamine, Lucie, Claudia, Ophélie, Vasiliya, Stéphane, Julien et tous ceux qui ont travaillé au 2^{ème} étage.

Je remercie Hugues et Valérie pour leur intérêt tout au long de l'avancement de mon projet ; ainsi que toute leur équipe. Je pense bien sûr à Cécile et à Caroline, pour tous nos repas et pauses-café partagées ; à Marie-Claude, pour ses conseils et discussions ; mais encore à Michiko, à Florence, à Omar et toutes les personnes croisées au 3^{ème} étage.

Je remercie les membres de la plateforme technologique du bâtiment Hayem et notamment Niclas pour son aide précieuse pour la microscopie. Merci également à Stéphane, pour son enthousiasme et son temps passé avec moi à son microscope, ainsi que Judith, pour ses conseils sur la dynamique des protéines.

Je remercie chaudement Rodney, pour m'avoir accueilli dans son équipe pour mon stage de M1, et être depuis resté un véritable mentor.

Je remercie la Ligue Nationale Contre le Cancer d'avoir financé ma quatrième, et si importante, année de thèse.

La thèse ce n'est pas seulement un travail en laboratoire, mais une petite partie de vie, partagée également en dehors du labo. Ainsi je remercie tous mes amis hors-paillasse : Claire, sans ses toutes ses sous unité, la polymérase fait trop d'erreurs, Nicolas, pour nos discussions, nos tennis, nos rires et nos lectures partagées ; bien sûr Sam & Paul, on s'imaginait soutenir nos thèses en même temps, tu as changé de direction en cours de route mais tu restes ma meilleure amie ; Mathilde & Clément, Rosie & Julien, Eléonore & Norman, Anaïs, et Marie, pour votre amitié. Je remercie le Magistère de génétique, pour m'avoir permis ses rencontres formidables, aussi bien professionnelles que personnelles. Je pense également à Théo, à Caro, à Salomé, et à Cordi pour toutes ces bières bues ensembles !

Devenir chercheur n'était certes pas inscrit dans mes gènes, mais je crois qu'ils ont été l'environnement propice pour le faire émerger, merci à toute ma famille pour leur soutien, parfois sans bien savoir ce que je faisais dans mon laboratoire. Je remercie surtout mes parents, pour la liberté qu'ils m'ont accordé de trouver ma voie, pour leur bienveillance à toute épreuve, pour la curiosité qu'ils m'ont transmise, et pour leur amour. Je pense fortement à mes grands-parents, qui n'auront pas connu la fin de cette aventure, mais qui sont avec moi, dans mes pensées.

Enfin, pour ta patience et ton soutien durant toutes ses années, malgré mon caractère et mes retards chroniques, malgré tous mes défauts et mes angoisses, tu m'as soutenu, poussé et aidé, merci Pauline. Merci de partager ma vie...

TABLE OF CONTENTS

Table of contents

Acknowledgments	6
List of abbreviations	18
List of figures	22
INTRODUCTION	26
I - Genetic and epigenetic regulations of DNA.	26
A - Structure and organization of chromatin	26
Nucleosome and chromatin	26
Chromatin states: euchromatin and heterochromatin	29
B - Epigenetic regulations of chromatin	32
Histone post-translational modifications	33
1. Acetylation	34
2. Methylation	36
DNA methylation	39
Variants of H2A	45
1. macroH2A	45
2. H2A.X	46
Variants of H3	47
1. CENP-A, the centromeric H3	47
2. The H3.3 histone variant	48
H3.3-associated chaperones	50
C - The DAXX-complex chaperone	53
II - Spatial compartmentalization of the nuclear space.	56
A - Three-dimensional folding and radial positioning of chromatin	56
B - Lamina-Associated Domains	59
1. Nuclear envelope and definition of the lamina-associated domains	59
2. Protein composition of the nuclear periphery	62
3. Functions and dysfunctions of LADs	65
C - Pericentromeric heterochromatin	68
1. Pericentromeric heterochromatin and chromocenters organization	68
2. Protein composition of PCH and maintenance mechanisms	71
3. Biological functions of pericentromeric heterochromatin	75
D - Telomeres	78
1. Localization and definition of telomeric heterochromatin.	78

2. Protein composition of telomeres _____	79
3. Influence of telomeres _____	81
E - Transposable Elements _____	83
1. Localization and definition of TEs _____	83
2. Regulation of TEs _____	86
3. Diversity of functions of the transposable elements _____	90
F - Nuclear Bodies _____	92
The Nucleolus _____	92
1. Definition of the nucleolus _____	93
2. The nucleolus as dynamic compartment _____	94
3. Diseases associated with nucleolar dysfunction _____	95
PML NBs _____	96
1. Definition and roles of PML NBs _____	96
2. Interplay of PML with DAXX, H3.3 and chromatin _____	99
<i>III - Embryonic stem cell as a model of embryonic development and chromatin</i>	
<i>specifies. _____</i>	103
Embryonic development and embryonic stem cells _____	103
1. Definition of the embryonic development and pluripotent cells _____	103
2. Different levels of pluripotency in in vitro cultures _____	106
3. Pluripotency in a chromatin context _____	109
<i>Appendix to the introduction _____</i>	118
Review 1 _____	118
<i>Objective of the thesis _____</i>	132
Evaluation of the role of Daxx in heterochromatin maintenance in pluripotent cells _	132
<i>RESULTS _____</i>	136
Publication 1 – In preparation _____	136
Other results concerning Daxx at PCH _____	168
Methods _____	168
RESULTS _____	172
Deeper characterization of DAXX function in pluripotent cells _____	172
1. Loss of Daxx results in transcriptional 2C-like signature _____	172
2. DAXX contributes to the radial positioning of chromocenters _____	173
3. DAXX contributes to peripheral heterochromatin organization and silencing of LADs _____	175
4. LINE1 elements upregulation contributes to the accumulation of DNA damages in the	
absence of Daxx _____	178
Characterization of the role of PML in DAXX-mediated pericentromeric heterochromatin	
organization _____	180

1. PML is essential for pluripotent cell survival upon DNA hypomethylation _____	180
2. DAXX accumulation at PCH is independent of PML _____	182
3. PML contributes to organization and radial localization of PCH _____	183
4. Loss of Pml induces alteration of peripheral heterochromatin and loss of LADs silencing upon ground-state conversion _____	184
Characterization of DAXX domains necessary for PCH clustering _____	186
1. DAXX-mediated PCH clustering is independent of ATRX interaction _____	186
2. Post-translational regulation of DAXX _____	188
CONCLUSIONS _____	198
DISCUSSION _____	202
1. DAXX is essential for prolonged culture upon DNA hypomethylation and maintains chromatin identity of pluripotent cells. _____	202
2. Mechanism of DAXX-PML recruitment at PCH upon loss of DNA methylation. _____	203
3. DAXX and SETDB1 participate in re-establishment of heterochromatin state following active DNA demethylation-induced DNA damages. _____	205
4. DAXX maintains pericentromeric heterochromatin organization. _____	209
5. Roles of DAXX-SETDB1 at other genomic regions _____	214
6. Activation of heterochromatin regions can generate DNA damages and IFN signaling ____	216
7. DAXX interactions and post-translational modifications _____	218
8. Roles of DAXX and pericentromeric regions in pathologies _____	221
RESUME SUBSTANTIEL DE LA THESE EN FRANCAIS _____	226
Introduction _____	226
Résultats _____	227
Discussion _____	230
REFERENCES _____	234
RESUME _____	304
English _____	304
Français _____	304

LIST OF ABBREVIATIONS

List of abbreviations

2i - 2 inhibitors

5mC - 5-methyl-cytosine

5hmC - 5-hydroxy-methyl-cytosine

5fC - 5-formyl-cytosine

5caC - 5-carboxylcytosine

A

AC - Astrocyt

AICDA – activation-induced cytidine deaminase

ALT - Alternative-lengthening of telomeres

ATAC - Assay for transposase-accessible chromatin

ATM - Ataxia telangiectasia mutated

ATRAX - α -thalassemia/mental retardation syndrome protein

APE-1 - AP endonuclease 1

APC - Adenomatous polyposis coli

APL - Acute promyelocytic leukemia

B

BER - Base-excision repair

C

CABIN - Calcineurin binding

CENP-A - Centromeric protein A

CFP1 - CXXC finger protein 1

CHD - Chromodomain helicase DNA-binding domain

CT - Chromosome territory

D

DamID - DNA methyl transferase

DAMP – Damage-associated molecular pattern

DAPI - 4',6-diamino-2-phenylindole

DAXX - Death-domain associated protein

DFC - Dense fibrillar compartment

DKC1 - Dyskerin protein 1

DDR - DNA damage response

DNA - Desoxyribonucleic acid

DNMT - DNA methyl-transferase

DSB - Double-strand break

E

EM - Electron microscopy

EP400 - E1A binding protein p400

ERE - Endogenous retroelement

ERV - Endogenous retrovirus

(m)ESC - (murine) embryonic stem cell

F

FC - Fibrillar center

FISH - Fluorescent *in situ* hybridization

G

GC - Granular component

I

ICF - Immunodeficiency, centromeric instability and craniofacial abnormalities

ICM - Inner cell mass

IFN - Interferon

iPSC - Induced pluripotent stem cells

H

HAT - Histone acetyl transferase

HDAC - Histone deacetylase

HGPS - Hutchinson-Gilford progeria syndrome

HIRA - Histone regulator A

HJURP - Holliday junction recognition protein

HR - Homologous recombination

K

KDM - Histone lysine demethylase

KMT - Histone lysine methyl-transferase

KoRV - Koala retrovirus

KRAB - Krüppel-associated box

L

LAD - Lamina associated domain

cLAD / fLAD - constitutive / facultative
LAD

LBR - Lamin B receptor
LIF - Leukemia inhibitory factor
LINE - Long interspersed element
LLPS - Liquid-liquid phase-separation
LTR - Long-terminal repeats
LSD1 - Lysine-specific histone demethylase

M

MBD - Methyl-binding domain
MDM2 - Mouse double minute 2
MEF - Murine embryonic fibroblast
MLL - Myeloid/lymphoid or mixed-lineage leukemia-associated
MMLV - Moloney murine leukemia virus
MLV - Murine leukemia virus

N

NBS1 - Nibrin 1
NLS - Nuclear localization signal
NET - Nuclear envelope transmembrane
NGS - Next-generation sequencing
NHEJ - Non-homologous end-joining
NAD - Nucleolus associated domain
NB - Nuclear body
NOR - Nucleolus organizer region
NPC - Neuronal progenitor cell

P

PCH - Pericentromeric heterochromatin
PCNA - Proliferating cell nuclear antigen
PML - Promyelocytic protein
polyQ - Polyglutamine
PTEN - Phosphate and tensin homolog
PRC - Polycomb repressive complex

S

SAFB - Scaffold attachment factor B
SAHF - Senescence-associated heterochromatin foci
scRNA-seq - Single-cell RNA-sequencing
SIM - SUMO-interacting motif
SINE - Short interspersed element
SSB - Single-strand break
SUMO - Small ubiquitin like modifier

R

RAR α - Retinoic acid receptor α
RPA - Replication protein A

T

TE - Transposable element
TET - Ten-eleven translocation
TIR - Terminal inverted repeats
TAD - Topologically associated domain
tRNA - Transfer RNA
TERT - Telomerase
TERRA - Telomere repeat-containing RNA
T-loop - Lariat-like structure
TREX1 - Three-prime-repair exonuclease 1
TSA - Trichostatine A
TSS - Transcription start site

U

UBN - Ubinuclein
UHRF1 - Ubiquitin-like containing PHD and RING finger domains 1

Z

ZFP - Zinc-finger protein

LIST OF FIGURES

List of figures

Figure 1 Nucleosomal organization of chromatin and nucleosome repartition. _____	27
Figure 2 Different chromatin compaction states. _____	30
Figure 3 Landscape of histone post-translational modifications. _____	34
Figure 4 Schematic of histone acetylation and associated ‘readers’. _____	35
Figure 5 Histone methyltransferases and their associated phenotypes. _____	37
Figure 6 DNA methylation machinery and mechanism. _____	42
Figure 7 Histone variants. _____	45
Figure 8 Histone variant H3.3 structure and function. _____	52
Figure 9 The H3.3-chaperone DAXX, structure, localization and function. _____	54
Figure 10 Spatial compartmentalization of the nuclear space. _____	57
Figure 11 Localizations of chromosomes within the nuclear space. _____	58
Figure 12 Lamina associated domains. _____	60
Figure 13 Proteins associated with lamina associated domains. _____	63
Figure 14 Changes in nuclear lamina interactions upon differentiation and ‘unlocking’ theory. _____	66
Figure 15 Organization of pericentromeres. _____	70
Figure 16 Heterochromatin composition and transcriptional state of pericentromeres. _____	74
Figure 17 Importance of pericentromeric satellite regulation. _____	76
Figure 18 Organization and composition of telomeric DNA. _____	81
Figure 19 Overview of the classes of transposable elements in mouse. _____	84
Figure 20 Multiple proteins ensure transcriptional repression of ERVs. _____	88
Figure 21 PML proteins assemble into PML nuclear bodies. _____	97
Figure 22 PML NBs as a storage center for H3.3-chaperones and interaction with chromatin. _____	101
Figure 23 Murine early embryonic development. _____	105
Figure 24 Signaling pathways in pluripotent cells in vitro. _____	108
Figure 25 Chromatin changes along early embryonic development. _____	111
Figure 26 Pericentromeric maintenance in totipotent and pluripotent cells. _____	114
Figure 27 Absence of Daxx results in 2C-like transcriptional profile. _____	173
Figure 28 DAXX contributes to the radial positioning of chromocenters. _____	174
Figure 29 DAXX contributes to peripheral heterochromatin organization. _____	175
Figure 30 Loss of Daxx impairs the silencing of genes within LADs. _____	177
Figure 31 LINE1 activation contributes to the accumulation of DNA damages in the absence of Daxx. _____	180
Figure 32 Generation of Pml KO ESCs. _____	181
Figure 33 DAXX accumulation at PCH is independent of PML. _____	182
Figure 34 PML contributes to pericentromeric heterochromatin organization. _____	184
Figure 35 Loss of Pml induces alteration of H3K9me2 peripheral signal upon ground-state conversion. _____	185
Figure 36 Absence of Pml induces the loss of LAD-genes upon ground-state conversion. _____	186
Figure 37 DAXX-mediated PCH clustering is independent of ATRX interaction. _____	187
Figure 38 SUMOylation but not SIM domain of DAXX seem implicated in PCH clustering. _____	189

Figure 39 Recruitment of H3.3 and PML upon DAXX targeting to PCH. _____	190
Figure 40 Model displaying the function of DAXX at pericentromeric heterochromatin and the consequences of its loss. _____	199

INTRODUCTION

INTRODUCTION

I - Genetic and epigenetic regulations of DNA.

Carrier of the genetic information, deoxyribonucleic acid (DNA) is the basic unit of life. Constituent of DNA, the 4 nucleic acids were identified early on by Albrecht Kossel at the University of Berlin, although there was no evidence that DNA was indeed the molecule responsible for hereditary information. The first observations of DNA in cells were made by Walther Flemming. He coined the term of chromatin as the compact DNA he observed was refractory to light under the microscope. He observed that the chromatin was passed on from the mother to the daughter cell during a process that he named mitosis.

A - Structure and organization of chromatin

The first complete theory that DNA was the molecule required for inheritance of traits was published by Walter Sutton and Theodor Boveri in 1902. The actual set of experiments clearly demonstrating the role of DNA were carried by Oswald Avery in 1944. He qualified DNA as the “transforming principle”. This discovery led many groups to try to identify the structure of this molecule. The famous double-helix structure was identified by James Watson, Francis Crick, Maurice Wilkins and Rosalind Franklin in 1953 (Watson and Crick 1953).

All cells of the organism carry the same DNA sequence and however, different cells and tissues coexist in one individual. How can it be that the same information gives rise to different outcomes? Although DNA serves as template, not every gene is transcribed within the same cell. In 1942, in a seminal paper, Conrad Waddington coined the term ‘epigenetics’ to bring together the different phenotypes exhibited by different cells. This is notably the case during embryonic development. From the zygotic single cell to a whole organism, many cell divisions and cell identities will be required.

In this first part, I will describe the organization of DNA into chromatin and the two main types of chromatin structure.

Nucleosome and chromatin

The DNA molecule is not merely floating naked into the nuclear space but is rather found has a complex structure of nucleic acids and proteins. DNA folds around small basic and positively charged proteins called histones. Four types of canonical histones exist in eukaryotes - H2A, H2B,

H3 and H4. They form multimeric complexes - H2A-H2B and H3-H4 that assemble into an octamer to form a nucleosome. DNA wraps itself onto nucleosomes, where a sequence of 148bp of DNA surrounds one nucleosome. This organization of nucleosome-DNA forms the chromatin and implicates repeating units all along the DNA molecule that could give the observed flexibility of this molecule (Kornberg and Thomas 1974; Kornberg 1974). DNA wraps 1.75 turns around a nucleosome. The crystal structure of nucleosomes interaction with DNA was only obtained in 1997 (**Figure 1A**)(Luger *et al.* 1997).

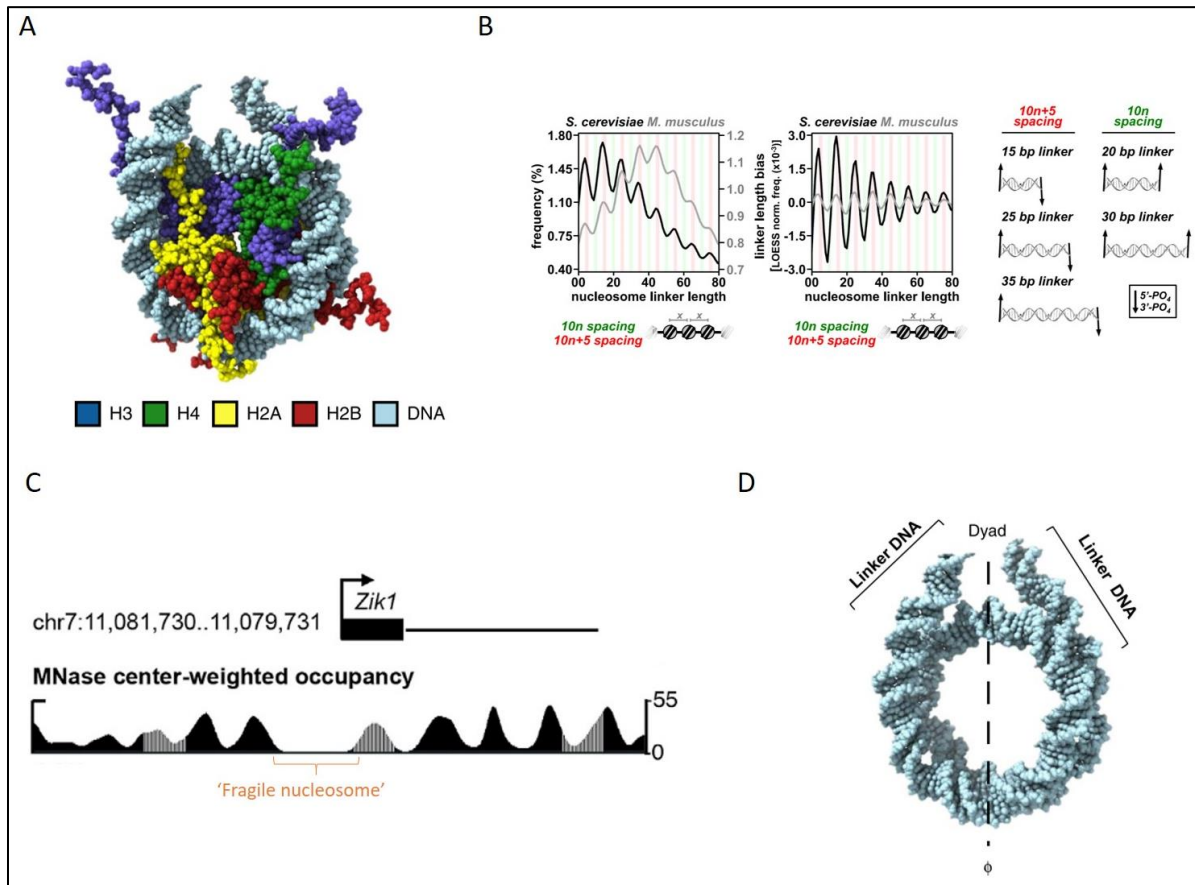


Figure 1| Nucleosomal organization of chromatin and nucleosome repartition. (A) Crystal structure of a nucleosome consisting of a histone octamer and DNA. (B) Nucleosome spacing in *S. cerevisiae* and *M. musculus* that favor two different types of inter-nucleosome distances. (C) MNase-seq profile displaying nucleosome occupancy near a transcription start site (TSS). In orange is highlighted a fragile nucleosome region which is strongly unstable. (D) DNA wrapped around a nucleosome. At the top of the dyad lies the linker inter-nucleosome sequence. A and D are from Zhou, Gaullier and Luger, *Nat. Struc. Mol. Biol.* 2019. B is from Gibson *et al.*, *Cell* 2019. C is adapted from Voong *et al.*, *Cell* 2016.

X-ray crystallography of a nucleosome-DNA complex at high resolution demonstrated the folding of chromatin, but also that some part of the histones were not facing the inside of the structure but were rather turned outside to DNA contacts. These domains are the N-terminal domains of the histones and called histone “tails” that can carry many subsequent post-translational modifications that are essential for chromatin functions. These modifications will be addressed in the second part of the introduction.

Although all eukaryotes display a nucleosomal organization of chromatin, the nucleosomes are not equally distributed among the genome. Furthermore, the spacing of nucleosome is of great importance and varies from species to species (Baldi 2019). The spacing between nucleosomes have different impacts on chromatin processes, notably for transcription as the presence of nucleosomes can profoundly impact the binding of transcription factors (Zhu *et al.* 2018a). In *Saccharomyces cerevisiae*, the baker's yeast, the average spacing between nucleosome is about 15bp, whereas in mouse it is mostly about 45bp. Furthermore, it was observed across eukaryotes that evolution favored a spacing biased toward $10n+5$ (15, 25, 35...) but depleted for $10n$ (10, 20, 30...) (Gibson *et al.* 2019; Voong *et al.* 2016) (**Figure 1B**). Very recently, it was demonstrated that distances between nucleosomes could even participate in the phase-separation properties of nucleic acids (Gibson *et al.* 2019). Gibson *et al.* showed that histone proteins have the intrinsic ability to form molecular condensates. Phase-separation capacities could be modified according to histone post-translational modifications and transcription factor bindings. These results suggest that chromatin organization and chromatin processes might be regulated by physical principles. The stability of the nucleosome depends on its genomic localization. Interestingly, most species display around the transcription start site (TSS) of genes a nucleosome-depleted regions which is surrounded by strongly phased nucleosomes as observed by MNase studies (Hughes *et al.* 2012). Using a chemical mapping of nucleosomes, it was recently shown that at the TSS and transcription termination site lied 'fragile' nucleosomes which are unstable and easily displaced during transcription (Voong *et al.* 2016) (**Figure 1C**).

Between nucleosomes, DNA can be enriched into linker histones (**Figure 1D**). Linker histones have been conserved along evolution, although more diversity is observed than for nucleosomal-histones. Histone composition can drastically change the biophysical properties of the chromatin fiber and histone concentrations can vary between different regions of the genome. Mammals have eleven linker histone H1 proteins and it is likely that they have overlapping yet different roles according to cell type and metabolic state. In mouse, H1 protects around 20bp in mouse, and genetic deletion of H1 lead to embryonic lethality, suggesting a crucial role for H1 on the cell physiology (Fan *et al.* 2003). Linker histones H1 are tightly linked to chromatin condensation, even though they have been historically less studied. Indeed, H1 presence is usually correlated with a higher chromatin condensation, as observed in for rod photoreceptors of the mouse retina where it corresponds to the increase of the nucleosomal repeat length from 190 to 206bp together with H1 accumulation (Popova *et al.* 2013). Other studies have shown that H1 mediates local chromatin compaction and subsequent gene silencing (Kim *et al.* 2015; Chen *et al.* 2014).

These results illustrate that the very nature of chromatin, the nucleosomal organization, the spacing between nucleosomes and the presence of linker histones can modify DNA-related processes.

Chromatin states: euchromatin and heterochromatin

The mammalian genome measures roughly 2 meters long, yet it needs to fit inside a 10 μm -diameter nucleus. Thus, chromatin must be tightly condensed. The mammalian genome measures roughly 2 meters long, yet it needs to fit inside a 10 μm -diameter nucleus. Thus, chromatin must be tightly condensed. The first observations of chromatin using DNA dyes allowed the identification of two main types of chromatin - heterochromatin and euchromatin. Euchromatin corresponds to open, decompacted and transcribed regions of the genome, whereas heterochromatin dovetails with close, compacted and repressed regions (**Figure 2A**). Subsequent molecular and genomic techniques gave more insights into the meaning of these two-chromatin types categorization.

The classical view of DNA folded around nucleosomes gave rise to the vision of a 10nm-fiber that allows two physical properties - the positive charges of the histones are neutralized by the negative charges given by the phosphate DNA backbone and secondly, it provides clues of how the 2m of the genome can be compacted to fit inside a 10 μm nucleus. The 10nm fiber was observed by electron microscopy (EM) in 1975 and then referred in textbooks as the bead-on-a-string model (Olins and Olins 1973). As this 6-fold compaction given by the 10nm fiber organization could not account for the different chromatin states observed by microscopy studies, it was proposed that chromatin could be organized as a repeated higher-order structure - the 30nm fiber (Finch and Klug 1976) (**Figure 2B**). Furthermore, euchromatin is sought to represent only 10% of the genome, which clearly indicates that most of the genome is organized into the more condensed heterochromatin state (Fussner *et al.* 2011). The 30nm fiber was thus suggested to be a physical organization of chromatin which involves DNA compaction. Several 30nm fiber models were proposed that recapitulated the physical properties of such chromatin as the solenoid, the helix zigzag, the cross-linker or the supranucleosome models (Fussner *et al.* 2011). Each of these models proposed a view for nucleosome arrangements within the three-dimensional space that relied on EM observations of extracted chromatin and theoretical modeling. Yet, the very existence of 30nm fiber remains controversial and some authors argue that the 10nm folding could well-

enough explain the different compaction levels and that the 30nm fiber was never actually observed *in vivo* in another model that the starfish sperm nuclei (Horowitz *et al.* 1994; Fussner *et al.* 2011).

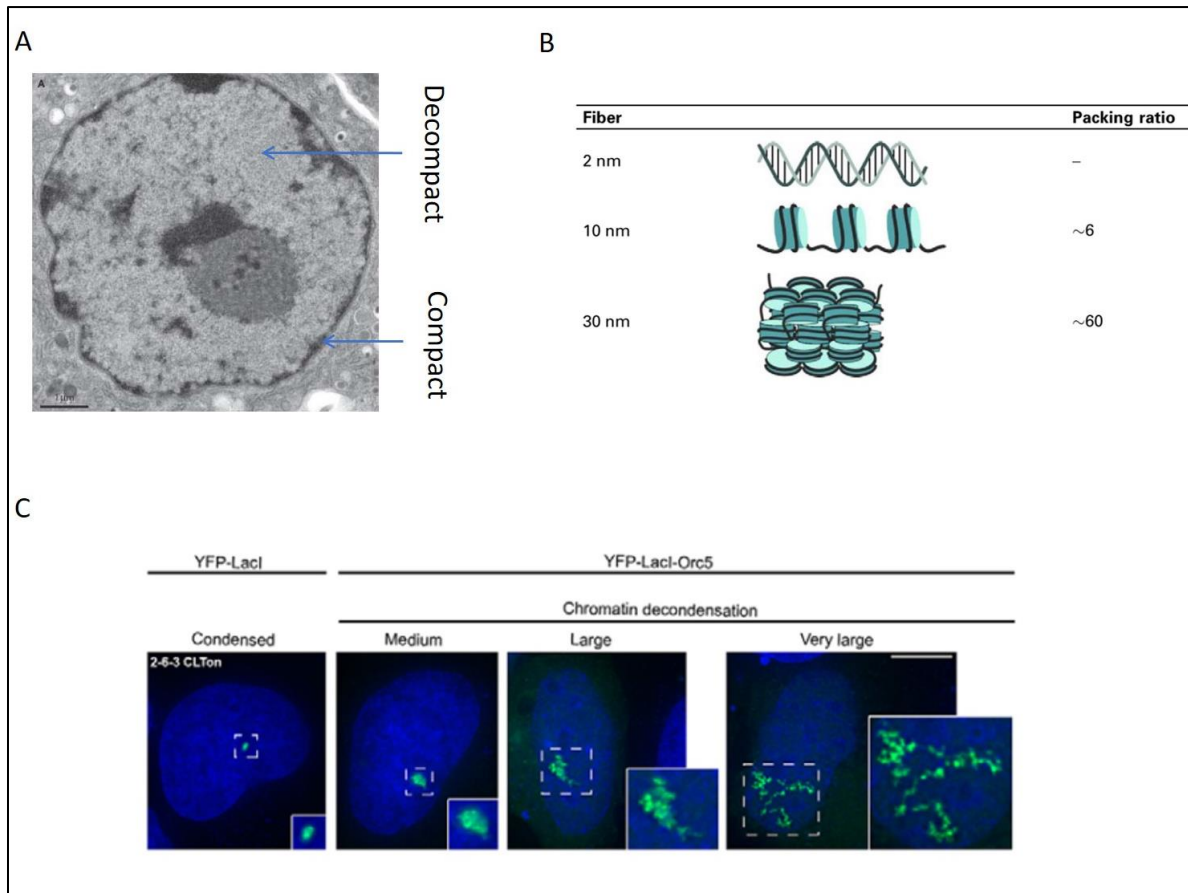


Figure 2 | Different chromatin compaction states. (A) Electron microscopy picture of a mammalian nucleus. In light grey is the decompact, open and active euchromatin whereas in dark grey lies the compacted, closed and inactive heterochromatin. **(B)** Theoretical states of chromatin compaction and the corresponding packing ratio obtained from these configurations. **(C)** Live-cell imaging of a LacO array visualized by a LacI-YFP reporter. On the left is a compact locus, whereas on the right is shown different decompaction state from medium to a very large decondensation. A is adapted from Akthar and Gasser, *Nat. Rev. Gen.* 2006. B is from Fussner, Ching and Bazett-Jones, *Trends in Biochem. Sciences* 2011. C is from Giri *et al.*, *J. Cell Science* 2016.

Evidence of large-scale chromatin compaction was established a long time ago for the inactive X chromosome. In mammals, females carry two X chromosomes coming from the two parents. Yet, only one remains active in the cell. The other one is silenced and compact. This compaction form the long-known Barr body (Barr and Bertram 1949). Already visible with a DNA dye staining, FISH studies have further confirmed this phenomenon, the inactive X chromosome appearing as a small and compact FISH signal whereas the active X is less compacted and takes more space with a more diffuse fluorescence signal. This was also appreciated on polytene chromosomes of *Drosophila melanogaster* for which active regions also appear to be more decompact (Berkaeva *et al.* 2009). A later study demonstrated that the same-sized Mb domains occupied different proportion of the nucleoplasm depending on the gene-content of the regions. This indicates that different

degrees of chromatin compaction are observed, and it seems to correlate with the transcriptional status of the region.

To assess the molecular compaction state of chromatin at specific loci, different strategies have been adopted. The firsts used are molecular techniques such as DNaseI and MNase. Indeed, these strategies stemmed from early characterization of promoter regions. These techniques have then be used to assess genome-wide the regions that display a more open or closed chromatin state, when the accessibility to digestion was high or low respectively (Henikoff *et al.* 2011). The development of the HiC technique to probe all chromatin interactions genome-wide revealed that the genome globally segregates into two particular compartments - A and B, which correspond respectively to an active and inactive chromatin states. A and B compartments spatially segregate from one another and form the basis of the three-dimensional organization of chromatin that I will deeply describe in a next chapter. The HiC technique that probe all chromatin interactions genome-wide could also be used to assess chromatin compaction state of one locus as it is the intensity of close-by interactions for each locus. It has been used to study the impact of polycomb on gene repression during differentiation (Kundu *et al.* 2017).

Correlation with ChIP-seq data have revealed that compacted and decompacted regions were each enriched for particular set of proteins and histone modifications, and also correlated with the A and B chromatin compartments. Indeed, the strongest correlation include the enrichment of histone acetylation for open regions, whereas closed regions are enriched for histone methylation, that I will describe in a later chapter. Interestingly, Filion *et al.* proposed that in addition to the observed open or closed chromatin, more subtle chromatin compaction states coexist within the cell and might arise from the action of different set of factors (Filion *et al.* 2010). These results suggest that while chromatin can either belong to the A or B compartments, compaction state is finely regulated to allow the different DNA-related processes to happen.

More recent studies have used a novel assay for transposase-accessible chromatin (ATAC) followed by high-throughput genome sequencing (Buenrostro *et al.* 2013). This technique allows for a genome-wide cartography of chromatin accessibility. It has been improved to look at allele-specific gene transcription, which gives a deeper understanding of genomic regulation, at the level of specific gene-units (Xu *et al.* 2017). The authors observed an unexpected allele-specific regulation of chromatin compaction, yet the allelic choice could be randomly established and did not rely on the parental origin. This study points out that not only chromatin state regulation happens at specific regions of the genome, but that it can also be regulated at particular gene-unit and at the level of the chromatid.

It was though for a long time that chromatin compaction was a direct visualization of the transcriptional state of the locus. It is now demonstrated that it is not always the case. Chromatin decondensation can indeed precede gene activation, and it is now believed that decompaction of a locus might prime a gene to allow a faster activation when needed. This was observed for the immunological memory of T cells and macrophages (Bevington *et al.* 2016). This was also hypothesized and then demonstrated for the upregulation upon differentiation of specific genes in pluripotent cells (Peric-Hupkes *et al.* 2010; Therizols *et al.* 2014).

Since the 1960's, studies have tried to understand lymphocyte activation. It was observed early on that upon activation, the cells would drastically change their nuclear size, RNA production levels and would increase global histone acetylation. It was only recently elucidated how activation of lymphocytes could trigger overall chromatin decondensation. Chromatin firstly goes away from the repressive nuclear periphery, and then a large MYC-dependent genome reorganization takes place, where long-range contact decrease and short-range contacts increase. This MYC-dependent reorganization is visible as histone nanodomain clusters are dissolve into mononucleosome domains (Kieffer-Kwon *et al.* 2017). Interestingly, chromatin condensation state can vary when cells are kept in culture, suggesting that *in vitro* culture conditions might hamper the possible conclusions (Oh *et al.* 2013).

Compaction state of peculiar loci have been confirmed using fluorescent in situ labeling (FISH). It has notably been used during the natural decompaction of specific loci upon differentiation of mouse pluripotent cells (Williams *et al.* 2006). Further characterization of compaction state have been assessed by live-cell imaging of particular loci, displaying striking differences between a compacted and a decompacted locus (**Figure 2C**)(Giri *et al.* 2016). However, it remains to understand how biophysical properties of the chromatin fiber is controlled.

B - Epigenetic regulations of chromatin

The term 'epigenetics' was developed in 1942 by the developmental biologist Conrad Waddington. He introduced the concept of epigenetics to link genotypes and phenotypes in a will to gain insights into the role of the genetic regulation of development. Nowadays, epigenetics usually refers to the heritable genetic information that does not involve changes in DNA sequences. Epigenetic information thus relies onto the chemical modification of either DNA or histones.

DNA folds around nucleosomes, which are composed of the four canonical histones in most of the chromatin. However, other histones have emerged during evolution for specific functions. Histones are considered as very stable proteins with half-lives of several months to year

in non-dividing cells, opening the question of how chromatin could be maintained in case of unwanted disruption such as transcription or damages.

Canonical histones are transcribed during S-phase and are crucial for proper DNA replication. Histone genes are short genes, with no introns, organized in multiple tandem repeats of 10 to 17 gene units to ensure large production of proteins. Histone genes have no polyadenylation sequence on 3' end but end with a stem loop followed by a purine-rich region that is complementary to the U7 snRNA. Histone mRNAs are regulated by the stem loop binding protein and the U7 snRNA (Marzluff *et al.* 2002). Histone variants have the capacity to be transcribed outside of mitosis, suggesting an important role, particularly in non-dividing cells. Histone variants genes often contain introns and are only present in one or two copies in the genome. Different variants have been identified for the histones H2A and H3, that I will describe in the following subsection. Interestingly, H4 does not have any variant, and it is one of the most slowly evolving protein, with divergence only described for unicellular eukaryotes (Malik and Henikoff 2003). Histone variants usually differ from canonical ones by only a few amino acid substitutions, but these changes are often found within the globular core of the proteins, thereby modifying their interactions between histone-histone and histone-DNA. I will hereby present some H2A and H3 variants.

All the nucleosomal histones can be post-translationally modified. These modifications have been linked to chromatin regulation and compaction state. Some proteins can modify histones, and act as 'modifiers', some can read the modifications, they act as 'readers' and some can remove it, acting as 'erasers'. It was proposed that these proteins act in a coordinated manner, thus forming a dynamic system that Jenuwein, Strahl and Allis called the 'histone-code' hypothesis (Strahl and Allis 2000; Jenuwein and Allis 2001). An important number of studies now supports this theory and research is now focusing on disease-related histone modification, implicating either histone or histone-modifying proteins mutations. Changes in the histone composition of specific modifications of histone are crucial to regulate chromatin properties such as the compaction state.

Histone post-translational modifications

For a long time, histones were considered as passive organizational proteins. Since then, many histone modifications were observed, yet their role revealed a great complexity system. Many types of post-translational modifications were identified - acetylation and methylation are the major ones, but there is also phosphorylation, ubiquitylation, sumoylation, citrullination, glycosylation, carbonylation, crotonylation, propionylation, ADP-ribosylation, biotinylation, N-formylation,

butyrylation, proline and aspartic acid isomerization and the recently discovered dopaminylation, that have been observed so far (**Figure 3**). The histone code is getting more and more complex as some residues like lysine 9 and 27 of histone H3 can be modified by different post-translational modifications, suggesting that the dynamic and combination of post-translational modifications is crucial for proper chromatin regulation. Globular core of histones can be modified, but many of the associated modifications studied in relation to genome regulation lie at the N-terminal tails of histones. I will only focus on the two most common - acetylation and methylation.

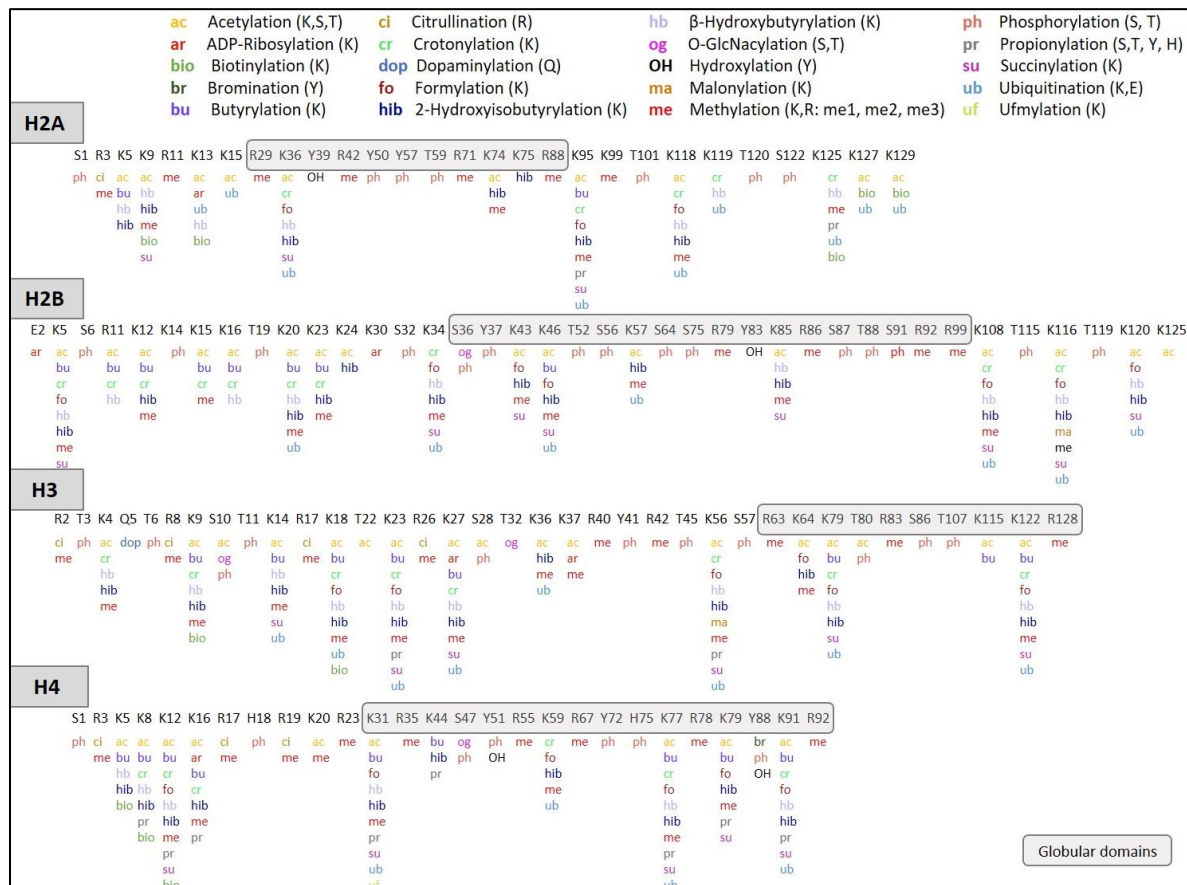


Figure 3| Landscape of histone post-translational modifications. For each canonical histone residues are indicated the reported post-translational modifications. Many of the modifications are observed on the N-terminal tails but the globular cores are also subjected to chemical modifications.

1. Acetylation

Acetylation is carried by histone acetyltransferase (HAT) enzymes. The major HAT in mammals are the TIP60, the P300/CBP and GCN5 complexes, but more proteins have the capacity to acetylate histone tails. All canonical histones can be acetylated, but the amino acids vary from one to another. Some lysines of newly synthesized H3 and H4 are modified before incorporation and then deacetylated, before properly modified to establish genomic patterns (Sobel *et al.* 1995). Lysines are the most often acetylated residues and only one acetyl group can be added.

It was the first histone modification associated with gene regulation (Brownell *et al.* 1996; Kuo *et al.* 1996; Taunton *et al.* 1996). Acetylated histones are associated with open chromatin as the negative charge can neutralize the positive one from the lysine and weakens the interactions between the DNA and the nucleosomes (Shahbazian and Grunstein 2007). Histone acetylation increases before the mRNA production, suggesting that this modification is indeed preceding and regulating transcription (Pogo *et al.* 1966). Deacetylation is carried by histone deacetylases (HDAC), and HAT and HDAC act dynamically to ensure transcriptional regulation of the genome (**Figure 4A**).

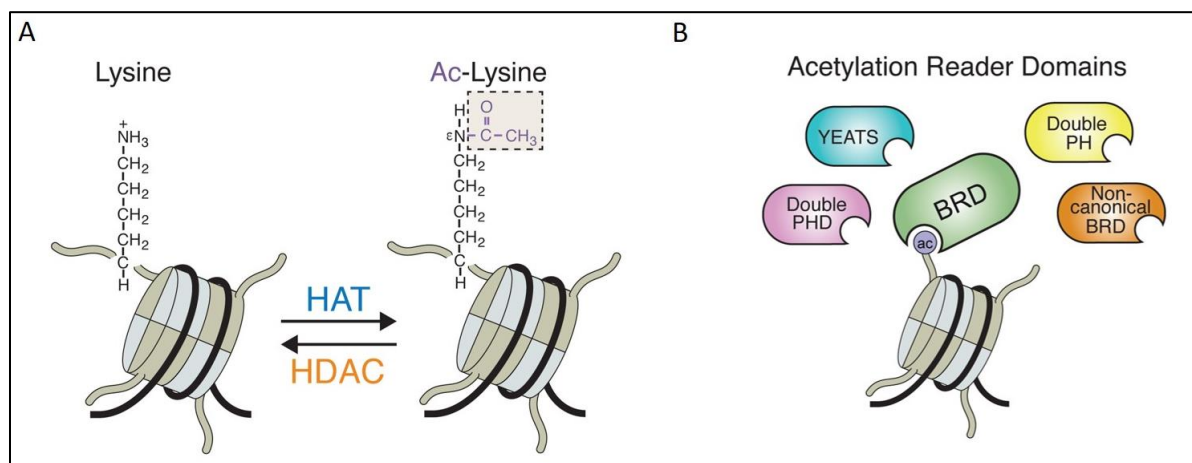


Figure 4 | Schematic of histone acetylation and associated ‘readers’. (A) Scheme of a nucleosome displaying one N-terminal histone tail with a lysine residue either acetylated or nor. The acetyl-group is added by a histone acetyl-transferase (HAT) and removed by a histone deacetylase (HDAC). (B) The different domains acting as ‘readers’ of an acetylated residue. The bromodomain (BRD) being the most common one. From Gong, Chiu and Miller, *PLoS Gen.* 2016.

The most common modifications observed are H3K9ac, H3K14ac, H3K27ac and H4K16ac. At the chromatin levels, they mostly appear as peaks present at regulatory regions. Although acetylation is mainly linked to activation, some reports observed that in specific conditions, HDAC recruitment was correlated with activation, suggesting a more complex view with cycles of acetylation-deacetylation taking place at active genes, yet it remains clear that silenced heterochromatin is devoid of acetylation (Wang *et al.* 2002, 2009). Histone acetylation is associated with high accessibility of DNaseI digestion and decompacted chromatin (Ridsdale *et al.* 1990; Hebbes *et al.* 1994). Genome-wide, histone acetylation is enriched at active promoters but not within gene bodies. H3K9ac and H3K14ac co-occupy many regulatory elements in murine embryonic stem cells (mESCs) and their enrichment correlates with transcription intensity (Karmodiya *et al.* 2012). The authors observed that H3K9ac and H3K14ac-rich promoters display low levels of DNA methylation, suggesting interplay between different types of epigenetic modifications. HATs are crucial for cell regulation, and their deletion results in either embryonic

lethality, as observed for Gcn5 and P300, or defects at later stages of differentiation as reported for CBP (Phan *et al.* 2005; Kasper *et al.* 2010).

Interestingly, acetylation of histones has also been implicated in transcriptional repression. Indeed, H4K16 must be deacetylated to enable chromatin compaction (Shogren-Knaak *et al.* 2006). It renders HDAC proteins as crucial in proper organization of chromatin, as indicated by the disruption of heterochromatin clusters when cells are treated with the HDAC inhibitor trichostatine A (TSA) (Taddei *et al.* 2001). HDAC functions have been conserved along evolution as both yeast and mESCs were shown to regulate telomeric heterochromatin via histone deacetylation (Dan *et al.* 2015).

Acetylation of histones can be recognized by different proteins, often containing a bromodomain such as BRD4, which has been implicated in many cancers and genetic syndromes (Olley *et al.* 2018). Other domains have the capacity to recognize and bind to acetylated histones (**Figure 4B**). Genome regulation appears to be a combination of histone modifications and binding of different factors, indicating multiple layers of control and complexity.

2. Methylation

Long before to be understood as histone methylase, factors crucial for proper development were discovered in genetic screens in *Drosophila* and called trithorax and polycomb proteins (Schuettengruber *et al.* 2017). It was later demonstrated that these proteins were not only implicated in the regulation of *Hox* gene expression but had a broad variety of functions, explained by the fact that they regulate histone methylation profiles. Histone methylation can be associated with different genomic regions depending on the residue. Methylation is performed by histone methyltransferase enzymes, both arginine and lysine residues can be methylated, but as the main methylated sites identified are lysine residues, these enzymes are called lysine methyltransferases (KMTs). Many proteins belong to this family of enzymes, and each one is specialized for one residue, yet some can achieve the same enzymatic process to ensure the robustness of the system. For each residue, a histone lysine demethylase (KDMs) exist that perform the opposite action of removing the methyl site (**Figure 5A**). Histone lysine methylation can exist in three states, according to the number of methylation group added - mono- (me1), di- (me2) or tri- (me3) methylation. Combination of the methylation state and the underlying residue specify different chromatin states. The catalytic activity of KMTs often reside in their SET domain (Rea *et al.* 2000).

H3K4me1 is an activating mark only found at enhancers, whereas tri-methylation of the same residue is specific to promoters (Heintzman *et al.* 2007). H3K36 and H3K79 methylation are found over gene bodies of active genes (Bannister *et al.* 2005; Wang *et al.* 2008). Methyltransferase

(EED), the suppressor of *zeste* (SUZ12) and the CAF1 histone-binding proteins RBBP4 and RBBP7 (Schuettengruber *et al.* 2017). The enzymatic activity is mediated by EZH1 or EZH2 (Cao *et al.* 2002). Identified for its role on body patterning by regulating *Hox* genes, polycomb proteins have now been implicated in many processes including X inactivation, genomic imprinting or cell cycle control. Furthermore, mis-regulation of polycomb was observed in many cancers, suggesting a broad range of gene regulation in many different cell types (Plath *et al.* 2003; Terranova *et al.* 2008; Hidalgo *et al.* 2012; Comet *et al.* 2016). Polycomb proteins have been linked to the maintenance of ES cell identity and depletion of PRC1 components leads to derepression of lineage-commitment genes (Endoh *et al.* 2008). Interestingly, in both flies and mammals, polycomb proteins display a spatial organization into small nuclear foci that stabilizes transcriptional silencing (Saurin *et al.* 1998; Grimaud *et al.* 2006; Terranova *et al.* 2008). At the level of the chromatin, polycomb proteins have been implicated in the regulation of local chromatin loops but also higher-order organization and chromatin compaction states (Vieux-rochas *et al.* 2015; Entrevan *et al.* 2016; Boyle *et al.* 2020). Specific targeting of EZH2 to a locus induced increased contacts with other H3K27me₃-rich domains, showing that the presence of polycomb can reorganize higher-order chromatin folding (Wijchers *et al.* 2016)

Histone 3 methylation of lysine 9 are associated with constitutive heterochromatin, whereas methylation of lysine 27 is associated with facultative heterochromatin and developmental processes. The two enzymes Prdm3 and prdm16 have been described as H3K9me₁ methylases (Pinheiro *et al.* 2012). H3K9me₂ is catalyzed by the G9a and G9a-like protein (GLP), whereas K9me₃ is performed by the Suv39H1 and 2 and SETDB1 (also named ESET) (**Figure 5A**). H3K9me₂ is a hallmark of chromatin lying at the nuclear periphery, whereas H3K9me₃ is a hallmark of pericentromeric and telomeric heterochromatin, regions that will be covered in chapter 2. Although Suv39H1/2 and SETDB1 have different preferences in genomic localization, they can act within the same complex, further illustrating the redundancy that can take place (Fritsch *et al.* 2010)

Many demethylases, named lysine demethylases (KDMs) have been identified, such as the jumonji-domain-containing (JMJD) family that notably removes H3K9me₃, or ubiquitously transcribed tetratricopeptide repeat, X chromosome (UTX) that mainly removes H3K27me₃ (**Figure 5A**) (Agger *et al.* 2007; Lee *et al.* 2007). Demethylases, like their methylase counterparts often carry specific affinity for a modified residue, although there is some level of redundancy between KDMs, such as lysine specific demethylase 1 (LSD1) which demethylates H3K4me₁ and me₂, but also H3K9me₁ and me₂ as well, suggesting more variability than previously imagined (Shi *et al.* 2004; Metzger *et al.* 2005).

Both methylases and demethylases carry essential roles, yet to date it seems that although they act redundantly, many of them show embryonic lethality at different times of development when depleted (**Figure 5B**). For example, deletion of Setdb1 results in very early embryonic lethality before the implantation stage, whereas deletion of MLL1 display organogenesis defects for myeloid and lymphoid lineages and lethality around 7 to 10 days after implantation (**Figure 5C**) (Jambhekar *et al.* 2019). Furthermore, overexpression of LSD1 is frequently observed in cancers, indicating that proper regulation of both methylation and demethylation processes are crucial for genome regulation (Kahl *et al.* 2006). Unlike acetylation, histone methylation does not *per se* impact chromatin compaction and its impact on chromatin state likely resides in the activity of specific ‘readers’.

The use of genome-wide analysis of ChIP experiments has allowed a deeper understanding of histone modification repartition throughout the genome. Histone methylation profiles show striking features with H3K4 or H3K27me being locally restricted to regulatory regions, whereas H3K36me goes over the Kbs length of gene bodies, and H3K9me spreads over Mbs domains. These assays performed in a large variety of conditions and cell-types has given a comprehensive resource to better understand the gene regulation mechanisms but also has helped apprehending the chromatin folding into chromatin states.

The many proteins identified in the methylation processes suggests both specific roles for each enzyme, but also redundant pathways that act to ensure robustness of the gene regulation programs. Histone methylation can be recognized by different proteins, notably via chromo-domain-containing proteins, giving rise to an additional layer of regulation. Finally, KMT activities are not limited to histones and many non-histone proteins can be post-translationally modified and then regulate gene regulation.

DNA methylation

Not only histones can have additional modification, but the DNA itself can be epigenetically marked, notably via the methylation. Methylation of 5th carbon of cytosine (5mC) is a well-known and characterized epigenetic modification of DNA. It has been deeply investigated in many cellular contexts. It is well conserved as it is found in the animal kingdom, in plants and some fungi, although it is not present in the baking yeast *Saccharomyces cerevisiae* and barely detectable in *Drosophila melanogaster* (Takayama *et al.* 2014).

Cytosine methylation is mainly restricted to CpG contexts. Interestingly, the genome is globally depleted for CpG sequences with about 28 million sites. Originally, CpG were described

at promoters where it was observed as 1 or 2 Kbs of methylation-rich sequences called CpG islands. CpG islands are often found unmethylated across all tissues. In fact, only about 10% of genomic CpG lie in promoters. For the majority of CpG sites scattered in the genome, 60 to 80% is methylated (Smith and Meissner 2013).

DNA methylation is established by different enzymes called DNA-methyl transferases (DNMTs) (**Figure 6A**). Highly conserved enzymes, three DNMTs exist in mammals, with an additional fourth enzyme specific to rodents. DNMT3A and DNMT3B are *de novo* enzymes that will catalyze the reaction onto an unmethylated DNA sequence. Unique to rodents, DNMT3C emerged via duplication of the DNMT3B gene and methylates promoters of young retrotransposons in male germ cells (Barau *et al.* 2016). DNMT2 enzyme carries no effect on DNA and its activity is instead limited to transfer RNA (tRNA) cytosines (Goll *et al.* 2006). DNMTs activities rely on the DNMT3L co-factor that stabilizes and facilitates DNMT3A activity (Chedin *et al.* 2002; Veland *et al.* 2018). DNA methylation is a very dynamic process. Indeed, once added during development, 5mC must be re-established at each mitosis, or it will be lost in a passive way. If there is no maintenance of the DNA methylation mark, it is diluted as an unmodified cytosine is incorporated in the newly synthesized strand. DNMT1 is a maintenance enzyme that, upon recognition of a hemi-methylated DNA fiber, will add a 5mC onto the complementary strand. DNMT1 is constitutively expressed, yet it undergoes an increased abundance at the entry of the S-phase to add the 5mC at each hemi-methylated CpG replicated (Kishikawa *et al.* 2003). DNMT1 is recruited to replication forks via interactions with proliferating cell nuclear antigen (PCNA) and ubiquitin-like containing PHD and RING finger domains 1 (UHRF1). UHRF1 binds to the parental methylated sites via its SET and RING associated (SRA) domain and recruits DNMT1 to methylated the newly synthesized DNA strand (Bostick *et al.* 2007; Arita *et al.* 2008; Avvakumov *et al.* 2008).

Furthermore, in order to provide gene regulation, DNA methylation must be erased at need. It is the role of the ten-eleven translocation (TET) family of enzymes, which have the capacity to convert 5-methylcytosine into 5-hydroxymethylcytosine (5hmC) (**Figure 6B**) (Tahiliani *et al.* 2009). It was observed that TET1 bind to CpG-rich promoters of active genes, yet downregulation of Tet1 alone does not lead to a downregulation of all its targets, indicating redundant functions via TET2 and TET3 enzymes (Wu *et al.* 2011). Interestingly, TET1 is also important for gene silencing as it recruits PRC2 at developmental gene promoters (Wu *et al.* 2011). TET proteins display differential tissue expression with TET1 being strongly expressed in embryonic stem cells. TET1 is essential for ESC maintenance *in vitro*, as TET1 depletion downregulates expression of the pluripotency factor Nanog (Ito *et al.* 2010). Mouse deficient for either TET1 or TET2 or both

are viable, yet the TET1/TET2 double KO displayed reduced 5hmC and increased 5mC patterns and presented postnatal abnormalities with notably some female infertility (Dawlaty *et al.* 2013). Deletion of Tet3 results in neonatal lethality (Gu *et al.* 2011). Recruitment of TET1 to promoters does not only rely onto 5mC as depletion of DNA methylation does not prevent its binding. With the expected possible dilution of DNA methylation in case there would be no maintenance, TET enzymes provide an additional and active mechanism of DNA demethylation. It is likely that these two mechanisms act redundantly to ensure efficient DNA demethylation and epigenetic erasure (Hackett *et al.* 2013b, 2013a). Recent studies suggested that TET enzymes have the ability to convert 5mC to 5hmC and then 5mC to 5-formylcytosine (5fC) and then to 5-carboxylcytosine (5caC), other cytosine derivatives (**Figure 6C**) (Ito *et al.* 2011).

The enzymatic activity of TET enzymes creates oxidation and can induce cytidine deaminase (AICDA)-mediated deamination (Cortellino *et al.* 2011). The uracil-guanidine and hydroxyuracil-guanidine produces a mismatch recognized by the thymine DNA glycosylase (TDG), a protein from the base-excision repair (BER) pathway. *In vivo*, TDG depletion leads to embryonic lethality, as it is required for active demethylation of lineage-specific promoters (Cortellino *et al.* 2011). TDG only removes 5fC and 5caC but not 5hmC and requires the DNA replication machinery (Maiti and Drohat 2011). The action of TDG creates abasic sites in the genome that are resolved through BER and restores an unmodified cytosine (**Figure 6C**). TET proteins can bind to any modified cytosine, yet it has higher affinity for 5mC and 5hmC (Hu *et al.* 2015). Hu *et al.* suggested that 5hmC is a relatively stable mark that could act as a regulatory modification. The action of TDG and subsequent BER can generate a single-strand break (SSB) via the action of the AP endonuclease 1 (APE-1). The SSB is restored by XRCC1 and the DNA ligase 3 (Weber *et al.* 2016). Yet, because CpG are present as a dyad in the genome, both cytosine can be differentially oxidized. The action of TET and TDG onto both strands can then lead to two SSB occurring at the same time, thus generating a double-strand break (DSB), although it seems to be a rare event, suggesting that active demethylation of the two strands occurs iteratively to avoid destabilization of the locus (Weber *et al.* 2016).

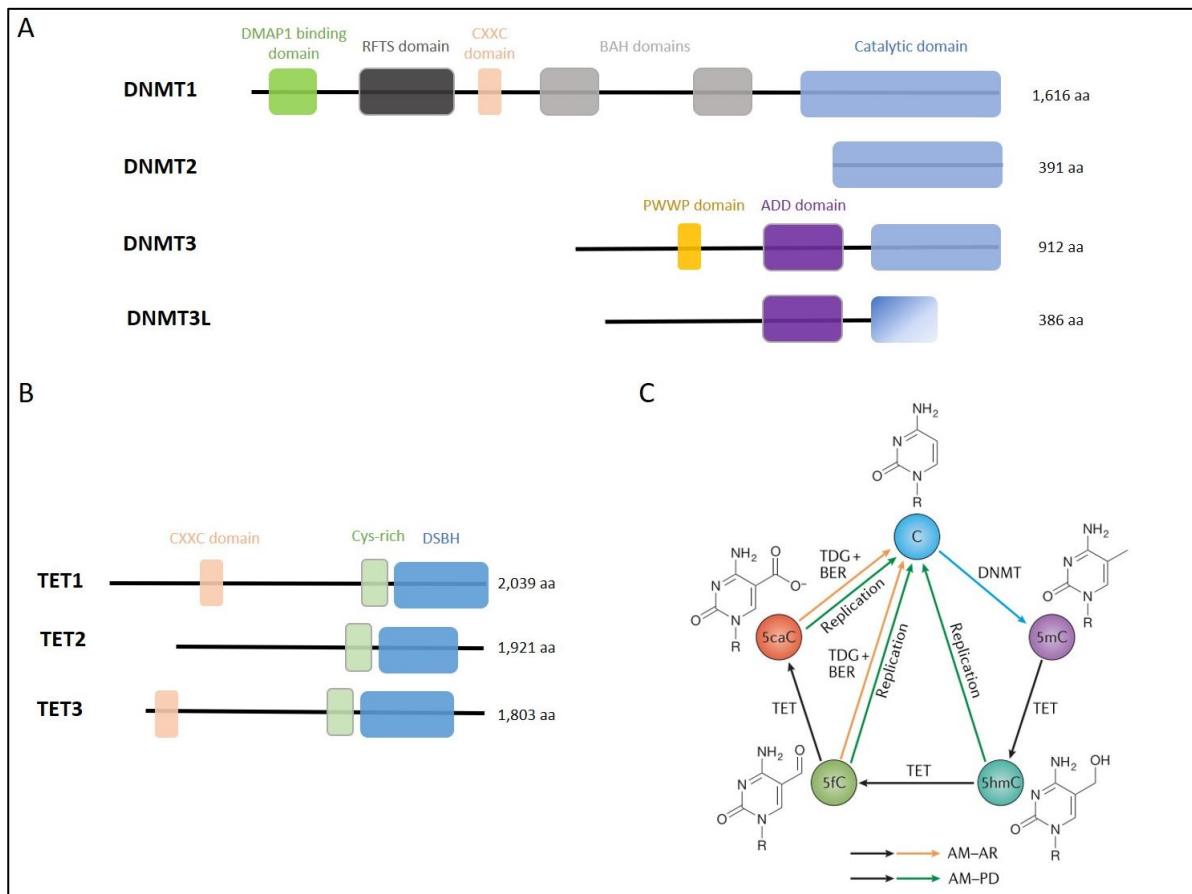


Figure 6 | DNA methylation machinery and mechanism. (A) Scheme of the four main DNMT proteins and their different peptidic domains. DNMT3 possesses two members A and B that are highly similar. **(B)** The three main TET enzymes with their corresponding protein motifs. **(C)** Life cycle of a methylated cytosine. A DNMT first adds a methyl-group onto the cytosine (5mC). A TET enzyme can then oxidize the 5mC into a hydroxy-methyl (5hmC). 5hmC can be lost passively through replication or further oxidized into a formyl-cytosine (5fC) or a carboxyl-cytosine (5caC). 5fC or 5caC modifications can ultimately generate double-strand breaks if not resolved via TDG. AM-AR = active modification-active removal, AM-PD = active modification-passive dilution, TDG = Thymine DNA glycosylase, BER = Base excision repair. C is from Wu and Zhang, *Nat. Rev. Gen.* 2018.

The presence or absence of a modification will induce the recruitment and action of different co-factors. CpG sequences not only recruit DNMTs when methylated to maintain its status but also numerous additional partners. Notably, the methyl-binding domain-containing family of enzymes (MBD) is heavily recruited to 5mC. A prominent member of the MDB family is the ubiquitously expressed MeCP2 protein, yet other proteins contain a MDB and can be differentially expressed (Wood *et al.* 2016). MecP2 functions as a transcriptional repressor, notably via the recruitment of the NCoR/SMRT co-repressor complex (Lyst *et al.* 2013). CHIP experiments revealed that MeCP2 binds to CpG across all the genome, suggesting that it acts mainly as a global repressor rather than in a promoter-specific manner (Skene *et al.* 2010). Indeed, MeCP2 deficiency results in global changes in genes and repeated elements transcriptional upregulation. Unmethylated CpG at promoters can be bound by CXXC finger protein 1 (CFP1) that recruits the H3K4 methyltransferase SETD1, which allows to maintain an open, unmethylated region

(Thomson *et al.* 2010). Interestingly, depletion of Cfp1 reduced the levels of H3K4me3 at CFP1-targeted promoters without affecting the transcriptional level, suggesting that it does not *per se* regulate transcription (Clouaire *et al.* 2012).

DNA methylation acts in close relationship with histone modifications. There is a strong genome-wide correlation between DNA methylation and H3K9me3 (Meissner *et al.* 2008). DNMT3A can bind to unmethylated H3K4 via its ADD domain and this binding abolishes HP1 tethering to methylated H3K9 (**Figure 6A**). But in other contexts, DNMTs can bind to HP1 or H3K9 methylases and be recruited to H3K9me3-rich regions, suggesting synergistic action of H3K9me3 and 5mC. Another example is the UHRF1 protein that can physically interact with methylated H3K9 and this interaction increases the stability of the UHRF1 complex, suggesting additional mechanisms of recruitment and stabilization of DNMT complexes depending of the chromatin state of the targeted locus (Rothbart *et al.* 2012). The H3K27me3-modification can be observed at CpG-rich promoters that are devoid of DNA methylation. Furthermore, PRC2 can interact with TET1, further demonstrating the antagonist relationship between H3K27me3 and 5mC (Gu *et al.* 2018). Thus, DNA methylation, together with H3K9me3 is a hallmark of constitutive heterochromatin.

The DNA methylation machinery is crucial for cellular processes. Depletion of UHRF1 is sufficient to induce a global loss of DNA methylation and associated phenotypes, including embryonic lethality (Sharif *et al.* 2007). Highly similar, DNMT3A and DNMT3B act in a redundant manner, yet they both display embryonic lethality and some tissue-specificities, suggesting specific functions (Li *et al.* 1992; Okano *et al.* 1999). Cells in culture are also dependent on their DNA methylation machineries as their depletion generally results in cell death, except for embryonic stem cells which have the capacity to overcome the loss of DNA methylation (Tsumura *et al.* 2006; Dodge *et al.* 2005; Jackson-Grusby *et al.* 2001). Murine embryonic fibroblasts (MEFs) deficient for DNMTs display high levels of chromosome instabilities and apoptosis, and require P53 mutation to partially overcome the loss of DNA methylation (Jackson-Grusby *et al.* 2001; Dodge *et al.* 2005). ESCs are thus a useful model to study epigenetic modifications.

One well-characterize disease associated with impaired DNA methylation machinery is the ICF syndrome (immunodeficiency, centromeric instability and facial anomalies), a rare autosomal disorder with about 50 cases described worldwide (Jefferson *et al.* 2010). These patients present a mutation into *Dnmt3b* gene that gives a hypofunctional enzyme, due to a point mutation in 20q11.2 genomic *Dnmt3b* region. These patients notably display immunological disorders, such as reduced number of T-cells, and lymphocytes also present a characteristic centromeric instability of three chromosomes - 1, 9 and 16 that show a typical loss of DNA methylation of their pericentromeric

satellite repeats of class II. These phenotypes also happen in an ICF mouse model with the same point mutation of *Dnmt3b* (Ueda *et al.* 2006). Interestingly, other mutated genes have since been discovered such as *ZBTB24*, *CDCA7* and *HELLS* (Velasco *et al.* 2018). Although these genes are not directly involved in the DNA methylation machinery, their mutation all lead to hypomethylation of pericentromeric satellites (Thijssen *et al.* 2015). Generation of a zebrafish model bearing a mutation in the *zbtb24* gene resulted in the phenotypes of ICF syndrome (Rajshekar *et al.* 2018). Rajshekar *et al.* further observe that the loss of DNA methylation at pericentromeric induces the increase of satellite repeats which ultimately triggers an interferon response.

Pathologies can arise with defects not directly linked to the DNA methylation proteins but to 5mC ‘readers’. Hemizygous mutations in the X-linked *MeCP2* gene inducing a loss of function is lethal for males and results in the Rett syndrome for females (Amir *et al.* 1999). Rett syndrome is a severe neurological disorder, suggesting a crucial role for DNA methylation and *MeCP2* in the brain, the tissue where it is the highly expressed. The majority of *MeCP2*-reported mutation affect its methyl-binding domain, suggesting that it is its role as 5mC binding protein that is essential (Tillotson and Bird 2020).

DNA methylation has been the focus of many studies as it is frequently altered in many cancers. Interestingly, cancer cells usually display altered DNA methylation profiles, with lower levels at some locations and higher elsewhere. It can result from mutation arising within genes of the DNA methylation pathway or within genes controlling the precise localization of 5mC deposition. Most of the studies have focused on the CpG islands of promoters. Indeed, the TET enzymes are often mutated, as in myeloid cancers in which *TET2* is mutated (Delhommeau *et al.* 2009). DNA methylation defects not only arise from mutations in the DNA methylation machinery but can be induced by hypoxia in solid cancers, indicating that multiple pathways can lead to altered epigenetic modifications (Thienpont *et al.* 2016). However, it is now proposed that DNA methylation profiles undergo many changes along the aging of any individuals. Altered DNA methylation might arise in healthy tissue and only favor tumorigenesis upon mutation of another gene (Klutstein *et al.* 2016). Furthermore, tumors often emerge as clonal cell population, and DNA methylation patterns can vary from one cell to the other within the same cancer, highlighting the essential role of this epigenetic modification (Brocks *et al.* 2014).

Variants of H2A

Many variants of H2A have been identified, and a lot of them are restricted to specific species or tissues. Five full-length variants have been identified in mammals - H2A.X, H2A.Z, macroH2A, H2A.Bbd and H2A.J (not represented in the figure) (**Figure 7**). I will only describe two of them - macroH2A and H2A.X, which are involved in heterochromatin and genome stability respectively.

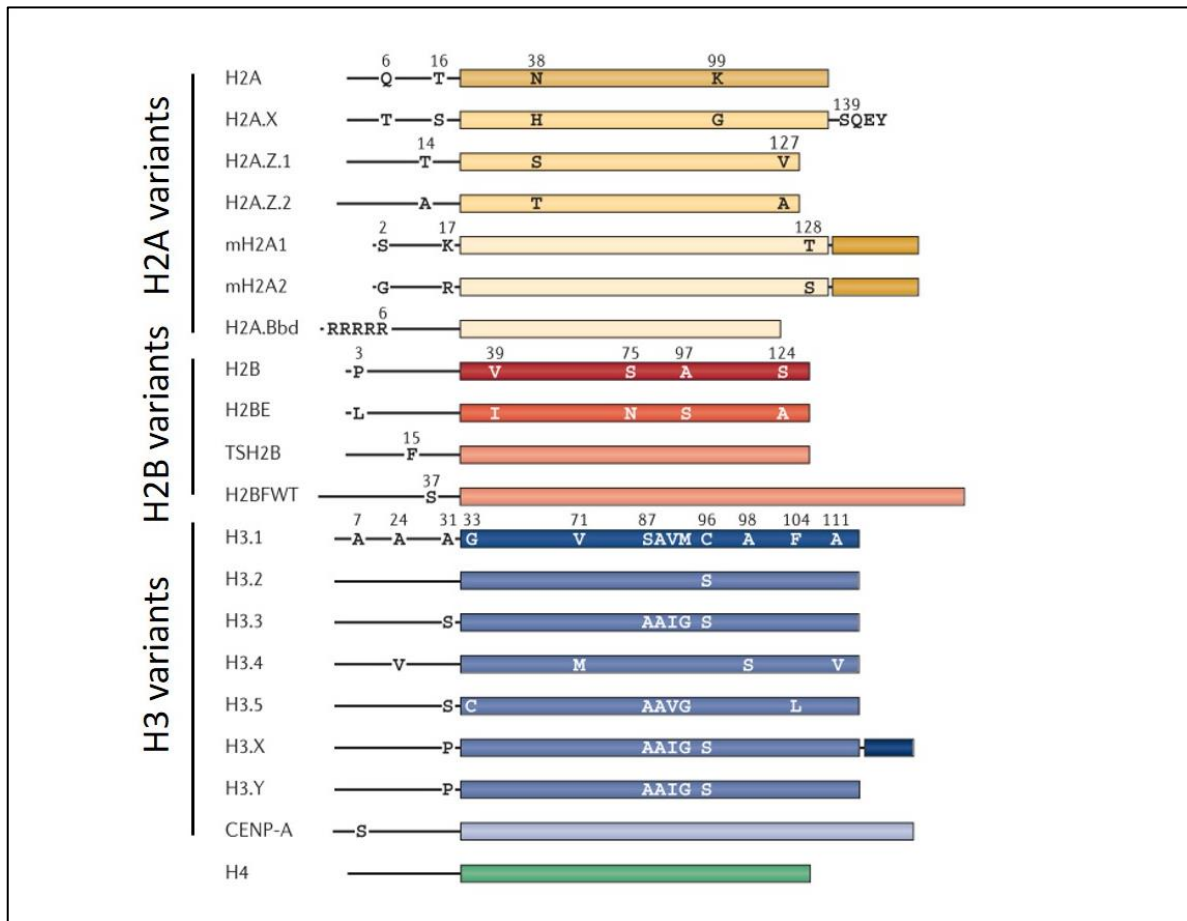


Figure 7 | Histone variants. Scheme of the various histone variants identified. They often differ by only a few mutations. Only histone H4 does not possess any identified variant. From Maze *et al.*, *Nat. Rev. Gen.* 2014

1. macroH2A

MacroH2A was first described in 1992 (Pehrson and Fried 1992). It is an unusual histone as it is composed of a tripartite structure where the N-terminal domain is linked to a non-histone macro domain through a lysine rich H1-like region. Thus, macroH2A is larger than its canonical counterpart as the macro domain itself is about 28kDa and originated from the highly conserved macro proteins. Two genes exist in mammals giving two macroH2A proteins 1 and 2 that can carry

different roles. MacroH2A is usually associated with repressed chromatin, notably onto the inactive X chromosome and during senescence when it localizes into senescence-associated heterochromatin foci (Zhang *et al.* 2005; Costanzi and Pehrson 1998). MacroH2A1 can associate with ATRX, which regulates its stability (Ratnakumar *et al.* 2012). Loss of Atrx increases macroH2A1 deposition at the α -globin gene and induces its silencing. Furthermore, recent reports suggest that macroH2A might important functions in chromatin organization. Indeed, macroH2A1 can associate with the nuclear lamina in interphase of mouse liver cells (Fu *et al.* 2015). Fu *et al.* further characterized the genome-wide localization of macroH2A and observed that it is enriched at the boundaries of lamina-associated domains, which I will define in a next section. While depletion of macroH2A does not impair LAMIN B distribution, it disrupted H3K9me3 localization. Another study indeed demonstrated that the loss of macroH2A disrupted H3K9me3 localization from heterochromatin and the compaction state of pericentromeric heterochromatin in embryonic stem cells (Douet *et al.* 2017).

However, recent studies have challenged this view as they point out that macroH2A might also be a positive regulator of transcription (Buschbeck *et al.* 2009; Gamble *et al.* 2010). Genome regulation via macroH2A can have important impact on cell identity as the depletion of macroH2A leads to the upregulation of the CDK8 colorectal oncogene and increased malignant phenotypes (Kapoor *et al.* 2010).

2. H2A.X

H2A.X is mostly known for its ability to be phosphorylated at the Serine in position 139 in human in response to DNA damages. In addition, H2A.X differs from H2A.1 by only four amino acids, that might give it specific nucleosomal properties, but this is currently not known. Interestingly, H2A.X is transcribed during S-phase the same way as canonical histones - its mRNA thus folds in a stem loop structure without polyA tails (Mannironi *et al.* 1989; Nagata *et al.* 1991). However, as a histone variant, it can be transcribed outside of S-phase that produces a longer mRNA that carries a polyA tail. Although some organisms, such as *Caenorhabditis elegans* and *Saccharomyces cerevisiae* does not possess a H2A.X variant, their respective H2A can be phosphorylated in response to DNA damage, indicating that the variant itself might not be necessary, yet the phosphorylation signaling is conserved throughout evolution. H2A.X represent from 2 to 25% of H2A in mammalian cells, depending on cellular types. Interestingly, H2A.X is not essential for mouse development, although mice displayed severe phenotypes such as growth retardation, immunodeficiency and male-specific infertility (Celeste *et al.* 2002). Celeste *et al.* described H2A.X deficiency results in increased levels of chromosomal instabilities due to impaired

recruitment of subsequent proteins of the DNA damage response pathway, implicating H2A.X as a crucial factor for DNA repair.

There are as many as 10^4 to 10^5 varied DNA lesions per day per mammalian cell due to both endogenous and exogenous sources (Hoeijmakers *et al.* 2009). Organisms have evolved and created several pathways known as the DNA-damage response (DDR) that allows them to repair their DNA. Among these are the homologous recombination (HR) which is mostly error-free and non-homologous end joining (NHEJ) which is more error-prone than HR (Heyer *et al.* 2010). After DNA lesions, specific kinases are activated and phosphorylates H2A.X on its Serine 139. γ -H2A.X signal fuses into nuclear foci in the minutes following DSBs (Rogakou *et al.* 1999). At the chromatin levels, γ -H2A.X signals spreads over distances that vary from species to species but is Mbs-long in mammals. It is estimated that $\sim 0.03\%$ of all H2A.X molecules are phosphorylated per double-strand break (DSB) (Kinner *et al.* 2008). Following DSBs, the ataxia telangiectasia mutated (ATM) kinase phosphorylates H2A.X in a process that requires nibrin 1 (NBS1) for optimum efficacy (Fernandez-Capetillo *et al.* 2002; Falck *et al.* 2005). γ -H2A.X accumulates around the site of the lesion in an asymmetrical manner and γ -H2A.X domains can extend up to 1.7Mb in human (Iacovoni *et al.* 2010). Deletion of both γ -H2A.X and ATM results in embryonic lethality (Zha *et al.* 2008). In response to other types of DNA damages, such as single-strand breaks resulting from replication stresses or UV damages, the other kinase ATR is active and can also phosphorylate H2A.X (Hanasoge and Ljungman 2007; Ward and Chen 2001). γ -H2A.X stands as a general signal for DNA lesions and occurs in both HR and NHEJ, rendering the H2A.X histone variant a crucial factor for genome stability.

Variants of H3

Different variants of histone H3 have emerged along evolution, although they do not present much genetic differences between them. About 8 variants have been described, yet only two are ubiquitously expressed, the other being transcribed in a tissue-specific manner. These two widely expressed H3 variants are H3.3 and CENP-A. I will briefly describe CENP-A and will then focus onto the H3.3 variant.

1. CENP-A, the centromeric H3

One peculiar chromosomal locus is the centromere. Indeed, it must be specifically recognized during mitosis to ensure faithful segregation of chromosomes.

Centromeric nucleosomes are enriched with the centromeric histone variant CENP-A (Centromeric protein A), which is only found there. Centromeric histone defines the centromeric identity more than the underlying sequence (Allshire and Karpen 2008). CENP-A is crucial for centromere identity and direct kinetochore assembly during mitosis (Müller and Almouzni 2014). The loss of Cenp-A results in the disorganization of the kinetochore (Goutte-Gattat *et al.* 2013). CENP-A is deposited by a specific chaperone, the Holliday junction recognition protein (HJURP) in a cell-cycle dependent manner (Dunleavy *et al.* 2009; Foltz *et al.* 2009). In telophase/early G1, HJURP binds to centromeric DNA and incorporates CENP-A. The timely control of HJURP depends on its phosphorylation (Müller *et al.* 2014). Crystal structure of CENP-A-containing chromatin was determined and described slight structural differences with H3-containing nucleosomes with notable differences in entrance and exit of DNA that display more flexibility (Tachiwana *et al.* 2011). The flexible ends of 13bp observed for CENP-A-containing nucleosome are essential for proper mitotic fidelity as it prevents H1 binding and compaction (Roulland *et al.* 2016). CENP-A nucleosomes are transmitted across S-phase in a HJURP-dependent manner, which in addition with newly synthesized CENP-A during G1-phase enables a stable inheritance of centromere identity (Zasadzińska *et al.* 2018).

CENP-A can be overexpressed in different cancers. Its expression correlates with malignant progression and could be used a predictive biomarker for breast cancers (Sun *et al.* 2016). In colon cancer, CENP-A is upregulated and assembled ectopically via the DAXX and HIRA chaperones (Nye *et al.* 2018). This ectopic formation of CENP-A nucleosomes can recruit kinetochore components at multiples localization and enhance the genomic instability and levels of DNA damages.

2. The H3.3 histone variant

H3.3 variant is encoded by two genes which are *H3 β a* and *H3 β b* in mouse and humans. The two proteins are identical, yet the two genes possess different untranslated regions (Krimer *et al.* 1993). H3.3 has only 4 to 5 amino acids different from canonicals H3.1 and H3.2, with only one amino acid change in the N-terminal tail and the other belonging to the globular histone core (**Figure 8A**). H3.3 is one of the most conserved protein among eukaryote, suggesting crucial roles for the cell. The two genes are expressed differentially depending on the cell type (Jang *et al.* 2015). H3.3 incorporation modify the structural properties of the chromatin. In the early embryonic development, H3.3 maintains a decondensed chromatin state and prevents genome instabilities (Jang *et al.* 2015; Lin *et al.* 2013). In vitro, H3.3 was observed to change the folding of chromatin arrays, inducing a more open conformation with increased spacing between nucleosomes (**Figure**

8B)(Chen *et al.* 2013). Chromatin condensation observed in H3.3 knock down correlates with higher levels of linker histone H1, but does not induce large transcriptional changes (Lin *et al.* 2013). Indeed, at the chromatin levels H3.3 is generally anti-correlated with the presence of the linker histone H1 (Braunschweig *et al.* 2009).

H3.3 was firstly observed at euchromatin enriched for active marks such as H3K4me2 and high PolIII occupancy in *Drosophila* and latter in mammals (Ahmad and Henikoff 2002; Mito *et al.* 2005; Jin *et al.* 2009; Goldberg *et al.* 2010). H3.3 is mainly observed enriched all along gene bodies, with peaks of occupancy at the promoter, yet preceded by a dip at the transcription start site, and the replacement rate of H3.3 is proportional to PolIII densities, suggesting that H3.3 is incorporated during transcription to compensate the loss of H3.1 during the progression of the PolIII (Mito *et al.* 2005). When looking at specific inducible genes such as *Ifit1*, Tamura *et al.* had showed that upon interferon treatment, *Ifit1* is transcribed and H3.3 occupancy increases, yet H3.3 stays enriched long after the transcription ceased demonstrating that H3.3 enrichment at gene bodies is not merely the result of the elongation process (Tamura *et al.* 2009). Interestingly, finer characterization of H3.3 occupancy revealed that it is not only enriched at genes and promoters, but also to regulatory elements, and unexpectedly to heterochromatin regions such as telomeres, indicating previously unappreciated roles for this H3 variant (Goldberg *et al.* 2010). Assessment of the dynamic of H3.3 incorporation revealed different turnover rates along the genome (**Figure 8C**). Promoters and enhancers presented a fast H3.3 turnover rate, whereas gene bodies and transcription end sites displayed a lower turnover rate (Ha *et al.* 2014; Kraushaar *et al.* 2013; Deaton *et al.* 2016).

Interestingly, in euchromatin regions, H3.3 is enriched at nucleosome-free regions, notably the +1 nucleosome at the promoter, possibly creating a high nucleosome turnover at this position, thus enhancing the accessibility for additional transcriptional factors (Jin *et al.* 2009). This nucleosomal instability comes from the presence of both H3.3 and H2A.Z in the same nucleosome (Yukawa *et al.* 2014). Furthermore, the gap created by nucleosome eviction at sites of transcription are filled by H3.3, as observed for the inducible *Hsp70* gene in *Drosophila* (Schneiderman *et al.* 2012). Many genes retain a memory of their transcriptional state. It was demonstrated using nuclear-transplant embryos that the *MyoD* muscle-lineage gene could keep a transcriptional state for 24 cell divisions without the proper network of transcription factors. Defined as a memory, the transcriptional state of *MyoD* was shown to be dependent on the lysine 4 of H3.3, pointing to a possible role for H3.3 in epigenetic marking of specific promoters in the genome (Ng and Gurdon 2008). It was observed that non-nucleosomal histones are post-translationally modified before incorporation into chromatin, and that could impact on the later modifications of histones, indicating another layer of regulation by histone variants (Loyola *et al.* 2006).

In embryonic stem cells, H3.3 carry additional roles that are lost during cellular differentiation. First observations that H3.3 was present at heterochromatin regions came during cell-cycle observations of the H3.3-specific phosphorylation of serine 31 that displayed a pericentromeric localization during metaphase (Hake *et al.* 2005). Although observed at heterochromatin loci in somatic cells, H3.3 is particularly important for heterochromatin in ESCs. It is observed enriched at different DNA tandem repeats such as telomeres and transposable elements (Goldberg *et al.* 2010). The presence of H3.3 is crucial for the proper silencing of these regions. Indeed, loss of H3.3 enrichment at telomeres is associated with a decrease in H3K9me3 signal and subsequent telomere integrity (Ivanauskiene *et al.* 2014; Udugama *et al.* 2015). H3.3 occupancy at endogenous retroviruses (ERVs) was also demonstrated to be crucial for their transcriptional repression and associated H3K9me3 enrichment (Elsässer *et al.* 2015). Interestingly, heterochromatic H3.3 possess a low turnover rate, except at satellite sequences where it has a high dissociation rate, yet dependent on the replication machinery (Ha *et al.* 2014).

H3.3 is essential for mouse development. Mice lacking only one *H3f3a* or *b* gene is viable but generates fertile individuals. Depletion of both genes results in early embryonic lethality at the implantation stage (Jang *et al.* 2015). In agreement with the genetic experiments performed by Jang *et al.*, the knock-down of one or both H3.3 genes by zygotic microinjection led to the same conclusions (Lin *et al.* 2013). Impossibility to reach the blastocyst stage has been proposed to rely on the lysine 27 residue of H3.3 (Santenard *et al.* 2010). Moreover, H3.3 is essential for proper gametogenesis (Tang *et al.* 2015). Even embryonic stem cells, which have a particular chromatin state, that I will develop in the last part of the introduction, and cannot survive more than a few divisions without H3.3 because of increased genome instabilities, thus resembling to heterochromatin-related defects (**Figure 8D**) (Jang *et al.* 2015).

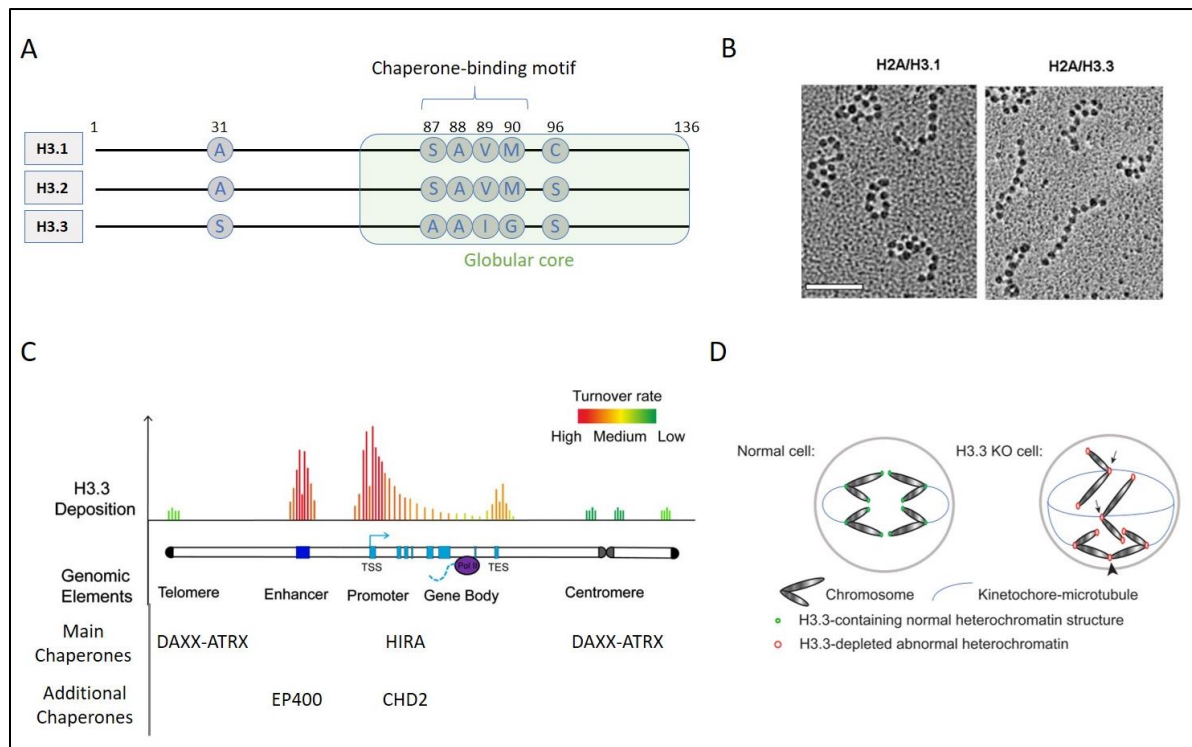
H3.3-associated chaperones

This ‘double face’ of the histone variant H3.3 arise from two main deposition pathways (Szenker *et al.* 2011). In euchromatin, H3.3 is deposited via the histone regulator A (HIRA) complex (Ray-gallet *et al.* 2002). HIRA is in a complex with two other proteins - calcineurin binding protein 1 (CABIN1) and ubinuclein (UBN). H3.3/H4 dimers bind to the HRD domain of UBN1 (Ricketts *et al.* 2015). H3.3 is deposited at heterochromatin sites by the death-domain associated protein (DAXX) and alpha-thalassemia/mental retardation syndrome X-linked protein (ATRAX) complex,

that I will describe in the next sub-section (Drané *et al.* 2010). Apart from these main identified deposition pathways, other chaperone can bind and incorporate H3.3 within the chromatin (**Figure 8C**). In euchromatin regions, H3.3 often co-localizes with the histone variant H2A.Z at ‘nucleosome-free’ regions of regulatory elements (Jin *et al.* 2009). In human cells, it was observed that the E1A binding protein p400 (EP400) that is part of the pre-initiation complex and a known chaperone of H2A.Z could, together with H2A.Z, incorporate H3.3 at promoter and enhancer regions (Pradhan *et al.* 2016). Pradhan *et al.* demonstrated that the presence of both H2A.Z and H3.3 enhanced transcription *in vitro*. H3.3 was implicated in the myogenic differentiation in mouse. Skeletal muscle differentiation relies on the action of the master regulator MyoD, a transcription factor that activate myogenic-lineage genes to induce differentiation. Harada *et al.* reported that the chromodomain helicase DNA-binding domain 2 (CHD2) binds to both MyoD and H3.3 during myogenic differentiation. CHD2 incorporates H3.3 at MyoD targeted promoters prior to differentiation, suggesting that H3.3 serves as a poised mechanism for subsequent activation (Harada *et al.* 2012). Deletion of Chd2 in this context does not impair H3.3 deposition at housekeeping transcribed genes. The related chromatin remodeling factor CHD1 was also interacting with HIRA and regulating H3.3 deposition in *Drosophila* embryos (Konev *et al.* 2007). In humans, both CHD1 and CHD2 can modulate transcription-coupled deposition of H3.3 (Siggens *et al.* 2015). These results indicate that although two main H3.3 deposition pathways exist in all cell types; alternative chaperones might have emerged for specialized functions in different tissues or time of life.

In line with the idea of specialized roles of H3.3 according to specific cell types, additional roles for H3.3 were described in murine ESCs. Some developmental genes are silenced by the polycomb repressive complex 2 (PRC2) and the recruitment of PRC2 is facilitated by H3.3 deposition at these promoters (Banaszynski *et al.* 2013). Indeed, deletion of H3.3 impaired PRC2 presence and ESCs presented difficulties to differentiate, highlighting the crucial role played by H3.3 in pluripotent cells. Interestingly, H3.3-rich PRC2 loci display a low histone turnover rate (Deaton *et al.* 2016). During the early embryonic development, in the zygote, methylation of the lysine 27 of H3.3, achieved by polycomb, is essential for developmental progression, strengthening

the connection between polycomb regulation and H3.3 (Santenard *et al.* 2013).



Many factors have been identified interacting with H3.3-containing complexes. In

Figure 8 | Histone variant H3.3 structure and function. **(A)** Scheme of the H3.3 protein compared to the two canonical H3.1 and H3.2 histones. Highlighted are the 4 to 5 amino acid changes of H3.3 that are mainly observed within the globular core. **(B)** Nucleosomal chromatin fiber reconstituted in vitro carrying either H3.1 or H3.3-nucleosomes. Presence of H3.3 is associated with a decondensed structure of the chromatin. **(C)** Scheme of the turnover rate of H3.3 at its enriched positions along the chromosome. Above are indicated the preferential and additional chaperones described for H3.3 that are locus-specific. **(D)** Scheme of the role of H3.3 in embryonic stem cells. Lack of H3.3 induces defects in chromosome segregation during mitosis. B is from Chen *et al.*, *N.A.R.* 2013. C is adapted from Huang and Zhu, *Bioessays* 2014. D is from Jang *et al.*, *Genes & Dev.* 2015.

Drosophila and human cell lines, the oncogene DEK was proposed to act as a H3.3-chaperone (Sawatsubashi *et al.* 2010). Interestingly, the RPA complex was found in a shRNA screen as a partner of HIRA-H3.3 complexes (Zhang *et al.* 2017). Replication protein A (RPA) is a single-strand DNA binding protein implicated in DNA replication and DNA repair. In human cells, it was demonstrated that RPA regulated transcriptional directionality at gene promoters. RPA enabled HIRA-mediated H3.3 deposition at regulatory elements, and its deletion impaired transcription (Zhang *et al.* 2017). Although implicated in DNA replication, a well-studied role of RPA lies during the repair of DNA damages. Because of its capacity to be transcribed during the whole cell cycle, H3.3 was thought to be important for DNA repair mechanisms to reconstitute the chromatin. In human cells, UV exposure generates DNA damages that induce the recruitment of HIRA. HIRA deposits newly synthesized H3.3 histones at the lesion site and that primes the locus for later transcriptional reactivation (Adam *et al.* 2013). In chicken DT40 cells, H3.3 was also identified to be crucial for UV-damage recovery, notably to complete DNA replication (Frey *et al.*

2014). Depletion of H3.3 renders the cell more sensitive to UV damages, suggesting a broad effect of this variant on both replication fork progression and DNA repair mechanisms. Luijsterburg *et al.* proposed that one role of H3.3 at sites of DNA damage could be chromatin expansion. Indeed, the authors observed that CHD2 is recruited at DNA breaks and includes chromatin expansion and H3.3 deposition (Luijsterburg *et al.* 2016). The presence of H3.3 is not merely for chromatin reconstitution as it can impact later steps of NHEJ (non-homologous end joining) repair.

C - The DAXX-complex chaperone

DAXX is a very interesting protein. Historically described as a pro-apoptotic protein, Daxx is a 120KDa protein encoded on the chromosome 17 in mouse. It has diverse been reported to act on diverse cellular pathways. Indeed, DAXX is a multi-task protein that has been identified as an interactor of many proteins in proteomic screens (Yang *et al.* 1997). Yang *et al.* showed that DAXX induced apoptosis response when overexpression with the intracellular domain of FAS. Furthermore, DAXX could activate the JNK kinase ASK1 (also called Map3K5) via direct interaction, then leading to an apoptosis response (**Figure 9A**)(Chang *et al.* 1998). However, opposite results suggested that DAXX might also repress apoptosis (Meinecke *et al.* 2007).

DAXX interacts with the tumor-suppressor protein P53 upon overexpression (Gostissa *et al.* 2004). P53 is a key signaling protein implicated in the cellular response upon DNA damages or oncogene-activation and leads to cell-cycle arrest, apoptosis or senescence. P53 is a short-lived protein and its stability is controlled by other proteins such as the mouse double minute 2 (MDM2) protein. DAXX notably controls the stability of MDM2 via direct interaction. Upon DNA damages, DAXX dissociates from MDM2, which induces its auto-degradation and allows P53 signaling (Tang *et al.* 2006; Zhao *et al.* 2004).

DAXX-regulation of apoptosis signaling may happen via other protein interactions. Indeed, DAXX have been implicated in the regulation of the phosphate and tensin homolog (PTEN) tumor-suppressor protein via PTEN deubiquitylation (Song *et al.* 2008). In glioblastoma, a study reported that PTEN bind to DAXX and could regulate H3.3 deposition (Benitez *et al.* 2017). In the common PTEN deficient glioblastoma, depletion of DAXX presented a synthetic growth defect phenotype.

The first hint that Daxx was indeed interacting with histone proteins was that it could interact with the centromeric CENP-C during interphase (Pluta *et al.* 1998). In 2010, Drané *et al.* purified the human H3.3 histone variant from human HeLa cells and performed mass spectrometry experiments to isolate interactant of H3.3. They observed that DAXX and ATRX interacted with H3.3 and regulated its heterochromatin deposition (Drané *et al.* 2010). H3.3 binding to DAXX is due to the recognition of H3.3 glycine 90 residue and DAXX glutamine 225 residue in human (**Figure 9B**). DAXX then wraps 40% of the accessible surface of the dimer H3.3/H4, highlighting how a single amino acid substitution in histone can have a crucial impact (Elsässer *et al.* 2012; Lewis *et al.* 2010).

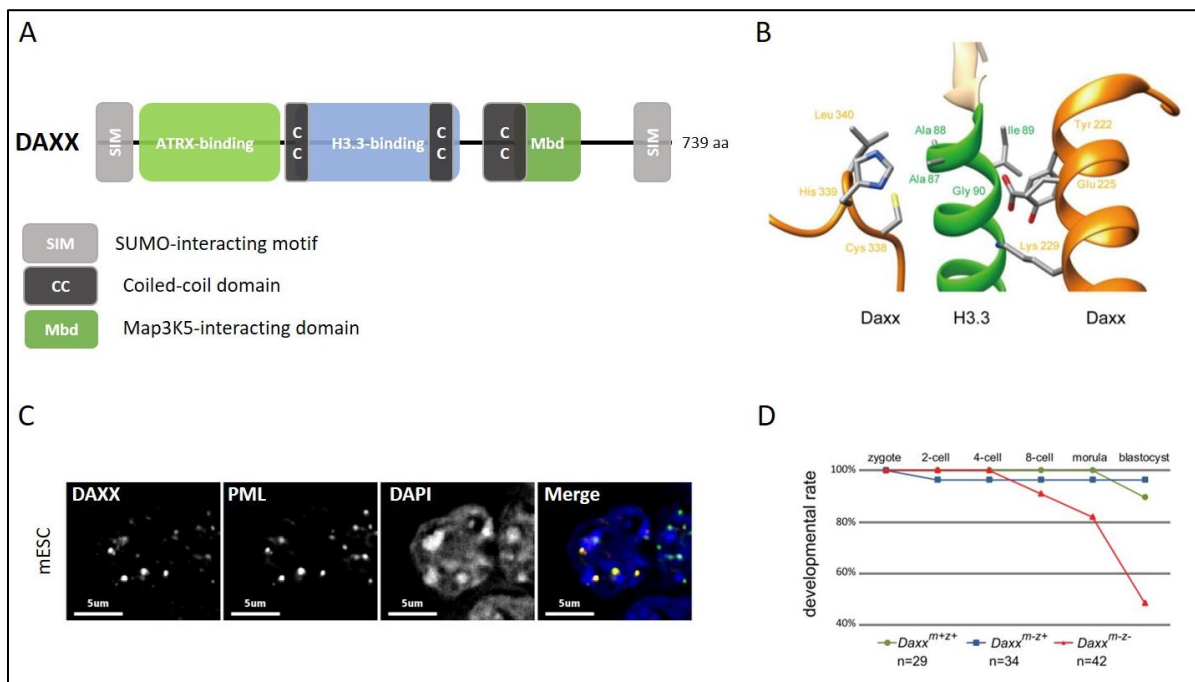


Figure 9 | The H3.3-chaperone DAXX, structure, localization and function. (A) Scheme of DAXX protein and its different domains. (B) Structures of DAXX and H3.3 showing their interaction domain, mediated by the specific amino acid H3.3G90 and DAXXY222 and G225. (C) DAXX localizes within PML nuclear bodies in murine embryonic stem cells. (D) Daxx-deficient embryo die before the implantation stage and the majority does not reach the blastocyst stage. B is from Huang and Zhu, *Bioessays* 2014. C is from personal unpublished data. D is from Liu *et al.*, *EMBO J.* 2020.

DAXX localizes at PML nuclear bodies (NBs) within the nucleus (**Figure 9C**). Its localization and activities are regulated by post-translational modifications such as SUMOylation. Small-ubiquitin like modifier (SUMO) are small peptides that can bind to proteins to modify its function and stability. DAXX contains two sumo-interacting motifs (SIM), at the C and N-termini, but the most important one is the N-terminal SIM which controls its interaction with PML. I will deeply describe the DAXX-PML interaction in the PML part of this introduction. However, C-

terminal SIM seems implicated in other functions such as the regulation of transcription factors' interactions (Escobar-Cabrera *et al.* 2011).

Intriguingly, Daxx *-/-* mice die at an early embryo stage, E9.5, and present high levels of apoptosis markers (Michaelson *et al.* 1999). A recent paper confirmed the essential role of Daxx and presented a more detailed picture where Daxx-deficient embryo die even before gastrulation at the morula or blastocyst stage, suggesting an essential role in first stages of development (**Figure 9D**) (Liu *et al.* 2020). At the zygote and 2-cell stage, DAXX and H3.3 are recruited to pericentromeric heterochromatin in a DPPA3-dependent manner (Arakawa *et al.* 2015). Moreover, deletion of *Dppa3* impaired Daxx and pericentromeric satellites expressions, and ectopic expression of DAXX restored H3.3 deposition and pericentromeric expression.

Because H3.3 can be incorporated during all the cell cycle and not only during S-phase, post-mitotic tissues like accumulate H3.3, and this effect increases along the life (Piazzesi *et al.* 2016; Maze *et al.* 2015; Tvardovskiy *et al.* 2017). In post-mitotic neurons, DAXX is phosphorylated in response a calcium-dependent signaling, and in turn incorporates H3.3 at regulatory regions (Michod *et al.* 2015). Furthermore, H3.3-specific and DAXX or ATRX driver mutations were observed in pediatric glioblastoma, indicating heterochromatin-associated H3.3 is crucial even in somatic tissues (Schwartzentruber *et al.* 2012; Wu *et al.* 2012). The observed mutations for H3.3 were the K27M and G34R/V. Furthermore, H3.3 might physiologically be impacted in finer phenotypes, particularly in the brain where its transcription and incorporation is increases in human and mouse suffering from depression (Lepack *et al.* 2016). H3.3 plays a critical role in the nucleus accumbens that regulates the reward circuitry and mood. Blocking H3.3 activity was performed by antidepressants therapeutics and released the depressive disorder. DAXX-mediated H3.3 deposition is implicated in the neuronal activation of a particular set of genes and loss of Daxx impairs their transcriptional induction (Michod *et al.* 2012). The histone variant H3.3 and its chaperone DAXX are of particular importance as they carry multiple roles, during embryonic development, but also in somatic cells.

Together, these results indicate that H3.3 is implicated in a wide diversity of processes. At heterochromatin regions, H3.3 is deposited via the DAXX-ATRAX complex. However, DAXX itself may carry additional ATRAX and H3.3-independent roles as observed for ERV regulation, showing another layer of complexity (Hoelper *et al.* 2017).

II - Spatial compartmentalization of the nuclear space.

Genome activity is regulated at different levels. At the chromatin state, epigenetic modifications such as histone post-translational modifications or DNA methylation, can modify the compaction state of the chromatin and thus regulates binding of transcription factors. Furthermore, it has recently emerged that the chromatin is not randomly positioned within the nucleus and its three-dimensional organization acts as an important regulator for all chromatin processes, from transcription to DNA repair and replication (Bickmore and Van Steensel 2013).

In mammalian genomes, only about 2% of the genome encodes form proteins. Thus, the vast majority of the genome was qualified as “junk DNA” (Ohno 1972). It was observed that an important part of this non-coding genome overlapped with previous microscopic descriptions of heterochromatin. Recently, NGS techniques have enabled a more comprehensive view of these genomic regions. An important amount of evidence has emerged to suggest that heterochromatin subcompartments serve as nuclear landmarks for spatial chromatin organization and genome regulation.

I will firstly describe the 3D organization of chromatin within the nucleus. I will then define the two major spatial landmarks of heterochromatin - the lamina-associated domains located at the nuclear periphery, and the chromocenters within the center. Another smaller heterochromatin feature consists of the telomeric regions. Lastly, spreading between spatial heterochromatin landmarks and euchromatin, the transposable elements are part of the heterochromatin components that compose half of the genome but are scattered and do not assemble into a unique compartment (**Figure 10**). I will present each of these four heterochromatin features with the associated network of proteins that regulate them.

A - Three-dimensional folding and radial positioning of chromatin

This higher-order organization of chromatin was observed at first using microscopy-based techniques. In 1928, using DNA-staining dyes, Emil Heitz coined the term “heterochromatin” as he noticed that some regions of the chromosomes were densely-stained. He went even further in this characterization as he could specify that some regions are always densely-stained, whereas other

are only heterochromatic in some cells (Passarge 1979; Allshire and Madhani 2017).

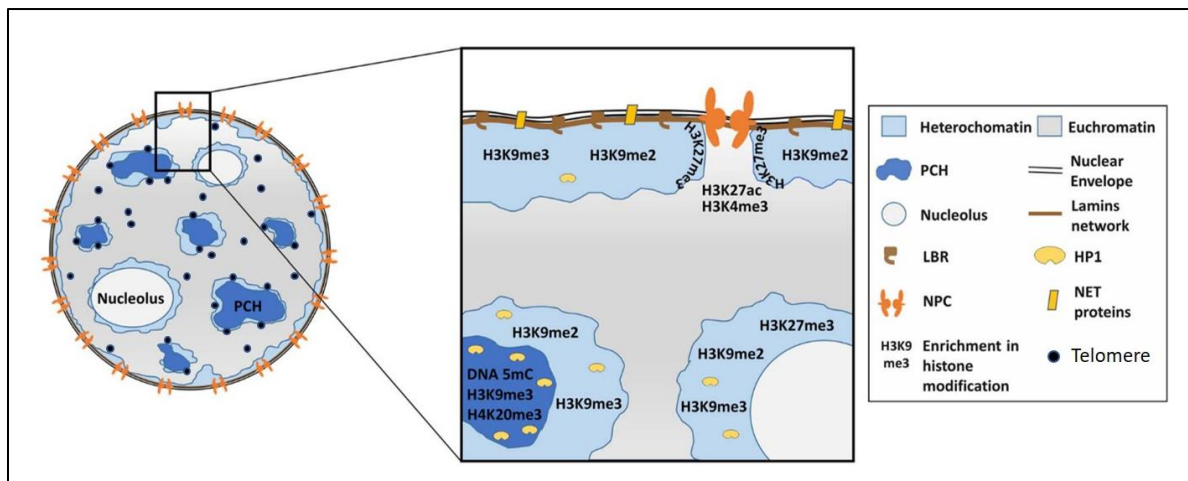


Figure 10 | Spatial compartmentalization of the nuclear space. Scheme of a mammalian nucleus. Different landmarks define nuclear heterochromatin sub-compartments. The nucleus is defined by a nuclear envelope segregating the nucleus from the cytoplasm. The nuclear lamina is only interrupted by the nuclear pore complexes. Heterochromatin regions lie at the nuclear periphery. PCH clusters into large foci serving as anchors for heterochromatin regions. Half of telomeres are located close to the PCH foci because of the acrocentric structure of murine chromosomes, the other half is randomly distributed within the nuclear space. The nucleolus serves as anchoring landmark for heterochromatin regions. All heterochromatin-associated landmarks are enriched for specific histone modifications such as H3K9me2 and H3K9me3. PCH = pericentromeric heterochromatin, HP1 = heterochromatin protein 1, NPC = nuclear pore complexes, LBR = lamin B receptor. Adapted from Canat *et al.*, *Brief. Funct. Genomics* 2020.

The idea that chromosomes must have delimited spaces in the nucleus was proposed early on by Carl Rabl and later developed by Theodor Boveri, whom worked on horse worms and coined the term of chromosome territory (CT) (Boveri 1909). Yet, EM studies have diminished this theory as it only reported an intermingling of chromatin in interphase nuclei. In the 1990's and 2000's, researchers have studied the organization of the genome into CTs using hybridization techniques. These advances were mainly due to the development of chromosome-specific probes that could be used in FISH experiments. Once probes were designed for specific chromosomes, it enabled the visualization of the different CTs coexisting in cells (Bolzer *et al.* 1999). CTs were observed to exist for each human chromosome in lymphoid cells (Boyle *et al.* 2001; Bolzer *et al.* 2005). Interestingly, this organization is conserved in primates and in mice, suggesting a putative functional role) (Tanabe *et al.* 2002).

The CT organization reflects that each chromosome segregates in the nuclear volume. Further studies have examined the radial organization of the genome - how the chromosomes positioned themselves in accordance to nuclear lamina. At chromosomal scale, it was observed that radial positioning was regulated by the gene-content, the higher the gene-density the more central the chromosome appears. Yet, even for one chromosome, finer-scale observations revealed a general rule for which gene-dense regions tend to more centrally located (**Figure 11**). This

localization is sought to be dependent on the transcription activity (Bickmore and van Steensel 2013).

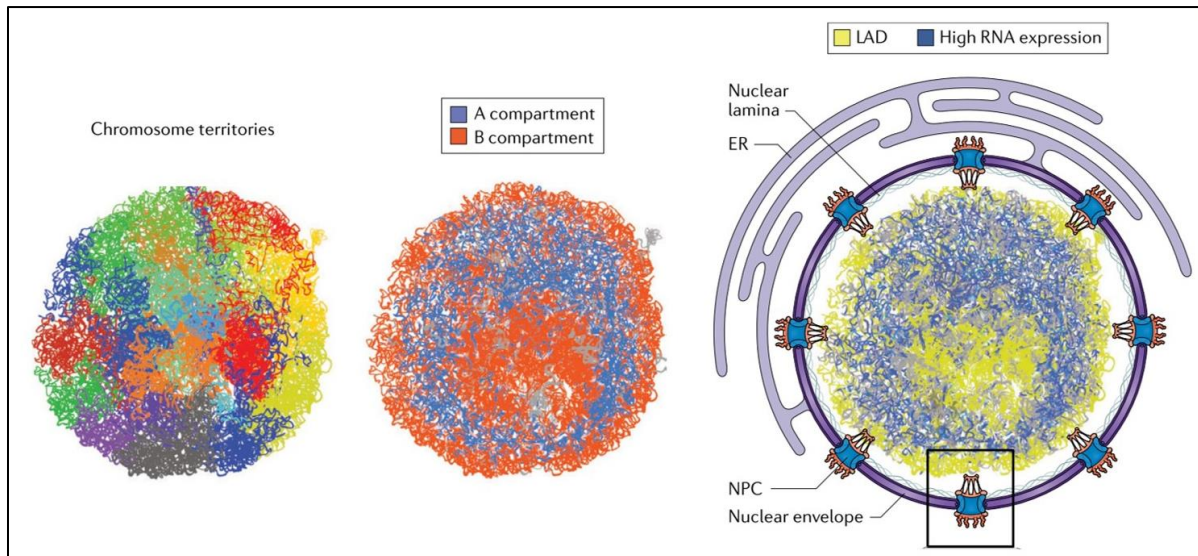


Figure 11 | Localizations of chromosomes within the nuclear space. On the left is a modeling of the chromosome territories observed in a mammalian nucleus. Each color represents a particular chromosome. In the middle is a modeling of the A and B chromatin compartment with the A compartment in blue encompassing open and transcribed regions and lies mostly within the nuclear interior. In red is the B compartment that corresponds to closed and inactive regions of the genome that lies notably at the nuclear periphery but also in the nuclear interior where it can associate to nuclear landmarks such as PCH. On the right is a modelling of the genome based on LAD status. LADs are displayed in yellow and are, by definition, mostly enriched at the nuclear periphery, although a substantial fraction of LADs are found within the nuclear interior, probably associated with pericentromeric clusters, illustrating the high overlap between heterochromatin compartments. Non-LAD regions are mostly gene-rich domains that are highly transcribed and represented in blue and mostly observed around the center of the nuclear space. LAD = lamina-associated domains. From Buchwalter, Kaneshiro and Hetzer, *Nat. Rev. Genetics* 2019.

The study led by Lieberman-Aiden *et al.* showed that the genome could be organized as fractal globules, yet the HiC realized was only 1Mb-resolution scale. In 2012, three groups co-discovered, using high-resolution HiC that each chromosome was organized into topologically-associated domains (TADs). Organization into TADs was observed in mammalian cells (Nora *et al.* 2012; Dixon *et al.* 2012), as well as in drosophila at the same time (Sexton *et al.* 2012). TADs are Mb-domains partitioning of the mammalian genomes, and of about 100kb-size in *Drosophila*. They are defined as the intra-TAD contacts are much higher than the inter-TAD contacts. The overall TAD-organization of chromosomes is mostly invariant between cell types, although a number of TAD boundaries appear to be cell-type specific (Dixon *et al.* 2012). TADs correspond to the basal topological organization of the genome and it correlates with other genomic features, such as the DNA replication domain (Pope *et al.* 2014). TADs were firstly described in cell population. The use of single-cell HiC techniques provided a more comprehensive picture (Nagano *et al.* 2013). Nagano *et al.* observed that whereas intra-chromosomal domains were conserved, inter-chromosomal domains were not and displayed a high cell-to-cell variability. This study reinforced

the chromosomal territory organization and noted that only active regions of the chromosome tended to localize at the territory's boundaries.

Altogether, these studies reveal a complex spatial organization at multiple scales. Chromosomes tend to segregate into specific territories and chromatin regions displaying the same state have increased contacts. In addition to chromosome-specific organization, inter-chromosome interactions arise from spatial compartmentalization of the genome.

B - Lamina-Associated Domains

The major heterochromatin subnuclear compartment correspond to the periphery of the nuclear space. Genomic regions that localize close to the nuclear envelope are called lamina-associated domains (**Figure 11**).

1. Nuclear envelope and definition of the lamina-associated domains

The periphery of the nucleus is defined by the nuclear envelope. The nuclear envelope is a double membrane barrier with one side, the inner nuclear envelope, facing the nuclear space and the other, the outer nuclear envelope, facing the cytoplasm. The outer nuclear membrane is contiguous with the endoplasmic reticulum, indicating a strong interconnection between nuclear and cytoplasmic events. Yet, the inner and outer nuclear envelopes have different protein networks and regulation. The nuclear envelope is underlined by the nuclear lamina, a filamentous meshwork composed of lamin proteins. The nuclear lamina and the inner nuclear envelope are highly interacting networks. Four lamin proteins have been described - A, B1, B2 and C. Lamins A and C are derived from an alternative splicing event of the same gene unit, whereas lamins B1 and B2 comes from two separate genes (Fisher *et al.* 1986; Mckeeon *et al.* 1986; Weber *et al.* 1990). Lamins B1 and B2 are ubiquitous, whereas expression of LAMINA/C is tissue-specific (Eckersley-maslin *et al.* 2013; Röber *et al.* 1989; Constantinescu *et al.* 2006; Solovei *et al.* 2011). Other transmembrane-proteins have been identified that are located within the nuclear envelope. Entitled NET (nuclear envelope transmembrane) proteins have been mostly identified in the last two decades. Tens of NET proteins have been described, many of them only expressed in a cell-type specific manner (Wong *et al.* 2014; Schirmer *et al.* 2003).

The lamin meshwork and the nuclear envelope are only interrupted by the nuclear pore complexes that allow the complex communication between the nucleus and the rest of the cell. It was suggested early on during the 1960's by electron microscopy that the nuclear lamina forms a repressive environment with a visible layer of dense and compact chromatin surrounding the nuclear space (**Figure 12A, Figure 12B, Figure 12C**)(Comings 1968; van Steensel and Belmont 2017). The observations that the inactive X chromosome in female cells was often seen at the periphery suggested that the peripheral localization might concern only some genomic regions (Dyer *et al.* 1989). Indeed, further FISH (fluorescent in situ hybridization) analysis using defined genomic sequences reported that the peripheral localization correlated with gene-poor domains as the gene-rich chromosome 19 was reported to be more centrally located than the gene-poor chromosome 18 which is preferentially found at the periphery (Croft *et al.* 1999). Interestingly, translocation of a 20Mb region of chromosome 18 was demonstrated to be sufficient for a peripheral localization (Croft *et al.* 1999). This correlation is not restricted to chromosomes 18 and 19 but is a general rule for all human chromosomes (Boyle *et al.* 2001).

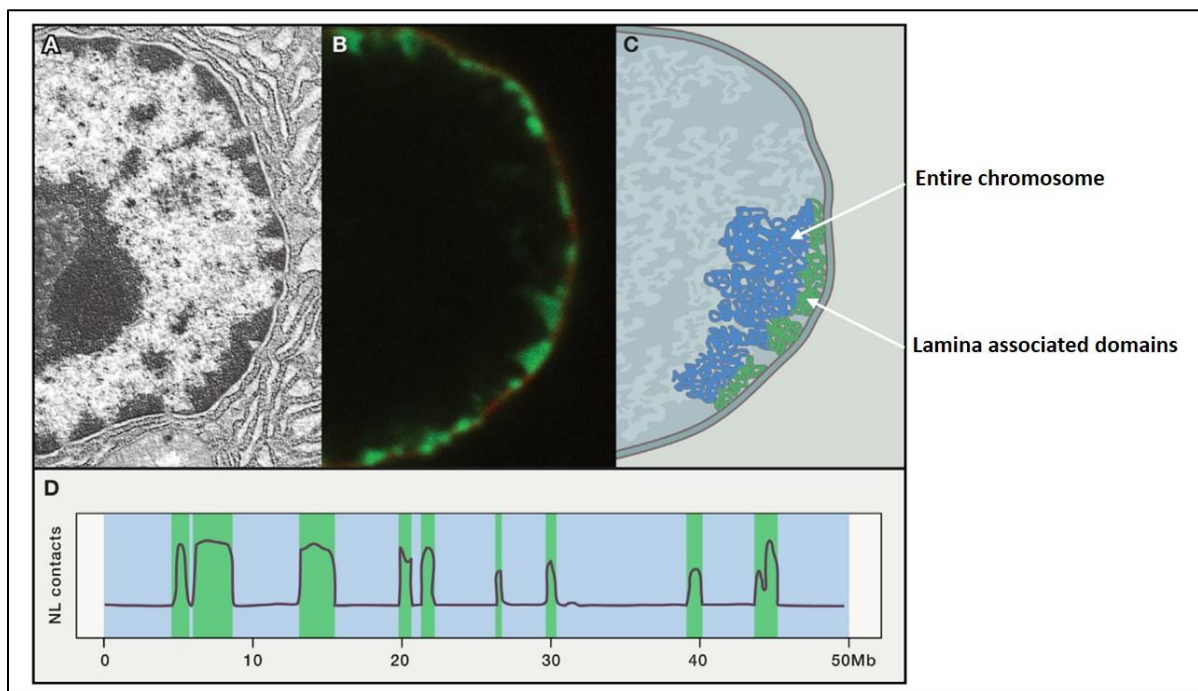


Figure 12 | Lamina associated domains. (A) Electron microscope image showing a mammalian nucleus. An electron-dense layer of chromatin is observed at the nuclear periphery. Other electron-dense heterochromatin regions are observed within the nuclear interior, notably around the nucleolus. (B) Imaging of LADs. In green is the m6A-tracer binding to genomic regions methylated by the LaminB-DamID. In red is a staining of Lamin B. (C) Cartoon illustrating the folding of one chromosome. The entire chromosome drawn in blue faces the nuclear interior, whereas LADs of this chromosome, drawn in green, specifically lie at the nuclear periphery. (D) Scheme of a DamID genome-wide profile showing nuclear lamina (NL) contact intensities. LADs are depicted in green. Adapted from van Steensel and Belmont, *Cell* 2017.

Genome-wide mapping of peripherally positioned genes were produced using a technique called DNA adenine methyltransferase identification (DamID). The DamID relies on the bacterial

DNA methyltransferase that adds a methyl group onto an adenine instead of a cytosine, thus the only adenine methylated observed during the genome-wide DNA sequencing results from the DamID (Van Steensel and Henikoff 2000). To identify regions interacting with the nuclear lamina, the methyltransferase is fused to LAMINB (**Figure 12D**). Widely used in *Drosophila melanogaster* and human cells, the DamID has produced a comprehensive view of the genomics regions preferentially in close proximity to the nuclear lamina that were named lamina-associated domains (LADs) (Pickersgill *et al.* 2006; Guelen *et al.* 2008). LADs have been confirmed by other approaches such as ChIP-seq, and in other organisms like mice or *Caenorhabditis elegans* (Poleshko *et al.* 2017; González-Aguilera *et al.* 2014). The general rules assessed by FISH experiments were confirmed and refined. In mammalian cells, over 1000 LADs are observed. LADs are large domains of 0.1 to 10Mb long, that in total represent about 40% of the genome. They carry heterochromatin hallmarks as LADs are A/T-rich regions and gene-poor regions. Interestingly, LADs are overall conserved, devoid of synteny breakpoints, and although the sequence is not, the A/T-rich feature is constant between mouse and human, suggesting that the radial positioning is evolutionary important (Meuleman *et al.* 2013). Furthermore, the genes present in LADs are lowly expressed. As heterochromatin regions, LADs replicate during the late S phase (Hiratani *et al.* 2010).

Assayed in population of millions of cells, no information could be obtained about the number of LADs effectively contacting the nuclear lamina in each nucleus. In fact, only about 30% of LADs are positioned at the periphery in each cell (Kind *et al.* 2013). Using a memory-approach of the DamID via a fluorescent m6A-tracer, the authors could visualize the LADs contacting the nuclear lamina but also follow their fate during the next cell cycle. They observed that during interphase LADs displayed a confined dynamics at the nuclear periphery but they are dislodge during mitosis and do not seem to act as anchoring points for the novel domains that will associate with the nuclear lamina during this second interphase (Kind *et al.* 2013). Single cell genome-wide characterization of DamID sequencing signal then provided evidence that association with the nuclear lamina involve multiple lamina interactions rather than long stretches of association. Regions contacting the lamina are extremely gene-poor segments, suggestion a potential structural role for these contact points (Kind *et al.* 2015a).

What have these DNA sequences special to be located at the nuclear periphery, is it encoded in the DNA or is it an epigenetic feature? Apart from the A/T enrichment, a GAGA motif was frequently observed in the *Igh* and *Cyp3a* LADs. Furthermore, it was demonstrated the GAGA motif-containing sequence of a few Kbs was sufficient to induce lamina association and transcriptional repression at another genomic location (Zullo *et al.* 2012). In another study by Bian *et al.*, a dissection of the beta-globin *Hbb* locus identified three regions sufficient for peripheral

targeting that were also a few Kbs in length (Bian *et al.* 2013). Sequence-specific targeting mechanisms seems to be conserved throughout evolution as it was also proposed in yeast that some particular sequences called DNA zip code, here located in some gene promoters, were sufficient to target other genomic regions to the nuclear periphery (Ahmed *et al.* 2010). However, GAGA repeats do not seem to be particularly in LADs genome-wide, suggesting additional mechanisms (Guelen *et al.* 2008).

It was described that the *Igf* gene and the neuronal regulator *Mash1* were localized at the periphery of progenitor cells and were relocalized to the nuclear interior in more differentiated cells and correlated with their transcriptional activation (Kosak *et al.* 2002; Williams *et al.* 2006). Observed for particular genes, it was then demonstrated that association with the nuclear lamina reflected the transcriptional status for a large majority of LAD-genes (Peric-Hupkes *et al.* 2010; Kind *et al.* 2013). Some regions always associate with the nuclear lamina and are called constitutive LADs (cLADs), whereas some only associate in a cell-type specific manner and are named facultative LADs (fLADs), that only partially correlate with the transcriptional status of the region (Peric-Hupkes *et al.* 2010).

Studies have observed in many tissues the sequences and underlying genes interacting with the nuclear lamina, yet it remains to understand the protein composition of the nuclear periphery that allows such a silencing and positioning effects.

2. Protein composition of the nuclear periphery

The first genome-wide characterization of the sequences associated with the nuclear lamina revealed that the genes present in genes were repressed (Pickersgill *et al.* 2006). LADs strongly correlate with positive enrichment in heterochromatin marks such as - high H3K9me2 and H3K9me3, low H3K4me2 and H4 acetylation and high H3K27me3, CTCF and YY1 binding at the LAD borders (Guelen *et al.* 2008; Wen *et al.* 2009; Harr *et al.* 2015). LADs are not enriched with high DNA methylation levels (Berman *et al.* 2011). In *Drosophila*, depletion of the B-type lamin induced a loss of nuclear lamina interaction for many genes (Kohwi *et al.* 2013; Shevelyov *et al.* 2009). Interestingly, in mESCs, lamins are not essential for LADs, showing that additional proteins are required to maintain this localization (Amendola and van Steensel 2015). It was observed that A-type lamins could interact with chromatin regions, intriguingly both hetero- and euchromatin (Gesson *et al.* 2016; Harr *et al.* 2015; Kubben *et al.* 2012). Although, deletion of LaminA induced a relocalization away from the nuclear lamina, it was not associated with a loss of repression, suggesting that the nuclear lamina might be important for peripheral anchoring in some tissues but that the repressive compartment is largely due to other proteins (Harr *et al.* 2015; Kubben *et al.*

2012).

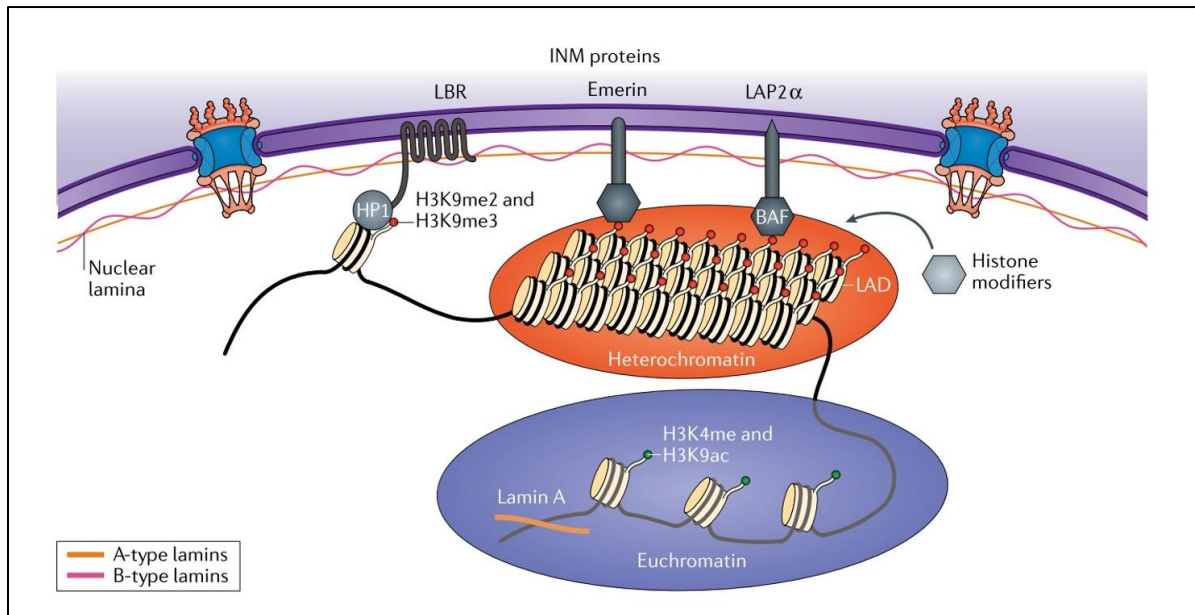


Figure 13 | Proteins associated with lamina associated domains. Proteins from the nuclear lamina such as LBR, Emerin and LAP2 α can bind to chromatin-associated factors. Heterochromatin LADs are enriched in specific histone modifications such as H3K9me2 and me3, subsequently bound by ‘readers’ like HP1. LaminB is exclusively observed within the nuclear lamina whereas some LaminA can bind to non-LADs of the genome. From Buchwalter, Kaneshiro and Hetzer, *Nat. Rev. Genetics* 2019.

Deeper investigations revealed that the enzymes responsible for the compacted heterochromatin state of LADs were important for their peripheral localization. Zullo *et al.* identified that a GAGA-containing sequence could drive a nuclear lamina association, and further demonstrated that it relies on the binding of the cKrox factor in complex with HDAC3 and the lamina protein Lap2 β (Zullo *et al.* 2012). Treatment with the HDAC inhibitor trichostatin A (TSA) led to an increased expression of heterochromatin-genes (Finlan *et al.* 2008). It was reported that the function of HDAC3 in LADs was not restricted to its enzymatic activity. Indeed, deletion of HDAC3 impaired the cardiac-lineage gene *Actc1* peripheral positioning. While complementation with a catalytically dead HDAC3 mutant was sufficient to restore its nuclear association, an HDAC3 mutant unable to bind Lap2 β could not (Poleshko *et al.* 2017). It is interesting to note that HDAC3 $-/-$ mice die during embryonic development, enzymatic-dead HDAC3 mice are viable, possibly highlighting a structural role for HDAC3 (You *et al.* 2013). Tissue-specific NETs could also have a role in proper establishment of LADs and gene activation, as exemplified during myogenesis, where myoblast specific NET tether myotubes genes to the periphery to ensure robust repression (Robson *et al.* 2016). Lamin B-receptor (LBR) is expressed in many cell types. Interestingly, in the cell-types where LBR is not expressed, such as retinal rod cells of nocturnal mammals or olfactory sensory neurons in mouse, no heterochromatin compartment is visible at the periphery (Solovei *et al.* 2009; Clowney *et al.* 2012; Solovei *et al.* 2013). Furthermore, LBR might

be implicated in the recruitment of some loci such as the inactive X chromosome (Chen *et al.* 2016). Nuclear pores may contribute to gene tethering at the nuclear periphery as reported for NUB93 and NUP153, which binds to enhancers sequences (Ibarra *et al.* 2016). Deletion of NUP153 in murine ESCs impaired the pluripotency state by the loss of silencing at differentiated genes that correlated with a spatial relocation away from the periphery (Jacinto *et al.* 2015). In a genome-wide screen, many proteins were found to disrupt heterochromatin localization at the nuclear periphery, which included DNA methylation proteins, histone chaperones, but also proteins implicated in the maintenance of repressive histone modifications (Shachar *et al.* 2015). Many proteins are acting together to ensure the proper localization and silencing of heterochromatin at the nuclear periphery, these proteins can be linked to the nuclear envelope or associated with repressive chromatin state, suggesting a redundancy of pathways to ensure higher robustness of nuclear envelope tethering. High-throughput integration of reporter genes at 27,000 different genomic positions revealed that although LADs globally act as repressive environment, the silencing effect vary from positions to positions, suggesting local effects of particular proteins (Akhtar *et al.* 2013).

The prominent histone modifications associated with LADs are H3K9me2 and H3K9me3 and have thus been the focus of many studies (**Figure 10, Figure 13**). Bian *et al.* have identified three peripheral targeting sequences within a transgenic HBB locus. They observed that the peripheral anchoring of the transgene was abolished in a Suv39h1/2 double KO (Bian *et al.* 2013). Intriguingly, H3K9me3 is the prominent feature of pericentromeric heterochromatin (PCH), and PCH do not localize at the nuclear lamina. Deletion of the H3K9 di-methylase induced the lamina detachment of the endogenous beta-globin genes, suggesting that H3K9me2 and H3K9me3 may have partially overlapping function in nuclear tethering, and the two marks ensure a robust peripheral localization (Bian *et al.* 2013). It was observed that integration of large transgene into the *C. elegans* genome led to accumulation of H3K9me3 and that these transgene localized at the nuclear periphery (Towbin *et al.* 2010). Interestingly, using a genetic screen for peripheral localization in *C. elegans*, Towbin *et al.* discovered that the histone lysine methylase pathways was essential. Indeed, they observed that depletion of either the S-adenosil-methionine proteins or the methyltransferase enzymes led to a central relocation of their reporter (Towbin *et al.* 2012). A latter study reported that the CEC-4 protein directly binds to H3K9 mono, di and tri-methylated. CEC-4 localizes at the nuclear envelope independently of H3K9 methylation (Gonzalez-Sandoval *et al.* 2015). Interestingly, CEC-4 is required for the anchoring of heterochromatin domains at the nuclear lamina, but not for its repression. Furthermore, the action of genome-anchoring of CEC-4 is only visible in worm embryo, but not in adult larvae. Deletion of *cec-4* impairs the differentiation of

embryo toward a muscle cell-type (Gonzalez-Sandoval *et al.* 2015). These results suggest that redundant pathways for genome anchoring coexist within the nucleus, and that some of these pathways are tissue-specific. No orthologs of CEC-4 have been identified in mammals, yet, other proteins may carry the same function. The PRR14 protein in human was described as localizing in the inner nuclear envelope in interphase and it has the capacity to bind to HP1 (Poleshko *et al.* 2013). Poleshko *et al.* proposed that PRR14 functions in recognizing heterochromatin regions via HP1 binding during mitosis and then guide the heterochromatin-bound regions toward the periphery when the nuclear envelope is reformed. It was recently demonstrated that an additional factor acting in differentiated tissues in *C. elegans* was the MRG1 protein. Intriguingly, MRG-1 binds to euchromatin regions and is involved in histone acetylation, indicating that euchromatin domains also play a role in heterochromatin compartmentalization (Cabianca *et al.* 2019).

In conclusion, different pathways are at play, from epigenetic histone-modifications and particular ‘readers’ to nuclear lamina proteins, to ensure proper localization and repression of LADs.

3. Functions and dysfunctions of LADs

From all the studies characterizing the nuclear periphery, it emerges that it acts as a repressive compartment. Yet, different phenotypes accompany the loss of peripheral anchoring, sometimes leading only to a relocalization, sometimes to a loss of the transcriptional repression. Does this compartmentalization have functional roles in genome regulation? Genetic deletion of B-types lamins in mouse impair organogenesis, although without affecting transcription levels, suggesting a crucial role of the nuclear envelope on the cellular architecture and on the organism (Kim *et al.* 2011).

There is a good genome-wide correlation of radial positioning and transcriptional state of a locus in a given cell-type. Yet this correlation is not complete. Indeed, using murine embryonic stem cells (ESCs) and two subsequent differentiated states - neuronal progenitor cells (NPCs) and astrocytes (ACs), it was demonstrated that repressed genes associated with the nuclear lamina in ESCs lose their peripheral localization in NPC if they are activated. Vice-versa, genes that are repressed in NPC gain nuclear lamina association (Peric-Hupkes *et al.* 2010). Although it works as a general rule, some genes detach from the lamina in NPCs, yet are only activated at later developmental stages, suggesting they might enter an “unlocked” state as the authors coined it, so they can be expressed at a later stage more efficiently (**Figure 14**). Association and disassociation concern single gene units as well as multigene regions. Detachment of nuclear lamina is conserved

for other cell differentiation programs such as cardiac or muscle commitment (Poleshko *et al.* 2017; Robson *et al.* 2016).

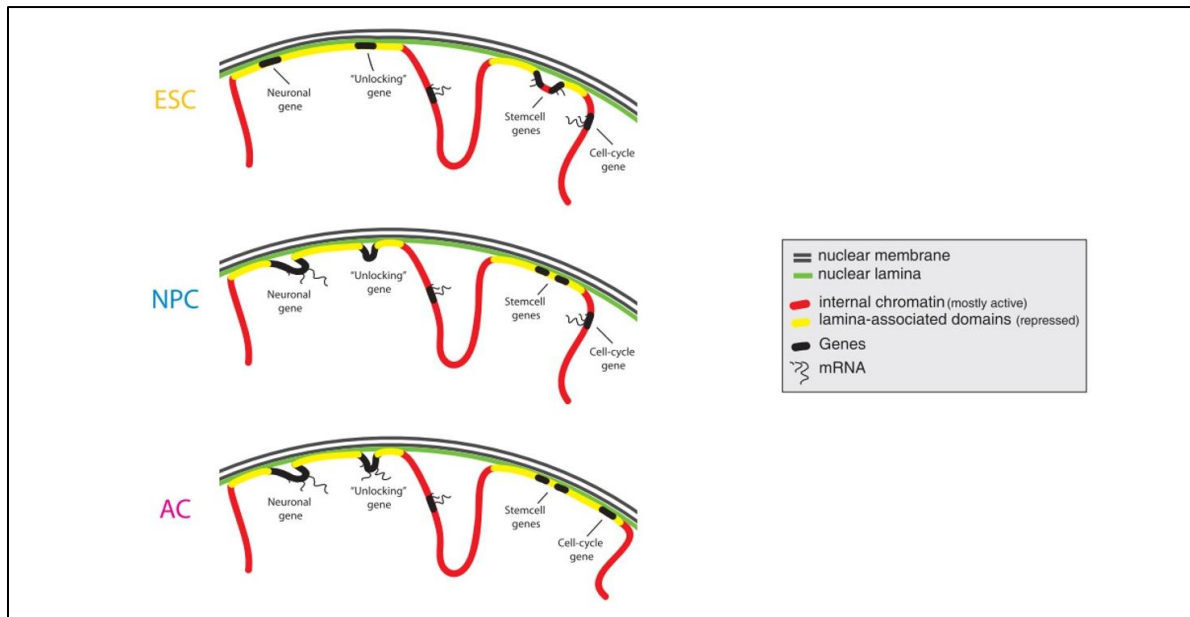


Figure 14| Changes in nuclear lamina interactions upon differentiation and ‘unlocking’ theory. The nuclear periphery acts as a repressive compartment for LADs. Some LADs are cell-type specific and called facultative (fLAD). Inactive neuronal gene on the left localizes at the periphery in ESCs and changes positioning and transcriptional state in NPC.s Active stem cell gene on the right faces the nuclear interior in ESCs and is repressed and gain lamina-interaction upon differentiation into NPCs. The gene in the middle is inactive and localizes at the nuclear periphery in ESCs, upon NPC differentiation, it relocalizes away from the periphery upon NPC differentiation but in a poised state and is only activated upon AC differentiation. ESC = embryonic stem cell, NPC = neural precursor cell, AC = astrocyte. From Peric-Hupker *et al.*, *Mol. Cell* 2010.

It remained to understand the cause-consequence relationship. Artificial locus-tethering to the nuclear periphery resulted in gene silencing, although with different efficiencies depending on the reporter (Kumaran and Spector 2008; Finlan *et al.* 2008; Harr *et al.* 2015). Yet, forced transcriptional activation of a LAD-gene induce relocalization toward the nuclear interior (Therizols *et al.* 2014). It was further shown that the transcriptional activation of a LAD-gene was not the cause of its detachment but rather a consequence of the change in chromatin state. Indeed, targeting of the particular DEL peptide that only decompacted the locus without transcriptional activation led to the relocalization toward the nuclear interior (Therizols *et al.* 2014). Furthermore, the central localization is maintained for several mitosis even when the peptide is lost, suggesting that epigenetic mechanisms maintain the decompacted state and radial positioning of the locus (Therizols *et al.* 2014).

Nuclear periphery as a compartment can encompass up to ~40% of the genome. Although not all LADs are at the periphery in each cell, it represents a large amount of DNA that is subjected to all DNA-related process and might encounter DNA breaks. In flies, reports suggest that DNA breaks occurring in heterochromatin are delocalized toward the nuclear periphery via the structural

maintenance of chromatin proteins 5 and 6 (SMC5 and SMC6) (Ryu *et al.* 2015). These results suggest that the nuclear periphery might act as a compartment for heterochromatin repair. A recent study further demonstrate that histone-modification are important in the DNA damage response as demethylation of H3K9 via KDM4A is essential to complete DNA repair only at heterochromatin loci (Janssen *et al.* 2019). Interestingly, DNA lesions occurring in LADs in mammals display a delay in the DNA damage response activation and are less resolved using homologous recombination (HR) but rather via non-homologous end joining (NHEJ) (Lemaître *et al.* 2014). Despite the discrepancies between organisms, it seems that the radial positioning of chromatin can influence repair pathway choice and kinetics.

Descriptions of the nuclear envelope and lamina-associated domains in various tissues revealed that many pathologies presented an unusual nuclear chromatin compartment, either from the chromatin-associated modifications or directly from the nuclear envelope. A whole family of pathologies is called 'laminopathies' as the common ground of these disorders is the impaired nuclear lamina, and notably mutations in the *Lamin A* gene (Mattout *et al.* 2006). Laminopathies are degenerative disorders with a broad range spectrum, such as the Hutchinson-Gilford progeria syndrome (HGPS) which is a premature aging pathology or the Emery-Dreifuss muscular dystrophy that display perturbed heterochromatin (Perovanovic *et al.* 2016). Laminopathies result from an accumulation of mutant LAMIN A that induces a disturbed nuclear lamina (Goldman *et al.* 2004). Since LAMIN A has been implicated in the spatial distribution of heterochromatin, heterochromatin localization in laminopathies has been scrutinized (Solovei *et al.* 2013). Using a *C. elegans* model, Harr *et al.* demonstrated that a point mutation in the unique *Lamin A* gene mimicked many of the Emery-Dreifuss syndrome phenotypes, including hyper-sequestration of heterochromatin at the nuclear periphery. Interestingly, deletion of the CEC-4 protein, which is involved in H3K9me3-binding, rescued the effect of the Lamin A mutation, suggesting a strong interconnection between nuclear lamina and histone-modifications in the peripheral tethering and phenotypic impact of laminopathies (Harr *et al.* 2020).

Radial positioning can be affected in numerous diseases such as cancers. Indeed, changes in *Lamin A* gene is often observed in human cancers (Willis *et al.* 2008; Johnson *et al.* 2004). Furthermore, by looking at the spatial localization of cancer-associated genes, Meaburn *et al.* described a global reorganization of the 3D-genome organization during normal and tumorigenic cell differentiation. A number of genes changed their radial localization in cancerous cells, independently of their transcriptional status (Meaburn and Misteli 2008). Specific gene repositioning was reproducible between individuals in the case of breast cancer, suggesting a potential function of this repositioning (Meaburn *et al.* 2009). For particular breast cancer subtypes,

it was demonstrated that large multiple gene-unit regions were undergoing transcriptional changes (Rafique *et al.* 2015). Rafique *et al.* observed that the regions displaying changes in expression were concomitantly decompacted and relocalized away from the nuclear periphery in an estrogen-dependent manner. Although, the presence at the nuclear periphery was not assessed, large regions encompassing differences in chromatin compaction were described for bladder cancers as well (Vallot *et al.* 2015). These reports suggest that environmental clues such as hormones might regulate the chromatin folding changes observed in cancers and that the nuclear periphery might be a key contributor to the gene-expression alterations.

Lamina-associated domains encompass ~40% of the mammalian genomes. Chromatin association with the nuclear lamina is stochastic but controlled by diverse epigenetic pathways thus ensuring proper formation this nuclear sub-compartment. As an important repressive heterochromatin domain, the LAD-genes are lowly if expressed. The integrity of the nuclear lamina and LADs is crucial for the cell biology and defects in LADs positioning and silencing is often observed in diseases.

C - Pericentromeric heterochromatin

A large portion of the genome consists of repeated DNA sequences. One well-known example is the pericentromeric heterochromatin (PCH) regions that surround centromeres.

1. Pericentromeric heterochromatin and chromocenters organization

PCH regions are mainly composed of satellite sequences tandemly repeated that can vary from one species to another. In human, pericentromeric regions consist of three different satellite sequences that are tandemly repeated over large genomic distances (>4Mb). These three different repeat sequences are called satellites. In human, the I, II and III satellites are dispersed in a chromosome-specific pattern. In mouse, tandem repeats of pericentromeric regions are the major satellites, whereas centromeric repeats are the minor satellites. Major satellite sequences are A/T-rich 234bp tandemly repeated in a head to tail fashion for 1,000 to 10,000 times per chromosomes, forming Mbs-long domains (**Figure 15A**)(Martens *et al.* 2005). Although major satellites are virtually identical between all chromosomes, recent reports suggest that some chromosome-specific tandem repeats might exist (Komissarov *et al.* 2011). In human, satellite sequences represent ~3% of the genome and in mouse, satellites represent from 3 to 8% of the genome depending on the report (Martens *et al.* 2005; Komissarov *et al.* 2011). Major satellites display high

sequence similarities (Vissel and Choo 1989). The importance of satellites in the genome can vary as it is ~20% in *Drosophila melanogaster* and even ~50% in some plant species (Garrido-Ramos 2017). Murine chromosomes are all acrocentric with one arm being only composed of satellite and telomeric sequences. However, human chromosomes can be either metacentric, sub-metacentric and acrocentric, with different lengths of the two arms.

Although satellite repeats are dispersed within the nucleoplasm, some species such as *D. melanogaster*, mice and some plants show a striking clustering of PCH into chromocenters (**Figure 10, Figure 15A**) (Guenatri *et al.* 2004). This could also be the case for human in particular condition like blood lymphocytes (Alcobia *et al.* 2000). This clustering was first identified by DNA-staining dyes. Specific purification of chromocenters in murine cells followed by DNA sequencing suggest that while the majority of DNA sequences in chromocenters are major satellites, ~30% might be other repeated elements such as LINE1 and ERVs (Ostromyshenskii *et al.* 2018). It is not perfectly understood how this clustering is mediated but a AT-hook protein named D1 in *Drosophila*, conserved from mouse (HMGA1) to flies, was recently identified (Jagannathan *et al.* 2018). Furthermore, it was showed that this clustering is mediated by a dynamic interplay between different players. Indeed, the Prod protein, which binds to the particular {AATAACATAG}_n satellite sequence was found to act with D1 in chromocenter clustering in flies (Jagannathan *et al.* 2019). H4K20me₃ also seems required for proper PCH clustering, as deletion of the Suv4-20H1/2 enzymes result clustering defects (Hahn *et al.* 2013). Interestingly, deletion of the Suv39H1/2 enzymes does not impact chromocenter formation. However, deletion of the H3K9me₁ methyltransferases Prdm3 and Prdm16 completely disintegrate DAPI-rich foci and impairs major satellite clustering (Pinheiro *et al.* 2012).

All murine cells display chromocenters, as observed by DAPI-dense foci. Yet, not all cells display the same number of chromocenters. Most somatic cells present small and round DAPI foci, while embryonic stem cells have more diffuse chromocenters, which might be a consequence of the more decondensed chromatin state contained in pluripotent cells. The radial positioning of the chromocenters changes along development (Solovei *et al.* 2004). This spatial organization is of major importance for the maintenance of the heterochromatin properties of these compartments as forced-tethering to the nuclear envelope prevents proper establishment of heterochromatin marks during early embryo (Jachowicz *et al.* 2013). But in mouse embryonic stem cells, it was reported that PCH regions were bound by Lamin proteins, suggesting an interconnection between heterochromatin compartments (Saksouk *et al.* 2014). Some cells present a chromocenter clustering pattern strikingly different, such as retinal cells of nocturnal mammals which only have a unique, large and central DAPI-dense focus (Solovei *et al.* 2009). Intriguingly,

this conformation seems to be evolutionary favored as a physical way to improve light collection, suggesting crucial role of PCH organization for cellular and tissue physiology.

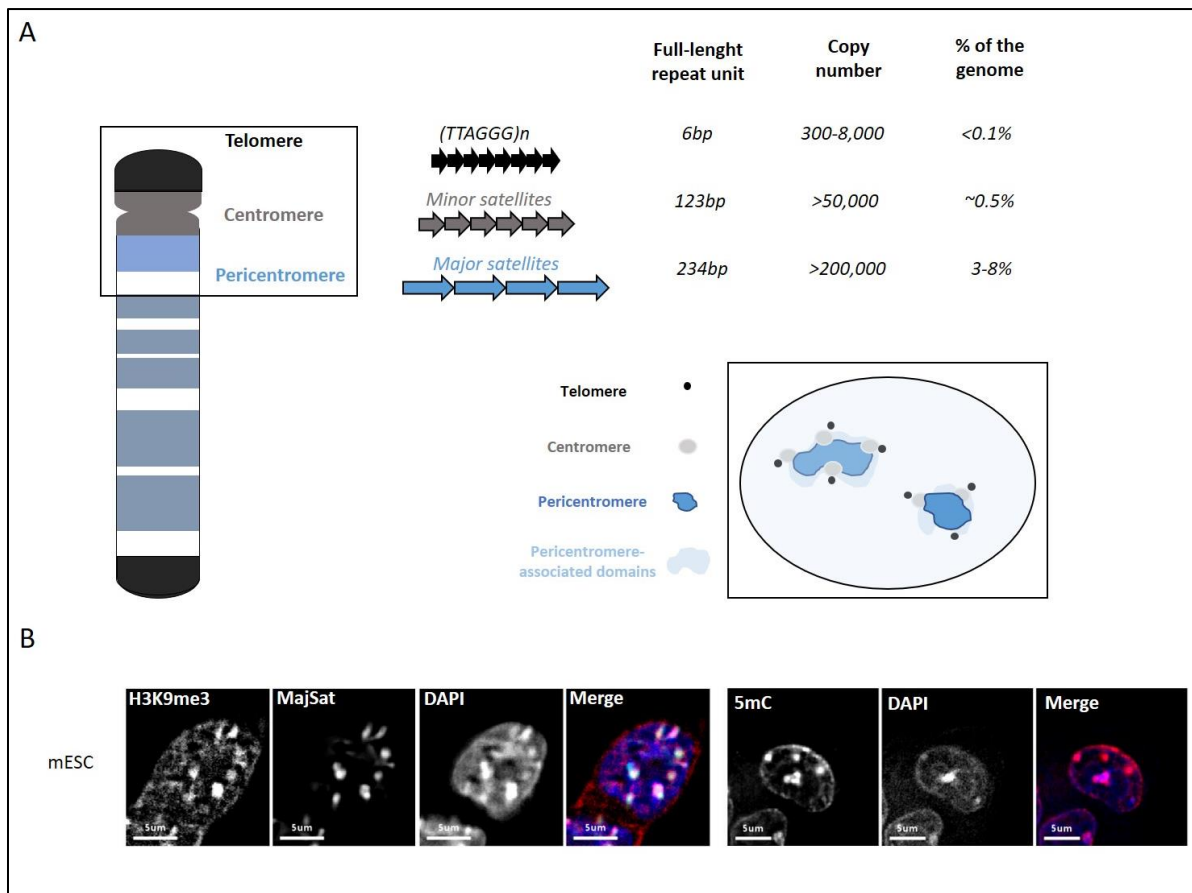


Figure 15 | Organization of pericentromeres. (A) Left, scheme of mouse chromosome. White zones represent euchromatin regions, whereas dense zones represent heterochromatin regions. Highlighted are the telomere, centromere and pericentromere regions with a zoom onto their repeated sequences. Right, table showing sizes, copy number and percentage of telomere, centromere and pericentromere regions in mouse. Bottom, scheme of the spatial organization of constitutive heterochromatin with the pericentromeres that merge to form big chromocenters. At the periphery of chromocenters are observed the centromere and closely located telomere, as well as pericentromere-associated domains. (B) Representative immunofluorescence pictures of H3K9me3 histone modification, major satellite repeats and 5mC DNA methylation in murine ESCs. B is from personal unpublished data.

These chromocenters composed the majority of the so-called constitutive heterochromatin. Yet, it also serves as an anchoring landmark for some facultative heterochromatin regions. FISH observation of unique loci revealed that the α and β -globin gene relocalized away from chromocenters upon activation (Francastel *et al.* 1999; Brown *et al.* 2001). Using the 4C technique to genome-wide map the regions interacting with the major satellite repeats, de Laat's lab has identified around 1 000 regions they called pericentromere-associated domains (PADs) (Wijchers *et al.* 2015). These regions show a great overlap with LADs, together with more distinctive feature like H4K20me3 enrichment, which is enriched at chromocenters. This redundancy between compartment can be explained by a competition between the two compartments - the nuclear periphery and the chromocenters. This competition phenomenon was nicely illustrated using a

transgene intergration in mouse cells (Bian *et al.* 2013). It is proposed that the choice between the two compartments might be based on H3K9me3 content (Bian *et al.* 2013; Kind *et al.* 2015b). Interestingly, they observed that higher levels of H3K9me3 was associated with a peripheral localization, although LADs are enriched in H3K9me2 whereas PCH are enriched in H3K9me3. In ESCs, LADs form large domains spanning an average of 1Mb. PADs form smaller domains. Upon differentiation, LADs sizes remain constant whereas PADs increases, indicating a reinforcement of PADs contact with PCH. Furthermore, Wijchers *et al.* observed that differentiation-induced PADs are transcriptionally silenced before their association with PCH, suggesting that this association is not the primary cause of their silencing but rather a compartmentalization of repressed regions. These results suggest that different mechanisms regulate peripheral and pericentromeric heterochromatin, and these regulation are likely influenced by cell-type particularities.

2. Protein composition of PCH and maintenance mechanisms

PCH are maintained via epigenetic-based protein modifications, that are dynamically regulated. It serves as a good model to study heterochromatin. These regions were identified almost twenty years ago as enriched in specific epigenetic modifications such as depletion in histone acetylation, H3K9me3 and subsequent HP1 binding, and DNA methylation (**Figure 15B**).

The Suv39h enzyme trimethylates H3K9 to allow HP1a binding (Martens *et al.* 2005). There is an interplay between Suv39h ‘writer’ enzyme and the HP1a ‘reader’ protein that helps heterochromatin spreading along these regions by avoiding competition between these two proteins (Al-Sady *et al.* 2013). Other heterochromatin marks are also found at PCH (**Figure 16A**). Some other histone modifications are dependent on H3K9me3 for establishment, such as H4K20me3 (Schotta *et al.* 2004). H4K20me3 is established via the Suv420h enzyme. This enzyme not only methylates histone H4 but is also important for PCH compaction as its loss results in a decompaction and a scattering of chromocenters. Suv420h can also interact with cohesins (Hahn *et al.* 2013). The histone modification H3K64me3 however appears to be dependent of the presence of H3K9me3, but not on DNA methylation or HP1, suggesting that multiple pathways act independently to ensure proper heterochromatin conformation of the PCH (Lange *et al.* 2013). Multiple isoforms of HP1 exist in mammalian cells - α , β and γ . Of interest, each isoform can carry different roles, and they are found at different positions within the nucleus. Although the most known heterochromatic protein, it was recently observed that depletion of HP1 α , but not the other two, led to an even more compact heterochromatin state (Bosch-Presegué *et al.* 2017). HP1 was

also found to interact with structural proteins such as CTCF. These data suggest that PCH are fine-tune heterochromatic compartment with tight links to genome organization.

DNA methylation is another important feature of pericentric regions and is maintained there during DNA replication via UHRF1 and DNMT3A and DNMT3B (**Figure 16A**) (Papait *et al.* 2007; Bachman *et al.* 2001). However, loss of DNA methylation does not impact the formation of chromocenters (Saksouk *et al.* 2014). Pluripotent cells with low DNA methylation levels display increased levels of H3K27me3 at PCH (Tosolini *et al.* 2018). Because of its importance as huge DNA repeats, PCH has been used as a model to study the dynamic protein network implicated in the heterochromatin maintenance (Müller-Ott *et al.* 2014). A more detailed view was obtained using pitch technique and revealed that loss of DNA methylation or H3K9me3 was compensated by the Bend3 protein that then recruited PRC2 and the NuRD complex (Saksouk *et al.* 2014). In addition to the numerous proteins that acts at PCH, there is a dynamic interplay between all these players. Long-though to be transcriptional activators, some transcription factors may help for the heterochromatinization process of PCH. PAX3 and PAX9 transcription factors bind within PCH regions and repress transcription of these repeats and their depletion leads to a dramatic derepression of the mouse major satellites (Bulut-Karslioglu *et al.* 2012). Additional transcription factors are implicated in major satellite regulation. Indeed, the SNAIL1 protein via interactions with the H3K4 deaminase LOXL2 controls pericentromeric transcription (Millanes-Romero *et al.* 2013). This SNAIL1-LOXL2 pathway acting at pericentromeres is crucial for the epithelial-to-mesenchymal transition of mesenchymal cells, suggesting a broad impact of heterochromatin regulation. Furthermore, it was observed that the major pluripotency factor NANOG could also regulate heterochromatin organization as its deletion leads to a decompaction of the chromocenter in embryonic stem cells, and the forced expression in epiblast stem-cells when it is not supposed to be active could also decompact PCH, showing an intricate relationship between heterochromatin organization and pluripotency (Novo *et al.* 2016). NANOG directly binds to pericentromeric repeats and additional factors such as SALL1, which controls Nanog-mediated regulation of PCH (Novo *et al.* 2016). The regulation of PCH is not only dynamic according to cell state, but also for dividing cells, each mitosis represents a challenge. Indeed, at each mitosis, heterochromatin must be reinstalled after DNA replication. KAP1 protein that is usually involved in retrotransposon repression is involved in this process in MEF cells (Jang *et al.* 2018).

The heterochromatin state is a barrier to transcription. However, transcription of major satellites and the production of RNAs seems important for proper establishment of the repressive environment (**Figure 16B**). Indeed, deletion of Dicer in murine ESCs led to elevated transcription of PCH satellites together with a loss of H3K9me3 (Kanellopoulou *et al.* 2005; Murchison *et al.*

2005). Deletion of Dicer results in early embryonic lethality (Bernstein *et al.* 2003). Major satellites are constitutively transcribed, however in a cell-cycle dependent manner with the more abundant transcripts observed in late G1 phase (Lu and Gilbert 2007). Quiescent cells do not have detectable major satellite transcripts. PCH RNAs are produced by RNA polymerase II and can be sense or anti-sense, although both are not expressed at the same levels. Upon stress exposure, human cells display an elevated levels of satellite III transcripts (**Figure 16B**)(Jolly *et al.* 2004; Valgardsdottir *et al.* 2008). Satellite III RNAs accumulate at nuclear stress granules and disturb segregation of chromosomes during the following 24h, suggesting a role in satellite RNAs in chromosomal instability (Giordano *et al.* 2020). It was later observed, in mouse embryonic stem cells, that the RNA produced from major satellite repeats could stabilize SUV39h binding, allowing a better enzymatic activity (Velazquez Camacho *et al.* 2017). Interestingly, SUV39h protein has a higher affinity for RNA than DNA and this binding is independent of H3K9me3, indicating its ability to induce heterochromatin formation (Shirai *et al.* 2017). During early development, a strand-specific burst in major satellite transcription is necessary to properly form PCH clustering (Probst *et al.* 2010). Intriguingly, ESCs with high levels of DNA methylation show correspondingly higher transcription of major satellites than lowly methylated ESCs (Tosolini *et al.* 2018). Furthermore, not only major satellite RNAs but potentially additional RNAs might be important to establish the heterochromatin environment at chromocenters. In muscle cells, it was observed that a lncRNA, Chro1, helps targeting DAXX/ATRX to pericentromeric regions and deposit H3.3 (Park *et al.* 2018). Loss of either DAXX, ATRX, H3.3, Chro1 or RNA transcription affects the 3D-organization of PCH and the muscle differentiation. Interestingly, DAXX can relocate away from PML NBs toward centromeric and pericentromeric repeats in human cells subjected to heat shocks (Morozov *et al.* 2012). Morozov *et al.* demonstrate that the lack of Daxx represses satellite transcription and destabilizes histone-modifications associated at pericentromeric regions. These results suggest that DAXX might carry an important role in the reformation of heterochromatin following stress-induced transcription of satellites. ATRX usually localizes at pericentromeric regions (McDowell *et al.* 1999).

Together, these studies show an additional and essential layer of regulation whereby heterochromatin must be transcribed to establish a proper repressive state.

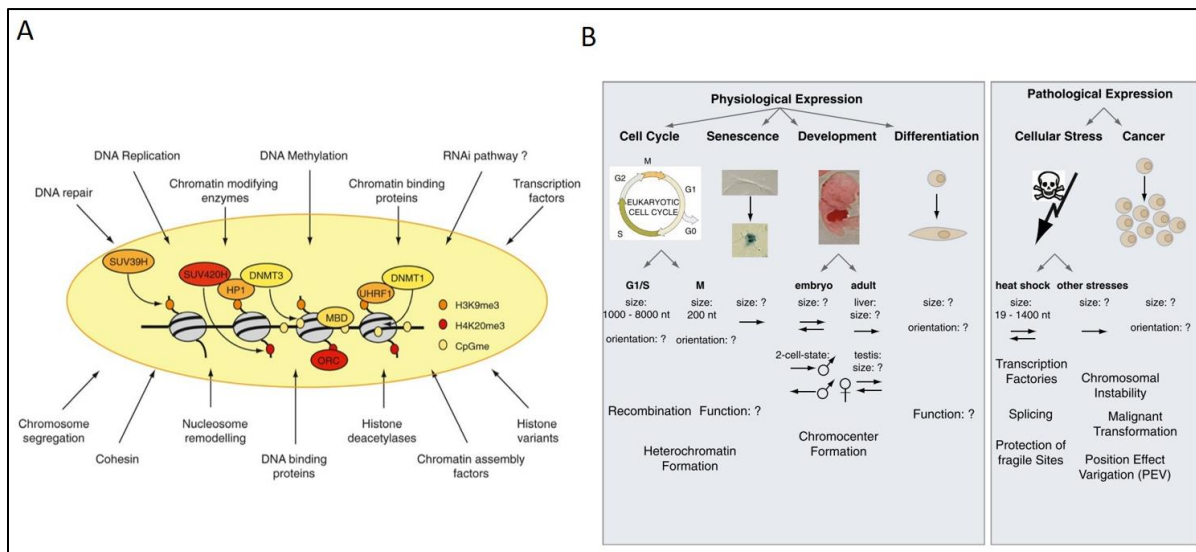


Figure 16 | Heterochromatin composition and transcriptional state of pericentromeres. (A) Heterochromatin state of pericentromeres is maintained via the action of multiple proteins. DNMT proteins maintain high levels of DNA methylation, which is then bound by MBD-containing proteins. Histone H3 are notable modified on lysine 9 by SUV39H1/2 enzymes that tri-methylates this residue, which can then recruit HP1. Histone H4K20me3 is established by SUV4-20H1/2 enzymes. Histone deacetylases remove histone acetylation, further contributing to the compact state of chromatin. **(B)** Satellite repeats can be physiologically transcribed under some circumstances. Transcription of pericentromeres is important for heterochromatin formation as observed in G1-phase or during the early embryonic development. However, transcription of satellite sequences is observed under pathological conditions as in case of cellular stresses such as heat shock, or in some cancers. From Saksouk, Simboeck and Déjardin, *Epigenetics & Chromatin* 2015.

Once H3K9me3 is established, HP1a can bind to this modification. In addition, it was observed that induced SUMOylation of HP1a could induce its targeting to pericentric heterochromatin even in the absence of Suv39h and H3K9me3 (Maison *et al.* 2011). Additional studies advanced our comprehension of this mechanism showing that SENP7, a SUMO protease, was necessary for HP1a retention at PCH (Maison *et al.* 2012). This retention is modulated by the two PxVxL domains of SENP7 that binds HP1a and the presence of SENP7 directly regulates HP1a mobility (Romeo *et al.* 2015). Other proteins than HP1 can also be SUMOylated. This is the case of IKAROS, a zinc-finger protein that binds to PCH repeats (Cobb *et al.* 2000). IKAROS localization is independent of SUMOylation but its enzymatic activity is, indicating that not only the right proteins must be targeted to the right compartment but they then need additional modification to play their role (Gómez-del Arco *et al.* 2005). These data demonstrate that pericentric heterochromatin foci are the result of a dynamic interplay between histone and non-histone proteins, that can all be post-translationally modified, thus adding complexity but also robustness in heterochromatin formation and maintenance.

A new perspective regarding chromocenter has recently emerged. Indeed, HP1, a main component of chromocenter was shown to undergo liquid-liquid phase separation (LLPS) in vitro and in vivo (Strom *et al.* 2017; Larson *et al.* 2017). Binding of HP1 results in the reshaping of nucleosome and increases nucleosome-nucleosome interaction, thus favoring a compact heterochromatin state (Sanulli *et al.* 2019). HP1-marked chromocenters exhibit dynamic patterns of foci fusions during in the embryo (Strom *et al.* 2017). Formation of biomolecular condensates seems to be a key feature in the dynamic organization of PCH. However, the exact capacity of HP1 to mediate undergo phase-separation is still under debate (Erdel *et al.* 2020). Nucleosomes carry some LLPS properties when incorporated in chromatin, adding a force to the formation of particular subcompartments (Gibson *et al.* 2019). Moreover, major satellite transcripts can interact with the scaffold attachment factor B (SAFB) that promotes PCH organization via LLPS (Huo *et al.* 2019). It is thus likely that PCH organization results from LLPS and non-LLPS mechanisms.

3. Biological functions of pericentromeric heterochromatin

Chromocenters serve as anchoring landmarks for PADs (Wijchers *et al.* 2015). Using a LacO integrated in a non-PAD genomic locus, Wijchers *et al.* observed that targeting of a LacR in fusion with the chromodomain of Suv39H1 was sufficient to induce repositioning of the LacO array near chromocenter and induced its transcriptional repression. Interestingly, the same group latter demonstrated that recruitment of Suv39H1 indeed reproduced the chromodomain recruitment, however, the recruitment of a Suv39H1 lacking its chromodomain resulted in an efficient silencing of the *LacO* locus, but not in its repositioning toward chromocenters (Wijchers *et al.* 2016). These results suggest that, although chromocenters act as a tether for repressed PAD regions, repression of a locus is not sufficient to induce its spatial relocalization.

Pericentromeric regions were first thought to protect centromeres, as the deletion of heterochromatin proteins can lead to genomic instabilities. It is the case for the SUV39H1/2 and the SUV4-20H1 and 2 enzymes that both display higher levels of chromosomal abnormalities (Peters *et al.* 2001). Depletion of SUV4-20H1/2 enzymes resulted in impaired cohesin recruitment at major satellites and increased chromosomal segregation defects in MEF cells (**Figure 17B**) (Hahn *et al.* 2013). Furthermore, depletion of HMGA1, which is involved in chromocenter clustering results in elevated levels of DNA damages and formation of micronuclei (**Figure 17A**) (Jagannathan *et al.* 2018). It is now clear that heterochromatin regions must be tightly repressed and spatially organized to ensure proper cell physiology.

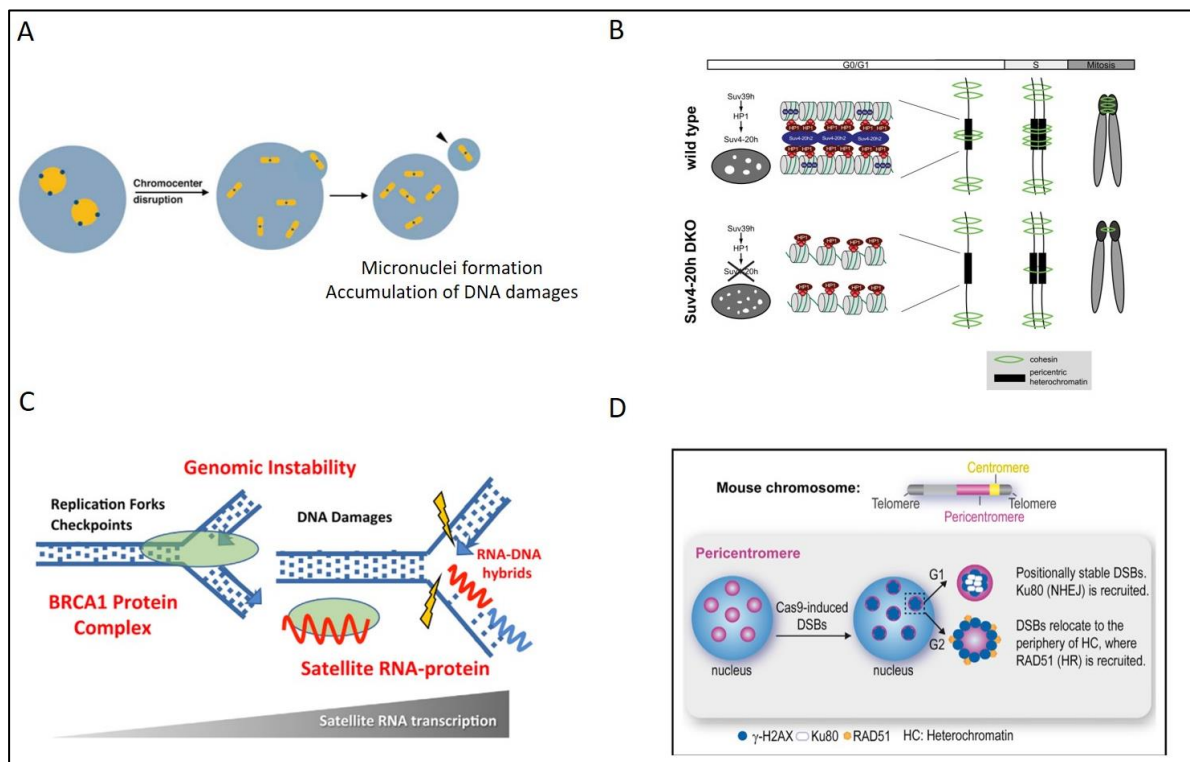


Figure 17 | Importance of pericentromeric satellite regulation. (A) PCH of different chromosomes cluster together. Loss of clustering impairs cohesion of chromosomes and generates micronuclei formation during interphase and induces accumulation of DNA damages. (B) SUV4-20H1/2 enzymes provide H4K20me3-modification. Deletion of Suv4-20H1/2 results in loss of cohesin recruitment at PCH and mis-segregation of chromosomes. (C) High levels of pericentromeric satellites are observed in Brca1-null breast cancers. RNA produced can destabilize DNA replication forks and generates R-loops, ultimately leading to genomic instabilities. (D) Chromocenters represent highly compact constitutive heterochromatin and particular DNA repair strategies have thus evolved to ensure proper stability of PCH regions. In G1-phase of NIH 3T3 cells, DSBs arising in chromocenters are mainly repaired by NHEJ within the sub-nuclear compartment. However, in G2-phase, DSBs relocate toward the periphery of chromocenters and are resolved via HR. A is adapted from Jagannathan and Yamashita, *Cold Spring Harbor Symp. Quant. Biol.*, 2017. B is from Hahn *et al. Genes & Dev.* 2013. C is from Zhu *et al., Mol. Cell* 2018. D is from Tsouroula *et al. Mol. Cell* 2016.

Defects in the DNA methylation machinery also lead to chromosomal instability, as it is the case in the ICF syndrome where Dnmt3b is mutated (Xu *et al.* 1999). In this syndrome, a specific instability of the chromosomes 1, 9 and 16 is observed, which are more GC-rich than other

satellites and thus more prone to DNA demethylation. This is consistent with the fact that they carry more HSat II than other chromosomes, and this phenotype also happens when using the 5-azacytidine drug to impair DNA methylation (Prada *et al.* 2012). Intriguingly, Alzheimer patient cells are more prone to 5-azacytidine-induced DNA demethylation at pericentromeres of chromosomes 1, 9 and 16 (Marques Paya *et al.* 1998). Alzheimer disease results from the appearance of intracellular aggregates of the microtubule-associated protein TAU in neuronal cells. In neuronal cultures, TAU localizes at chromocenters. Depletion of Tau or aggregation of Tau in Alzheimer disease disturb PCH organization and localization of H3K9me3 and HP1 at PCH (Mansuroglu *et al.* 2016). Misregulation of TAU generates widespread heterochromatin decondensation, aberrant gene expression and higher levels of DNA damages (Frost *et al.* 2014). These studies established a novel role of TAU in PCH organization that impact neurodegeneration.

Frontotemporal dementia and amyotrophic lateral sclerosis are neurological disorders resulting from hexanucleotide G4C2 (Proline-Arginine - PR) repeat expansions in the C9orf72 locus. Expression of the poly(PR) peptide revealed its association with PCH (Zhang *et al.* 2019b). Zhang *et al.* observed that poly(PR) localization at chromocenters disrupted HP1 α transcription and localization and induced the upregulation of many families of transposable elements. The presence of poly(PR) diminished HP1a LLPS capacities *in vitro*. Upregulation of repeated elements is observed in patients suffering from frontotemporal dementia and amyotrophic lateral sclerosis (Prudencio *et al.* 2017).

Furthermore, upregulation of satellite sequences is often seen in different cancers, such as pancreatic and breast cancers (Ting *et al.* 2011; Zhu *et al.* 2011). In breast cancer, it is proposed that the tumor-suppressive role of BRCA1 could result from its role in maintaining heterochromatin organization, and Brca1 depletion leads to a drastic change in chromocenter organization and strong transcriptional de-repression of the DNA satellite sequences in both mice and human (Zhu *et al.* 2011). Satellite RNAs alone can generate DNA damages and recruit BRCA1, which ultimately induces tumor formation, as observed from RNA microinjection experiments (Zhu *et al.* 2018b). Increased levels of satellite transcription in breast cancer cells destabilizes DNA replication forks, that in turn increases the levels of R-loops and can ultimately generate genomic instabilities, further highlighting the importance of transcriptional regulation of satellite repeats (**Figure 17C**).

It is proposed that heterochromatin is more refractory to γ -H2A.X accumulation in human cells, although in murine, specifically-induced DSBs within constitutive heterochromatin regions induces γ -H2A.X foci formation (Cowell *et al.* 2007; Tsouroula *et al.* 2016). Interestingly, DNA lesions at PCH in G1-phase are stably positioned within chromocenters and mostly repaired via NHEJ whereas DSBs occurring in S or G2-phase are relocalized toward the periphery of the

chromocenters and mostly repaired via HR, suggesting different heterochromatin environment at PCH regions along the cell cycle (**Figure 17D**)(Tsouroula *et al.* 2016).

Pericentromeric heterochromatin represent an important fraction of the nuclear constitutive heterochromatin. PCH assemble into DAPI-dense chromocenters in multiple species and its repressive environment is redundantly and dynamically established and maintained. Pericentromere clustering into chromocenters has been implicated in genome integrity and the high level of divergence among satellite sequences has been proposed to underlie hybrid incompatibility (Jagannathan and Yamashita 2017). PCH dysregulation can lead to genome instability and diseases.

D - Telomeres

Telomeres constitute the other main constituent of the constitutive heterochromatin and its regulation is particularly important for cell viability.

1. Localization and definition of telomeric heterochromatin.

Telomeres are the regions located at each end of the chromosomes, that comprise hundreds of repeats of the {TTAGGG} DNA sequence, highly conserved in eukaryotes (Meyne *et al.* 1989; Moyzis *et al.* 1988). Interestingly, not all organisms possess particular telomeric sequences as the *Drosophila melanogaster* for which chromosome ends consist of an array of non-LTR retrotransposons (Pardue and Debaryshe 2003). Telomeric tandem repeats assemble into a lariat-like structure (T-Loop) which shields the DNA end (**Figure 18A**) (Shay and Wright 2019; Griffith *et al.* 1999). The length of the telomeres varies greatly from species to species, from 300bp in yeast to 10-15Kbs in human and 20-60Kbs in mice (Jain and Cooper 2010). From 300 to 8,000 telomeric repeats represents about 0.1% of the genome.

In mammals, the double-stranded part of telomeres is composed of nucleosome like other regions of the genome, whereas yeast telomeres are devoid of nucleosomes (Makarov *et al.* 1993; Jain and Cooper 2010). Furthermore, it appears that the nucleosome density at telomeres can vary in a cell-cycle dependent manner (Galati *et al.* 2012). Telomeric repeats are transcribed and produce the well-conserved G-rich RNA TERRA (telomere repeat-containing RNA), which lengths from 0.1 to 10Kbs (Azzalin *et al.* 2007).

In yeast, it has been known for year that telomeres cluster in 3 to 6 foci, 8 times less than the number of telomeres, and are located close to the nuclear envelope (Kupiec 2014).. These foci are dynamics and are generated by random associations-dissociations of individual telomeres (Hozé *et al.* 2013). Telomeres spatial positioning within the nuclear space is less clear in mammals (**Figure**

10). A first report in human lymphocyte indicated that telomeres are not close to the nuclear lamina and rather tended to be within the nuclear interior (Amrichová *et al.* 2003). More recent studies showed that human telomeres organization depends on the cell-cycle and that in G1 telomeres are associated with the nuclear lamina (Crabbe *et al.* 2012). This was confirmed by genome-wide studies using the new MadID technique (Sobecki *et al.* 2018). Furthermore, reports have shown light on the interaction between telomeric proteins and the nuclear lamina network, suggesting interconnections between heterochromatin sub-compartments (Wood *et al.* 2014).

Interestingly, mice have acrocentric chromosomes. This creates a specific spatial organization of telomeres as half of the telomeres are located near to chromocenters, and the other half are dispersed throughout the nucleoplasm (**Figure 10**). In human, chromosomes can be metacentric, sub-metacentric or acrocentric. Such chromosome organization might be important for the generation of nuclear subcompartments.

2. Protein composition of telomeres

In somatic cells, there is a telomere attrition at each mitosis, which is responsible of the 'Hayflick limit' that postulates that each cell possess only a limited number of cell division before activating senescence signaling (Hayflick and Moorhead 1961; Shay and Wright 2005; Daniali *et al.* 2013). Interestingly, telomere shortening along the life resulting from DNA replication and the many damages it can generate acts as a barrier to tumor formation, as a minimal length of only one chromosome ends can trigger a cellular growth arrest signaling (Hemann *et al.* 2001).

Because of the replication process that uses a DNA template, chromosome ends face the 'end replication problem' (Watson 1972). Evolution has selected the use of the telomerase protein that can extend the 3' ends of chromosomes (Shay and Wright 2019). Telomere ends are maintained via the telomerase (TERT) protein, which bears a reverse transcriptase activity (**Figure 18B**)(Greider and Blackburn 1987). Indeed, ectopic expression of telomerase rescues the shortening of telomeres and extend the life-span of cells (Bodnar *et al.* 1998). TERT functions with an RNA component (TERC) that provides a template for its activity, the dyskerin protein (DKC1) and other associated proteins such as TCAB1, NHP2 and NOP10 (Shay and Wright 2019). The structure of the telomerase bound to DNA was only recently obtained (Nguyen *et al.* 2018). Telomerase expression is limited to embryonic and adult stem cells, whereas most somatic tissues have no detectable telomerase expression (Cohen *et al.* 2007). When expressed, telomerase elongates only seven per cent of the shortest telomeres at each S-phase, suggesting an efficient control of telomere elongation (Teresa Teixeira *et al.* 2004).

Many proteins act throughout the cell-cycle to ensure telomere-protection from DNA damages. Among these proteins are the TRF proteins that can control telomere length (van Steensel and de Lange 1997). TRF1, TRF2, RAP1 and TIN2 together form the shelterin complex that act in different ways to protect telomeres and avoid DNA damages (**Figure 18B**)(de Lange 2018). The sheltering complex does not act alone but rather recruits, when needed other proteins like TPP1, POT1, RPA or 53BP1. 53BP1 was indeed demonstrated as promoting non-homologous end joining by increasing chromatin mobility, suggesting that telomere localization and movement within the nucleoplasm is of particular importance (Dimitrova *et al.* 2008). Telomere protein composition is dynamic and can be cell specific. Studies have focused on identifying all the proteins present at particular loci, notably telomeres by developing the PICCh technology (Déjardin and Kingston 2009). TRF2, via its basic N-terminal domain, can bind DNA in a sequence-independent manner to branched DNA, which notably includes the T-Loop structure (Schmutz *et al.* 2017).

Many cancer cells for example have evolved a telomerase-independent pathway called ALT (Alternative-Lengthening of Telomeres) that stabilizes telomere length using recombination when heterochromatin might be compromised (Voon *et al.* 2016). This process was recently showed to be highly dynamic and rely on phase-separation mechanism (Min *et al.* 2019). Indeed, in ALT-positive cancer cells, telomeres tend to cluster in PML NBs. Min *et al.* have constructed an artificial system to generate phase-separation clustering of telomeres using an array of polySUMO chains. They observe that, when co-overexpressed with Bloom (BLM) helicase in human cells, this induced ALT-phenotypes that relied on both TRF2 and RAD52. Interestingly, TRF2 must be SUMOylated to induce the ALT-pathway, a SUMOylation process favored by PML-concentration of SUMO peptides. Interestingly, although embryonic stem cells express TERT, they display a related telomeric organization with high levels of PML NBs colocalization (Chang *et al.* 2013). PML NBs contain DAXX, which increases its telomeric localization upon DNA demethylation (He *et al.* 2015). DAXX and PML maintain the heterochromatin state of telomeres via H3.3 deposition and subsequent lysine 9 trimethylation (Udugama *et al.* 2015). Indeed, telomeric heterochromatin is enriched in H3K9me3-histone modification. Although Suv39H1/2 dKO cells display telomere defects, more recent observations suggest that the main enzyme responsible for H3K9me3 at telomeres might be SETDB1 (Karimi *et al.* 2011; Elsässer *et al.* 2015; Gauchier *et al.* 2019; García-Cao *et al.* 2004).

Telomere length vary greatly between species due to the differences in telomere constitution and maintenance mechanisms. Protection of DNA ends is essential to prevent undesired recombination events and DNA damages which can arise at DNA ends.

(Robin *et al.* 2014). The length of the telomere can influence expression of the Isg15 gene which is not in contact with telomeric heterochromatin nor activated via DNA damages signaling at the DNA ends (Lou *et al.* 2009). Using an adapted HiC technique, Robin *et al.* have mapped genomic association with telomeres and described that at least three genes located in subtelomeric regions. Telomeric loops can extend to up to 10 Mb away from DNA ends and may thus regulate chromatin state of many loci in a mechanism the authors called telomere position effect over long distances (Robin *et al.* 2014). Telomere position effect has been conserved throughout evolution as it is also important in yeast where telomere loops can regulate expression of genes located up to 20 Kbs away (Gottschling *et al.* 1990; Bruin *et al.* 2001). These results highlight that heterochromatin telomeric chromatin might have additional roles in global chromatin organization and gene silencing that extend beyond its locus.

A rare event can lead to upregulation of the telomerase gene, which is propagated within the subsequent cancer. The TERT promoter is embedded within a CpG island. Changes in TERT promoter is often associated with TERT transcription in cancers (Lee *et al.* 2019; Liu *et al.* 2017). TERT transcription is regulated by transcription factors bindings its promoter and aberrant transcription factor such as MYC can enhance transcriptional activity of the telomerase gene (Wang *et al.* 1998a). Furthermore, genomic mutation can arise in TERT promoter and promotes its expression such as observed for melanoma (Huang *et al.* 2013). The vast majority of cancer cells display TERT expression, yet ~10 – 15% use the ALT-mechanism (**Figure 18B**)(Bryan *et al.* 1997).

Marzec *et al.* decided to assess all genome locations where TRF2 was binding in ALT-positive cells. They observed that TRF2 binds to many locations throughout the genome, and interestingly at NR2C/F binding sites (a hormone regulated nuclear receptor). NR2C/F promotes spatial proximity of telomeres and favors telomere-telomere recombination necessary for ALT. It can trigger insertion of telomeric sequences into the genome, creates fragile sites and promotes genomic instability. Thus, ALT-cancer cells-genomic instability might be partially explained by telomere defects (Marzec *et al.* 2015). ALT-positive cancer cells often display deactivating mutations in Daxx, H3.3 or Atrx genes (Jiao *et al.* 2011; Heaphy *et al.* 2011; Ahvenainen *et al.* 2018; Schwartzenruber *et al.* 2012; Clynes *et al.* 2015; Napier *et al.* 2015; Barthel *et al.* 2017; Voon *et al.* 2016). ATRX regulates cohesion of sister chromatid and when lost, cancer cells display defective cohesion and increased non-homologous recombination leading to genomic instability (Ramamoorthy and Smith 2015). Interestingly, it was recently observed that ALT-mechanism is not a consequence of a lack of heterochromatin at telomeres, but rather results from heterochromatin formation via the SETDB1 methyl-transferase (Gauchier *et al.* 2019). Gauchier *et al.* report that ALT characteristics appear as an excess of heterochromatin features like H3K9me3

provided by SETDB1 and that depletion of Setdb1 can suppress ALT phenotypes. These results suggest that telomeric heterochromatin must be tightly regulated to avoid genomic instabilities.

Mutations of the main component of telomere maintenance are also implicated in the dyskeratosis congenita disorder, such for telomerase and dyskerin (Mitchell *et al.* 1999; Armanios *et al.* 2005). Dyskeratosis congenita is a rare disease affecting different tissues. Patients display skin hyperpigmentation, nail dystrophy and aplastic anemia, which can be accompanied from pulmonary and liver fibrosis. It mainly affects regenerative tissues via the increase of chromosome instability due to lower levels of telomerase and associated shorter telomeres (Mitchell *et al.* 1999). Nowadays, many genetic diseases have been linked to telomere dysfunction and are referred to as telomeropathies (Holohan *et al.* 2014).

Telomeres are important constituent of the constitutive heterochromatin. Their localization and maintenance mechanisms can differ from cell to cell. Their stability is particularly important for the cell and defects in telomere protein can lead to enhanced genomic instabilities and diseases.

E - Transposable Elements

About 70 years ago, Barbara McClintock proposed that a phenotypic characteristic of maize could be explained by transposition of mobile genetic elements (McClintock 1956). Although this claim was welcomed with skepticism at that time, she was later rewarded for her discovery. In the early 2000's, the publication of the human genome shed the light on the fact that protein-coding genes account for merely 2% of the entire genome. In total, about half of mammalian genomes are composed of transposable elements (TE) and virtually all organisms contain TEs, which are scattered all along the genome.

1. Localization and definition of TEs

Two classes of TEs exist. Class I corresponds to retrotransposons that can have LTR sequences or non-LTR. Class I retrotransposon uses a reverse-transcription phase that allows these elements to undergo duplicative transposition - at each transposition, their number increases. Class II are DNA transposons that can be either autonomous or non-autonomous. Class II DNA transposons do not use a reverse-transcription step and integrate with a cut and paste mechanism. They are first excised from the genome and then integrated elsewhere, thus they do not increase their abundance. Class I TEs use an RNA intermediate and they are transcribed by the RNA Polymerase II. Thus, they must be tightly regulated. TEs have coevolved with their host genomes and transcription and integration events have been used by the host as an adaptive force yet

important regulation pathways have emerged to restrain this capacity to avoid disastrous integrations. Many families coexist within mammalian genomes and the sum of TEs present within an organism is called its endovirome (Friedli and Trono 2015).

Class II TEs are DNA transposons that move by cycles of excision-insertion and as such their number stays constant and are thus the less important group of TEs (**Figure 19**). They possess short terminal inverted repeats (ITR) and members of this family include the Tigger and Charlie elements (Smit and Riggs 1996). DNA transposons have given rise to essential human genes such as the RAG recombinase that generates the wide variety of antibodies (Huang *et al.* 2016; Zhang *et al.* 2019a). Yet, as no such transposons are still active in humans, I will mainly focus on the TEs class I.

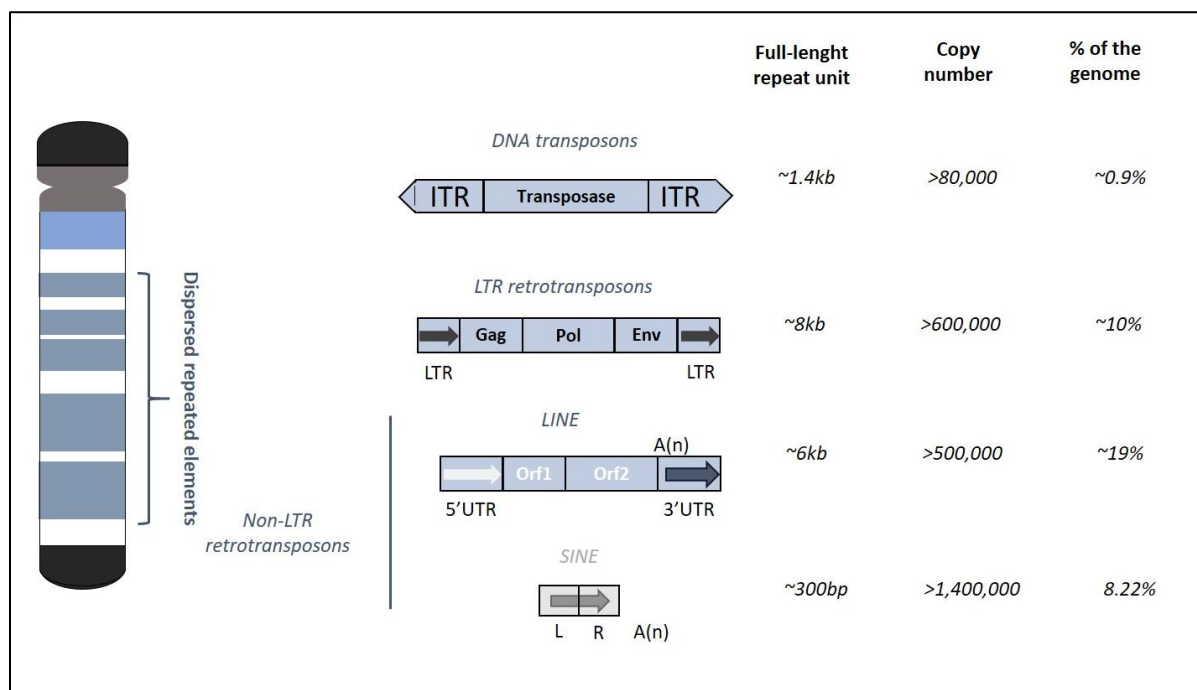


Figure 19 | Overview of the classes of transposable elements in mouse. Class II TEs represent the DNA transposons. Of about 1.4Kbs in length, they only represent up to 0.9% of the murine genome. They transpose via a cut and paste mechanism. Class I TEs are mobile via a copy-paste mechanism, which increases their number at each transposition. LTR retrotransposons, such as IAP elements, possess LTR repeats at ends. About 3.13% of the murine genome is composed of these elements, and many ‘solo-LTR’ are observed, remnants of past transpositions. Non-LTR elements comprise the LINE and the SINE elements. LINE elements are present within heterochromatin regions and are the most abundant families of TEs. ORF2 carries endonuclease and reverse-transcriptase activities. SINE elements are found within euchromatin regions. They do not encode for proteins and thus rely of the ORF2 of LINE to retrotranspose. Data from Mouse Genome Sequencing Consortium, *Nature* 2002.

Class I TEs can be referred to as endogenous retroelements (EREs) and is divided into two categories - long terminal repeats (LTR) and non-LTR elements. EREs account for 90% of all TEs in mouse and human genomes (Beck *et al.* 2011). While LTR elements encode the gag and pol proteins that are related from retroviral proteins, yet they do not transcribe the envelope protein, which precludes their existence within the host cell. These elements are named endogenous retroviruses (ERVs) (**Figure 19**). ERVs are 7 to 9 Kbs length but LTR sequences might recombine

and leave solitary 'solo' LTR throughout the genome, that represent the majority of the observed LTR sequences (Chuong *et al.* 2017). In human, at least 31 families of ERVs have been described based on sequences homology and they display almost no transposition activity, except for one HERVK (Mayer *et al.* 2011; Marchi *et al.* 2014; Feschotte and Gilbert 2012). In mouse however, more recent ERVs are described - the intracisternal A particles (IAP) and ETn/MusD which are still active and are responsible for about 10% of the spontaneous mutations (Maksakova *et al.* 2006). LTR-containing endogenous retroviruses arise from an ancient infection of germ cells by an exogenous retrovirus as it was exemplified for IAP which has lost its envelope gene but gained a reticulum endoplasmic targeting signal allowing a complete intracellular replicative cycle (Ribet *et al.* 2008). Non-LTR class I TEs comprise the short and the long interspaces nuclear elements (SINEs and LINEs). SINEs are 300 bp length but present in about 1.8 million copies, the larger member of this family being the *Alu* element in human and the B1 and B2 families in mouse, from which only ~1,000 are still active (**Figure 19**). SINEs are non-autonomous elements as they do not encode for any proteins and thus rely on the transcription of the LINEs, which impacted their rate of insertions that diverge greatly among species. *Alu* elements encode for small components of RNA polymerase III promoter and a polyA tail. LINEs are about 6 Kbs length and encode for two proteins - ORF1 and ORF2. ORF1 encodes for an unknown protein and ORF2 encodes for a protein that carries endonuclease and reverse-transcriptase activities. LINE1 possess a CpG-rich internal promoter recognized by the RNA Pol II. LINEs represent ~20% of the human and mouse genomes with ~950,000 copies found (**Figure 19**). However, many of these copies are degenerated sequences and only 10,000 are full-length elements, from which ~100 are active (Friedli and Trono 2015). Each family of young TEs display very high similarities among members, making it difficult to assess by sequencing technologies, but along evolution, each element will degenerate.

The different TEs display diverse integration preferences. SINEs are mainly observed in gene-rich euchromatin regions, however the exact insertion site varies between intergenic, intronic and even exonic regions (Versteeg *et al.* 2004). Interestingly, younger *Alu* seems to exhibit a LINE-like integration profiles which is enriched in heterochromatin regions. Prescott Deininger proposes that young *Alu* elements are removed from heterochromatin during evolution (Deininger 2011). Furthermore, euchromatin highly-transcribed regions might be more accessible for *Alu* elements. On the contrary, older LINE-1 and ERVs are preferentially observed in heterochromatin regions, suggesting that they are evolutionary removed from euchromatin (Lander *et al.* 2001). These discrepancies between integrations preferences rely on the chromatin state and associated-proteins that are recruited at each localization.

2. Regulation of TEs

To avoid any detrimental retrotransposition of LINE and ERVs, cells have evolved diverse repression mechanisms. Repressive mechanisms rely either on chromatin modifications to prevent transcription, or on the use of viral protection machineries.

Cellular factors have emerged to prevent integration of exogenous and endogenous retroviruses which are part of an innate immunity system. Such pathways use proteins like the APOBEC family, which have a cytidine deaminase activity and carry a post-transcriptional control over TEs (Harris *et al.* 2003; Mangeat *et al.* 2003; Esnault *et al.* 2005). APOBEC enzymes convert C-to-U during the reverse transcription of the nascent retroviral DNA, acting as a general mechanism to limit the effect of retroviruses by a G-to-A hypermutation. Other proteins such as the three-prime-repair exonuclease 1 (TREX1) mediates reverse transcripts-degradation of LINE1 and IAP (Stetson *et al.* 2008). TREX1 is part of the IFN-stimulatory DNA (ISD) response that senses viral infection within the cell, suggesting common mechanisms at play. Other factors of the ISD response that actively suppresses retroviral infection, notably the TRIM5 α which recognizes retroviruses capsid could have evolved to prevent endogenous retroviral integration along the evolution (Kaiser *et al.* 2007; Pertel *et al.* 2011). Moreover, the density and positioning of nucleosomes at a genomic locus can also modulate the integration frequency for murine leukemia virus (MLV) (Benleulmi *et al.* 2015). Other cellular strategies can exert a post-translational control over retroviral proteins. The cellular factor TEX19.1 is expressed upon hypomethylation of pluripotent cells and can bind to and stimulates the polyubiquitination of the ORF1 protein produced by LINE1 elements (Maclennan *et al.* 2017). Polyubiquitination of ORF1 protein leads to its degradation and prevents new genomic insertions. These results suggest that selected networks of cellular immunity to prevent viral infection might apply or be rewired to counteract endogenous retroviruses integrations.

Contrary to exogenous viral infection, the cellular factors preventing ERV insertions are only necessary if they are expressed in the first place. Chromatin modifications associated with heterochromatin are established to maintain proper silencing of these sequences. DNA methylation at CpG is a common mechanism in mammals to ensure transcriptional repression of TEs (**Figure 20**). Indeed, loss of DNA methylation via the depletion of Uhrf1 for example, results in the upregulation of LINE1 and IAPs (Bostick *et al.* 2007; Sharif *et al.* 2007). DNA methylation likely exerts its function via methyl-binding proteins such as MeCP2 as patients suffering from Rett syndrome display higher levels of LINE1 expression in the brain, indicating that TEs are regulated in a tissue-specific way (Muotri *et al.* 2010). Other proteins act to ensure the proper establishment of DNA methylation profiles. The pluripotency factor DPPA3 protects the specific genomic

localizations against DNA demethylation and its loss results in the diminution of IAP but not LINE1 DNA demethylation (Nakamura *et al.* 2007). Upon depletion of the lymphoid-specific helicase 1 (LSH1), cells display large DNA demethylation, notably at IAP, LINE1 and SINE B1, which results in the loss of repressive histone modifications and upregulation of their transcription (Huang *et al.* 2004; Dennis *et al.* 2001; Yan *et al.* 2003; Yu *et al.* 2014).

Histone methylation, notably the H3K9me3 is observed at a wide variety of TEs - LTR and non-LTR ones (Bulut-Karslioglu *et al.* 2014; Kondo and Issa 2003; Martens *et al.* 2005; Mikkelsen *et al.* 2007). However, deletion of each protein from the H3K9me3 maintenance pathway display a somehow specific deregulation pattern. Deletion of Suv39H1 and 2 seems to impair repression of full-length LINES in pluripotent but not differentiated cells (Bulut-Karslioglu *et al.* 2014). Interestingly, pluripotent embryonic stem cells present an ERV-dependent repressive H3K9me3 mediated by the other H3K9me3 methylase SETDB1 (Matsui *et al.* 2010). Matsui *et al.* demonstrated that LTR-containing TEs such as IAP and MusD were regulated by H3K9me3-mediated deposition of SETDB1, but not non-LTR elements like LINE1. Although H3K9me3 is enriched at these elements, it is not the only histone modification as H4K20me3 is observed too. Yet, deletion of H4K20me3 methylases Suv420H1 and 2 did not impair neither H3K9me3 enrichment nor ERV expression, suggesting that it is not required for proper repression but might only strengthen the repressive environment. H3K9me3 enrichment correlates with the presence of KAP1 (also named TRIM28) (**Figure 20**) (Matsui *et al.* 2010). In fact, KAP1 recognizes endogenous retroviruses such as IAPs, but also exogenous retroviruses such as MLV and then recruits SETDB1 to establish an H3K9me3 chromatin state, as depletion of KAP1 induces the loss of H3K9me3 at IAPs (Rowe *et al.* 2010; Wolf and Goff 2007). Furthermore, KAP1 act as a scaffold for a large complex comprising SETDB1 but also the histone deacetylase containing NuRD complex and the H3K9me3-binding protein HP1, thus creating a local heterochromatin state (Wolf *et al.* 2008; Macfarlan *et al.* 2011; Schultz *et al.* 2001; Sripathy *et al.* 2006). The KAP1-mediated silencing of ERVs is limited to the embryonic development, when the level of DNA methylation is low (Rowe *et al.* 2010). MLV is targeted by KAP1 because of its primer binding site (PBS), a sequence complementary to proline tRNA (Wolf and Goff 2007). Transcriptional repression of the two alleles of exogenous Moloney murine leukemia virus (MMLV) is asynchronously mediated and it is likely that it reflects an iterative silencing process that may also control endogenous TEs (Schlesinger *et al.* 2014). Histone-modification based silencing mechanisms are particularly important in murine embryonic stem cells. Indeed, mESCs are refractory to exogenous viral infections (Teich *et al.* 1977). Furthermore, mESCs can overcome the absence of DNA methylation for proper survival and ERV repression. It is proposed that additional chromatin pathways specific

to pluripotent cells have emerged to ensure the transcriptional silencing of TEs and avoid any mutational potential during the embryonic development (Leung and Lorincz 2012). Yet, further studies will likely present a finer comprehension of TE repressive processes and a better understanding of the reciprocal impact of both histone modification-based and DNA methylation mechanisms and how they both influence each other and ensure a complex and robust silencing of TEs (Turelli *et al.* 2014).

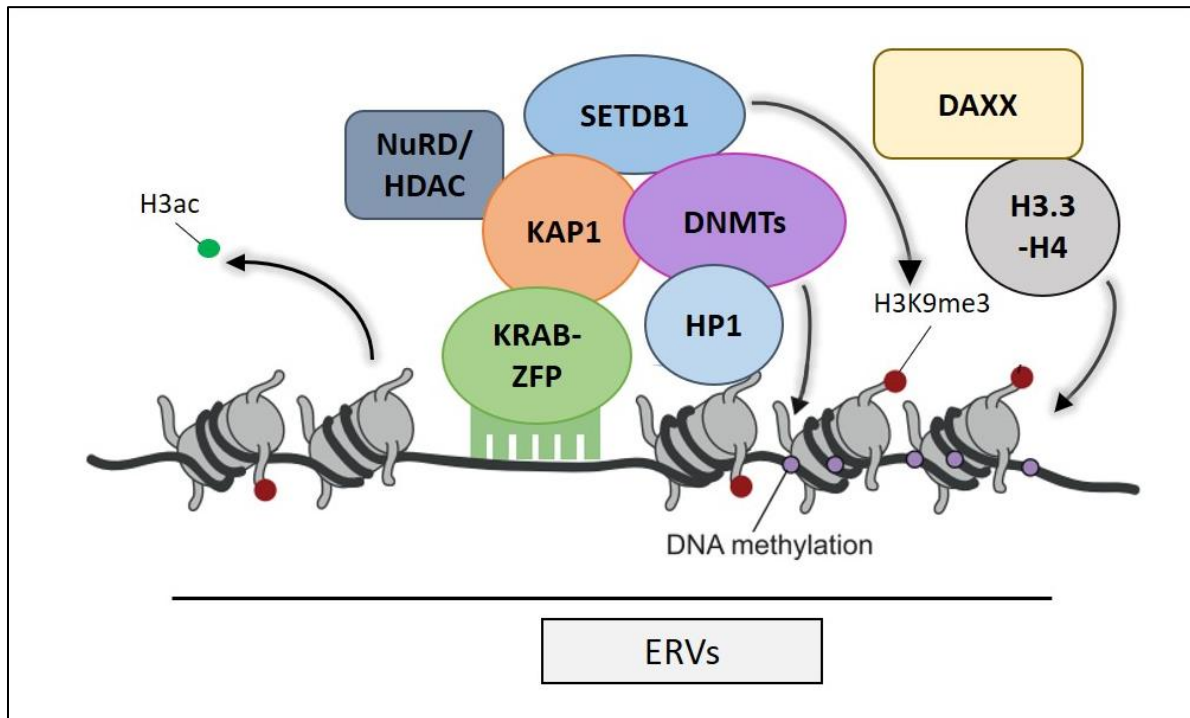


Figure 20 | Multiple proteins ensure transcriptional repression of ERVs. KRAB-ZFPs bind to DNA and recruit KAP1. KAP1 binds to diverse heterochromatin-related proteins and enables heterochromatin formation at ERV sequences. Among the recruited proteins are DNMTs that methylate DNA, SETDB1 which trimethylates H3K9, subsequently bound by HP1 and NuRD/HDAC complexes that remove histone acetylation. DAXX can also be part of SETDB1/KAP1 complex and deposits H3.3-H4 dimers into these heterochromatin regions. Adapted from Ecco, Imbeault and Trono, *Development* 2017.

KAP1 association with chromatin is mediated by its DNA-binding co-factors - the krüppel-associated box domain-zinc finger (KRAB) proteins, one of the largest family of transcription factors in mammals (Huntley *et al.* 2006). KRAB zinc-finger proteins (ZFPs) are composed of one KRAB and two C2H2 zinc-finger domains. The KRAB domain allows interaction with KAP1, whereas the zinc-finger domains mediate the binding to specific DNA sequences (Yang *et al.* 2017). During the evolution path, TEs have degenerated from their original sequence, yet they still need to be suppressed by cellular factors. KRAB-ZFPs are rapidly evolving proteins, and notably the zinc-finger domains (Liu *et al.* 2014). This particular feature of KRAB-ZFPs have likely arise as a co-evolution arms race between TEs, that try to escape transcriptional silencing, and repressive cellular factors, that are selected on their ability to bind a diverse range of targets (Thomas and Schneider 2011; Jacobs *et al.* 2014). Although essential for the embryonic development, the role of

KRAB-ZFPs seems restricted to the pluripotent cells, suggesting that these proteins initiate the silencing of ERVs during mammalian development and become dispensable upon cell differentiation (Wolf *et al.* 2015). Furthermore, from genome-wide sequencing data, it seems that KRAB-ZFP-repressive role happens at ERVs, but also at non-LTR retrotransposons including LINES and SINEs (Jacobs *et al.* 2014).

At the chromatin level, it was recently observed that the histone chaperone complex DAXX/ATRAX could regulate the transcriptional activities of a subset of ERVs via H3.3 deposition in embryonic stem cells (**Figure 20**)(Elsässer *et al.* 2015). Using a ChIP-reChIP strategy, Elsässer *et al.* observed that H3.3K9me3 is particularly enriched at ERV sequences, as well as DAXX and ATRAX. Depletion of H3.3 leads to a loss of the transcriptional repression of IAPs and MusD repeats, suggesting a particular function for H3.3 in the maintenance of K9me3-heterochromatin compartment in pluripotent cells, which is coherent with its role in K9me3-enrichment at telomeres in these cells (Udugama *et al.* 2015). The amount of H3.3K9me3 is drastically reduced in Setdb1 KO cells, suggesting that DAXX/ATRAX-deposition of H3.3 functions in the same repressive pathway than the SETDB1-KAP1 complex, and reciprocally, the levels of KAP1 are reduced when cells lack the H3.3 variant (Elsässer *et al.* 2015). The authors observed a physical interaction between DAXX and KAP1, that is independent of the presence of H3.3, and thus proposed that DAXX functions in the KAP1-SETDB1 complex at a subset of ERVs to establish the local heterochromatin environment, which could then be maintained by SUV39H1/2 enzymes (Bulut-Karslioglu *et al.* 2014). Intriguingly, DAXX/ATRAX complex-binding sites increases upon DNA demethylation, and notably at LTR-containing ERVs, concomitantly with an increase of H3K9me3 signal (He *et al.* 2015). Furthermore, depletion of Daxx or Atrx results in the upregulation of IAPs, that the author attributes to the loss of H3K9me3. However, DAXX-mediated silencing of ERVs can happen via an ATRAX-dependent and an ATRAX-independent pathway (Hoelper *et al.* 2017). Hoelper *et al.* propose that H3.3 stabilizes DAXX, and that H3.3 thus carries a role in the DAXX-H3.3-ATRAX silencing pathway; but they suggest that an additional DAXX-SETDB1-KAP1-HDAC1 pathway might favor silencing of specific ERVs without ATRAX nor H3.3 incorporation. Another report assessed the role of ATRAX in creating a local heterochromatin environment at IAP sequences (Sadic *et al.* 2015). Sadic *et al.* further reported that ATRAX binds to a short region of 160bp from the *gag* gene present in over 600 IAP elements. This short sequence was sufficient to induce the silencing of an exogenous DNA fragment and was thus called SHIN standing for short heterochromatin inducing sequence. These results suggest that multiple factors are acting differentially to ensure the proper silencing of TEs.

Because of the high diversity of TE sequences, many cellular proteins target only a subset of elements to create a common local heterochromatin environment consisting in DNA methylation and H3K9me3. This local heterochromatin compartment can vary according to the cell type, with the DNA methylation being the prominent repressive factor in somatic cells, whereas H3K9me3 pathway seems to be key during the embryonic development.

3. Diversity of functions of the transposable elements

TEs have had a great impact on the evolution of their host genomes. When they are embedded into a local repressive environment, TEs are part of the broader heterochromatin and B compartment in the nucleus. Because of their important number of individuals, TEs likely play a role in the maintenance of the three-dimensional folding of chromatin (Cournac *et al.* 2016). In *Drosophila*, the *gypsy* DNA retrotransposon contains many binding sites for transcription factors and acts as an insulator domain. The insulation role of *gypsy* is mediated by the formation of a local loop for regions surrounding the insulator, suggesting that *gypsy* retrotransposon can regulate higher-order chromatin folding (Byrd and Corces 2003). Furthermore, mammalian genomes are notably organized via the action of the CTCF transcription factors. Interestingly, Schmidt *et al.* analyzed CTCF-binding sites across diverse mammalian species and discovered highly conserved motifs corresponding to a two-part sequence separated by 20 or 21bp (Schmidt *et al.* 2012). Interestingly, the CTCF-binding sequences in mouse, rats, dogs and opossum are present within SINEs. The authors proposed that repeat-drive CTCF-binding sites expansion result from waves of SINE retrotransposons activities over the evolution of mammalian genomes (Schmidt *et al.* 2012). TEs may thus represent an important source of evolution of the spatial organization of the genome. LINE1 expression can be regulated by the condensin II protein, which suggest that although LINEs might maintain the 3D-folding of the genome, their expression is also controlled by the spatial organization (Ward *et al.* 2017).

Furthermore, upon the loss of repressive marks and the subsequent transcriptional activation, TEs become a strong force to modulate the global compaction state of the genome. This particular feature is exploited by mammalian genomes during the early embryonic development. Indeed, following fertilization, the embryo possess a densely compact genome and upon the loss of DNA methylation, the 2-cell state correlates with peaks of expression of LTR and non-LTR endogenous retrotransposons (Fadloun *et al.* 2013). It was proposed that the global transcription of repeated elements was a mean to achieve a fast and robust general decompaction of the genome coinciding with the first transcription activity of the zygotic genome (Jachowicz *et al.* 2017). I will discuss this point more thoroughly in the last part of the introduction.

While cells adopt a wide variety of factors to repress the expression of TEs, some have been ‘domesticated’ and their expression is tolerated or even essential for cell survival (Lowe and Haussler 2012). Lowe and Haussler searched for putative regulatory elements that originated from mobile elements such as SINE, LINE and ERVs, and they detected over 280,000 possible sequences that presented cross-species constraint and a purifying selection, without any detectable RNA transcript. The authors propose that about 20% of regulatory sequences in human might have emerged from the domestication of TEs, suggesting that TEs have indeed served as a source of non-coding regulatory sequences. Demonstration of such ‘exaptation’ was performed by Bejerano *et al.* which described an enhancer perfectly conserved in human, mouse and rat that originated from a SINE retrotransposon active in an ancient organism and still active in the Indonesian coelacanth (Bejerano *et al.* 2006). The authors thus called this element a ‘living fossil’ as it is still active in one specie and shown that this element indeed could serve as a regulatory element for a reporter gene. Differentiation of regulatory T cells depends on FOXP3 factor and it was observed that a conserved enhancer of FOXP3 that lie in one of its introns is derived from a retrotransposon and is specific to placental mammals (Samstein *et al.* 2012). This regulation is crucial for the proper development of regulatory T cells to allow maternal-fetal tolerance during pregnancy. This hypothesis was already though to be important for promoter regulation of a gene, such as for the salivary amylase gene which in human requires the presence of an ERV to maintain its tissue-specific expression (Ting *et al.* 1992). These results indicate that co-option of TEs to become regulatory elements have happened and these events likely arise as an additional mean to confer specific spatio-temporal control of gene expression (Thompson *et al.* 2016). TEs are crucial modulator for the evolution of their host genome, however, trans-species transmission of TEs must be happening via exogenous source of retroviruses and propagation as endogenous retroviruses could then shape the new host genome. Endogenization of a retrovirus is ongoing in koalas where the koala retrovirus (KoRV) has invaded only a subpopulation of animals, but is present in germ cells and is transmitted to the progeny (Tarlinton *et al.* 2006; Fiebig *et al.* 2006). These results indicate that not only the present ERVs, but also exogenous retroviruses could play a role in genome regulation.

Although important player for genomic evolution, TE transcription and integration can be detrimental for the cell. Indeed, about 10 % of spontaneous mutations in mouse and 50% in *Drosophila* arise from *de novo* insertions of TEs and in human, more than 120 pathologies are linked to *de novo* insertions (Cosby *et al.* 2019). TEs overexpression is sometimes a consequence of particular disease, such as the Rett syndrome for which patients display elevated LINE1 retrotranspositions (Muotri *et al.* 2010). LINE1 upregulation of transcription or retrotransposition

is a hallmark of many cancers (Burns 2017). Loss of DNA methylation is often observed in certain cancers, which thus express higher levels of LINE1 RNA due to a loss of repressive marks. Hypomethylation of LINE1 was correlated to enhanced genomic instability and poor prognosis for non-small-lung, colon and breast cancers (Daskalos *et al.* 2009; Ogino *et al.* 2008; van Hoesel *et al.* 2012; Saito *et al.* 2010). Upregulation of TEs can lead to the increase of the interferon response in acute myeloid leukemia (Cuellar *et al.* 2017). In lung cancers, it is observed that LINE1 upregulation correlates with enhanced new insertions (Iskrow *et al.* 2010). Furthermore, the capacity to perform genome-wide DNA and RNA sequencing as led to propose a role for TEs in tumorigenesis, as LINE1 insertions in somatic cancer cells are preferentially observed at genes that are frequently mutated in these cancers (Lee *et al.* 2012). Colorectal cancer often originates from a mutation in the adenomatous polyposis coli (APC) tumor suppressor gene. It was reported early on that a LINE1 insertion could occur within the APC gene as it was observed for patient cells (Miki *et al.* 1992). It recently demonstrated that LINE1 integration events could indeed lead to the disruption of one APC allele as a consequence of the derepression of an active LINE1 in non-tumor cells (Scott *et al.* 2016). When combined with a spontaneous mutation on the other APC allele, it could lead to cancer. Thus, active TEs represent an important source of variation that can potentially drive tumorigenesis, as well as creating genomic instability when it happens as passenger mutations.

In conclusion, transposable elements are important modulator of genome function and evolution. TE sequences can be coopted by the host genome to generate new regulatory system that take advantages of their activities and transcription factor binding sites. Yet the lack of repression exerted by the host cells can lead to undesired mutations and pathologies.

F - Nuclear Bodies

Different nuclear bodies have been observed in cells. Contrary to the heterochromatin compartments presented above, the main common characteristic of nuclear bodies is the enrichment of certain proteins and not specific chromatin domains. Indeed, high concentration of some proteins can generate membrane-less organelles, which can carry specific functions.

The Nucleolus

The nucleolus was the first sub-nuclear compartment identified. However, comprehensive understanding of its assembly and functions required a long time.

1. Definition of the nucleolus

Firstly observed during the 19th century, the nucleolus was not the center of attention of many biological studies until the realization that nucleolus arises at specific loci that was called the nucleolus organizer regions (NORs) by Barbara McClintock in 1934 (Pederson 2011). Within the nucleolus are the rDNA genes encoding for ribosomal RNAs which are actively transcribed. The nucleolus organizes as a tripartite organelle. The fibrillar center (FC) correspond to the multiple rDNA genes, the dense fibrillar compartment (DFC) is made from the synthesis of rRNAs and the granular component (GC) is the place of ribosome assembly (Tiku and Antebi 2018). Because of its function of ribosome biogenesis, the nucleolus regulates the metabolic state of the cell. Thus, active cells have large and numerous nucleoli whereas cell cycle arrest reduces the size of the nucleolus. In mammalian cells, nucleoli must reassemble after each mitosis around NORs. rDNA transcription is carried by the efficient RNA Polymerase I. Many additional small nucleolar RNAs and proteins reside within the nucleolus and participate into the transcription and maturation processes. Not all rDNA genes are transcribed within the same cell at the same time. Furthermore, associated proteins such as UBF are essential in this process as depletion of UBF changes rDNA genes from an active to an inactive state (Sanij *et al.* 2008). The nucleolus is a specialized sub-nuclear compartment that comprises DNA, RNA and proteins and carries the essential ribosomal biogenesis function.

The nucleolus act as a nuclear landmark and can associate with chromatin regions (Canat *et al.* 2020). Human centromeres were observed to specifically localize closely to the nucleolus (Carvalho *et al.* 2001). Furthermore, entire large regions could interact with the nucleolus as reported for the X inactive chromosome, in which case, the nucleolar association seems necessary for proper silencing (Zhang *et al.* 2007). Initial genome-wide identification of genomic regions that could associate with the nucleolus described the nucleolus-associated domains (NADs) which encompassed ~4% of the human genome and confirmed that is mostly corresponds to heterochromatin regions such as satellite repeats and transposable elements (Németh *et al.* 2010). Further characterization of NADs revealed that the ~1600 heterochromatin regions in fact cover ~40% of the human genome (Dillinger *et al.* 2017). Human NADs are ~800Kb long on average and correspond to classical heterochromatin regions with a low gene content and enrichment of repressive histone modifications and present a high overlap with LADs. Interestingly, although nucleoli are strongly reorganized upon senescence, NADs largely retain their nucleolar association and display only moderate changes in expression. The regions displaying the major reorganization upon senescence being centromeric and pericentromeric satellites, which disassociate from the nucleolus (Dillinger *et al.* 2017). Intriguingly, peripheral tethering of LADs is compromised in

senescent cells, suggesting different anchoring pathways to nuclear landmarks for LADs and NADs (Lenain *et al.* 2017). Characterization of NADs in mouse cells revealed a more complex picture. Vertii *et al.* observe two classes of NADs coexisting in murine embryonic fibroblasts. Class I NADs correspond to typical heterochromatin domains and present a high overlap with LADs, repressive histone marks and late DNA replication, whereas class II NADs represent a facultative heterochromatin signature with H3K27me3 signal and a more early replication timing (Vertii *et al.* 2019). Interestingly, the authors observe using DNA FISH that while class I appears either next to nucleolus or close to the nuclear periphery, the class II exclusively associate with the nucleolus. As the class II NAD is absent in ESCs, the author conclude that class II NAD corresponds to developmental genes which are only silenced upon differentiation (Vertii *et al.* 2019)

2. The nucleolus as dynamic compartment

The nucleolus is a particularly dynamic membrane-less organelle. Indeed, it self-assemble via liquid-liquid phase separation (LLPS), which depends on its transcriptional activity (Berry *et al.* 2015). Each sub-compartment (FC, DFC and GC) forming the nucleolar undergo LLPS and assemble into distinct liquid phases which do not mix together (Feric *et al.* 2016). Feric *et al.* propose that each liquid phase's properties facilitated sequestration, transcription and maturation of the ribonucleoproteins. Furthermore, not only the transcription process but also the nascent transcripts drives the formation of the nucleolar sub-compartments (Yao *et al.* 2019). Treatment with 1,6-hexanediol, which impairs LLPS seems to increase the number of nucleoli and prevented association of NAD, with a stronger effect for class II NAD, suggesting differences in anchoring mechanisms (Vertii *et al.* 2019).

The number of nucleoli is dependent on the metabolic state of the cell. For example, fusion events happen upon senescence, with only one giant nucleolus visible (Dillinger *et al.* 2017). In ESCs, rDNA genes lack repressive histone modifications due to lower levels of DNA methylation, which results in extensive transcription (Savić *et al.* 2014). rDNA genes obtain heterochromatin feature upon differentiation and inhibition of heterochromatin formation impairs ESC differentiation, underlying the importance of this mechanism. Around half of the ~400 rDNA genes are expressed in somatic cells. During the early development, one copy of each NOR is marked for later inactivation in somatic cells in a process that is clonally retain and resemble the X inactivation memory (Schlesinger *et al.* 2009). Nucleoli are strongly reorganized during embryogenesis. Transcription of rDNA genes only starts at the end of the 2-cell state but it is essential for further division (Coura Koné *et al.* 2016). From the zygote to the 4-cell state, the nucleolus appears as the nucleolus precursor body (NPB) which are mostly devoid of activity as

transcription of the rDNA genes happens at the periphery of the NPB (Kresoja-rakic and Santoro 2019). In the zygote and 2-cell state, pericentromeres appear as a ring-shape around NPBs and only organize as chromocenters from the 4-cell state (Aguirre-Lavin *et al.* 2012). These results highlight that the nucleolus is a dynamic sub-nuclear compartment, both in terms of assembly but also as an organelle that undergoes changes in shape and composition.

3. Diseases associated with nucleolar dysfunction

Center of ribosome biogenesis, the nucleolus bears a critical role in the cell. However its functions extend beyond this role as it has been implicated in many other cellular processes such as tRNA processing, pre-mRNA splicing and telomerase sequestration (Wong *et al.* 2002; Bertrand *et al.* 1998; Falaleeva *et al.* 2016). Furthermore, the nucleolus acts as a sensor for signaling pathways. Indeed, upon insulin treatment, the insulin receptor substrate 1 translocates within the nucleus, localizes specifically at the nucleolus and an increase in rRNA synthesis (Tu *et al.* 2002).

Heterochromatin surrounding the nucleolus provides stability for the silenced rDNA genes. Alteration of heterochromatin using the 5-azacytidine drug or by deleting the Su(var)3-9 gene in *Drosophila* results in rDNA instability and generates extrachromosomal rDNA circles that ultimately lead to senescence (Gagnon-Kugler *et al.* 2009; Peng and Karpen 2007). Furthermore, because of the high levels of transcription, the nucleolus undergoes many RNA-DNA hybrids, which are called R-loops and must be resolved via topoisomerases. Indeed, preventing topoisomerase activity impairs nucleolar organization (Govoni *et al.* 1994; Christensen *et al.* 2004). rDNA genes also appear to be prone to recombination, especially in some cancers (Stults *et al.* 2009). Intriguingly, ALT-positive cancer cells and ESCs depleted for Atrx display high levels of rDNA copy loss (Udugama *et al.* 2018). Udugama *et al.* describe that ribosomal DNA instability in Atrx-mutated results from impaired H3.3 deposition and subsequent heterochromatin formation at rDNA genes, suggesting that rDNA repeats are partly silenced via the same pathway than the more typical heterochromatin.

PML NBs

Promyelocytic (PML) proteins are ubiquitously expressed and assemble into 5 to 30 nuclear bodies (NBs) of 0.1 to 1 μm in diameter dispersed within the nuclear space. PML NBs have been implicated in many biological processes.

1. Definition and roles of PML NBs

PML is essential for the formation of the PML NBs and recruits many proteins such as SP100, DAXX or SUMO peptides. It acts as a hub for protein post-translational modifications like SUMOylation and ubiquitination and have been associated to a wide variety of DNA-related processes (Lallemand-Breitenbach and de Thé 2010). PML was identified as an oncoprotein in fusion with the retinoic acid receptor α (RAR α) in acute promyelocytic leukemia (APL) (Dyck *et al.* 1994; Daniel *et al.* 1993; Weis *et al.* 1994). PML and RAR α fusion arise from the t(15 -17) translocation and leads to the mis-localization of RAR α in the nucleus and expression of PML-RAR α is sufficient to lead to APL phenotypes in mouse. Furthermore, APL therapy - a combination of retinoic acid and arsenic induces the degradation of PML-RAR α and the reorganization of PML NBs (Nasr *et al.* 2009; Ablain *et al.* 2014). PML belongs to the tripartite-motif (TRIM) family and carries a RING domain that can bind to the SUMO E2 ligase UBC9, two B-boxes and a coiled-coiled domain required for homodimerization (**Figure 21A**) (Duprez *et al.* 1999; Tao *et al.* 2008; Kastner *et al.* 1992). Seven isoforms have been described in human, but only two in mouse, that in each species are generated by alternative splicing of the C-terminal region (Condemine *et al.* 2006). The different isoforms might carry distinct function, either for PML or for NB formation, which would likely explain the differences of NBs observed across cell types and conditions. PML is mainly a nuclear protein as it carries a nuclear localization sequence (NLS) on its exon 6, yet, about 10% of PML proteins might reside or shuttle into the cytoplasm where it can have other functions such as regulation of signaling pathways (Giorgi *et al.* 2010; Lin *et al.* 2004; Carracedo *et al.* 2011).

Acting as a hub for post-translational modifications, PML NBs concentrate the SUMO E2 ligase UBC9 and PML is heavily SUMOylated, along with the additional proteins sequestered into PML NBs. SUMOylation might be a recruitment pathway via the SUMO-SIM (SUMO-interacting motif) interactions of the different proteins. Indeed, PML mutants that cannot be SUMOylated can still generate NBs but subsequent partners recruitment is impaired (Shen *et al.* 2006; Sahin *et al.* 2014). Although PML NBs are easily visible under the microscope, 90% of PML proteins are diffuse in the nuclear space (Lallemand-Breitenbach and de Thé 2010). The consensus mechanism

for NB formation is that PML shell forms via PML-PML interactions, and that subsequent SUMOylation favors recruitment of SIM-containing proteins (**Figure 21B**). Recently, a biophysical model was proposed to explain PML NBs formation that could undergo a liquid-liquid phase separation process, which could be a physical principle to enhance PML concentration and render NB formation easier (Shin *et al.* 2018; Banani *et al.* 2017, 2016). It was also reported that polySUMO-polySIM interactions could induce liquid-liquid phase separation, thus suggesting that SUMOylation of PML and other partners might reinforce the stability of PML NBs (Min *et al.* 2019).

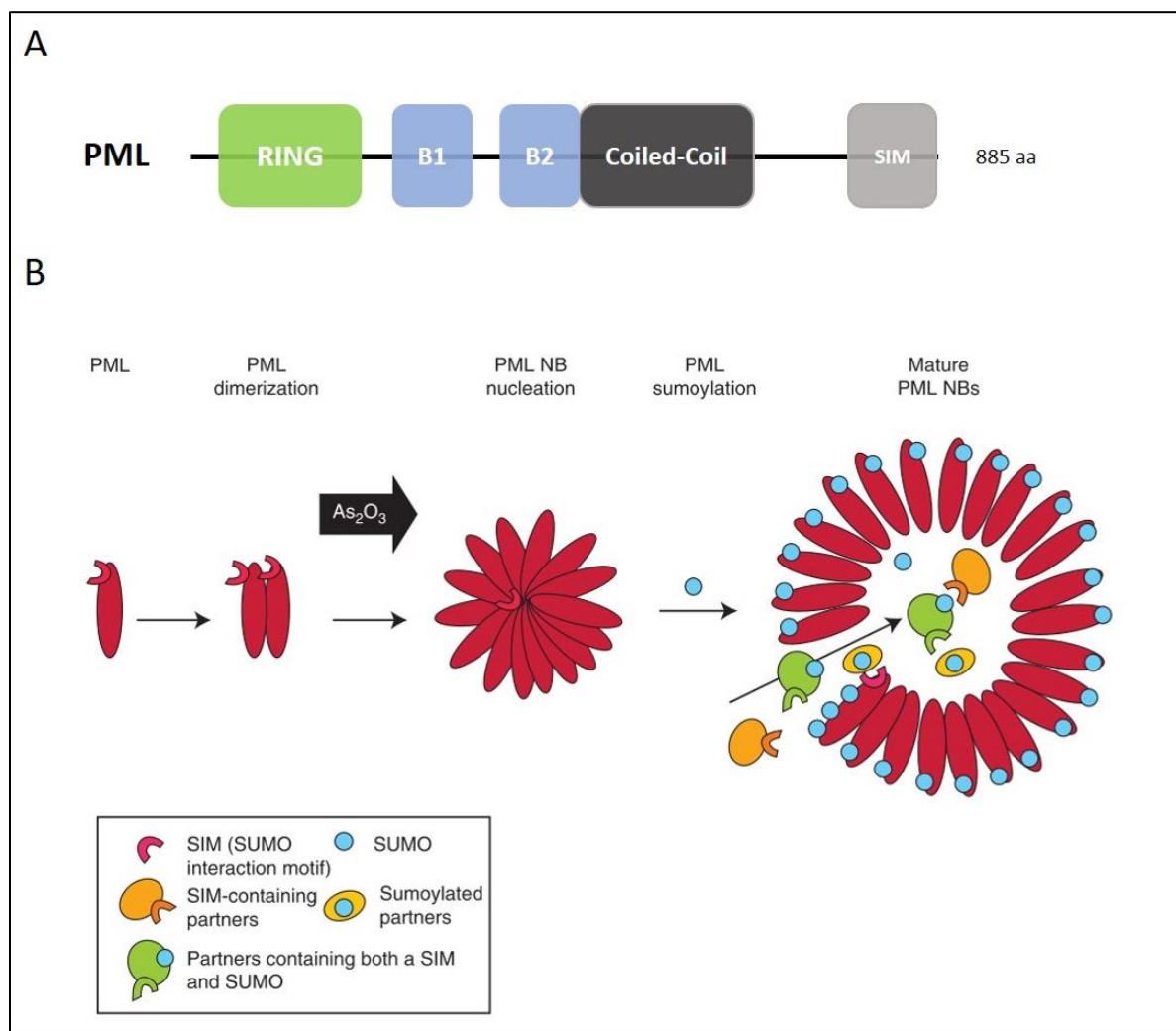


Figure 21 | PML proteins assemble into PML nuclear bodies. (A) Scheme of the PML protein and its domains. PML, also named TRIM19 (TRI-partite Motif 19) possesses a RING (Really Interesting New Gene) domain, two B1 and B2 zinc-finger boxes and a multimerization coiled-coil domain. Each of these domains is important for nuclear body assembly. (B) PML proteins can dimerize and then multimerize to form nuclear bodies that serve as a storage center for various other proteins that mostly contain a SIM domain. SUMO-SIM interaction allows recruitment of PML NB partners. PML NBs serve as hubs of post-translational modifications and notably SUMOylation. B is from Lallemand-Breitenbach and de Thé, *Cold Spring Harbor Persp. Biol.* 2010.

PML is an important sensor of cellular stresses, such as oxidative stress, which induces assembly of NBs. In fact, PML does not form many NBs *in vivo* in physiological cells but only

display high number of NBs in inflammatory tissues, suggesting that in vitro cultured cells exhibit constitutively high levels of oxidative stress (Terris *et al.* 1995). PML NBs often contain P53 protein and it was shown that PML is required for ROS sensing and subsequent P53 activation, via the regulation of P53 post-translational modifications in mouse (Niwa-Kawakita *et al.* 2017). Thus, PML regulates ROS levels in the nucleus. PML-dependent regulation of P53 is also true in human where reformation of PML NB upon arsenic treatment of APL cells induces a P53-senescence pathway (Ablain *et al.* 2014). However, deletion of Pml gene does not impair growth and survival of mice, yet defects in hematopoietic and apoptotic functions are observed (Gang Wang *et al.* 1998; Wang *et al.* 1998b). Yet, Pml $-/-$ mice exhibit neocortex hematopoietic defects, suggesting important roles in further differentiation and maintenance of tissues (Regad *et al.* 2009; Gang Wang *et al.* 1998). PML is also implicated in the control of protein quality as it can promote degradation of misfolded proteins via SUMOylation of the misfolded protein and recruitment of the SUMO-dependent ubiquitin ligase RNF4. In a spinocerebellar ataxia disease, a polyglutamine (polyQ) syndrome, PML NBs colocalize with the misfolded proteins and it was further demonstrated that depletion of Pml could increase polyQ phenotypes in mouse (Janer *et al.* 2006; Guo *et al.* 2014). These results indicate that PML is an important player in the regulation of cellular homeostasis.

The shape of PML NBs can vary according to the cell state. In human embryonic stem cells, PML NBs were reported to adopt different conformations upon differentiation and can appear as linear rods or rosettes (Butler *et al.* 2009). These unusual PML NBs appear to spatially interact with LaminA and centromeres, suggesting a role for PML in the organization of the heterochromatin in the nucleus. Upon LaminA depletion, PML NBs are perturbed, further indicating that PML interacts with the nuclear lamina, as it was proposed in a descriptive study where the isoform II of PML tend to associate with the inner membrane of the nuclear envelope (Stixova *et al.* 2012; Condemine *et al.* 2006). Intriguingly, the unprocessed LaminA progerin accumulates at PML NBs in the aging disease HGPS (Hutchinson-Gilford Progeria Syndrome) (Harhoury *et al.* 2017). In HGPS, PML NBs display increased abnormal shapes such as long threads inside the nucleoplasm resulting from PML isoform 2 along aging, and these peculiar PML NBs perturb DNA repair processes and transcriptional regulation of PML NB-associated genes (Wang *et al.* 2020). Shape and localization of PML NBs have been described in stressed and senescent human cells, which display large PML NBs at the nucleolus (Condemine *et al.* 2007). The unusual rods and rosettes PML NBs do not contain the classical other partners SP100, DAXX nor SUMO, suggesting that protein composition of the nuclear bodies might influence its functions (Butler *et al.* 2009).

2. Interplay of PML with DAXX, H3.3 and chromatin

Classical PML NBs do not contain chromatin, yet it contains the histone chaperone DAXX, its co-factor ATRX and sometimes HIRA (**Figure 22A**). DAXX and HIRA are the two histone chaperones specific for the histone variant H3.3, which is observed at PML NBs in some cells and notably upon overexpression of H3.3 (**Figure 22B**)(Delbarre *et al.* 2013). The presence of HIRA within PML NBs seems to be quite rare in normal conditions but increases in senescence cells, where HIRA transiently localizes at PML NBs (Zhang *et al.* 2005). Senescence cells are characterized by a strong higher-order chromatin reorganization with the appearance of senescence-associated heterochromatin foci (SAHF) (Narita *et al.* 2003). In senescence cells, DAXX also associates with PML NBs and recruits there the newly synthesized H3.3 (Corpet *et al.* 2014). Newly synthesized H3.3 is mostly observed at sites of active transcription, but although it is not found in SAHF, enrichment of H3.3 increases at constitutive heterochromatin regions such as pericentromeres. Interestingly, PML NBs act as a storage center for H3.3 and depletion of PML impairs the deposition at both euchromatin and heterochromatin, highlighting a strong interconnection between PML NBs and H3.3 (Corpet *et al.* 2014). The link between H3.3 and PML is mediated by DAXX as only DAXX, and not ATRX, is crucial for H3.3-H4 dimers targeting to PML NBs (Delbarre *et al.* 2013).

In interphase nuclei, it was reported that PML NBs can associate preferentially with different loci such as the MHC class I gene cluster and the TP53 locus and regulates its transcriptional activity (Shiels *et al.* 2001; Kumar *et al.* 2007; Sun *et al.* 2003). The fact that PML might associate to chromatin loci shed new light on the role of the NBs as regulators of the compartmentalization of the nucleus. Attempts to characterize the chromatin interactions with PML NBs observed that they tend to preferentially associate with active regions, suggesting a role for PML NBs in the transcriptional activity (Wang *et al.* 2001; Ching *et al.* 2013). PML can regulate gene expression, it is notably the case for the *Id2* gene. At the *Id2* promoter, PML mediates SETDB1 binding and repression of the locus. Interestingly, SETDB1 is a constitutive member of PML NBs since the early embryogenesis (**Figure 22C**). Furthermore, it is an essential member of PML NBs as Setdb1 depletion results in the loss of NBs without affecting the total level of PML proteins (Cho *et al.* 2011). PML NBs have also been linked to the KAP1 repressor as KAP1 forms foci adjacent to PML NBs upon differentiation (Briers *et al.* 2009). PML was reported to control the expression of many genes, especially in ESCs where PML is proposed to be an important regulator of pluripotency, although the action of PML in genome regulation could be indirect (Hadjimichael *et al.* 2017).

Interestingly, a recent study described a role for PML in regulating the higher-order organization of chromatin and loss of Pml resulted in the alteration of heterochromatin compartments (Delbarre *et al.* 2017). The regions regulated by PML are named PML-associated domains and are enriched in H3K9me3, a mark that they tend to lose upon Pml depletion because of an impaired DAXX-mediated H3.3 deposition. Yet other regions can be affected by the loss of Pml. Pml-null mouse fibroblasts displayed higher levels of H3.3 into constitutive heterochromatin regions such as subtelomeres, centromeres and pericentromeres (Spirkoski *et al.* 2019).

The role of the histone variant H3.3 on heterochromatin maintenance is clearly visible in embryonic stem cells as H3.3 provides the telomeric H3K9me3 (Udugama *et al.* 2015). Moreover, PML NBs colocalize with some telomeres in ESCs and cancer cells with the alternative-lengthening of telomeres (**Figure 22D**)(Draskovic *et al.* 2009; Chang *et al.* 2013). Depletion of Pml decreases H3.3 levels and affects telomere integrity in embryonic stem and ALT-positive cancer cells (Ivanauskiene *et al.* 2014; Osterwald *et al.* 2015). In murine embryonic stem cells, the DAXX-mediated deposition of H3.3 at telomeres is further regulated by the oncoprotein DEK. Indeed, loss of DEK induces the relocalization of PML and DAXX away from telomeres and increased the incorporation of H3.3 into chromosome arms (Ivanauskiene *et al.* 2014). Ivanauskiene *et al.* propose that non-nucleosomal H3.3 is stored into PML NBs and from then can be recruited by its chaperones. After depletion of DEK, the pool of non-nucleosomal H3.3 is reduced and H3.3 is no longer observed at PML NBs. On the opposite, in the case of Daxx depletion, the soluble pool of H3.3 increases as it is less incorporated in the chromatin. Thus, it emerges a model whereby newly synthesized H3.3 would be directed to PML NBs in a DAXX-dependent manner and be stored until further necessity.

PML NBs can associate with chromatin regions. One of the functions of PML is the activation of an antiviral response. It was further observed that in response to herpes simplex virus (HSV) infection, the HSV genome is embedded within PML NBs and is chromatinized via H3.3 incorporation and H3K9-methylation (Cohen *et al.* 2018). Interestingly, H3.3 incorporation is mediated by both chaperones DAXX and HIRA in this context, but this mechanism is dependent on PML. PML NB formation also occurs during HIV and other retroviruses infections, where it mediates a DAXX-dependent control of HIV reverse-transcription (Dutrieux *et al.* 2015). From all these studies, it appears that PML might be an important regulator of heterochromatin, notably via its interactions with DAXX and H3.3.

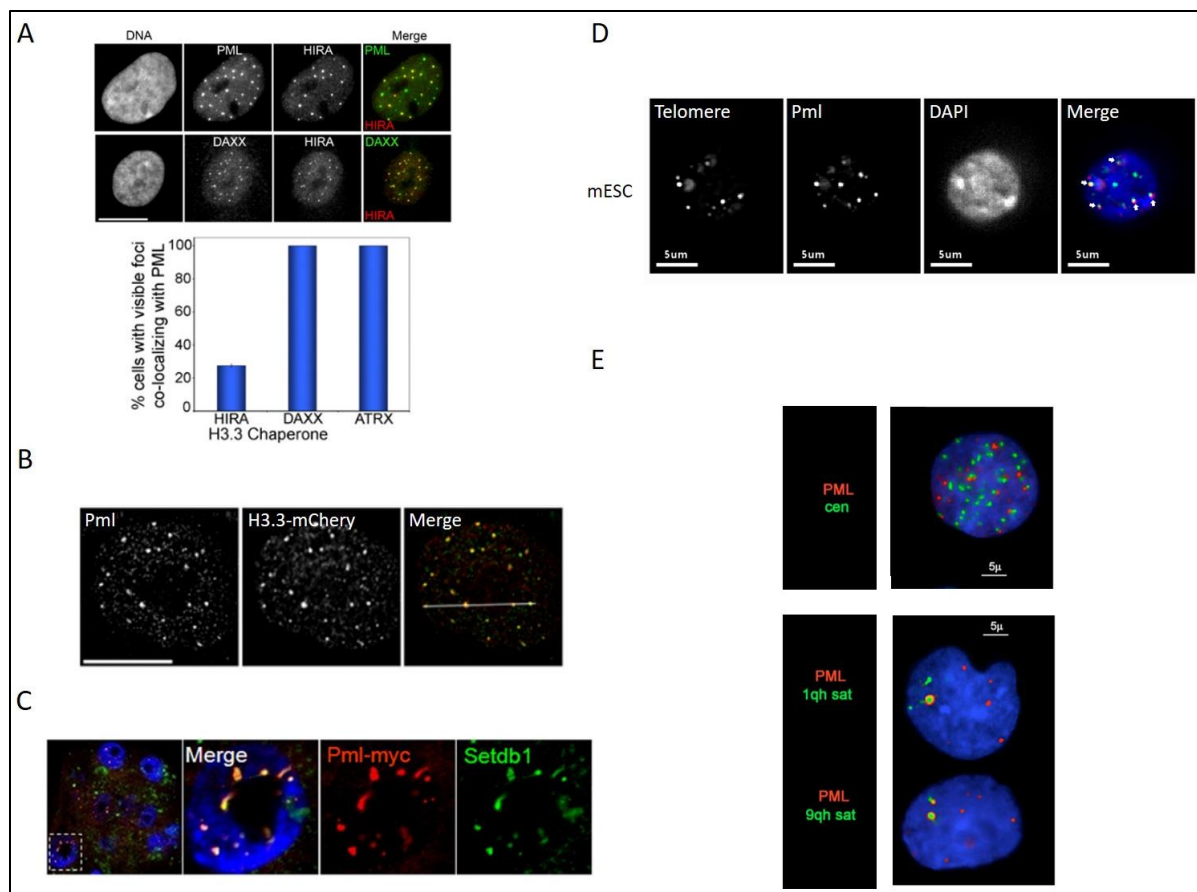


Figure 22 | PML NBs as a storage center for H3.3-chaperones and interaction with chromatin. (A) H3.3-chaperones HIRA, DAXX and ATRX can localize within PML NBs. (B) Over-expression of H3.3 leads to its accumulation at PML NBs, which serve as storage center before chromatin deposition. (C) The H3K9 tri-methylase enzyme SETDB1 localizes at PML NBs, this is notably visible in the early embryo. Deletion of Setdb1 impairs the formation of PML NBs. (D) In murine embryonic stem cells, PML can be found at some telomeres, visible here with the presence of the telomeric repeats in red and PML in green. (E) Pictures of lymphocytes of control (top) or ICF patients (bottom) (Immunodeficiency, Centromeric instability and Facial abnormalities). The ICF syndrome is caused by mutation in DNMT3B and results in hypomethylation, notably at pericentromeres of the chromosomes 1, 9 and 16. Interestingly, pericentromeric satellites of these three chromosomes are found within PML NBs. A and B are adapted from Delbarre *et al.*, *Genome Res.* 2013. B is from Cho *et al.*, *J. Biol. Chem.* 2011. D is from personal unpublished data. E is from Luciani *et al.*, *J. Cell Science* 2006.

In the ICF syndrome, which is a consequence of a mutation in the DNMT3B gene, a reported phenotype is the instability of the centromeres of three chromosomes - 1, 9 and 16. These three centromeres are the most GC-rich and they undergo the strongest DNA demethylation. It was observed that lymphocytes of ICF patients display atypical PML NBs that are bigger than classical ones (**Figure 22E**). Called ‘giant NBs’, they form a scaffold for the classical SUMO, SP100 and DAXX proteins, and interestingly, they contain chromatin regions marked with HP1 (Luciani *et al.* 2005). It was observed that giant PML NBs form onto the pericentromeric regions of the chromosomes 1, 9 and 16 and are enriched in DNA repair proteins such as BLM, BRCA1 and TOPOIII α (Luciani *et al.* 2006). These structures are exclusively observed in G2 phase and the authors proposed that it could be a mechanism to reform heterochromatin after S-phase.

Not only in the ICF syndrome could PML NBs sequester DNA repair protein. Proteins such as BRCA1, RAD51 or MRE11 can transit through PML NBs (Boichuk *et al.* 2011; Carbone *et al.* 2002). Furthermore, PML NBs could act as sensors of DNA damages for upon DNA damages, the number of PML NBs increases due to fission events of the existing NBs and this mechanism is dependent on DNA damage response (DDR) checkpoints ATM, ATM, NBS1 and CHK2 (Dellaire *et al.* 2006). The function of PML in DDR seems to be at a late stage, as the loss of Pml does not impair DNA damages signaling such as γ H2AX and RAD51 foci formation, but diminished by up to 20 fold the efficiency of homologous recombination (Yeung *et al.* 2012). Yet a more recent study suggest that the initial recognition of DNA damage might be delayed when Pml is absent (Di Masi *et al.* 2016). Because of the possible localization of BRCA1 and RAD51 inside PML NBs, it was proposed that defects in DDR might arise from the mislocalization of these proteins if there is no PML NBs and that could be an important feature of APL pathogenesis (Voisset *et al.* 2018). Together, these studies indicate that PML is a multivalent interactor that plays different roles in the regulation of DNA-related processes. One of the functions of PML might reside in its ability to form NBs that could help concentrating proteins at specific nuclear localizations.

III - Embryonic stem cell as a model of embryonic development and chromatin specifies.

All cells of the organism originate from a unique one, the zygote, created by the fusion of the two parental gametes. Cell-types is not a DNA property, rather the expression of a defined set of genes. A lot of phenotypic changes happen during the embryonic development, from zygote to birth. Indeed, many differentiation programs start after the implantation stage, during gastrulation, with the appearance of the three layers that will compose all the organism - mesoderm, endoderm and ectoderm. Cells then commit lineage differentiation, a definitive process, that erase their pluripotent capacities.

Pluripotency has intrigued biologists for a long time and is still not completely understood. I will here present the early mouse embryonic development, then the use of pluripotent cells in cultures and their use to gain developmental insights. Finally, I will present pluripotency from a chromatin viewpoint.

Embryonic development and embryonic stem cells

Understanding the developmental properties of human and mouse has been the focus of many research groups for above a century. Yet, this has proven to be a complex question to tackle. Embryonic development is an extremely complex suite of events that includes cell differentiation, tissue morphogenesis and growth of the organism. The use of pluripotent cells has been a key technology to better understand the early embryogenesis. *In vivo* experiments have yielded important discoveries and remain crucial to assess the relevance of molecular events identified *in vitro*. However, because of the inherent difficulties to get *in vivo* materials, the use of pluripotent stem cells in culture is particularly adapted to dissect molecular events.

1. Definition of the embryonic development and pluripotent cells

Embryonic development consists of the route from the zygote to birth, that includes many stages (Saiz and Plusa 2013).

Pre-implantation development starts in the oviducts until the blastocyst stage when the uterine implantation takes place at around E4.5 in mouse and E7 in human (**Figure 23**). Totipotency is defined as the capacity to generate all cellular tissues, including the embryo and extra-embryonic tissues. Embryonic cells are totipotent up to the 4-cell state. Between the 4-cell and blastocyst state, some of the embryonic cells differentiate to give rise to the extraembryonic

tissues - the trophoctoderm and the primitive endoderm which are observed at the periphery of the embryo. The trophoctoderm will give the placenta, whereas the primitive endoderm will form the yolk sac. The rest of the cells at the blastocyst stage form the inner cell mass (ICM) which consist of pluripotent cells able to differentiate into all tissues of the organism (Shahbazi and Zernicka-goetz 2018).

During these cell divisions, many transcriptional changes arise, giving specific transcriptomic signatures. Within the blastocyst, the three tissues present distinct signatures - ICM cells composed of the naïve pluripotent epiblast present high OCT4, NANOG and REX1, KLF2, KLF17 and ESSR β whereas the trophoctoderm cells display high Cdx2, EOMES and KRT8 transcription, and the primitive endoderm high GATA6, SOX17 and GATA4 signaling (Shahbazi and Zernicka-goetz 2018). At the implantation stage, specific signaling pathways act to ensure proper polarized specialization of the embryo. One key signal is the activation of NODAL by the epiblast, that activates BMP4 in the adjacent extraembryonic tissue, which in turn activates WNT3 in the epiblast (Ben-haim *et al.* 2006). These transcriptomic signatures have getting more and more exhaustive and precise with the arrival of new NGS (next-generation sequencing) technologies such as single cell RNA sequencing. Single-cell RNA-seq (scRNA-seq) studies have generated a comprehensive timeline of gene activation from mouse to human (Xue *et al.* 2013). ScRNA-seq has determined that for about 12 to 24% of autosomal genes there is a random monoallelic expression that occurs independently of the other allele (Deng *et al.* 2014). It has given unprecedented deepness for cross-species comparisons and helped identify transcriptional variation and conservation such as GATA6, SOX17 and GATA4 sequential activation in primitive endoderm from primates to humans (Boroviak *et al.* 2018). Many of the transcriptional changes seen before gastrulation are linked to chromatin regulation, which I will discuss in the last part of this introduction.

This deeper understanding of the pathways implicated during acquisition and loss of pluripotency have been under the focus on researches for decades. It was necessary to understand the *in vivo* transient pluripotency to get to *in vitro* maintained pluripotency cultures.

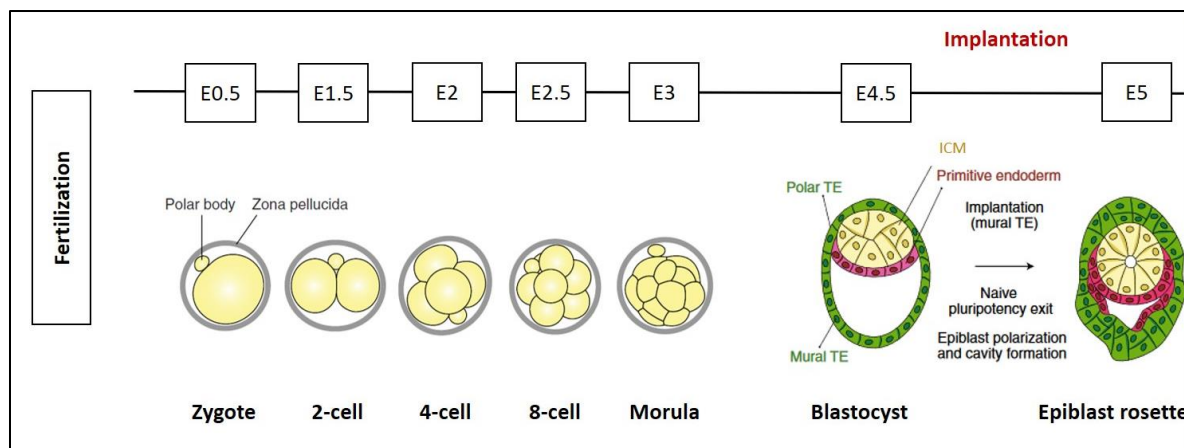


Figure 23 | Murine early embryonic development. At the fertilization, the two gametes fuse to form the zygote. The first 4 days of development consist in numerous cell division and the embryo reaches a 2-cell stage, 4-cell stage, 8-cell stage, then the morula. Around E4, the embryo forms the blastocyst in which three cell types co-exist. Two cell-type will form the extra-embryonic tissues: the trophoblast in green that will give the placenta and the primitive endoderm in purple which will give the yolk sac. The inner cell mass in yellow will differentiate into the whole organism. At E4.5, the blastocyst can implant within the uterus and then form the epiblast. ICM = inner cell mass. Adapted from Shahbazi and Zernicka-Goetz, *Nature Cell Biol.* 2018 and Saiz and Plusa, *Reproduction* 2013

The 1950's have witnessed the emergence of the *in vitro* culture conditions for embryonic cells that have paved the way for today's culture conditions (Hammond 1949; Whitten 1956). Researchers have firstly tried to cultivate the whole pre-implantation embryo until 1981 when two teams isolated embryonic stem cells (ESCs) from mouse ICM blastocysts (Evans and Kaufman 1981; Martin 1981). In the post-implantation embryo, ICM cells have converted into the epiblast before giving rise to the other tissues. Epiblast stem cells have been derived and cultured *in vitro* to help elucidate this first primed state of pluripotency (Brons *et al.* 2007; Tesar *et al.* 2007). The defined set of additional factors necessary for pluripotent epiblast stem cell-derived cultures FGF2 and ACTIVIN-A can be used to generate epiblast-like stem cells from cultured ESCs, however epiblast stem cells do not rely onto the LIF factor essential for ESCs (Hayashi *et al.* 2011). Extraembryonic ectoderm cells can also be cultured *in-vitro* (Tanaka *et al.* 1998). Furthermore, mixing ESC and TSC can generate blastocyst-like structures that highly resemble to *in vivo* blastocysts, including the formation of a pro-amniotic cavity, indicating that ESCs possess essential intrinsic properties (Rivron *et al.* 2018).

These studies have shed light on the early embryonic development and have further shown the differences between human and mouse development. Moreover, not all *in-vitro* mouse stem cell cultures can be applied to humans. Murine and human ESCs share some resemble but also some differences indicating that the *in vitro* culture of mESC or hESC does not correspond to the exact same pluripotency, however it can be smoothen by particular culture conditions (Davidson *et al.* 2015; Gu *et al.* 2012). Indeed, whereas murine ESCs grow as domed colonies, human ESCs grow as more flat colonies like murine epiblast stem cells. Moreover, they do not rely onto the

exact same signaling pathways. Human embryonic stem cells in culture resemble to both murine epiblast stem cells and embryonic stem cells, suggesting that pluripotency might to some extent be specie-specific (Schnerch *et al.* 2010).

Human ESCs presented a high therapeutic interest until 2007. Indeed, the possibility to differentiate ESC to any cell-type held great promises and many *in vitro* differentiation pathways have been described. From 2007 and during the following years, induced pluripotent stem cells (iPSCs) were generated from murine and human somatic cells, by overexpressing the pluripotent factors - OCT4, KLF4, SOX2 AND C-MYC (Takahashi and Yamanaka 2006; Takahashi *et al.* 2007). Induced pluripotent stem cells display an ESC-like transcriptomic regulation and 3D-chromatin organization, suggesting common pluripotency networks for embryonic and somatic cells (Krijger Lodewijk *et al.* 2016; Guenther *et al.* 2010).

2. Different levels of pluripotency in *in vitro* cultures

ESCs pluripotency is partly defined as the capacity to generate chimera embryos when injected in a blastocyst. Yet, in *in-vitro* studies, researchers often only look at transcriptional markers associated with pluripotency that I will briefly describe here. Classical pluripotency markers usually consist of the so-called ‘Yamanaka factors’ that are sufficient to reprogram somatic cells - OCT4, KLF4, SOX2, C-MYC; and some non-Yamanaka as NANOG, ESSRB and REX1. These factors are transcription-factors that act within complex signaling pathways. OCT4 is transcribed from the *Pou5f1* gene that stands for octamer-binding transcription factor 4 (Kellner and Kikyo 2010). Although OCT4 is not involved in the initiation of totipotency, it appears to be crucial for pluripotency in both mouse and humans, as deletion of the *Pou5f1* impairs embryogenesis after the blastocyst stage (Nichols *et al.* 1998; Fogarty *et al.* 2017). Inactivation of Oct4 in human and murine ESCs induce a loss of pluripotency and differentiation into neural ectoderm cell-type (Bertero *et al.* 2016; Thomson *et al.* 2011). The *Pou5f1* gene is under the control of OCT4 and SOX2 binding, which creates a regulatory feedback loop (Okumura-Nakanishi *et al.* 2005). KLF4 stands for Krüppel-Like Factor 4, it is also a transcription factor. Its proper expression is crucial to normal development, as mice lacking this gene die rapidly after birth (Villarreal *et al.* 2010). SOX2 belongs to the SRY-related HMG box family of transcription factors and is expressed in the pre-implantation embryo, but also later in the epiblast (Huang *et al.* 2015). Deletion of *Sox2* impairs pluripotency both *in vivo* and *in vitro*, likely via its crucial role in OCT4 regulation (Masui *et al.* 2007; Avilion *et al.* 2003). NANOG is a Q50 homeodomain-containing transcription factor. Interestingly, NANOG is not essential for embryonic development, yet it is required for germline formation (Chambers *et al.* 2007).

Culturing embryonic stem cells requires special medium conditions. First culture media in the 1980's relied on mouse embryonic fibroblasts (MEFs) as feeders for ESCs in addition to fetal bovine serum. Yet, it was identified that MEFs produced the leukemia inhibitory factor (LIF), which activates the JAK-STAT3 signaling pathway. So, ESCs could be kept in culture without MEF feeder when LIF was added to the serum-based medium (Williams *et al.* 1988). These cells exhibit the classical pluripotency-associated factors - OCT4, KLF4, NANOG and ESSR β expression. They retain their pluripotency capacities as injection into blastocysts could generate chimeras, they are thus naïve stem cells. I will refer to this culture condition as the 'standard' ESC serum/LIF condition.

Although well-defined, the 'standard' serum culture condition uses a fetal bovine serum, which we do not know its complete chemical composition. Furthermore, it has been realized that 'standard' medium culture of ESCs was sufficient for chimera's formation (Nagy *et al.* 1993; Bradley *et al.* 1984). However, *in vitro* pluripotency differs from its *in vivo* counterpart observed in the ICM as ESCs display some transcriptional changes (Plusa and Hadjantonakis 2014; Boroviak *et al.* 2014). Research groups have tried to use serum-free medium for ESC culture conditions to get pluripotent cells that would match *in vivo* ICM cells. In 2008, a study led by Austin Smith described the 3i (3 inhibitors) medium able to maintain naïve pluripotency of mESCs that they called the ground state of pluripotency without LIF (Ying *et al.* 2008). Ying *et al.* were not only able to cultivate ESC in a serum-free medium, but they also demonstrated that the activation of the STAT3 signaling is dispensable for maintaining of pluripotency, and ESCs instead required the complete inhibition of differentiation-signaling, indicating intrinsic pluripotent capacities of these cells. An alternative 2i/LIF medium was adopted to overcome the reduced proliferation observed in 3i medium. 2i/LIF-medium is obtained using small-molecule inhibitors for the GSK3 and MEK3 pathways (**Figure 24**). Intriguingly, the MEK-ERK signaling pathway is inhibited in this medium, yet genetic ablation of ERK impedes ESC culture, suggesting a MEK-independent role for ERK signaling (Chen *et al.* 2015). Furthermore, differences in signaling pathways at play in 2i/LIF or serum cultures are exemplified by the observation that the Klf2 knock-out, a factor regulated by ERK, is only lethal in the 2i/LIF medium (Yeo *et al.* 2014). A proteomic study confirmed those transcriptomic and genetic studies, the authors also observed differences in metabolism between the two medium conditions and reported a lower reactive oxygen species levels in 2i/LIF (Taleahmad *et al.* 2015). Cells cultured in 2i/LIF condition retain proper differentiation capacities, indicating that a metastable state, such as serum-based condition, is not necessary for lineage-commitment (Marks *et al.* 2012).

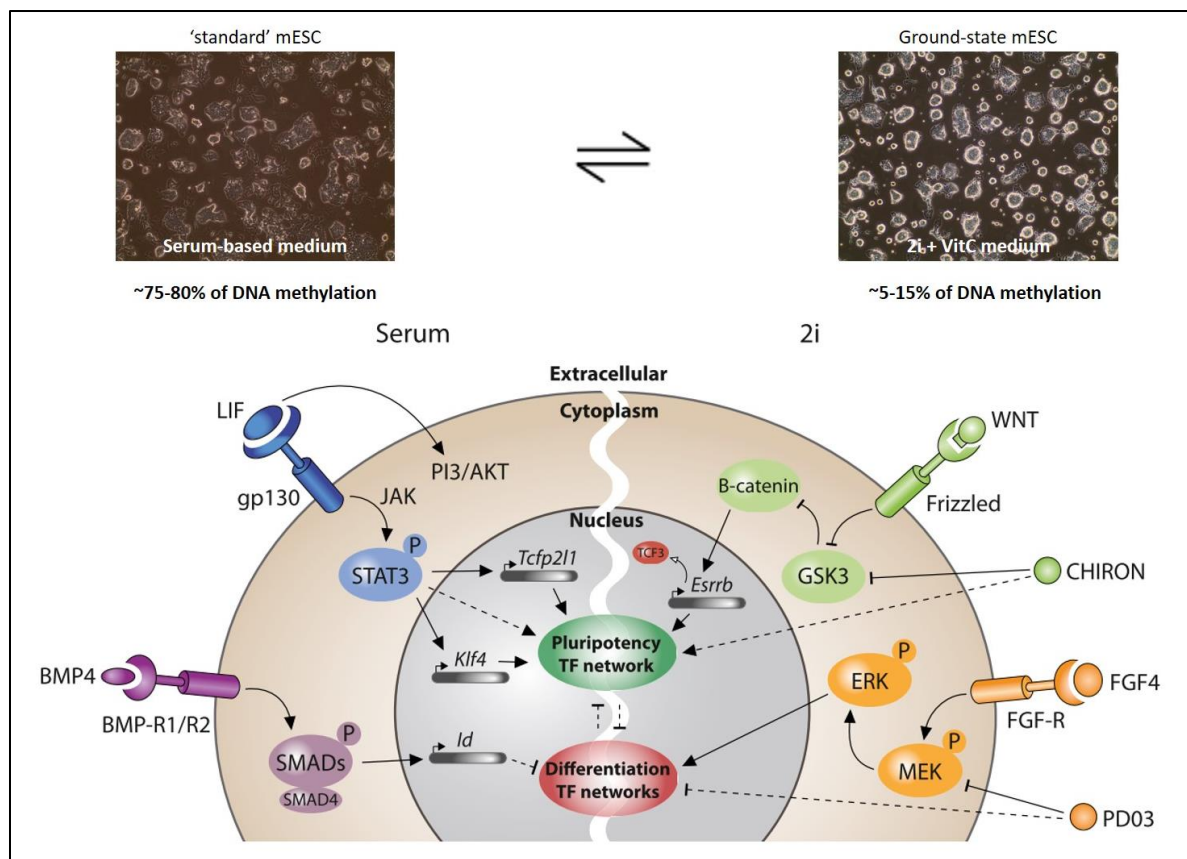


Figure 24 | Signaling pathways in pluripotent cells in vitro. ESCs grow as dome-shaped colonies in both serum-based 'standard' medium and ground-state 2i/LIF + VitC medium. Serum-cultivated ESCs display 75 to 80% of DNA methylation levels, whereas conversion toward 2i/LIF + VitC reduces DNA methylation to 5 to 15%. However, pluripotency goes through different pathways. Serum-based ESCs activate the BMP4 receptor that ultimately represses lineage-specific genes. Addition of LIF to serum medium activates the STAT3 signaling pathways that activates pluripotency factors such as KLF4. Ground-state ESCs have 2 inhibitors in the medium that block the GSK3 and the MEK pathways that sustain activation of pluripotency factors. Ground-state ESCs are more homogeneous than 'standard' serum-grown cells. VitC = Vitamin C. Adapted from Hackett and Surani, *Cell Stem Cell* 2014. ESC-colonies pictures are from personal unpublished data.

Both serum and 2i/LIF culture conditions present the classical dome-shaped colonies formed by ESCs multiplication. Nonetheless, not all ESCs in in-vitro culture dish display the same morphology and transcriptional profile, suggesting a high heterogeneity. It was demonstrated using GFP-tagged REX1 marker, which should only be expressed in the ICM-derived cells (i.e. ESCs) and not in Epiblast stem cells. Yet, in serum-based culture, REX1-positive coexist with a REX1-negative population (Toyooka *et al.* 2008). Furthermore, even if REX1-negative cells are sorted, after five days of culture, half of the population present a Rex1-positive profile, indicating that a population of ESCs is a mix of transient and reversible states toward naïve and primed pluripotent cells (Toyooka *et al.* 2008). Deeper population-level genome-wide studies of the 'standard' and 2i/LIF conditions have been conducted. It was observed that 2i/LIF ESCs presented lower expression of differentiation-related genes that correlated with an increase of RNA Pol II-pausing at promoters, and importantly an increased expression of Nanog, while conserving the same differentiation capacities (Marks *et al.* 2012). These results were thought to arise from a

more homogenous cell-population in 2i/LIF, as assessed by scRNA-seq (Guo *et al.* 2016). This view is challenged by scRNA-seq suggesting that there is the same level of heterogeneity in the two culture conditions, although it does not concern the same set of genes, with lineage-commitment genes being completely silenced in 2i/LIF conditions (Kolodziejczyk *et al.* 2015). Differences between the two cultures arises in part from changes in the epigenome states, notably characterized by a lower DNA methylation level in 2i/LIF, which I will discuss in the next sub-part.

Consistent with some heterogeneity even for ground-state ESCs, 2cell-like stage observed by Macfarlan *et al.* are a rare ESC population in culture with only less than 1% of the cells (Macfarlan *et al.* 2012). 2cell-like ESCs activate a specific gene-set which closely resemble the *in vivo* 2-cell state embryo and they are totipotent cells as they can even generate extra-embryonic tissues such as the placenta and the yolk sac. Interestingly, activation of 2cell-related transcripts such as the Zscan4 cluster and MERVL transposable elements further increase the DNA demethylation (Eckersley-Maslin *et al.* 2016). It was observed that conversion toward this peculiar 2cell-like state could be further enhanced via depletion of some factors, notably chromatin-associated proteins that I will describe in the next section (Rodriguez-Terrones *et al.* 2018).

Finally, cells in culture display features of pluripotency, one should keep in mind that during the embryonic development, pluripotency is a transient state before lineage commitment. However, *in vitro* ESCs can be kept in cultures virtually indefinitely and it is likely that subtle changes may accumulate during prolonged culture.

3. Pluripotency in a chromatin context

Pluripotency results from signaling pathways that ultimately induce transcription factors. Yet, as defined in the second part of the introduction, chromatin is not merely binding sites for proteins, but also bears a complex three-dimensional organization. During development, many chromatin changes happen, some are large-scale like the building of the different heterochromatin compartments, and some are visible at finer-scale such as promoter reorganization.

Chromatin changes along development affect genomic loci with differences in histone modifications enrichment. This is notably the case for promoters which can only bear in pluripotent cells both H3K4me3 and H3K27me3-enrichments (Azuara *et al.* 2006). These promoters were thus called bivalent, because these two histone modifications do not usually colocalize. The genes are inactive but poised for later activation, although it was reported that they might be expressed at low levels even in ESCs (Herz *et al.* 2009). Bivalent promoters have been identified from the 8-cell stage to the blastocyst in the embryo, but also in other adult stem cell as hematopoietic or mesenchymal stem cells. Interestingly, it seems that the bivalency might have a

function during development as it is conserved in zebrafish (Vastenhouw *et al.* 2010). Furthermore, the number of bivalent promoters is reduced in ground-state ESCs compared to ‘standard’ serum ESCs, suggesting that the DNA methylation levels might play a role in promoter identities (Marks *et al.* 2012). In pluripotent cells, many genes display monoallelic expression, suggesting an even finer level of regulation (Xu *et al.* 2017). It was demonstrated that the monoallelic expression of some factors such as Nanog was essential at the ground state of pluripotency as the removal of

one allele of *Nanog* impaired proper development of the ICM (Miyanari and Torres-Padilla 2012). Thus, transcriptional regulation is important in the maintenance of pluripotency.

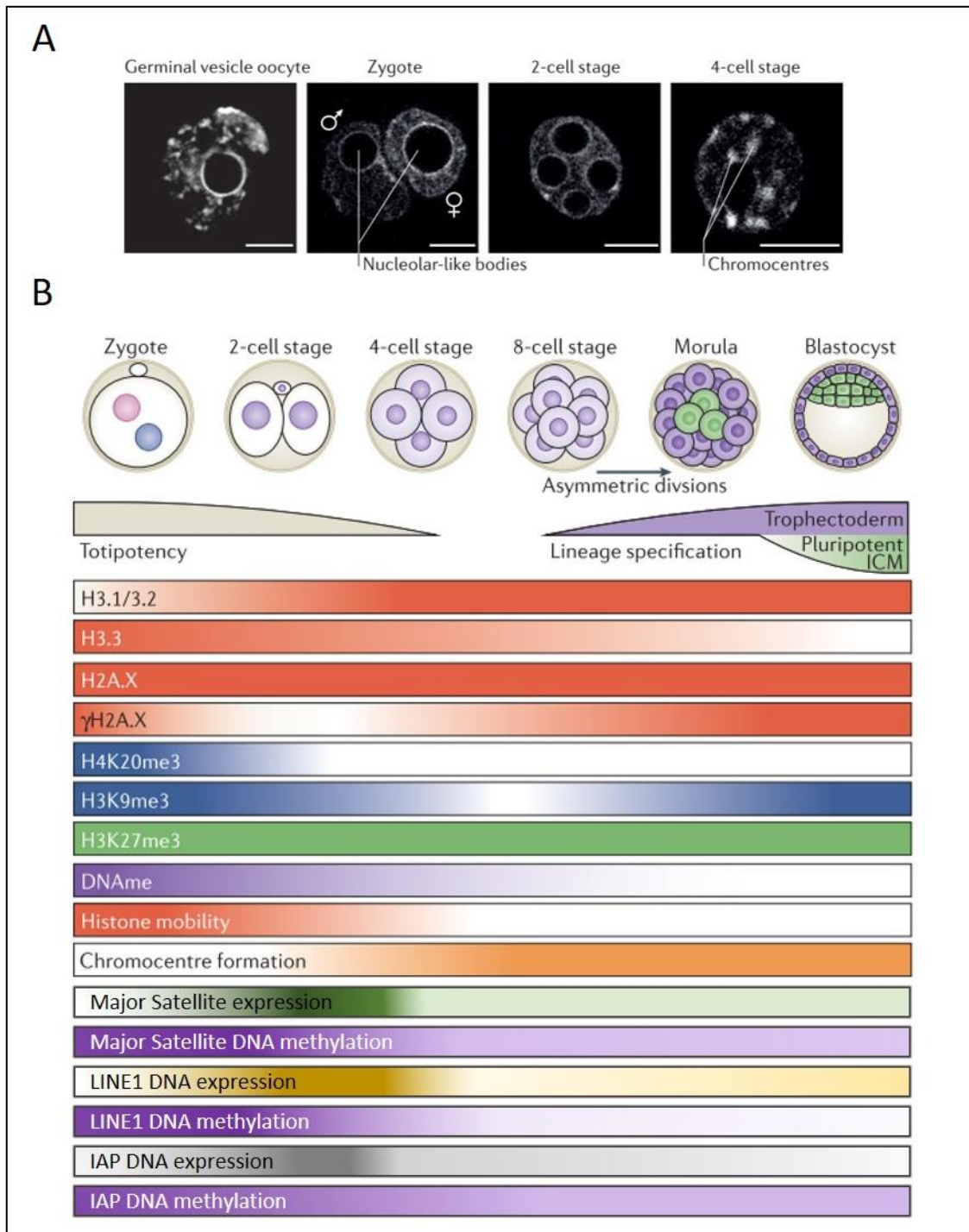


Figure 25 | Chromatin changes along early embryonic development. (A) Schematic of the early embryonic development, from the zygotic to the blastocyst stage. Below are depicted the global levels of histone modifications, chromatin features and heterochromatin transcription across pre-implantation embryo. (B) DAPI (4',6-diamidino-2-phenylindole)-staining of nuclei from the oocyte, the zygote, the 2-cell and 4-cell embryo. DAPI binds to A/T-rich regions, highlighting notably the pericentromeric satellites. PCH localize around nucleolar-like bodies until the 4-cell stage of development, when pericentromeric satellites assemble into well-defined chromocenters. Adapted from Burton and Torres-Padilla, *Nat. Rev. Mol. Cell Biol.* 2014.

At the zygote stage, there is no transcription from both parental genomes, all the proteins at play arise from the oocyte transcripts. An important event at the 2-cell stage in mouse, 4-cell stage in human, is the zygotic genome activation (ZGA), when the embryo starts its own transcription for the first time. At the ZGA, the chromatin becomes globally decondensed. How could the genome decompact all at once? It was noted that retrotransposon transcription is correlated with the pluripotent state, with a transcriptional burst at the 2-cell stage and a slow decrease along the development, that is following a loss of active marks onto the chromatin (**Figure 25B**)(Fadloun *et al.* 2013). It was further demonstrated that the activation of LINE1 elements was modulating global chromatin accessibility and that this activation and the subsequent silencing at later stages was required for proper maturation toward blastocyst (Jachowicz *et al.* 2017).

The first 4 to 5 days of the embryonic development are moments of intense changes. The major change, observed early on, is the wave of DNA demethylation from the zygote to the blastocyst, then the methylation is progressively restored (Howlett and Reik 1991). Genome-wide assessment of 5mC observed that the loss is global and at almost all genomic locations, excepts for imprinted-loci and some ERVs such as the young IAPs (**Figure 25B**)(Lane *et al.* 2003). Right after the zygote stage, the paternal genome becomes fully unmethylated, the maternal genome on the other hand will lose its DNA methylation over the next cell divisions (Ladstätter and Tachibana 2018). Around 20 imprinting control regions (ICRs) have been identified in both human and mouse (Barlow *et al.* 1991; Zwart *et al.* 2001; Ferguson-smith *et al.* 1991). ICRs are often CpG-rich regions that display differential methylation pattern in a parent-of-origin manner (Greenberg and Bourc'his 2019). Imprinted genes are thus methylated on only one of the two alleles such as IGF2 for which only the paternal allele is expressed, or the closely located H19 for which only the maternal allele is expressed, the reciprocal allele being methylated (DeChiara *et al.* 1991; Bartolomei *et al.* 1991).

ESCs in culture display ~75% of DNA methylation for all possible CpGs, indicating a strong level of DNA methylation which likely results from the *in vitro* serum culture conditions (Stadler *et al.* 2012). Recapitulating the changes in DNA methylation levels during early embryogenesis was only achieved with the use of the chemically defined 2i/LIF medium for ESCs (Ying *et al.* 2008). The scale and pattern of the observed DNA demethylation observed in culture resemble the one seen in the ICM at the blastocyst stage, as assessed by genome-wide bisulphite sequencing (Ficz *et al.* 2013). The addition of vitamin C to the 2i/LIF medium could further decrease the global level of 5mC and increase the level of 5hmC at the same time, via enhanced activity of the TET enzymes (**Figure 24**)(Blaschke *et al.* 2013). The decrease of 5mC was shown to be dependent on synergistic mechanisms, both passive and active. Indeed, the increase of the PRDM14 protein represses the action of the de novo methylases, whereas TET enzymes enhanced

the conversion from 5mC to 5hmC, inducing a rapid and genome-wide decrease of DNA methylation (Hackett *et al.* 2013a). A latter study complemented these results showing that the TET activation relied on the stabilization of JMJD2C, directly induced by MEK inhibition, and the PRDM14 activity was mediated by the G9A methyltransferase activity toward DNMT3A and DNMT3B (Sim *et al.* 2017). Interestingly, depletion of the three DNMT enzymes only partially upregulates the transcription of transposable elements, yet, converting the cells to the 2i/LIF medium induces a strong upregulation of TEs, suggesting synergistic mechanisms at play (Matsui *et al.* 2010). Walter *et al.* proposed that conversion of ESCs from a serum to a 2i/LIF medium induces a rapid genome-wide DNA demethylation that is comparable to what happens in the early embryo. Furthermore, they observed that cells respond to the loss of DNA methylation by an upregulation of TEs transcription during the first cell division only (Walter *et al.* 2016). Indeed, once in 2i/LIF for ~6 days, ESCs undergo a switch from a DNA methylation-based repression of TEs toward a histone modification-based control, which correlates with the downregulation of TEs. These results emphasize the capacity of ESCs to overcome the loss of DNA methylation, which mimics the physiological path of the early embryo.

The spatial architecture of chromatin is largely reorganized from the 2-cell to the epiblast. At the zygote and 2-cell stage, heterochromatin is mainly observed surrounding the pre-nucleolar bodies. Firstly, the pre-nucleolar bodies merge to give rise to the nucleolus where transcription of the rDNA takes place. Constitution of pericentromeric heterochromatin blocks into chromocenters is visible at the 4-cell stage (**Figure 25A**). Chromocenter formation arise during the 2-cell state of the embryo and coincides with a burst of transcription for the major satellites (**Figure 25B**)(Probst *et al.* 2010). It was further demonstrated that chromocenter formation required only reverse pericentric transcripts, but not the replication of the pericentromeric regions (Casanova *et al.* 2013). Interestingly, the two parental pericentromeric regions display different timing of replication, and knock-down of major satellite transcription impacted differentially maternal and paternal heterochromatin organization but was in any case sufficient to impair progression toward 4-cell embryo (Casanova *et al.* 2013). Furthermore, the spatial organization in itself is important for proper acquisition of histone modifications and heterochromatin regulation as forced-targeting of pericentromeric regions at the 2-cell stage to the nuclear lamina impaired the development toward blastocyst stage (Jachowicz *et al.* 2013). Interestingly, DAXX accumulates to pericentromeric regions at the zygotic and 2-cell stage, specifically in the male pronucleus in a, respectively, ATRX, DPPA3 and PRC1-dependent manners (**Figure 26A**)(De La Fuente *et al.* 2015; Arakawa *et al.* 2015; Liu *et al.* 2020). Loss of Atrx results in the overexpression of major satellite transcripts in the zygote, whereas the loss of Dppa3 induces a lower levels of major satellite RNAs at the 2-cell state. DPPA3

protects the genome against DNA demethylation at the zygotic state, notably at IAP elements (Nakamura *et al.* 2007). Depletion of PRC1 components or Daxx itself resulted in chromosomal instabilities and ultimately reduced the number of embryos reaching the blastocyst stage (Liu *et al.* 2020). Totipotent and pluripotent cells display constitutively high levels of DNA damage signaling, such as high expression of γ H2A.X. It is proposed that the high levels of γ H2A.X in the early embryo might not be linked to actual DNA damages as γ H2A.X foci are not colocalized with 53BP1 foci (Ziegler-birling *et al.* 2009). Intriguingly, the loss of DPPA3 induces 5hmC and γ H2A.X accumulation in pre-implantation embryos, suggesting that loss of silencing of TEs in the embryo and zygotic genome activation must be tightly regulated to avoid detrimental accumulation of DNA damages (**Figure 26B**)(Nakatani *et al.* 2015).

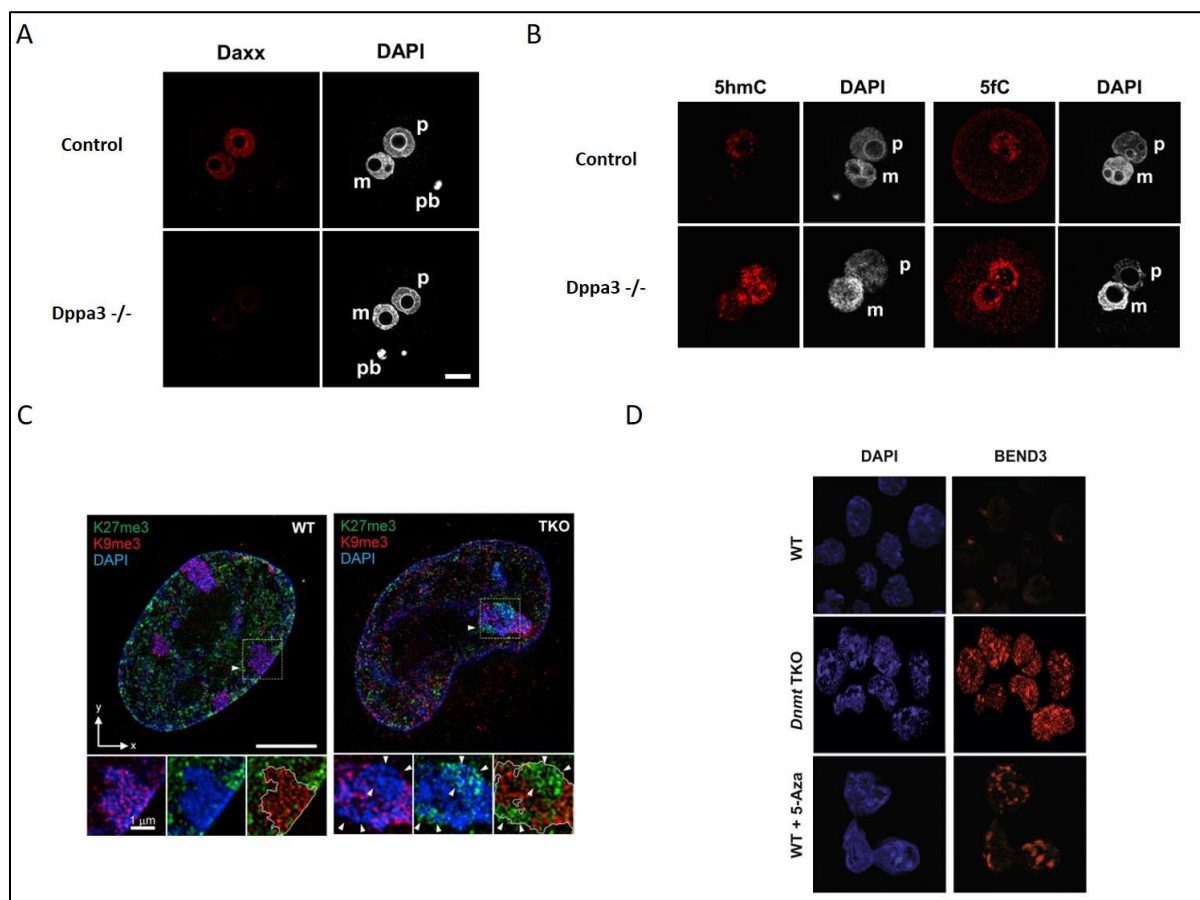


Figure 26 | Pericentromeric maintenance in totipotent and pluripotent cells. (A) In the paternal nucleus of murine zygote, DAXX accumulates at PCH in a DPPA3 (also named STELLA)-dependent manner. (B) Depletion of DPPA3 induces stronger active DNA demethylation at PCH, which in turns increases the levels of DNA damage. (C) Super-resolution picture of murine ESCs showing H3K9me3 enrichment at DAPI-dense PCH. However, in case of loss of DNA methylation such as in DNMT triple KO cells, the intensity of H3K9me3 signal reduces and chromocenters present overlapping signal with H3K27me3 mark deposited by polycomb proteins. Steric hindrance is visible as there is no colocalization of H3K9me3 and H3K27me3 signals. (D) Diminution of DNA methylation levels in ESCs, either by DNMT triple KO cells or 5-azacytidine treatment results in BEND3 accumulation at PCH. A is from Cooper *et al.*, *Cell Rep.* 2014. B is from Saksouk *et al.*, *Mol. Cell* 2014. C is adapted from Arakawa *et al.*, *Biochem. Biophys. Res. Comm.* 2015 D is adapted from Nagani *et al.*, *EMBO Rep.* 2015.

The DNA demethylation in 2i/LIF is notably visible at pericentromeric satellites (Tosolini *et al.* 2018). Although DNA methylation is an important epigenetic mark associated with constitutive heterochromatin maintenance, ESCs can overcome the loss of this modification. As mentioned in the second part of the introduction, pericentromeric organization also rely on the histone modification H3K9me3. Intriguingly, these two marks are dependent on one another as deletion of DNMTs results in the diminution of H3K9me3 and deletion of Suv39H1/2 induces the loss of DNA methylation (Saksouk *et al.* 2014). Indeed, H3K9me3 and H3K27me3 are non-overlapping modifications because of steric hindrance (**Figure 26C**). However, loss of DNA methylation or H3K9me3 enhances the recruitment of polycomb and NuRD proteins at nearly all major satellites to maintain the heterochromatin state, resembling the polycomb recruitment observed in the early embryo (Saksouk *et al.* 2014; Cooper *et al.* 2014). Saksouk *et al.* further shown that polycomb recruitment depended on the BEND3 protein (**Figure 26D**). Thus, heterochromatin state of pericentromeric regions can be maintained via multiple pathways according to the cellular state.

As developed in the second part of the introduction, heterochromatin is organized in multiple sub-nuclear compartments, one is the peripheral compartment with the LADs that are near the nuclear lamina. The dynamics of LADs during differentiation has been of great interest, although technical limitations made it difficult to explore within the pre-implantation embryo until very recently. The authors developed a single-cell DamID-LaminB1 approach with a low number of cells and performed it at four different time points from the zygote to the blastocyst (Borsos *et al.* 2019). They observed that zygotes displayed a LAD profile, whom 86% overlap with blastocyst-identified LADs, yet at the 2-cell stage 42% of the zygotic LADs reposition toward the nuclear interior, from which the majority were previously defined as cLADs, suggesting a broad and unusual LAD reorganization at the 2-cell stage. From the 2-cell stage to the blastocyst, some LADs lose their association, whereas other gain DamID signal in a transcription-dependent manner, as it was observed for the differentiation of mESCs (Peric-Hupkes *et al.* 2010). Interestingly, there are less transcriptional changes between LAD and non-LAD at the 2-cell stage than in other cell types, possibly a consequence of the more open chromatin state in these totipotent cells. Furthermore, TADs formation in the early embryo was not dependent on the DNA replication, but LAD acquisition was dependent on the parent-of-origin genome, with paternal LADs being broader, suggesting a stronger association. The authors observed that proper TADs establishment in the early embryo was dependent on the histone demethylase KDM5B, suggesting a strong importance of chromatin modification in this mechanism. To date, no study has reported differences in chromatin architecture between 2i/LIF and serum-based mESCs culture conditions. Formation of

TADs in the early embryo correlate with the ZGA but does not rely on transcription (Hug *et al.* 2017; Du *et al.* 2017). Furthermore, zygote cells have a low level of chromatin organization, and organization into TAD and A and B compartments is progressively acquired during the early development with strengthening of these features (Du *et al.* 2017). One could propose that at each division in the embryo, chromatin-related factors reinforce genome organization, thus preventing undesired conversion toward a more naïve state.

Pluripotent cells have an overall less condensed chromatin state, as it was described by assessing histone mobilities in ES and differentiated cells (Meshorer *et al.* 2006). In concordance with the less compacted chromatin, mESCs display high global transcriptional levels and differences in nucleosome distribution with a more homogeneous repartition in pluripotent cells, suggesting less defined chromatin subcompartments (Efroni *et al.* 2008; Ricci *et al.* 2015). Interestingly, it is proposed that this peculiar chromatin state could be a crucial regulator of pluripotency. Indeed, it was observed in high-throughput screenings that conversion from pluripotent ESCs to totipotent 2cell-like cells *in vitro* was enhanced when knocking-down chromatin-related factors (Rodriguez-Terrones *et al.* 2018; Ishiuchi *et al.* 2015; Cossec *et al.* 2018; Wu *et al.* 2020). The histone variant H3.3 is essential for embryonic development in mice, its lysine 27 residue being crucial for 2cell-state division (Santenard *et al.* 2010; Lin *et al.* 2013). H3.3 was also implicated in the maintenance of proper chromatin state. Indeed, depletion of H3.3 renders reprogramming more efficient (Fang *et al.* 2018). The SUMO-ligase UBC9 was also reported as a guardian of epigenetic state. Its removal allows ESCs to convert in a 2cell-like state, but also improves reprogramming efficiency of somatic cells into iPSCs (Cossec *et al.* 2018). These results suggest that totipotent, pluripotent and somatic cells possess differences in their chromatin organization, yet some factors used to maintain chromatin identity can play a role in different cellular states. Each state is not definitive, as reprogramming can be achieved. An emerging picture is that chromatin-related factors are crucial actors in maintaining cellular identities.

Many of the epigenetic-related factors mentioned in the second part of the introduction have been studied in different model organisms when possible. Intriguingly, most of these proteins were reported as embryonic lethal, although at different stages, such as the double knock-out of Dnmt3a and b, the H3K9-trimethylase Setdb1, the H3K9-dimethylases G9a and GLP (Li *et al.* 1992; Okano *et al.* 1999; Dodge *et al.* 2004; Tachibana *et al.* 2002, 2005). For the others H3K9-trimethylases Suv39h1 and 2, the double knock-out resulted in an increase in embryonic lethality and the remaining mice developed but were smaller and infertile (Peters *et al.* 2001). A similar observation was made for the knock-out of the Suv4-20h1 and 2 for which single KO did not present developmental defects but the double KO displayed perinatal lethality (Schotta *et al.* 2004).

These results indicate the crucial role played by epigenetic modifiers during development, but they also demonstrate the redundancy existing between these different enzymes as observed for the Suv39h and Suv4-20h enzymes. Specific deletion of HP1 proteins α , β or γ present different defects but no developmental arrest, although the triple KO is not reported (Brown *et al.* 2010). Only HP1 β KO present defects in cerebral cortex development (Aucott *et al.* 2008). Altogether, it seems that the heterochromatin state seems crucial in pluripotency control.


The early embryonic development follows different chromatin state, from totipotency to pluripotency to differentiated cells. Specific signaling pathways, that converge to chromatin regulation, correlate with each state. Indeed, it arises from recent studies that the regulation of cell physiology might happen from specific chromatin states. Notably, heterochromatin regulation seems essential in safeguarding cellular identity.

Appendix to the introduction

Review 1

Antoine CANAT, Adeline VEILLET, Amandine BONNET and Pierre THERIZOLS. Genome anchoring to nuclear landmarks drives functional compartmentalization of the nuclear space. *Briefings in functional genomics*, 2020.

Genome anchoring to nuclear landmarks drives functional compartmentalization of the nuclear space

Antoine Canat[‡], Adeline Veillet[‡], Amandine Bonnet and Pierre Therizols[†] [‡]

Corresponding author: P. Therizols, Laboratoire Génomes, Biologie Cellulaire et Thérapeutiques, Institut de Recherche St Louis, Université de Paris, CNRS UMR7212, INSERM U944, F-75010 Paris, France. Tel.: +33-1-5372-4058; E-mail: pierre.therizols@inserm.fr.

[‡]These authors contributed equally to this work.

Abstract

The spatial organization of the genome contributes to essential functions such as transcription and chromosome integrity maintenance. The principles governing nuclear compartmentalization have been the focus of considerable research over the last decade. In these studies, the genome–nuclear structure interactions emerged as a main driver of this particular 3D genome organization. In this review, we describe the interactions between the genome and four major landmarks of the nucleus: the nuclear lamina, the nuclear pores, the pericentromeric heterochromatin and the nucleolus. We present the recent studies that identify sequences bound to these different locations and address the tethering mechanisms. We give an overview of the relevance of this organization in development and disease. Finally, we discuss the dynamic aspects and self-organizing properties that allow this complex architecture to be inherited.

Key words: genome organization; nuclear pore complex; nuclear lamina; pericentromeric heterochromatin; chromosome 3D organization

Introduction

The studies of Carl Rabl and Theodor Boveri on salamander larvae and sea urchins at the turn of the 20th century demonstrated the non-random organization of chromosomes in the interphase nucleus. A few years later, Emil Heitz developed staining methods that distinguished gene-rich euchromatin from genetically inert heterochromatin [1]. Since then, the picture of the three-dimensional (3D) organization of the genome has become more complete mostly due to technological innovations made in the recent decades.

Chromosome conformation capture (3C) and its derived genome-wide methods showed that chromosomes occupy individual spaces with very low inter-chromosomal interactions, confirming the notion of chromosome territories observed by microscopy [2]. In most eukaryotes, chromosomes fold in a succession of large self-associating domains named

topologically associated domains (TADs) (reviewed in [3]). Inter-TAD interaction maps revealed the compartmentalization of the genome into two groups, segregating gene-rich, highly transcribed domains (A compartment) from gene-poor, transcriptionally repressed domains (B compartment). Although 3C-based methods have been crucial for measuring the frequency of physical interactions between genomic loci, they are intrinsically unable to indicate where these interactions occur in the nucleoplasm.

Nuclear organization of the genome also refers to the association of specific genomic regions with different membrane-less compartments. Nuclear landmarks, such as the nucleolus, the nuclear membrane and its nuclear pores and the chromocenters form discrete cellular structures. Genome tethering to the different landmarks is very well conserved through evolution, suggesting it is under selective pressure. For the past 25 years, many efforts have been made to characterize the interactions between

Antoine Canat is a PhD student at the Institut de Recherche Saint-Louis, Université de Paris.

Adeline Veillet is a post-doctoral fellow at the Institut de Recherche Saint-Louis, Université de Paris.

Amandine Bonnet is a post-doctoral fellow at the Institut de Recherche Saint-Louis, Université de Paris. Her research interests include the nuclear pore complex and transposable elements.

Pierre Therizols is a CNRS scientist in the unit 'Genome, Cellular Biology and Therapeutics', Institut de Recherche Saint-Louis. His research focuses on understanding how heterochromatin reorganizes in embryonic stem cells.

© The Author(s) 2020. Published by Oxford University Press. All rights reserved. For Permissions, please email: journals.permissions@oup.com

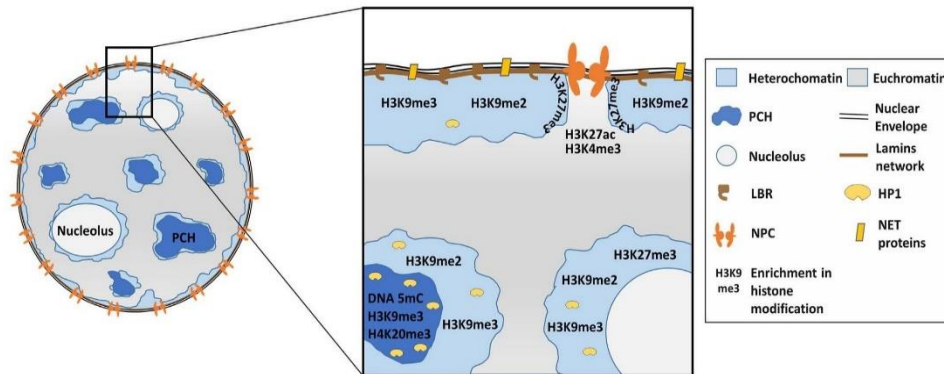


Figure 1. Conventional organization of a mammalian nucleus. Different landmarks contribute to genome segregation into functional compartments. The nuclear envelope defines the edge of the nucleus. The nuclear lamina is a meshwork of proteins that interact with heterochromatic genomic regions called lamina-associated domains (LADs), only interrupted by nuclear pore complexes (NPCs). The two main other landmarks—the chromocenter, composed of clustered pericentromeric heterochromatin (PCH), and the nucleolus—are surrounded by heterochromatin compartments, named pericentromere-associated or nucleolus-associated domains (PADs and NADs), respectively. Highlighted on the right is a small region of the nucleus with the histone marks associated with the different compartments. LADs at the periphery are enriched in H3K9me2/3 modifications and H3K27me3 at LAD borders [11]. LADs can interact with different lamina-associated proteins such as LBR and some NETs. PADs and NADs resemble LADs and are enriched in H3K9me2/3 modifications. A subset of NADs also presents high H3K27me3 [82]. Heterochromatin regions show different levels of HP1 with higher concentration at PCH. The NPC interacts with euchromatin domains, notably promoters and enhancers enriched in H3K27ac and H3K4me3 [41]. Ac, acetylation; me2/3, di- or tri-methylation; DNA 5mC, DNA methylation; HP1, heterochromatin protein 1; LBR, lamin B receptor; NET, nuclear envelope transmembrane protein.

the genome and the subnuclear compartments. In this review, we will discuss how different nuclear landmarks contribute to the non-random folding and positioning of chromosomes and the functional relevance of these interactions with a specific emphasis on mammals. We will consider the dynamic aspects of the genomic associations with the specific landmarks, highlighting recent results describing the mechanisms responsible for the reestablishment of these interactions after mitosis and their regulation during development.

The nuclear periphery

At the nuclear periphery, the nuclear lamina lines the inner nuclear membrane of the nuclear envelope interrupted by nuclear pore complexes (NPCs). Most eukaryotic cells display a radial nuclear organization with heterochromatin positioned at the nuclear periphery and around nucleoli, and the euchromatin located towards the nuclear interior (Figure 1). Evidence for the accumulation of dense chromatin regions at the nuclear periphery first came from electron micrographs in the 1960s [4,5]. At that time, the attachment of the inactive X chromosome to the nuclear membrane already suggested a role for the nuclear periphery in nuclear organization. The use of fluorescent in situ hybridization (FISH) experiments further confirmed that the inactive X chromosome is found preferentially at the nuclear periphery [6].

Nuclear lamina

The nuclear lamina (NL) forms a repressive environment that plays a role in the spatial organization of the chromosomes in the nucleus. It is comprised of lamin intermediate filaments and membrane-associated proteins. These intermediate filaments are made up of four lamin isoforms: lamins A, C, B1 and B2.

Exploration of the nuclear compartmentalization by FISH indicated that gene-poor regions preferentially associate with

the NL. Localization of the gene-rich human chromosome 19 was shown to have a more central position than the gene-poor chromosome 18, which preferentially associates with the nuclear periphery. Reciprocal translocations identified a 20 Mb region of chromosome 18 sufficient for the NL association [7]. This phenomenon is not limited to chromosomes 18 and 19, as most gene-poor chromosomes interact more often with the NL than gene-rich chromosomes [2]. At the gene level, studies further showed that developmental genes, such as the immunoglobulin H gene *Igh* and the proneural regulator gene *Mash1* are sequestered at the periphery of progenitor cells, but relocate towards the center of the nucleus before they get activated at further stages of differentiation [8,9]. These studies suggest a role for the nuclear periphery in development gene repression. However, these FISH studies are limited to a small number of specific genes.

Genome-wide characterization of the genome interactions with the NL were revealed by DNA adenine methyltransferase identification (DamID) experiments. In these studies, genomic loci in close proximity to the NL were identified using a fusion protein of DAM with a lamin protein. The adenine methylated DNA was then amplified and mapped to the respective genomes. This led to the discovery of lamina-associated domains (LADs) in *Drosophila melanogaster*, *Caenorhabditis elegans* and mammalian cells [10–13]. In mammalian cells, over 1000 LADs were identified. LADs are 0.1 to 10 Mb A/T rich regions that make up 30 to 40% of the genome. LADs replicate during the late S phase [14,15] and have low gene density. Most genes present in LADs are expressed at low levels [11].

Efforts have been made to find underlying genomic and epigenetic features that lead to association with the NL. Some LADs were found to contain GAGA repeats that direct lamina association and transcriptional repression [16]. In addition, loss of interactions between the NL and specific AT-rich motifs can lead to transcriptional permissiveness [17]. Loss of active chromatin marks, such as the deacetylation of histone H4 were

shown to be implicated in the repression of gene expression and NL localization. Periphery anchoring was found to be dependent on the repressive histone marks H3K9me2 and H3K9me3 for the β -globin gene cluster [18] and integrated gene arrays in *C. elegans* [19]. H3K9me2, H3K9me3 and H3K27me3 enrichment has also been correlated to LADs or LAD boundaries genome-wide (Figure 1) [11,20,21]. More recently, active marks on euchromatin were shown to play a role in NL anchoring and repression of heterochromatin in *C. elegans*. The *mrg-1* gene, which is involved in histone acetylation at euchromatin regions, is important for the NL localization of a heterochromatin reporter gene. Depletion of MRG-1 leads to aberrant recruitment of activators and active chromatin marks at heterochromatin and correlates with heterochromatin detachment from the NL [22]. Altogether, these studies suggest that post-translational chromatin marks can directly or indirectly affect NL association.

On the NL side, lamins and inner membrane proteins interact with heterochromatin at the nuclear periphery. Lamins have been shown to contribute to nuclear envelope association with the genome and transcriptional repression in *D. melanogaster* and *C. elegans* [23–25]. In contrast, in mouse embryonic stem cells, lamins appear dispensable for nuclear envelope interactions [26]. This discrepancy is most likely due to the redundant role of lamin B receptor (LBR) and lamin A/C in mice cells. Certain types of cells, such as mouse rod photoreceptors show an ‘inverted’ pattern of spatial organization, with a central mass of heterochromatin and euchromatin located towards the nuclear periphery [27]. These cells do not express lamin A/C or LBR. Interestingly, loss of both lamin A/C and LBR expression in all postmitotic cell types leads to a partially inverted chromatin configuration, and rod photoreceptor cells that express LBR can tether heterochromatin to the periphery [28]. Lamin A/C and LBR are therefore essential but redundant organizers of LADs. In addition, a number of tissue-specific nuclear envelope transmembrane proteins (NETs) contribute to chromosome positioning in the nuclear space (Figure 1) [29] and may be responsible for tissue-specific LAD–NL interactions [30]. Overall, radial organization is regulated at different levels, from the DNA sequence to the NE-associated anchoring factors. LAD tethering involves several redundant and overlapping pathways suggesting an important role for the radial organization.

Misregulation of the peripheral repressive compartment has significant functional consequences and is responsible for several diseases. Mutations in lamins and other NL proteins have been implicated in a number of human disorders. Missense mutations in *laminA* can cause Emery–Dreifuss muscular dystrophy (EDMD). *LaminA* mutations alter LADs in human muscle cell nuclei leading to perturbation of myogenic differentiation [31]. The NL also contributes to cellular senescence, a stress response that irreversibly suppresses cell proliferation. *LaminB* depletion during senescence leads to spatial reorganization of chromatin and changes in gene expression [32]. Moreover, in oncogene-induced senescence (OIS) models, most of the constitutive LADs (cLADs) are lost and the repressive activity of the NL is compromised [33]. Even though the function of altered LAD–NL interactions in EDMD and senescence still needs to be fully appreciated, it is clear that the radial genomic organization imposed by the NL is physiologically essential.

NPC

The NPCs are built of multiple copies of about 30 different proteins, called nucleoporins (Nups) that are organized into modular subcomplexes (for review [34]). The overall structure

of the NPC is conserved across eukaryotes with a structural core embedded within the nuclear envelope and peripheral structures extending towards the cytoplasm and the nucleoplasm, namely the cytoplasmic filaments and the nuclear basket, respectively. As the only gates between the cytoplasm and the nucleus, NPCs regulate the selective nucleocytoplasmic transport of proteins and RNAs. Over the last two decades, evidence has accumulated that NPCs are also key components of the 3D organization of the eukaryotic genomes.

The global role of NPCs in 3D genome organization is notably visible at the macromolecular scale with the NPCs being the only areas of the nuclear periphery systematically devoid of heterochromatin (Figure 1) [35]. Tpr, a Nup of the nuclear basket, was identified as essential for delimiting heterochromatin distribution and defining sub-nuclear compartments associated with the NPC [36]. Such chromatin boundary activities were first genetically characterized for Nups of the nuclear basket in yeast [37,38]. In *D. melanogaster*, NPC-interacting domains, defined by DamID, were also found to be significantly enriched in the chromatin insulator protein Su (Hw) [39,40]. Overall, these data suggest a strong conservation of the role of the NPCs as physical barriers to enclose different chromatin regions. The development of genome-wide techniques, like DamID or ChIPseq, led to the identification of NPC-interacting domains [41,42]. There is roughly the same number of contacts between the genome and the NPCs or the NL in human cells. However, the NPC–chromosome interactions are restricted to narrow sites of few kilobases (kb) (Figure 2), particularly enriched in promoter and enhancer regions, compared to the broader chromosomal domains of several hundreds of kilobases or kb associated with LADs [41].

Multiple functions and molecular mechanisms have been associated with these chromatin–NPC interactions. Genetically disentangled in yeast, these interactions are much more difficult to study in metazoan because of two main specificities: (i) some of the Nups have been described as dynamically associated with the NPC and also observed in the nucleoplasm [43,44] and (ii) the Nup composition of the NPC can vary in a tissue- or developmental stage-specific manner [45,46]. For instance, while a relocation of persistent DNA lesions has been clearly reported in yeast, a role for the NPC in DNA damage repair remains to be demonstrated in vertebrates [47]. In contrast, the function of the NPC in gene expression regulation has been conserved throughout evolution. The NPC-tethering of inducible genes upon transcriptional activation in yeast was first proposed to facilitate the coupling of mRNA synthesis and export, in agreement with the so-called ‘gene gating’ hypothesis [48]. Several recent examples illustrate the additional complexity that makes metazoan NPC an essential scaffold for implementing tissue-specific or signal-induced transcriptional programs [49–53]. Due to the transcriptional activation in their vicinity, NPCs have also been physically and functionally connected with stable regulated processes over time such as X dosage compensation in *Drosophila* and genomic imprinting in mammalian genome [54,55]. NPCs are associated not only with transcriptionally active loci but also with repressed ones [42,53,56]. More importantly, the delocalization of some loci from the NPC was correlated with a loss of silencing of these genes [57–59]. A third category of NPC-tethered genes has been described: inducible genes in a poised state. They are targeted to the nuclear periphery upon an initial stimulus and remain at the nuclear pore where they can be rapidly and robustly reactivated upon new stimuli. This ‘transcriptional memory’ relies on stabilization of chromatin loops by the NPC [60]. First described in yeast [61],

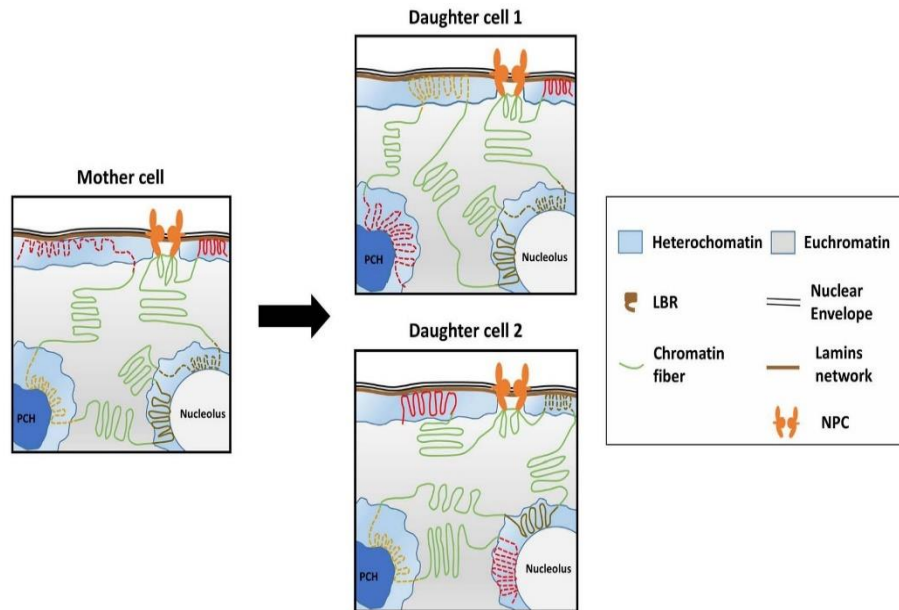


Figure 2. Inheritance of nuclear landmark associations throughout mitosis. Global organization of the genome is maintained upon cell division. Careful examination of the specific sequences however demonstrated a reshuffling of the genome [20]. Euchromatin is in green, and different heterochromatin domains are depicted in red, brown or yellow for LADs, NADs or PADs, respectively. In the mother cell, the genome is folded in a particular position. After mitosis, the genome is refolded around the different landmarks. Some domains, represented as dotted lines (PADs, LADs or NADs) can relocate to other subnuclear compartments of the same chromatin state. Some regions are constitutively found at the same nuclear position, showed here as full lines (LADs and NADs).

'transcriptional memory' has recently been described for the NPC-associated ecdysone-inducible genes in *Drosophila* [42].

Recently published data demonstrate a role for the nuclear basket in the organization of the lamin B1 network and the distribution of the NPCs within the nuclear envelope [62]. As expected, there is a constant interplay between the NPC and the NL. Further studies will be required to describe how they work together to ensure proper genome compartmentalization.

Pericentromeric heterochromatin clusters

When DAPI-stained, the nucleus of some species such as mouse, *Drosophila* or plants present distinctive dense foci called chromocenters (Figure 1). Chromocenters are mainly composed of the pericentromeric satellite DNA tandem repeats that surround centromeres. Pericentromeric heterochromatin (PCH) comprises from ~3% of the genome in human and mouse to ~50% of the genome in some *Drosophila* species (for review, see [63]). Human cells do not exhibit DAPI-dense foci, yet pericentromeric satellites still form clusters within the nucleoplasm [64,65]. PCH clustering is conserved through evolution despite the lack of conservation of satellite sequences, suggesting it is under selective pressure. Pericentromeric satellites are folded into constitutive heterochromatin, enriched in repressive epigenetic modifications such as H3K9me3, H3K64me3, H4K20me3 and DNA methylation (Figure 1). Many additional proteins, such as HP1 α and HMGA1, are found at PCH. They form a complex network of proteins acting together to ensure proper transcriptional repression [66]. Depletion in one of these heterochromatin factors generally compromises the chromatin state but does not impact the clustering [67–69]. These observations suggest that heterochromatin formation and clustering result from two separated

pathways. Very little is known about the mechanism driving PCH clustering. To date, only depletion of HMGA1 and H4K20me3 has been reported to alter chromocenters formation [69,70]. The molecular mechanisms supporting this clustering therefore need to be further investigated.

Defects in clustering were observed in different pathologies such as Alzheimer's disease and breast cancer [71,72]. Although the contribution of the clustering defect to disease etiology remains unclear, it is correlated to the derepression of satellite sequences, and higher DNA damage levels [71,72]. Interestingly, it was reported that altered PCH clustering induces severe genome instability reflected by micronuclei formation or mis-segregation of chromosomes, suggesting the importance of this clustering from mitosis to interphase [69,70]. Alongside maintaining chromosome stability, PCH clusters also serve as a scaffold for repressed genes. For example, the silent β -globin gene associates with chromocenters before relocating away from PCH upon activation [73,74]. Overall, chromocenters' functions remain elusive but they contribute to the safe transfer of chromosomes through mitosis and act as anchoring points for other heterochromatin domains.

Around 1000 regions, called pericentromere-associated domains (PADs), were identified to interact with PCH [75]. There is a striking overlap between PAD and LAD sequences suggesting the nuclear periphery and PCH form redundant repressive compartments (Figure 2). This redundancy can be illustrated by a competition between the nuclear periphery and chromocenters to bind silent transgenes in mouse cells [18]. Interestingly, the choice between periphery or chromocenter association seems to be dependent on H3K9me3 levels, with higher levels correlating with the periphery [18,21]. Overlap between LADs and PADs vary between cell types. In embryonic stem cells, gene-poor regions

form large LADs when associated to the nuclear envelope. In contrast, these regions associate with PCH as smaller interspaced domains [75]. Upon differentiation, neighboring PADs merge and form larger domains similar to LADs. These results suggest a different regulation for chromocenters and nuclear envelope associations. Future research is necessary to better characterize the extent of the observed redundancy.

Nucleolus

Discovered in 1835 by Wagner, the nucleolus was the first nuclear landmark identified. The tandem repeats of ribosomal DNA constitute the nucleolar organizer regions (NORs) and self-assemble into one or several subnuclear compartments by liquid-liquid phase separation [76]. The primary function of the nucleolus is the transcription of the different rRNAs and the maturation of ribonucleoproteins [77]. Nucleoli also form a scaffold for chromatin tethering. Electron micrographs of eukaryote nuclei generally exhibit large blocks of perinucleolar heterochromatin accumulating around the nucleoli (Figure 1). Pericentromeric and telomeric heterochromatin regions were first observed to stochastically associate with the nucleoli [78,79]. These results were later confirmed by NGS sequencing of DNA extracted from purified nucleoli from two different human cell lines [80,81]. Besides tandem-repeat heterochromatin, hundreds of large regions named nucleolar-associated domains (NADs) were identified. NADs are about 800 kb long on average, gene-poor, enriched in repressive histone marks and lowly transcribed.

At first glance, the high overlap between NADs and LADs suggests that they form two redundant compartments. However, more recent studies reveal a more complex nature for the perinucleolar compartment. The degree of redundancy between perinucleolar and peripheral heterochromatin varies between species. In murine fibroblasts, two classes of NADs were identified. Type I NADs display constitutive heterochromatin characteristics and frequently associate with the nuclear periphery. In contrast, type II NADs do not overlap with LADs and exhibit facultative heterochromatin attributes such as H3K27me3 (Figure 1) [82]. In *Arabidopsis thaliana*, there is a minor overlap between perinucleolar and peripheral heterochromatin, suggesting they form two distinct repressive compartments [83,84]. Functionally, it is accepted that the nucleolus and the nuclear envelope share the role of scaffolding repressive compartments where heterochromatin accumulates. However, during senescence, the perinucleolar and peripheral repressive compartments are differently affected. While LAD tethering is compromised in senescent cells [32,33], only minor changes in NAD organization were observed [65]. Interestingly, the maintenance of perinucleolar targeting could explain the few transcriptional changes observed in gene-poor regions upon senescence [32,33]. The perinucleolar and peripheral heterochromatins are therefore partially redundant, but the degree of redundancy depends largely on the species and physiological state of the cells.

Dynamic aspect of nuclear organization

Maps of the interactions between genomic domains and the different nuclear landmarks greatly improved our understanding of chromosome positioning and its impact on nuclear functions. Since these maps were generated from cell populations, they do not reflect the stochasticity and the dynamic nature of these interactions.

When a cell divides, genome-landmark associations are shuffled but the cells retain their global nuclear organization (Figure 2). Our current comprehension of genome positioning inheritance involves a combination of chromatin self-organization and stochastic associations with the landmarks discussed above. According to the model proposed by Falk *et al.*, interactions between heterochromatic regions are the main driver of nuclear organization [85]. By combining Hi-C, microscopy and polymer models, they conclude that strong heterochromatin interactions are essential and sufficient to achieve the segregation of active and repressive compartments. A biophysical mechanism contributing to the self-exclusion of the PCH compartment was recently discovered [86,87]. Phosphorylated HP1 α can form liquid-droplet structures mediated by multivalent weak interactions between its low-complexity protein domains. When bound to satellite sequences, HP1 α confers liquid-like properties to PCH, resulting in self-exclusion by liquid-liquid phase separation [86,87]. In contrast, the mechanism driving the transmission of gene-poor heterochromatin organization through mitosis remains largely unknown. Yet, converging results support the model of self-organization by phase separation. In Hi-C studies, the repressive compartment forms by preferential contacts between gene-poor regions [88,89]. In murine rod cells, the repressive compartment is maintained independently of nuclear envelope tethering [85]. In these cells, gene-poor regions occupy a specific volume segregated from euchromatin and PCH, suggesting some level of self-organization [27]. Polymer models satisfying phase separation criterion can predict the formation of a self-organized gene-poor compartment [85]. In these models, interactions between gene-poor regions result from phase separation, whereas nuclear envelope tethering is required to create a radial organization. Live imaging and single-cell DamID gave significant insights on the dynamic aspect of nuclear envelope associations. LAD association with the nuclear envelope is stochastic and only partially inherited through mitosis (Figure 2). Each LAD is tethered by multivalent interactions with the NL (Figure 2), and importantly, LADs from a same chromosome exhibit coordinated anchoring [20,21]. Altogether, these observations support the model of self-organization of the repressive compartment by phase separation. Additionally, stochastic associations of these self-assembled chromatin domains with nuclear landmarks determine their subnuclear localization.

Regulation of genome spatial positioning according to cell type is another important dynamic aspect of nuclear organization. NPCs have been reported to contribute to gene expression regulation during development. NPCs bind a number of cell-type-specific genes in human cells [41]. Upon embryonic stem cell differentiation, some genes relocate to NPCs prior to activation suggesting NPCs could mediate transcriptional priming [49]. Nup153 exerts a subtler regulation on both gene activation and repression to prevent neuronal progenitor cells differentiation [53]. This reflects the complexity of the regulation of the developmental transcriptional programs by the NPC. Although the molecular mechanisms remain to be fully elucidated, NPCs are therefore important landmarks that mediate spatial and temporal coordination of various factors and chromatin structures resulting in cell-specific transcriptional outputs.

Lineage commitment also modulates heterochromatin organization leading to thousands of changes in gene expression. Embryonic stem cells, with their ability to differentiate into a wide variety of cell types, are a model of choice to study the impact of lineage commitment on nuclear organization.

Upon differentiation, physical interactions between regions belonging to the heterochromatin compartment strengthen [89], correlating with the progressive compaction of heterochromatin during cell differentiation [15,90]. Concomitantly, genome tethering to the NL and chromocenters is reinforced in differentiated cells [12,91]. The vast majority of LADs and PADs remain associated to their respective landmarks in every cell type and are designated as constitutive (cLADs and cPADs) [12,75]. In zygotes, associations of constitutive LADs with the nuclear envelope are not inherited from the germ line but established *de novo* [92]. As active and repressive compartments segregate before zygotic transcriptional activation [93], nuclear envelope anchoring could be an early step of genome compartmentalization.

In contrast, the tethering of facultative LADs or PADs is modified. These regions can associate or detach from the repressive compartments in specific cell types [12,75]. For example, upon embryonic stem cell differentiation into neuronal progenitors, 847 genes detach from the nuclear edge while 633 genes are tethered [12]. Gene repositioning is strongly correlated to transcriptional changes: activation when a gene loses association with repressive landmarks and repression when it is anchored. About a third of the genes that detach from the nuclear periphery do not change transcriptional status. However, these genes are more likely to be activated at later stages of development supporting a model of gene relocation contributing to transcriptional priming. Interestingly, this unlocking mechanism is not restricted to protein coding genes. Indeed, the Bcl11b enhancer detaches from the nuclear envelope to form a loop with the promoter, facilitating transcriptional activation and T cell differentiation [94].

The important question of whether the NL and chromocenter associations are a cause or a consequence of transcriptional changes remains controversial. Ectopic transcriptional activation is sufficient to detach individual genes from nuclear envelope [95,96]. Reciprocally, artificial targeting of reporter constructs or chromosomes to the NL or to chromocenters is sufficient to repress the majority of genes even megabases away from the tethering site [75,97,98]. However, the influence of the NL or chromocenter on gene expression is very likely to be regulated at the gene level as some tethered genes escape silencing [91,97,99]. Indeed, the gene repression status in LADs seems to be based on both the intrinsic properties of promoters and on local chromatin features [100]. The reciprocal effect between the nuclear periphery positioning and transcription could be explained by self-organization of the repressive compartment. When brought to a repressive environment, the high local concentration of repressive factors may facilitate transcriptional silencing. Conversely, when a peripheral gene is activated, its chromatin state changes and phase separates from the neighboring repressive chromatin. This speculative model is supported by several observations indicating that chromatin state regulation plays a central role in gene repositioning. Inducing large-scale chromatin decondensation by recruiting a synthetic acidic-hydrophobic peptide is sufficient to relocate exogenous transgenes and endogenous facultative LAD genes towards the nuclear interior [95,96]. Histone acetylation regulation could be involved as both histone deacetylases and exclusion of histone acetylases are essential to maintaining the repressive state of LADs at the nuclear periphery [16,22,97]. The identification of new factors required for gene repositioning or phase separation of LADs will likely contribute to resolve the question of the cause-effect relationship between subnuclear localization and transcription.

Concluding remarks and future perspectives

Over the past decade, 3D genome organization has proved to be essential for many nuclear functions. The folding of the genome results from a synergistic combination of inter-chromatin interactions and anchors to discrete nuclear landmarks. In this review, we described how the nuclear envelope, NPCs, PCH and the nucleolus associate with particular genomic regions. We also discussed recent studies highlighting how the dynamic tethering to these different landmarks contributes to nuclear function compartmentalization.

Large domains of heterochromatin associate either with the NL, chromocenters or the nucleolus. The significant overlap between LADs, PADs and NADs substantiates the functional redundancy of these different repressive compartments. Their relative contributions vary between cell types and during processes like senescence [12,33,65,75]. The recent discovery of genomic domains that are exclusively associated with the nucleolus [82] implies there may be additional compartment specific roles. Studies are needed to further dissect the specific functions of each repressive compartment. Indeed, the nuclear periphery has been implicated in DNA repair pathway choice [101], but whether this function is limited to the nuclear periphery or is a broader feature of repressive compartments has to be addressed.

Interactions with the repressive compartments can facilitate gene silencing [75,97,98]. However, only correlations support a role for repressive compartment dissociation in transcriptional activation [12,75]. Although gene repositioning towards the nuclear interior can be independent of transcription [96], whether relocated genes are primed for transcriptional activation has yet to be clearly demonstrated.

Similarly, for NPC-associated regions, the transcriptional activation has been clearly associated with NPC tethering through artificial anchoring experiments performed in yeast [102–104]. However, conclusions driven from mammalian models are essentially based on correlations between a change in transcriptional status and a relocation from the NPC. The recent evidence that NPCs can also be a repressive environment strongly suggest a more complex picture of the NPC-associated subnuclear compartment [53,57,105]. Further studies will be required to precisely decipher whether the same molecular interactions underlie the active and repressive transcriptional environment.

Phase separation provides an energy efficient mechanism to functionally segregate the different domains of the genome. We are just beginning to understand how phase separation could regulate genome compartmentalization. Many factors able to promote phase separation will probably be discovered in the coming years. In particular, factors responsible for self-segregation of gene-poor regions remain unknown. The absence of nuclear envelope tethering in inverted nuclei should facilitate this task, since only heterochromatin interactions contribute to repressive compartment organization [85]. Like HP1, these factors will probably be well-characterized proteins with intrinsically disordered domains. For instance, in the NPCs, about a third of nucleoporins, named as FG Nups, contain 5 to 50 repeats of phenylalanine-glycine (FG) residues, which are interspersed by hydrophilic of charged sequences. These highly repetitive and disordered FG domains confer to FG Nups phase separation properties *in vitro* [106]. In a review, Pascual-Garcia & Capelson speculate that subnuclear compartments associated with NPCs could assemble by phase separation [107]. Post-translational modifications, such as SUMOylation, can confer phase sep-

aration properties to their targets [108]. These very dynamic modifications could significantly contribute to the stochastic association of the genome to the different nuclear landmarks. Phase separation models also bring new insights into human diseases and could lead to new therapeutic strategies. For example, in amyotrophic lateral sclerosis (ALS), Poly-PR and Poly-GR dipeptide-repeat proteins alter the phase separation of HP1 and NPM1, disturbing PCH and nucleoli compartmentalization [109,110].

The emergence of Crispr-derived tools already significantly contributed to our understanding of nuclear organization. The constant innovation in genome and epigenome engineering is crucial to experimentally test the more complex models brought by the compilation of Omics data and the new liquid droplet theories. The ability to efficiently knock out and knock in will facilitate the dissection of specific mechanisms, particularly for redundant pathways such as LAD tethering. Similarly, the role of specific epigenetic marks highlighted in this review can now be directly addressed with targeted recruitment of epigenetic modifiers such as histone deacetylases or demethylases to specific regions. Finally, the capacity of altering genome 3D organization and tethering an endogenous genomic locus to a specific landmark opens exciting perspectives for future studies [111].

Summary key points

- Anchoring the genome to discrete landmarks contributes to nuclear functions compartmentalization.
- Large domains of the genome associate with the nuclear lamina, pericentric heterochromatin or the nucleolus to form the heterochromatin compartment
- Heterochromatin tethering to repressive landmarks facilitates transcriptional repression and is required to protect genome integrity.
- Nuclear pore complexes are important platforms for coordinating spatial and temporal gene expression.
- Nuclear organization is inherited through cell division and development by dynamic genome interactions with the nuclear landmarks.

Funding

This work was supported by Agence Nationale de la Recherche (ANR-16-CE12-0003-01). A.C. acknowledges the support of Ecole Doctorale 'Hématologie – Oncogénèse – Biothérapies' (HOB). A.B. acknowledges the 'Who am I?' laboratory of excellence.

References

1. Allshire RC, Madhani HD. Ten principles of heterochromatin formation and function. *Nat Rev Mol Cell Biol* 2018;**19**:229–44.
2. Boyle S, Gilchrist S, Bridger JM, et al. The spatial organization of human chromosomes within the nuclei of normal and emerin-mutant cells. *Hum Mol Genet* 2001;**10**:211–9.
3. Bonev B, Cavalli G. Organization and function of the 3D genome. *Nat Rev Genet* 2016;**17**:661–78.
4. Comings DE. The rationale for an ordered arrangement of chromatin in the interphase nucleus. *Am J Hum Genet* 1968;**20**:440–60.
5. van Steensel B, Lamina-Associated Domains BAS. Links with chromosome architecture, heterochromatin, and gene repression. *Cell* 2017;**169**:780–91.
6. Dyer KA, Canfield TK, Gartler SM. Molecular cytological differentiation of active from inactive X domains in interphase: implications for X chromosome inactivation. *Cytogenet Cell Genet* 1989;**50**:116–20.
7. Croft JA, Bridger JM, Boyle S, et al. Differences in the localization and morphology of chromosomes in the human nucleus. *J Cell Biol* 1999;**145**:1119–31.
8. Kosak ST. Subnuclear compartmentalization of immunoglobulin loci during lymphocyte development. *Science* 2002;**296**:158–62.
9. Williams RRE, Azuara V, Perry P, et al. Neural induction promotes large-scale chromatin reorganization of the Mash 1 locus. *J Cell Sci* 2006;**119**:132–40.
10. Pickersgill H, Kalverda B, de Wit E, et al. Characterization of the Drosophila melanogaster genome at the nuclear lamina. *Nat Genet* 2006;**38**:1005–14.
11. Guelen L, Pagie L, Brasset E, et al. Domain organization of human chromosomes revealed by mapping of nuclear lamina interactions. *Nature* 2008;**453**:948–51.
12. Peric-Hupkes D, Meuleman W, Pagie L, et al. Molecular maps of the reorganization of genome-nuclear lamina interactions during differentiation. *Mol Cell* 2010;**38**:603–13.
13. González-Aguilera C, Ikegami K, Ayuso C, et al. Genome-wide analysis links emerin to neuromuscular junction activity in *Caenorhabditis elegans*. *Genome Biol* 2014;**15**:R21.
14. Hiratani I, Ryba T, Itoh M, et al. Global reorganization of replication domains during embryonic stem cell differentiation. *Plos Biol* 2008;**6**:e245.
15. Hiratani I, Ryba T, Itoh M, et al. Genome-wide dynamics of replication timing revealed by in vitro models of mouse embryogenesis. *Genome Res* 2010;**20**:155–69.
16. Zullo JM, Demarco IA, Piqué-Regi R, et al. DNA sequence-dependent compartmentalization and silencing of chromatin at the nuclear lamina. *Cell* 2012;**149**:1474–87.
17. Lund E, Oldenburg AR, Delbarre E, et al. Lamin A/C-promoter interactions specify chromatin state-dependent transcription outcomes. *Genome Res* 2013;**23**:1580–9.
18. Bian Q, Khanna N, Alvikas J, et al. β -Globin cis-elements determine differential nuclear targeting through epigenetic modifications. *J Cell Biol* 2013;**203**:767–83.
19. Towbin BD, González-Aguilera C, Sack R, et al. Step-wise methylation of histone H3K9 positions heterochromatin at the nuclear periphery. *Cell* 2012;**150**:934–47.
20. Kind J, Pagie L, Ortabozkoyun H, et al. Single-cell dynamics of genome-nuclear lamina interactions. *Cell* 2013;**153**:178–92.
21. Kind J, Pagie L, de Vries SS, et al. Genome-wide maps of nuclear lamina interactions in single human cells. *Cell* 2015;**163**:134–47.
22. Cabianca DS, Muñoz-Jiménez C, Kalck V, et al. Active chromatin marks drive spatial sequestration of heterochromatin in *C. elegans* nuclei. *Nature* 2019;**40**:47.
23. Kohwi M, Lupton JR, Lai S-L, et al. Developmentally regulated subnuclear genome reorganization restricts neural progenitor competence in drosophila. *Cell* 2013;**152**:97–108.
24. Shevelyov YY, Lavrov SA, Mikhaylova LM, et al. The B-type lamin is required for somatic repression of testis-specific gene clusters. *Proc Natl Acad Sci U S A* 2009;**106**:3282–7.
25. Mattout A, Pike BL, Towbin BD, et al. An EDMD mutation in *C. elegans* lamin blocks muscle-specific gene relocation and compromises muscle integrity. *Curr Biol* 2011;**21**:1603–14.

26. Amendola M, van Steensel B. Nuclear lamins are not required for lamina-associated domain organization in mouse embryonic stem cells. *EMBO Rep* 2015;16:610–7.
27. Solovei I, Kreysing M, Lanct Ot C, et al. Nuclear architecture of rod photoreceptor cells adapts to vision in mammalian evolution. *Cell* 2009;137:356–68.
28. Solovei I, Wang AS, Thanisch K, et al. LBR and lamin A/C sequentially tether peripheral heterochromatin and inversely regulate differentiation. *Cell* 2013;152:584–98.
29. Zuleger N, Boyle S, Kelly DA, et al. Specific nuclear envelope transmembrane proteins can promote the location of chromosomes to and from the nuclear periphery. *Genome Biol* 2013;14:R14.
30. Wong X, Luperchio TR, Reddy KL. NET gains and losses: the role of changing nuclear envelope proteomes in genome regulation. *Curr Opin Cell Biol* 2014;28:105–20.
31. Perovanovic J, Dell'Orso S, Gnochi VF, et al. Laminopathies disrupt epigenomic developmental programs and cell fate. *Sci Transl Med* 2016;8:335ra58.
32. Sadaie M, Salama R, Carroll T, et al. Redistribution of the Lamin B1 genomic binding profile affects rearrangement of heterochromatic domains and SAHF formation during senescence. *Genes Dev* 2013;27:1800–8.
33. Lenain C, de Graaf CA, Pagie L, et al. Massive reshaping of genome-nuclear lamina interactions during oncogene-induced senescence. *Genome Res* 2017;27:1634–44.
34. Lin DH, Hoelz A. The structure of the nuclear pore complex (an update). *Annu Rev Biochem* 2019;88:725–83.
35. Schermelleh L, Carlton PM, Haase S, et al. Subdiffraction multicolor imaging of the nuclear periphery with 3D structured illumination microscopy. *Science* 2008;320:1332–6.
36. Krull S, Dörries J, Boysen B, et al. Protein Tpr is required for establishing nuclear pore-associated zones of heterochromatin exclusion. *EMBO J* 2010;29:1659–73.
37. Dilworth DJ, Tackett AJ, Rogers RS, et al. The mobile nucleoporin Nup 2p and chromatin-bound Prp 20p function in endogenous NPC-mediated transcriptional control. *J Cell Biol* 2005;171:955–65.
38. Ishii K, Arib G, Lin C, et al. Chromatin boundaries in budding yeast: the nuclear pore connection. *Cell* 2002;109:551–62.
39. Kalverda B, Fornerod M. Characterization of genome-nucleoporin interactions in *Drosophila* links chromatin insulators to the nuclear pore complex. *Cell Cycle* 2010;9:4812–7.
40. Kalverda B, Pickersgill H, Shloma VV, et al. Nucleoporins directly stimulate expression of developmental and cell-cycle genes inside the nucleoplasm. *Cell* 2010;140:360–71.
41. Ibarra A, Benner C, Tyagi S, et al. Nucleoporin-mediated regulation of cell identity genes. *Genes Dev* 2016;30:2253–8.
42. Pascual-García P, Debo B, Aleman JR, et al. Metazoan nuclear pores provide a scaffold for poised genes and mediate induced enhancer-promoter contacts. *Mol Cell* 2017;66:63–76.e6.
43. Griffis ER, Altan N, Lippincott-Schwartz J, et al. Nup 98 is a mobile nucleoporin with transcription-dependent dynamics. *Mol Biol Cell* 2002;13:1282–97.
44. Rabut G, Doye V, Ellenberg J. Mapping the dynamic organization of the nuclear pore complex inside single living cells. *Nat Cell Biol* 2004;6:1114–21.
45. D'Angelo MA, Gomez-Cavazos JS, Mei A, et al. A change in nuclear pore complex composition regulates cell differentiation. *Dev Cell* 2012;22:446–58.
46. Ori A, Banterle N, Iskar M, et al. Cell type-specific nuclear pores: a case in point for context-dependent stoichiometry of molecular machines. *Mol Syst Biol* 2013;9:648–8.
47. Nagai S, Dubrana K, Tsai-Pflugfelder M, et al. Functional targeting of DNA damage to a nuclear pore-associated SUMO-dependent ubiquitin ligase. *Science* 2008;322:597–602.
48. Blobel G. Gene gating: a hypothesis. *Proc Natl Acad Sci* 1985;82:8527–9.
49. Liang Y, Franks TM, Marchetto MC, et al. Dynamic association of NUP98 with the human genome. *PLoS Genet* 2013;9:e1003308.
50. Liu Z, Yan M, Liang Y, et al. Nucleoporin Seh 1 interacts with Olig2/Brd7 to promote oligodendrocyte differentiation and myelination. *Neuron* 2019;102:587–601.e7.
51. Raices M, Bukata L, Sakuma S, et al. Nuclear pores regulate muscle development and maintenance by assembling a localized Mef2C complex. *Dev Cell* 2017;41:540–54.e7.
52. Su Y, Pelz C, Huang T, et al. Post-translational modification localizes MYC to the nuclear pore basket to regulate a subset of target genes involved in cellular responses to environmental signals. *Genes Dev* 2018;32:1398–419.
53. Toda T, Hsu JY, Linker SB, et al. Nup153 interacts with Sox2 to enable bimodal gene regulation and maintenance of neural progenitor cells. *Cell Stem Cell* 2017;21:618–34.e7.
54. Mendjan S, Taipale M, Kind J, et al. Nuclear pore components are involved in the transcriptional regulation of dosage compensation in *Drosophila*. *Mol Cell* 2006;21:811–23.
55. Sachani SS, Landschoot LS, Zhang L, et al. Nucleoporin 107, 62 and 153 mediate Kcnq1ot1 imprinted domain regulation in extraembryonic endoderm stem cells. *Nat Commun* 2018;9:2795.
56. Brown CR, Kennedy CJ, Delmar VA, et al. Global histone acetylation induces functional genomic reorganization at mammalian nuclear pore complexes. *Genes Dev* 2008;22:627–39.
57. Labade AS, Karmodiya K, Sengupta K. HOXA repression is mediated by nucleoporin Nup93 assisted by its interactors Nup188 and Nup205. *Epigenetics Chromatin* 2016;9:54.
58. Therizols P, Fairhead C, Cabal GG, et al. Telomere tethering at the nuclear periphery is essential for efficient DNA double strand break repair in subtelomeric region. *J Cell Biol* 2006;172:189–99.
59. Van de DW, Wan Y, Lapetina DL, et al. A role for the nucleoporin Nup170p in chromatin structure and gene silencing. *Cell* 2013;152:969–83.
60. Tan-Wong SM, Wijayatilake HD, Proudfoot NJ. Gene loops function to maintain transcriptional memory through interaction with the nuclear pore complex. *Genes Dev* 2009;23:2610–24.
61. Brickner DG, Cajigas I, Fondufe-Mittendorf Y, et al. H2A.Z-mediated localization of genes at the nuclear periphery confers epigenetic memory of previous transcriptional state. *Plos Biol* 2007;5:e81.
62. Fišerová J, Maninová M, Sieger T, et al. Nuclear pore protein TPR associates with lamin B1 and affects nuclear lamina organization and nuclear pore distribution. *Cell. Mol. Life Sci* 2019;76:2199–216.
63. Garrido-Ramos MA, Satellite DNA. An evolving topic. *Genes (Basel)* 2017;8:230.
64. Alcobia I, Dilão R, Parreira L. Spatial associations of centromeres in the nuclei of hematopoietic cells: evidence for cell-type-specific organizational patterns. *Blood* 2000;95:1608–15.

65. Dillinger S, Straub T, Németh A. Nucleolus association of chromosomal domains is largely maintained in cellular senescence despite massive nuclear reorganisation. *PLoS One* 2017;12:e0178821.
66. Saksouk N, Barth TK, Ziegler-Birling C, et al. Redundant mechanisms to form silent chromatin at pericentromeric regions rely on BEND3 and DNA methylation. *Mol Cell* 2014;56:580–94.
67. Martens JHA, O'Sullivan RJ, Braunschweig U, et al. The profile of repeat-associated histone lysine methylation states in the mouse epigenome. *EMBO J* 2005;24:800–12.
68. Lange UC, Siebert S, Wossidlo M, et al. Dissecting the role of H3K64me3 in mouse pericentromeric heterochromatin. *Nat Commun* 2013;4:2233.
69. Hahn M, Dambacher S, Dulev S, et al. Suv4-20h2 mediates chromatin compaction and is important for cohesin recruitment to heterochromatin. *Genes Dev* 2013;27:859–72.
70. Jagannathan M, Cummings R, Yamashita YM. A conserved function for pericentromeric satellite DNA. *Elife* 2018;7:1218.
71. Mansuroglu Z, Benhelli-Mokrani H, Marcato V, et al. Loss of tau protein affects the structure, transcription and repair of neuronal pericentromeric heterochromatin. *Sci Rep* 2016;6:33047.
72. Zhu Q, Pao GM, Huynh AM, et al. BRCA1 tumour suppression occurs via heterochromatin-mediated silencing. *Nature* 2011;477:179–84.
73. Francastel C, Walters MC, Groudine M, et al. A functional enhancer suppresses silencing of a transgene and prevents its localization close to centromeric heterochromatin. *Cell* 1999;99:259–69.
74. Brown KE, Amoils S, Horn JM, et al. Expression of alpha- and beta-globin genes occurs within different nuclear domains in haemopoietic cells. *Nat Cell Biol* 2001;3:602–6.
75. Wijchers PJ, Geeven G, Eyres M, et al. Characterization and dynamics of pericentromere-associated domains in mice. *Genome Res* 2015;25:958–69.
76. Feric M, Vaidya N, Harmon TS, et al. Coexisting liquid phases underlie nucleolar subcompartments. *Cell* 2016;165:1686–97.
77. Hernandez-Verdun D, Roussel P, Thiry M, et al. The nucleolus: structure/function relationship in RNA metabolism. *Wiley Interdiscip Rev RNA* 2010;1:415–31.
78. Carvalho C, Pereira HM, Ferreira J, et al. Chromosomal G-dark bands determine the spatial organization of centromeric heterochromatin in the nucleus. *Mol Biol Cell* 2001;12:3563–72.
79. Weierich C, Brero A, Stein S, et al. Three-dimensional arrangements of centromeres and telomeres in nuclei of human and murine lymphocytes. *Chromosome Res* 2003;11:485–502.
80. van Koningsbruggen S, Gierlinski M, Schofield P, et al. High-resolution whole-genome sequencing reveals that specific chromatin domains from most human chromosomes associate with nucleoli. *Mol Biol Cell* 2010;21:3735–48.
81. Németh A, Conesa A, Santoyo-Lopez J, et al. Initial genomics of the human nucleolus. *PLoS Genet* 2010;6:e1000889.
82. Vertii A, Ou J, Yu J, et al. Two contrasting classes of nucleolus-associated domains in mouse fibroblast heterochromatin. *Genome Res* 2019gr;247072:118.
83. Pontvianne F, Carpentier M-C, Durut N, et al. Identification of nucleolus-Associated chromatin Domains reveals a role for the nucleolus in 3D organization of the a. thaliana genome. *Cell Rep* 2016;16:1574–87.
84. Bi X, Cheng Y-J, Hu B, et al. Nonrandom domain organization of the Arabidopsis genome at the nuclear periphery. *Genome Res* 2017;27:1162–73.
85. Falk M, Feodorova Y, Naumova N, et al. Heterochromatin drives compartmentalization of inverted and conventional nuclei. *Nature* 2019;40:47.
86. Larson AG, Elnatan D, Keenen MM, et al. Liquid droplet formation by HP1 α suggests a role for phase separation in heterochromatin. *Nature* 2017;547:236–40.
87. Strom AR, Emelyanov AV, Mir M, et al. Phase separation drives heterochromatin domain formation. *Nature* 2017;547:241–5.
88. Lieberman-Aiden E, van Berkum NL, Williams L, et al. Comprehensive mapping of long-range interactions reveals folding principles of the human genome. *Science* 2009;326:289–93.
89. Bonev B, Cohen NM, Szabo Q, et al. Multiscale 3D genome rewiring during mouse neural development. *Cell* 2017;171(3):557–72.e24.
90. Ahmed K, Dehghani H, Rugg-Gunn P, et al. Global chromatin architecture reflects pluripotency and lineage commitment in the early mouse embryo. *PLoS One* 2010;5:e10531.
91. Wijchers PJ, Krijger PHL, Geeven G, et al. Cause and consequence of tethering a SubTAD to different nuclear compartments. *Molecular Cell* 2016;61:461–73.
92. Borsos M, Perricone SM, Schauer T, et al. Genome-lamina interactions are established de novo in the early mouse embryo. *Nature* 2019;569:729–33.
93. Du Z, Zheng H, Huang B, et al. Allelic reprogramming of 3D chromatin architecture during early mammalian development. *Nature* 2017;547:232–5.
94. Isoda T, Moore AJ, He Z, et al. Non-coding transcription instructs chromatin folding and compartmentalization to dictate enhancer-promoter communication and T cell fate. *Cell* 2017;171:103–19.e18.
95. Chuang C-H, Carpenter AE, Fuchsova B, et al. Long-range directional movement of an interphase chromosome site. *Curr Biol* 2006;16:825–31.
96. Therizols P, Illingworth RS, Courilleau C, et al. Chromatin decondensation is sufficient to alter nuclear organization in embryonic stem cells. *Science* 2014;346:1238–42.
97. Finlan LE, Sproul D, Thomson I, et al. Recruitment to the nuclear periphery can alter expression of genes in human cells. *PLoS Genet* 2008;4:e1000039.
98. Reddy KL, Zullo JM, Bertolino E, et al. Transcriptional repression mediated by repositioning of genes to the nuclear lamina. *Nature* 2008;452:243–7.
99. Kumaran RI, Spector DL. A genetic locus targeted to the nuclear periphery in living cells maintains its transcriptional competence. *J Cell Biol* 2008;180:51–65.
100. Leemans C, van der Zwalm MCH, Brueckner L, et al. Promoter-intrinsic and local chromatin features determine gene repression in LADs. *Cell* 2019;177:852–64.e14.
101. Lemaître C, Grabarz A, Tsouroula K, et al. Nuclear position dictates DNA repair pathway choice. *Genes Dev* 2014;28:2450–63.
102. Brickner JH, Walter P. Gene recruitment of the activated INO1 locus to the nuclear membrane. *Plos Biol* 2004;2:e342.
103. Taddei A, Van Houwe G, Hediger F, et al. Nuclear pore association confers optimal expression levels for an inducible yeast gene. *Nature* 2006;441:774–8.

104. Texari L, Dieppo G, Vinciguerra P, et al. The nuclear pore regulates GAL1 gene transcription by controlling the localization of the SUMO protease Ulp1. *Mol Cell* 2013;51:807–18.
105. Jacinto FV, Benner C, Hetzer MW. The nucleoporin Nup153 regulates embryonic stem cell pluripotency through gene silencing. *Genes Dev* 2015;29:1224–38.
106. Schmidt HB, Görlich D. Nup98 FG domains from diverse species spontaneously phase-separate into particles with nuclear pore-like permselectivity. *Elife* 2015;4:6281.
107. Pascual-Garcia P, Capelson M. Nuclear pores in genome architecture and enhancer function. *Curr Opin Cell Biol* 2019;58:126–33.
108. Min J, Wright WE, Shay JW. Clustered telomeres in phase-separated nuclear condensates engage mitotic DNA synthesis through BLM and RAD52. *Genes Dev* 2019;33(13–14):814–27.
109. Zhang Y-J, Guo L, Gonzales PK, et al. Heterochromatin anomalies and double-stranded RNA accumulation underlie C9orf72 poly (PR) toxicity. *Science* 2019;363.
110. White MR, Mitrea DM, Zhang P, et al. C9orf72 poly (PR) dipeptide repeats disturb biomolecular phase separation and disrupt nucleolar function. *Mol Cell* 2019;74:713–728.e6.
111. Wang H, Xu X, Nguyen CM, et al. CRISPR-mediated programmable 3D genome positioning and nuclear organization. *Cell* 2018;175:1405–17.e14.

OBJECTIVE OF THE THESIS

Objective of the thesis

Evaluation of the role of Daxx in heterochromatin maintenance in pluripotent cells

About half of mammalian genomes are composed of repeated DNA sequences that must remain silenced heterochromatin at all time. It is now well-established that heterochromatin maintenance is essential for proper cell physiology. Defects in heterochromatin are commonly observed in different diseases and can even drive tumorigenesis.

In somatic cells, heterochromatin regions, both dispersed and pericentromeric are constitutively silenced via high levels of DNA methylation, H3K9me3-modifications and subsequent binding of HP1 α . This peculiar heterochromatin organization arises during the early embryonic development. At the 2-cell stage, a major DNA repeats transcriptional burst, notably of the LINE1 family is proposed to facilitate genome-wide chromatin decompaction necessary for the zygotic genome activation. Interestingly, transcription of the major satellite repeats, composing the pericentromeric heterochromatin, is essential for the establishment of pericentromeric regions-clustering into chromocenters and mis-regulation of major satellite transcription at the 2-cell stage impairs further developmental capacity. Transcription of DNA repeats then decreases and is repressed from the blastocyst stage and later via high DNA methylation levels. Transcription of DNA repeats from the 2-cell to the blastocyst stage must then be tightly regulated independently of 5mC-based mechanisms.

Embryonic stem cells display lower levels of DNA methylation than differentiated cells. Indeed, DNA methylation marks are erased at the beginning of the embryonic development and are only re-established from the blastocyst stage from which are derived the embryonic stem cells. A useful model for the study of the embryonic development is the embryonic stem cells which can be cultivated *in vitro*. ESCs display all the characteristics of pluripotent cells - self-renewal and generation of all the tissues of the organism. However, when in culture, ESCs tend to accumulate DNA methylation increasing the differences from their blastocyst counterparts along time. A new culture medium was described in 2008 by Ying *et al.* which is composed of 2 inhibitors (2i) for the GSK3 β - and MEK3-pathways and convert the cells to a more physiological state with lower DNA methylation. DNA methylation can be further decreased upon addition of vitamin C into the 2i medium. Thus, pluripotent cells easily overcome the absence of DNA methylation, suggesting the existence of additional heterochromatin maintenance pathways in pluripotent cells. Some factors have already been described such as BEND3 and polycomb proteins at pericentromeres, and DAXX and SETDB1 for dispersed endogenous retroviruses.

Interestingly, DAXX localizes at PCH in the lowly methylated paternal genome in the first stages of development. However, genetic deletion of Daxx only impairs embryonic development at later stages, and Daxx $-/-$ embryos could not develop to the blastocyst state, suggesting a strong importance of DAXX in transitioning the embryonic cells toward a pluripotent state, when chromocenter formation arise.

DAXX is the heterochromatin-specific chaperone of the histone variant H3.3. H3.3 is a peculiar histone variant as it is enriched in both euchromatin and heterochromatin regions. Its deposition at euchromatin is achieved via the HIRA complex. H3.3 is essential for ESC viability and regulates chromosomal stability of both *in vitro* ESCs and in the embryo, suggesting crucial heterochromatin-related functions. Furthermore, it provides the H3K9me3-modification at telomeric regions and help heterochromatin silencing at some endogenous retrovirus elements. However, its role at major satellite repeats has mainly been envisioned as a transcriptional facilitator.

In the present work, I used ESCs as a model to study the role of DAXX in the maintenance of heterochromatin and gain deeper understanding of pericentromere regulation in pluripotent cells.

RESULTS

RESULTS

Publication 1 – In preparation

DAXX safeguards pericentromeric heterochromatin formation in embryonic stem cells

Authors - Antoine CANAT¹, Adeline VEILLET¹, Robert S. ILLINGWORTH², Emmanuelle FABRE¹, Pierre THERIZOLS^{1‡}

Affiliation -

¹Université de Paris, Laboratoire Génomes, Biologie Cellulaire et Thérapeutiques, CNRS UMR7212, INSERM U944, Institut de Recherche St Louis, F- 75010 Paris

²MRC Human Genetics Unit, Institute of Genetics and Molecular Medicine, University of Edinburgh, Edinburgh EH4 2XU, United Kingdom

‡ Corresponding author. Email - pierre.therizols@inserm.fr. Tel - +33-1-5372-4058

Abstract

Pericentromeric heterochromatin (PCH) regions consist of large arrays of major satellite repeats. PCH tend to cluster into large DAPI-dense structures called chromocenters which are enriched in H3K9me3 and DNA methylation. Chromocenter formation arise during the early embryonic development when the level of DNA methylation is low. However, the molecular pathways required to establish and maintain PCH organization in pluripotent cells remain unclear. Here, we uncover a novel essential role for the histone variant H3.3-chaperone DAXX in pluripotent cells upon ground-state conversion. We describe a novel function of DAXX in the maintenance of PCH organization. Indeed, we report that loss of DNA methylation via active DNA demethylation at PCH can lead to DNA damages and induce a massive accumulation of DAXX at chromocenters. Loss of DAXX impairs the organization of chromocenters and HP1 α dynamics. We further demonstrate that the H3.3-DAXX interaction is important to drive the recruitment of SETDB1 at PCH where it catalyzes H3.3K9me3.

Introduction

Most of the mammalian genome is composed of DNA repeats. In mouse, the major satellites form Mbs-arrays of constitutive heterochromatin that surround centromeres¹. Loss of silencing of satellite DNA is a hallmark of various cancer types and contributes to genomic instability. At the molecular level, constitutive heterochromatin exhibits epigenetic marks such as DNA methylation, H3K9me3 and HP1. Maintenance of H3K9me3 at major satellites rely on the SUV39H1/2 methyltransferases, whereas it strongly depends on the other K9me3 methylase SETDB1 at dispersed DNA repeats and telomeres^{2, 3, 4}.

The pericentromeric heterochromatin (PCH) of different chromosomes tend to aggregate to form large DAPI-dense heterochromatin clusters, called chromocenters. Defect in satellite clustering has been described different pathologies such as Alzheimer's disease or breast cancers and is often associated with higher DNA damages or chromosome segregation defects^{5, 6, 7, 8}. Chromocenters formation occurs at the 4-cell stage and expression of major satellite transcripts is necessary for the proper reorganization of pericentromeric heterochromatin proper developmental progression^{9, 10}. Factors responsible for the PCH clustering remain largely unknown. Interestingly, DAXX, a chaperone of the histone variant H3.3 specifically binds to PCH during the first stages of development, yet loss of Daxx only impairs development at later stages^{11, 12, 13}. However, the function of Daxx at PCH remains unknown in pluripotent cells.

In this paper, we decipher the role that DAXX plays at PCH in pluripotent embryonic stem cells. We found that DAXX is essential for ground-state ESCs survival. Furthermore, we observe that DAXX localizes to PCH to recruit SETDB1, facilitating heterochromatin reformation through H3K9me3 modification after DNA damages induced by active DNA demethylation.

Results

DAXX is essential for ES cell survival upon ground-state conversion.

To assess the role of Daxx in pluripotent cells, we generated a Daxx knock-out (KO) ES cell line. We targeted the exon 3 of the *Daxx* locus using the CRISPR/cas9 technology and confirmed the absence of DAXX mRNA and protein (Fig. 1A). The generated Daxx KO ES cell line did not present obvious changes in H3.3 protein levels. Consistent with previous reports, the lack of Daxx did not impair cell growth in serum-based ESCs culture condition¹⁴. In contrary of most epigenetic factor knockouts, the loss of Daxx did not impair the differentiation process. No growth nor morphological defects could be detected in Daxx KO ESCs after 5 days of culture in presence of retinoic acid (Fig. 1B). Since Daxx contributes to alternative pathways of heterochromatin formation independently of DNA methylation, Daxx KO and WT ESCs were grown into 2i medium supplemented with Vitamin C^{15,16}. In this medium, the level of 5mC is greatly reduced (Fig. S1A), allowing ESCs to reach the ground-state of pluripotency. Consistent with previous reports, no growth defect was detected for Daxx KO lines after 4 days of conversion (Fig. 1B)¹⁷. However, prolonged culture into 2i+VitC medium induced a severe decreased in cell viability. Compared to the parental WT line, only 12.6% of Daxx KO ESCs remained after 8 days of culture in 2i+VitC (Fig. 1B). No surviving cells could be detected after 9 to 10 days of conversion. These results indicate an essential role for Daxx in the maintenance of pluripotent cell survival upon ground-state conversion.

To evaluate the effect of the loss of Daxx onto the transcriptional landscapes of Daxx KO ESCs, we performed an RNA sequencing experiment for each of the culture conditions. Previous studies have demonstrated that Daxx binds to specific ERVs such as the IAP and ERVK elements, facilitating their silencing in ESCs¹⁷. As expected, we found that many ERV families were upregulated in Daxx KO ESCs in serum and ground-state conditions (Fig. 1C). Several LINE1 elements, notably the L1Md T and L1Md A families, which have not been reported to be regulated by DAXX before were also upregulated in pluripotent Daxx KO ESCs (Fig. 1C, S1B). The role of Daxx on transcriptional silencing is not limited to interspersed repeats, we detected a strong upregulation major satellites RNA in both serum and ground-state condition (Fig. 1C, S1B). The effect of Daxx onto DNA repeats was restricted to repeats transcribed by RNA-PolIII as the SINEs, transcribed by RNA-PolIII, were not affected. The mis-regulation of repeated element expression were significantly reduced upon retinoic acid differentiation supporting a specific role for DAXX in transcriptional silencing of DNA repeats when the level of DNA methylation is reduced. At the level of gene transcripts, the greatest differences between Daxx KO and WT cells were observed in pluripotent cells. With 1250 genes down-regulated and 1345 up-regulated ones ($-1 > \text{Log}(\text{FC}) > 1$; $\text{Pvalue} < 0.05$), ground-state was the most affected condition (Fig. 1D). Interestingly, nearly all the transcriptional changes were abolished upon differentiation with only 125 down-regulated and 8 up-regulated genes ($\text{Log}(\text{FC}) > 1$; $\text{Pvalue} < 0.05$). Compared to WT, DaxxKO cells showed similar response to medium changes for both 2i+VitC and retinoic acid addition, suggesting the loss of viability observed in 2i+VitC is not caused by a conversion defect (Fig. S1C).

To understand the potential cause for the reduced cell survival of ground-state Daxx KO ESCs, we searched for transcriptional pathways specifically deregulated in ground-state. Using a gene ontology algorithm for the most significantly mis-regulated genes ($\text{Pvalue} < 0.001$), we revealed that Daxx KO cells presented an overexpression of the type II interferon response and apoptosis, which is coherent with the reduced cell viability, and also transcriptional pathways linked to DNA repair such as P53, Toll-like receptor and EGFR1 signaling (Fig. S1D)^{18,19,20}. We noticed that among the most down-regulated pathways were the different types of DNA damage response (DDR) (Fig. 1E). We hypothesize that the reduced cell survival might arise from defects in DNA damage repair in the absence of Daxx.

DAXX accumulates at PCH upon ground-state conversion and DNA damages but is not part of DDR.

To better characterize the role of DAXX in ground-state ESCs, we decided to assess its localization by immunofluorescence. DAXX is a known partner of the PML nuclear bodies (NBs), membrane-less structures devoid of chromatin, forming hubs for post-translational modification²¹. As expected, in serum ESCs, DAXX is present as round foci of 0.3 μm in diameter on average that localizes at PML NBs (Fig. 2A, Fig. S2A). Intriguingly, upon ground-

state conversion, DAXX also accumulates at heterochromatin H3K9me3-rich foci surrounded by PML, forming large structures of 1.1 μm in diameter (Fig. 2A, Fig. S2A). H3K9me3/DAPI-rich foci in mouse correspond to chromocenters, formed by the clustering of pericentromeric regions of multiple chromosomes. We confirmed that the H3K9me3 regions were the pericentromeric heterochromatin by DNA FISH of the major satellites (Fig. 2B). DAXX relocalization at PCH is visible in half of ground state ESCs (Fig. 2C). Amongst those cells, 62% displayed only one PCH marked by DAXX, the remaining presenting 2 or ≥ 3 PCH-marked per nucleus. We conclude that upon ground-state conversion, DAXX relocalizes to major satellite repeats.

However, the presence of DAXX signal at a small fraction of chromocenters is different from the synchronized major satellite replication profile¹. Thus, Daxx recruitment does not result simply from replicative heterochromatin maintenance but requires a specific stimulus. The loss of Daxx induced the up-regulation of multiple DNA repeats (Fig. 1C). Previous studies have reported that loss of heterochromatin silencing could lead to increased DNA damages²². Moreover, we detected that DNA repair proteins were transcriptionally down-regulated in the absence of Daxx (Fig. 1E). We thus decided to assess DNA damage signaling in Daxx KO cells. A key signaling factor of DNA damages is the phosphorylation of the H2AX histone variant, which happens at the early stages of DNA lesion recognition²³. Because we detected a strong transcriptional upregulation of the major satellites and the spatial relocalization of DAXX, we decided to look for specific accumulation of γH2AX at pericentromeric heterochromatin. We counted the total number of γH2AX foci and evaluated if it was overlapping with a DAPI-rich focus. Interestingly, we observed that γH2AX foci appeared more at chromocenters in both WT and Daxx KO cells upon ground-state conversion (Fig. 2D). Hence, ground-state conversion induces DNA damage signaling at pericentromeric heterochromatin.

As increased levels of DNA damages were visible at chromocenters, we tested whether exogenously induced DNA damages could relocalize DAXX toward chromocenters. Hydroxyurea (HU) creates randomly positioned replication forks collapses that can ultimately generate double-strand breaks (DSBs). Random damages inflicted with HU treatment resulted in DAXX and PML accumulation at DAPI-rich foci in 30% of the cells (Fig. 2E). We decided to artificially generate DSBs at PCH to see if that would lead to the recruitment of Daxx. We designed a sgRNA targeting major satellites (Fig. S2B). When we expressed the catalytically dead Cas9 (dCas9), there was no relocalization of DAXX nor PML, while expression of the active Cas9 induced high γH2AX signal at PCH and DAXX and PML accumulation (Fig. 2E, S2B). Yet, each nucleus displayed a limited number of structures like in ground-state. Recruitment of

DAXX at pericentromeric regions can thus be triggered by DNA damages occurring at these locations.

Interestingly, γ H2AX is only visible within the DAXX-PML PCH-foci in ~50% of the cases during ground-state conversion, suggesting a somehow distinct recruitment mechanism than direct DNA damage response (Fig. S2C). It was reported that specific recruitment of NBS1, which is part of the MRN complex, could induce DNA damage response in the absence of DNA lesions²⁴. We thus artificially recruited NBS1 to major satellites using a Tale protein and while we observed the presence of γ H2AX, there was no PML relocalization (Fig. 2F, S2D). As NBS1 failed to recruit Daxx, we propose that DAXX is not part of DDR but rather comes at a later post-repair step of heterochromatin reformation.

DAXX relocalizes to PCH upon DNA damages induced by active DNA demethylation.

A major epigenetic change arising upon ground-state conversion is the strong reduction in DNA methylation levels, particularly at the major satellite repeats^{15, 25, 26}. The demethylation was shown to take place both passively and actively²⁷. Prolonged culture in ground-state condition drastically impaired Daxx KO cell survival (Fig. 1B). To test whether the loss of DNA methylation was the cause of cell death, we treated the cells with the 5-azacytidine drug that blocks the DNMTs activity. We observed that the loss of Daxx impaired proper cell survival upon 4 days of 5-azacytidine treatment (Fig. 3A). Because DAXX relocalized to pericentromeric regions upon ground-state conversion, we tested Daxx localization in 5-azacytidine-treated cells. Indeed, DAXX accumulated at H3K9me3- and DAPI-rich foci upon DNA demethylation and PML formed a giant shell around DAXX foci (Fig. 3B). DAXX-PML accumulation at PCH was visible in 29% of the cells (Fig. 3C).

We noted that upon ground-state conversion ESCs accumulated DNA damages at PCH and that artificially-induced DSBs led to DAXX recruitment (Fig. 2A, 2E). Active DNA demethylation via the TET enzymes can ultimately result in DSBs²⁸. Because loss of DNA methylation specifically induced the recruitment of DAXX toward pericentromeric regions, we wondered if DNA demethylation could be a cause of the observed DNA damages (Fig. 2D, 3B). We decided to recruit the catalytic domain of the TET1 enzyme that converts 5-methylcytosine (5mC) into 5-hydroxymethyl-cytosine (5hmC), using a Tale strategy. Targeted recruitment of TET1-catalytic domain (TET1CD) toward major satellite repeats led to the specific upregulation of major satellite transcripts of 2.5-fold, but not other repeats such as the IAPEz, confirming the specific action of the Tale (Fig. 3C). Targeting of the TET1CD induced a reduction in 5mC signal at DAPI-dense foci (Fig. S3A, S3B). We then performed immunofluorescence to assess if our Tale-construct generated DNA damages at pericentromeric heterochromatin. We noted that the Tale accumulated at DAPI-rich regions as expected and it induced multiple γ H2AX foci colocalizing with the Tale-flag signal, indicating enhanced DNA damages at PCH (Fig. 3D). To confirm that DNA damages generated by active

DNA demethylation were the main cause of Daxx recruitment, we looked at DAXX and PML localization. We observed that DAXX-PML foci at PCH were visible in the Tale-TET1CD condition and not in the Tale- Δ control (Fig. 3F). Interestingly, specific activation of major satellite repeats in serum condition using a Tale-MajSat-VP64 resulted in strong increase in major satellites RNAs as well as γ H2AX foci and DAXX-PML accumulation (Fig. S3D, S3E, S3F). However, as ground-state conversion leads to the silencing of pericentromeric regions, it suggests that the DNA damages arising in our cells do not result from increased activation (Fig. S1C). Hence, we conclude that accumulated DNA damages visible at major satellites can result from the DNA demethylation of pericentromeric regions.

DAXX maintains heterochromatin organization in pluripotent cells.

Changes in major satellites transcription often correlates with impaired spatial organization of chromocenters⁵. Since we observed an upregulation of major satellite repeats in Daxx KO cells, we decided to evaluate the organization of the pericentromeric heterochromatin clusters (Fig. 1C). We performed DNA FISH experiments against the major satellites and counted the number of foci. We observed that the number of chromocenters was increased in the absence of Daxx in both serum and ground-state ESCs (Fig. 4A). In agreement with the absence of phenotype in the Daxx KO cells upon differentiation, we detected the same number of major satellite foci in the differentiated condition. The increased of foci number was correlated with the diminution of the sizes of major satellites foci (Fig. S4A). Because the spatial organization of pericentromeric heterochromatin was affected, we then assessed the molecular state of these regions. We realized an MNase digestion of serum ESCs and observed that the lack of Daxx induced an enhanced chromatin accessibility (Fig. S4C). To understand the increased in chromatin accessibility, we expressed a GFP-HP1 α in both cell lines and performed FRAP experiments to measure the speed of fluorescence recovery (Fig. 4B). We observed that the half-recovery time was significantly lower in both serum and ground-state conditions in the absence of Daxx, suggesting a faster protein dynamic which agrees with the MNase accessibility results (Fig. 4B, S4C). However, the mobile fraction of GFP-HP1 α remained constant, suggesting that the same amount of proteins was bound to chromatin (Fig. S4B). These results indicate that Daxx is necessary for the proper organization of pericentromeric heterochromatin in pluripotent cells.

Interestingly, HP1 was reported to be able to undergo liquid-liquid phase-separation (LLPS)^{29, 30}. LLPS corresponds to particular biophysical properties including fusion-fission events as well as a dynamical behavior. Strom *et al.* observed that chromocenters boundaries displayed enhanced HP1 α variance, indicating a heterochromatin barrier impeding the diffusion of proteins, which is coherent with the tension surface exhibited by LLPS-driven biocondensates. We reasoned that higher HP1 α recovery rate might arise from altered heterochromatin barrier. We thus re-examined the FRAP data, looking at the intensity variation

along the duration of the movie (Fig. 4C). In WT cells, we noted that the variance levels were low in the nucleoplasm and only increased at chromocenters, reaching the highest peaks at the borders of chromocenters as previously reported. However, the variance from HP1 α in Daxx KO cells displayed a strikingly different pattern, with an increased variance levels in the nucleoplasm (Fig. 4C). We measured the variance at non-bleached chromocenters and observed a strong reduction of the peaks at the borders, suggesting a lower heterochromatin barrier. This effect was visible in both serum and ground-state conditions, however we noted that variance peaks in ground-state were higher for both WT and Daxx KO ESCs (Fig. 4C). Coherently with the increased dynamic of HP1 α , we note that the HP1 α variance at chromocenters borders is lower in Daxx KO ESCs, which could indicate that the loss of Daxx directly or indirectly affects heterochromatin barriers formed by LLPS capacities of HP1 α .

To evaluate the role of Daxx at major satellites, we specifically recruited DAXX using a Tale in Daxx KO ESCs in serum. The recruitment of DAXX induced a strong clustering of the major satellite signal, visible as a decrease in the number of foci by DNA FISH and a correlated increase in foci sizes (Fig. 4D). Furthermore, targeted recruitment of DAXX can overcome the normal spatial clustering as its recruitment in WT cells resulted in the same clustering phenotype (Fig. S4D). Overall, our data indicate that Daxx is sufficient to induce a spatial reorganization of pericentromeric heterochromatin.

DAXX recruits SETDB1 and mediates chromocenter clustering via H3.3K9me3 modification.

We next wondered what the function of DAXX at PCH could be. PCH are regions particularly enriched in H3K9me3 (Fig. 2A). SETDB1 is an H3K9me3 methyl-transferase that localizes within PML NBs³¹. We thus decided to assess whether SETDB1 also accumulated at pericentromeric heterochromatin upon DNA demethylation. In WT cells, we observed a strong signal of SETDB1 at DAPI-rich regions marked with DAXX and PML presence (Fig. 5A). However, in the absence of Daxx, we did not observe SETDB1 recruitment nor PML to DAPI-rich chromocenters but noticed that SETDB1 still localized at PML NBs (Fig. 5A, S5A). As DAXX is the heterochromatin-specific chaperone of H3.3, we knocked-down H3.3 expression and noted a strong reduction in PML-PCH relocalization upon DNA demethylation (Fig. S5B). We conclude that DAXX accumulates at PCH regions and then recruits PML and SETDB1 in an H3.3-dependent manner.

The main histone H3K9me3 methyl-transferases acting at pericentromeric heterochromatin are the SUV39H1/2 enzymes^{22, 32}. However, because SETDB1 is another H3K9me3 methyl-transferase, we wondered if it was recruited for its methylase activity. We took advantage of Suv39H1/2 double knock-out (Suv39dKO) ESCs in which H3K9me3 could only result from SETDB1 activity. Strikingly, Suv39dKO cells presented no growth defects phenotype upon ground-state conversion (data not shown). We confirmed that matched WT

ESCs presented DAXX-PML accumulation at H3K9me3-rich PCH (data not shown). We observed that while no H3K9me3 was observed in serum, specific foci were present in ground-state which colocalize with PML NBs at major satellites (Fig. 5B). The presence of H3K9me3 signal at PCH of Suv39dKO ESCs was reported in ground-state condition, yet it remained a mystery²⁶. Hence, SETDB1 can be recruited to PCH in a DAXX-dependent manner and exerts its tri-methylase activity.

As the targeted recruitment of DAXX induced a strong major satellites clustering, we asked if SETDB1 was recruited by the Tale-DAXX construct. While no SETDB1 signal was observed upon recruitment of the Tale- Δ , the Tale-DAXX displayed a strong SETDB1 signal (Fig. S5C). We noted that H3.3 was important for the pericentromeric localization of DAXX and wondered if H3.3 was important for SETDB1 recruitment as well (Fig. S5B). The DAXX-H3.3 interaction is mediated by the histone-binding domain of DAXX. It was reported that the tyrosine 222 residue in murine DAXX was responsible for the H3.3-binding¹⁴. We recruited a DAXX mutant in which we replaced the tyrosine 222 residue by an alanine (Y222A) and observed that the recruitment of SETDB1 was abolished (Fig. S5C). Next, to assess whether DAXX-mediated SETDB1 recruitment generated an enzymatic activity, we recruited our Tale constructs into the Suv39dKO ESCs. The recruitment of a Tale protein to the major satellite sequences did not increase the levels of H3K9me3 signal. However, upon DAXX targeting, we observed a strong accumulation of H3K9me3 signal by immunofluorescence (Fig. 5C). As expected from the absence of SETDB1 recruitment, targeting of the DAXXY222A mutant did not lead to any tri-methylase activity (Fig. 5C). The DAXX-mediated recruitment of SETDB1 induced H3K9 tri-methylation, that we propose to be specific of H3.3. However, to rule out a possible effect of any H3K9 tri-methylation that could arise at canonical H3, we recruited SUV39H1 and SETDB1 to major satellites. Although both constructs resulted in high H3K9me3, H3K9me3-rich chromocenters appeared as small foci different from the action of DAXX (Fig. 5C). Because the recruitment of SUV39H1 and SETDB1 results in a different phenotype from the DAXX recruitment, we reasoned that the function of DAXX-SETDB1 might rely on the modification of H3.3.

To evaluate the function of H3.3 in DAXX-mediated clustering, we first measured the clustering phenotype induced by DAXXY222A mutant recruitment. H3.3 binding-deficient DAXX did not induce any clustering of major satellites foci, like the recruitment of SUV39H1 or SETDB1 (Fig. 5D). We then depleted the endogenous pool of H3.3 using two specific siRNAs and overexpressed individual H3.3 constructs. H3.3-binding to DAXX is mediated by its glycine 90 residue and when it is replaced by the methionine residue, which is the H3.1 residue (G90M), it completely abolishes the H3.3-DAXX interaction³³. Depletion of endogenous H3.3 impaired the Tale-DAXX-mediated major satellite clustering (Fig. 5E). We confirmed that our H3.3 constructs were expressed at the same levels (Fig. S5E). Complementation of the loss

of endogenous H3.3 by a WT H3.3 rescued the tale-DAXX clustering, why complementation with the H3.3G90M mutant led to the symmetrical effect of the Daxx mutant without any clustering. Interestingly, when we expressed the H3.3K9A mutant, which cannot be post-translationally modified on its lysine 9, we observed an absence of pericentromeric clustering (Fig. 5E). From these results, we propose that the effect of Daxx on the pericentromeric heterochromatin is mediated through the specific tri-methylation of H3.3K9 via the methyltransferase SETDB1.

Discussion

In the present work, we describe a novel role of the H3.3-chaperone DAXX in pluripotent cell maintenance of pericentromeric heterochromatin.

Upon conversion toward a DNA hypomethylated condition, we notice that DAXX massively accumulates to chromocenters and drives PML recruitment (Fig. 2A, 3A). Intriguingly, previous reports described DAXX recruitment to pericentromeric regions in the early stage of embryonic development^{12, 13}. In the mouse embryo, DAXX-recruitment is controlled by diverse proteins such as DPPA3 and PRC1. Furthermore, upon loss of DNA methylation in pluripotent cells, PRC1 components and BEND3 are targeted to chromocenter to induce H3K27me3^{34, 35}. It remains to understand whether similar protein network regulates DAXX relocalization upon ground-state conversion. However, as PRC1 proteins and BEND3 appear at most chromocenters, notably in DnmtKO cells, whereas DAXX only localize at 1 to 3 PCH per nucleus, we think that it may be recruited by alternative mechanisms. Indeed, DAXX is increasingly recruited to ERV repeats in DnmtKO ESCs¹⁷. Interestingly, it was reported that ERV elements are present interspersed between major satellite repeats³⁶. Hence, we propose that DAXX might be recruited to these particular ERV sequences imbedded at chromocenters (PCH-ERVs), possibly after DNA damages.

Targeted recruitment of TET1 to major satellites could generate γ H2AX foci accumulation, demonstrating that active DNA demethylation can lead to DNA damages (Fig. 3D). We similarly observe that ground-state conversion drives the increase of the number of damaged chromocenters (Fig. 2D). Since exogenously induced DNA damages and hypomethylation of chromocenters lead to DAXX relocalization, we conclude that DAXX is recruited to major satellites following DNA damage (Fig. 2A, 2E, 3A). Interestingly, targeting recruitment of NBS1, although sufficient to induce γ H2AX accumulation, could not drive DAXX relocalization, suggesting that DAXX may not act within the DNA damage response (DDR), but rather at later steps to reform the heterochromatin state of the locus (Fig. 2F). Active DNA demethylation-induced DNA damages is often resolved via coordinated action of base-excision repair (BER), TDG and TET to avoid DSBs^{37, 38, 39}. However, CRISPR/Cas9 targeting leads to DSBs and can induce DAXX accumulation, although in serum, with higher levels of DNA

methylation. We observe discrete foci of γ H2AX at chromocenters, which could indicate the presence of rare DSBs. Future studies are required to assess the role of DAXX in DDR.

Chromocenters are highly enriched in H3K9me3-modification induced by SUV39H1/2 enzymes^{2, 22, 40}. Remarkably, we demonstrate that DAXX recruits SETDB1 to perform H3K9 tri-methylation activity at PCH, an action different from mere binding of SETDB1 or SUV39H1 (Fig. 5A, 5B, 5C). Since KDM enzymes have been implicated in DNA repair pathway choice and repair completion, we propose that the function of SETDB1 is to generate H3.3K9me3^{41, 42, 43}. More experiments are necessary to deeply understand the molecular events occurring at DSBs related to loss and gain of H3.3K9me3. Furthermore, the absence of Daxx impairs chromocenter organization (Fig. 4A). It is possible that the same mechanism we describe upon loss of DNA methylation takes place in serum. However, it remains to better characterize whether the binding of DAXX and SETDB1 in the presence of DNA methylation might be transient or localized at specific loci such as PCH-ERVs. Moreover, a recent understanding of chromocenter organization came from the observations that HP1 α could undergo LLPS^{29, 30}. Intriguingly, we notice that the absence of Daxx impairs the dynamics and alters heterochromatin barrier formation, suggesting a direct or indirect change in LLPS capacities of HP1 α (Fig. 4B, 4C). Since we show that the major satellite clustering induced by DAXX relies on the binding of H3.3 and recruitment of SETDB1 (Fig. 5C, 5D), there are perhaps undescribed differences of HP1 α binding to H3K9me3 and H3.3K9me3.

Finally, we describe an essential role of DAXX for cell survival in prolonged DNA hypomethylated conditions. We further observe that the function of DAXX at chromocenters is to induce H3.3 deposition and SETDB1 recruitment. Intriguingly, the loss of SETDB1 prevents cell survival in both pluripotent and leukemic somatic cells^{44, 45}. In that direction, future work should inquire whether this essential DAXX-mediated SETDB1 recruitment is limited to pluripotent cells and assess the vital role of DAXX upon chronic loss of DNA methylation.

References

1. Guenatri *et al.* J. Cell Biol. 2004
2. Martens *et al.* EMBO J. 2005
3. Matsui *et al.* Nature 2010
4. Fukuda *et al.* Genome Res. 2018
5. Zhu *et al.* Nature 2011
6. Mansuroglu *et al.* Sci. Rep. 2016
7. Jagannathan *et al.* eLife 2018
8. Hahn, *et al.* Genes & Dev. 2013
9. Probst *et al.* Developmental Cell 2010
10. Casanova *et al.* Cell Rep. 2013
11. Lewis *et al.* P.N.A.S. 2010
12. Arakawa *et al.* Biochem. Biophys. Res. Comm. 2015
13. Liu *et al.* EMBO J. 2020
14. Elsässer *et al.* Nature 2015
15. Ying *et al.* Nature 2008
16. Blaschke *et al.* Nature 2013
17. He *et al.* Cell Stem Cell 2015
18. Chou *et al.*, Dev. Cell 2014
19. Williams and Schumacher, Cold Spring Harbor Persp. Med. 2016
20. Russo *et al.*, Science 2019
21. Lallemand-Breitenbach and de Thé Curr. Op. Cell Biol. 2018
22. Peters *et al.* Cell 2001
23. Stucki and Jackson DNA Repair 2006

24. Soutoglou and Misteli, Science 2008
25. Leitch *et al.* Nature Struct. Mol. Biol. 2013
26. Tosolini *et al.* Sci. Rep. 2018
27. Hackett *et al.* Stem Cell Reports 2013
28. Nakatani *et al.* EMBO Rep. 2015
29. Larson *et al.* Nature 2017
30. Strom *et al.* Nature 2017
31. Cho *et al.* J. of Biol. Chem. 2011
32. Lehnertz *et al.* Curr. Biol 2003
33. Hoelper *et al.* Nat. Comm. 2017
34. Saksouk *et al.* Mol. Cell 2014
35. Cooper *et al.* Cell Rep. 2014
36. Ostromyshenskii *et al.* BMC Genomics, 2018
37. Weber *et al.* Nature Comm. 2016
38. Cortellion *et al.* Cell 2011
39. Santos *et al.* Epigenetics & Chromatin 2013
40. Burton *et al.* Nat. Cell Biol. 2020
41. Colmenares *et al.* Dev. Cell 2017
42. Janssen *et al.* Genes & Dev. 2019
43. Young *et al.* J. Biol. Chem. 2013
44. Wu *et al.* Cell Reports 2020
45. Cuellar *et al.* J. Cell Biol. 2017

Figure 1

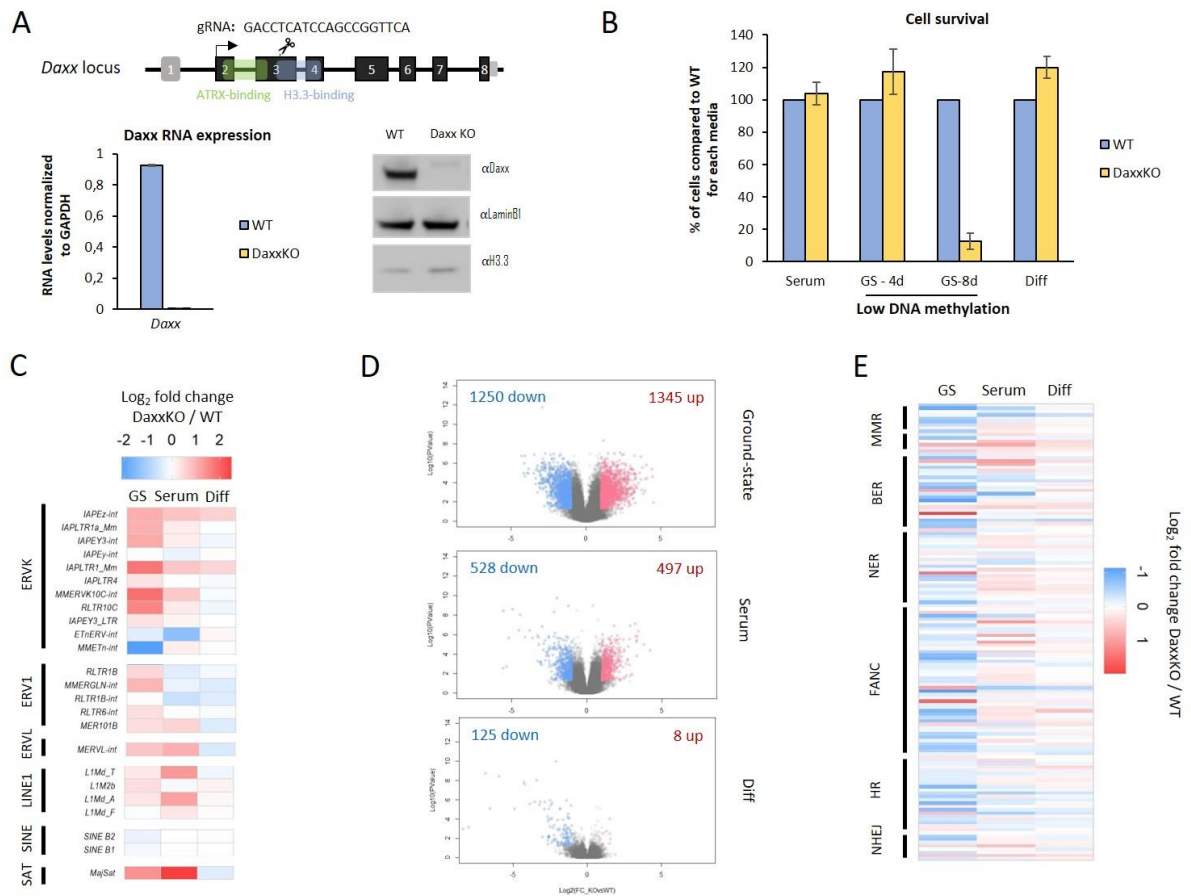


Figure 1| DAXX is essential for ES cell survival upon ground-state conversion. (A) Schematic of the *Daxx* locus and the sequence of the small guide RNA targeting exon 3. RT-qPCR experiment displaying mean of two biological replicates with SEM. Western blot correspond to one experiment from at least 2 biological replicates. **(B)** Quantification of the number of cells compared to WT in each culture condition. Histogram represents mean with SEM of 3 biological replicates for each condition except Diff which is the mean of two biological replicates. **(C)** Heatmap for different classes of transposable elements. Data are mean from RNA-seq experiments on 3 biological replicates. Major satellite transcription quantification was done by RT-qPCR from 3 biological replicates. **(D)** Volcano plot representing the number of differentially expressed genes in ground-state, serum or differentiated cells from RNA-seq experiments as in C. Differentially expressed genes in red for down-regulated or blue for up-regulated correspond to $\text{Log}_2(\text{FoldChange}(\text{KO}/\text{WT})) < -1$ or > 1 with $p\text{value} < 0.05$. **(E)** Heatmap for the genes belonging to the different DNA repair pathways. GS=Ground-state; Diff=Differentiation; MMR=Mismatch repair; BER=Base excision repair; NER=Nucleotide excision repair; FANCD1=Fanconi anemia pathway; HR=Homologous recombination; NHEJ=Non-homologous end joining.

Figure 2

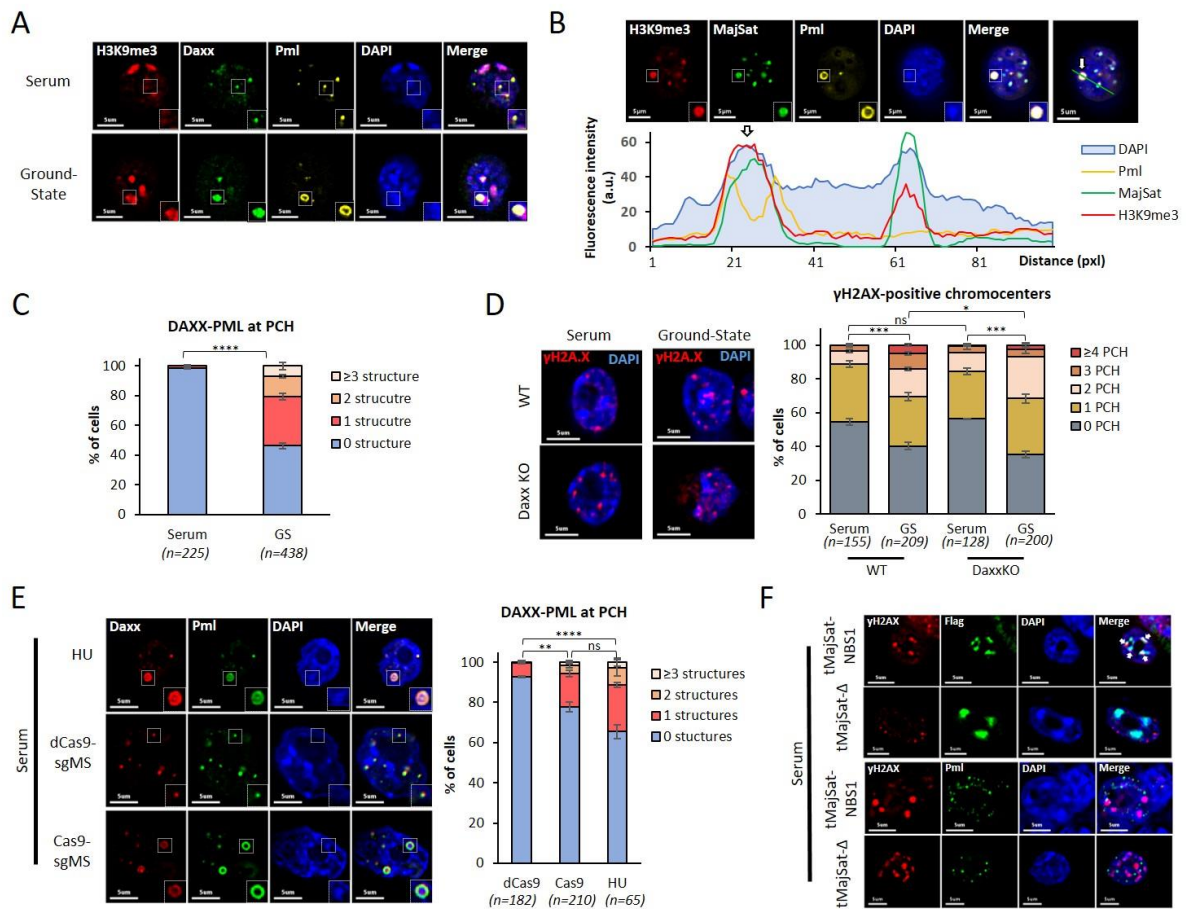


Figure 2 | DAXX accumulates at PCH upon ground-state conversion and DNA damages but is not part of DDR. (A) Representative immunofluorescence pictures showing DAXX, PML and H3K9me3 in serum-based or ground-state condition. White dashed square highlights a DAXX-PML NB (B) Representative immunofluorescence picture with H3K9me3, PML and major satellites DNA upon ground-state conversion. Intensity profile from the green line depicted onto the merged image. White arrow indicated an example of a DAXX-PML structure at PCH. White dashed square highlights a DAXX-PML structure at PCH. (C) Quantification of the mean number of DAXX-PML structures observed at PCH in serum-based or upon ground-state conversion. n=total number of nuclei analyzed from at least 3 biological replicates. (D) Immunofluorescence of yH2AX in WT or Daxx KO ESCs in serum or ground-state condition. Histogram displays the number of yH2AX foci observed localizing at DAPI-dense chromocenters. n=total number of nuclei analyzed from at least 3 biological replicates. (E) Representative pictures of DAXX and PML immunofluorescence in WT cells in serum subjected to HU treatment of dCas9 or Cas9 transfections. Histogram indicates mean number of DAXX-PML structures at PCH with SEM. n=total number of nuclei analyzed from at least 2 biological replicates. (F) Representative immunofluorescence pictures of yH2AX and Flag or yH2AX and PML in WT transfected cells with Tale-NBS1 construct. Chi-square tests were used for statistical analysis. GS=ground-state.

Figure 3

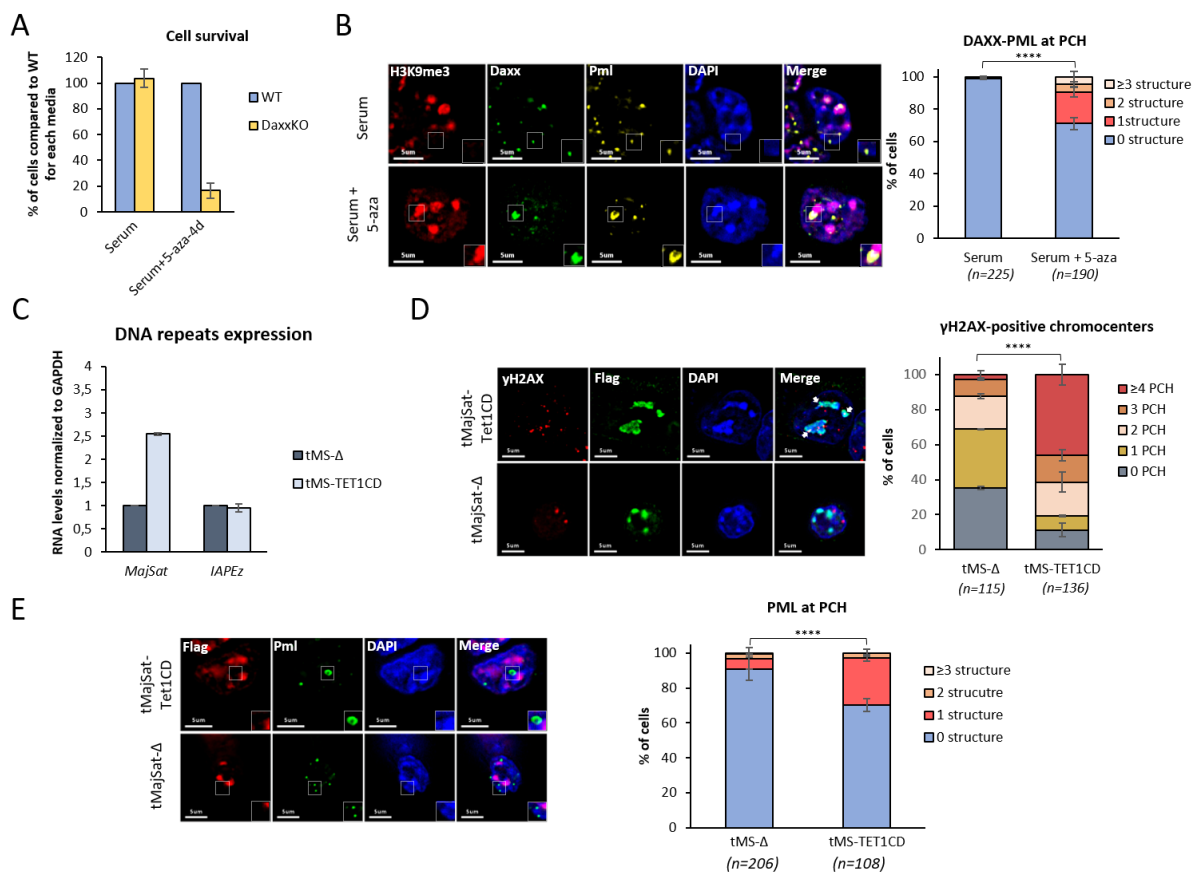


Figure 3 | DAXX relocalizes to PCH upon DNA damages induced by active DNA demethylation. (A) Quantification of the number of cells compared to WT in serum-based medium or after 5-aza treatment. Histogram represents the mean with SEM of 3 biological replicates. **(B)** Left, representative immunofluorescence pictures of H3K9me3, DAXX and PML in serum or 5-aza-treated cells. White dashed square highlights DAXX-PML NB. Right, quantification of the number of DAXX-PML structures at PCH observed in each condition. Histogram represents the mean with SEM of 3 biological replicates. n=total number of nuclei analyzed. **(C)** RT-qPCR to assess RNA levels of major satellite repeats or IAPEz in WT cells transfected with Tale-Δ or Tale-TET1CD. **(D)** Left, representative immunofluorescence pictures showing yH2AX and Flag in WT transfected cells with either Tale-Δ or Tale-TET1CD. Right, quantification of the number of yH2AX foci observed above DAPI-dense chromocenters. Histogram represents mean with SEM of two biological replicates. n=total number of nuclei analyzed. **(E)** Left, representative immunofluorescence pictures of Flag and PML in WT transfected cells with Tale-Δ or Tale-TET1CD. Right, quantification of the number of PML structures at PCH observed. Histogram represents mean with SEM of 2 biological replicates. n=total number of nuclei analyzed. Chi-square tests were used for statistical analysis. 5-aza = 5-azacytidine.

Figure 4

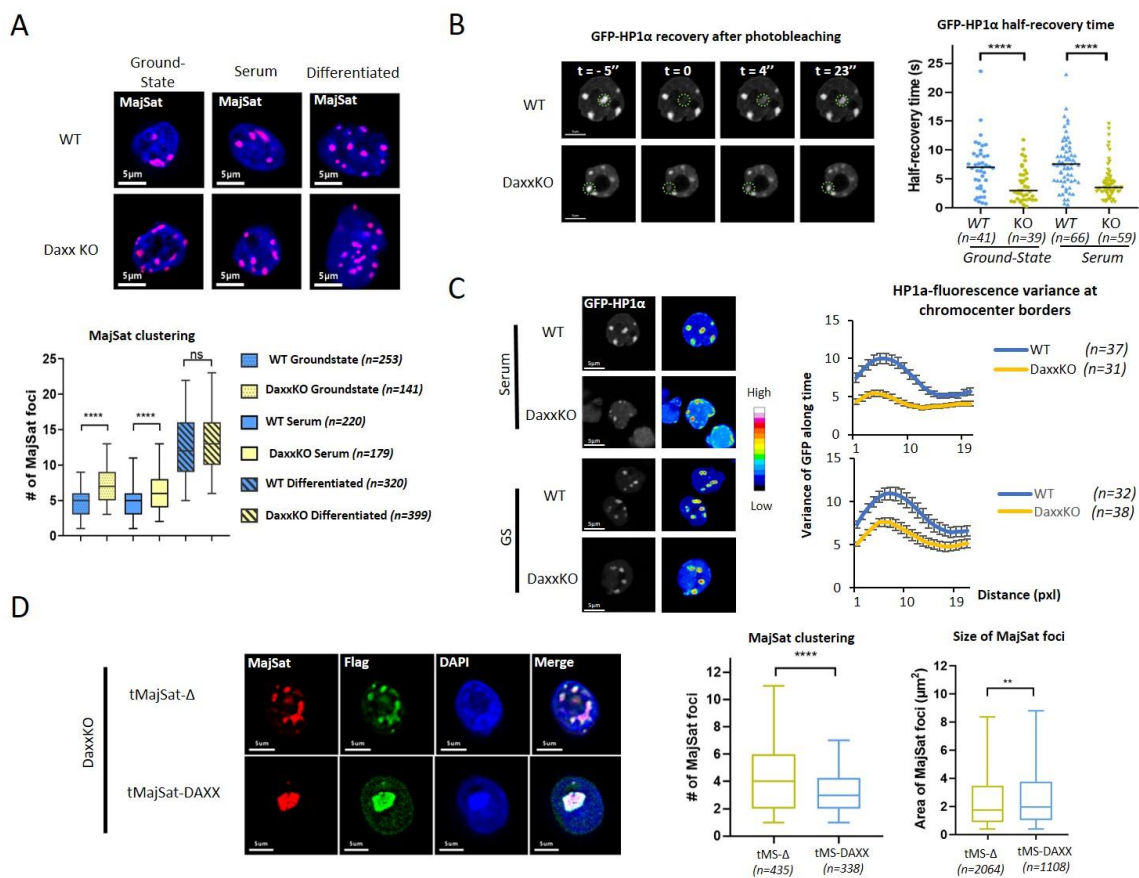


Figure 4 | DAXX maintains heterochromatin organization in pluripotent cells. (A) Top, representative major satellite DNA FISH pictures of WT and Daxx KO ESCs in serum, ground-state or differentiated conditions. Bottom, quantification of the number of major satellite foci counted on medium focal plane. Boxplot represent median of at least 3 biological replicates. n=total number of nuclei analyzed. **(B)** Left, representative pictures from FRAP experiments performed on WT and Daxx KO cells transfected with GFP-HP1α. T=-5'' corresponds to pre-bleach fluorescence. T=0 corresponds to the laser bleach pulse. T=4 and 23'' correspond to post-bleach recovery images. Right, quantification of half-recovery times for individual nuclei. n=total number of nuclei analyzed from 2 biological replicates. **(C)** Left, representative pictures of GFP-HP1α and corresponding variance in fluorescence intensities in serum-based or ground-state WT or Daxx KO ESCs. Right, graph displaying the variance along a 1µm line traced above non-bleached chromocenter borders. **(D)** Left, representative immunofluorescence pictures of major satellite and Flag for Daxx KO cells transfected with Tale-Δ or Tale-DAXX. Middle, quantification of the number of major satellite foci detected in medium focal plane. Right, quantification of the surface of each major satellite foci analyzed. Area was measured for each focus detected on medium focal plane. n=total number of nuclei analyzed from 4 biological replicates. Two-sided Mann-Whitney tests were used for statistical analysis.

Figure 5

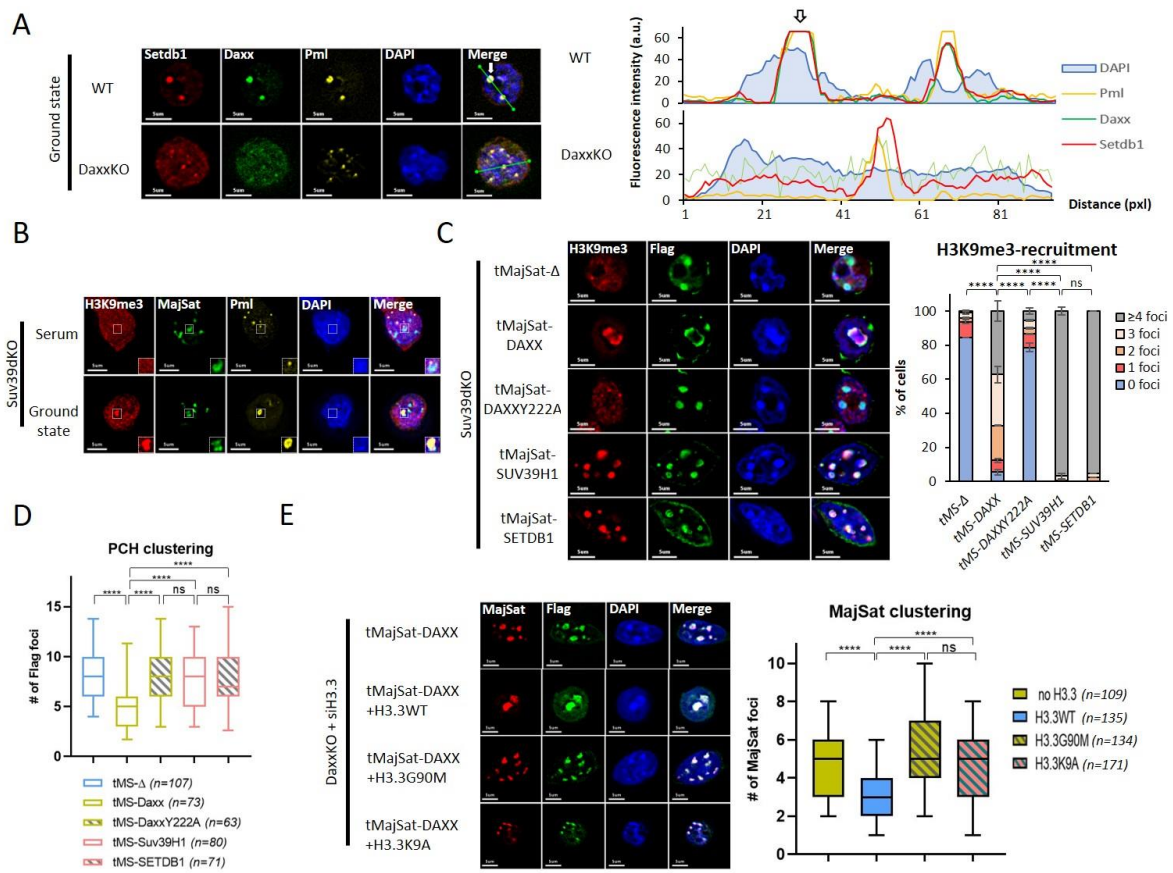


Figure 5 | DAXX recruits Setdb1 and mediates chromocenter clustering via H3.3K9me3 modification.

(A) Left, representative immunofluorescence pictures for SETDB1, DAXX and PML in WT or Daxx KO ESCs upon ground-state conversion. Right, fluorescence intensity profiles corresponding to the green line above the corresponding merge picture. White arrow indicates an example of DAXX-PML structure at PCH. **(B)** Representative immunoFISH pictures for H3K9me3, PML and major satellites in ground-state and serum Suv39H1/2 dKO ESCs. White dashed squares highlight a major satellite focus. **(C)** Left, representative immunofluorescence pictures for H3K9me3 and Flag in Suv39dKO serum ESCs transfected with Tale- Δ , Tale-DAXX, Tale-DAXXY222A, Tale-SUV39H1 and Tale-SETDB1. Right, quantification of the percentage of cells displaying H3K9me3 recruitment at Flag-DAPI-dense chromocenters. Histograms display mean with SEM from 2 biological replicates except for Tale-SetDB1. **(D)** Quantification of the number of Flag foci observed from C. Boxplot represent the 2 biological replicates with n=total number of nuclei analyzed. **(E)** Left, representative immunoFISH pictures for major satellite and Flag in Daxx KO serum ESCs transfected with siRNA against H3.3 with either no additional construct, H3.3WT, H3.3G90M or H3.3K9A. Right, quantification of the number of major satellite foci detected of medium focal plane. n=total number of nuclei analyzed from 2 biological replicates. Chi-square tests were used for statistical analysis of C. Two-sided Mann-Whitney tests were used for statistical analysis in D and E.

Methods

Cell lines

Feeder-free E14 mESCs were used for most experiment excepts otherwise notified. E14 mESCs were kindly provided by Pablo Navaro (Pasteur Institute). DaxxKO cell line was constructed using CRISPR/cas9 editing in E14 mESCs. Guide-RNA was designed using the online CRISPOR tool. Oligos were designed with a BbsI site on 5' to clone them into the pSpCas9(BB)-2A-Puro(pX459) v2.0 vector⁴⁶. Guide was designed carrying two guanines on 5' of the sequence to avoid off-target effects, as previously described⁴⁷. Feeder-free Suv39HdKO and corresponding WT R1 ESCs were obtained from Antoine Peters⁴⁸.

Culture conditions

Pluripotent cells were cultured either in a serum condition, defined as follow - DMEM (Gibco), supplemented with 10% of ESC-certified FBS (Gibco), 2-mercaptoethanol (0.05mM, Gibco), Glutamax (Gibco), MEM non-essential amino acids (0.1mM, Gibco), Penn-Strep (100units/mL, Gibco) and LIF (1000units/mL,) for serum condition. Serum-cultivated cells were grown on 0.1% gelatin-coated plates or stem cell plates (Stem Cell technology) at 37°C with 5% CO₂. Medium was changed every day and cells were passaged every 2 to 3 days. The other culture condition is the chemically defined serum-free 2i + VitC condition defined as follow - Neurobasal -DMEM/F-12 (50 -50, Gibco) medium, supplemented with N2 and B-27 supplements (Gibco), BSA fraction V (0.05%Gibco), 1-thioglycerol (1.5x10⁻⁴M, Sigma) and ESGRO 2 inhibitors (GSK3i and MEKi) and LIF (Merck). Vitamin C (L-ascorbic acid 2-phosphate, Sigma) was added at a concentration of 100µg/mL (Blaschke *et al.* 2013). Cells were grown on 0.1% gelatin-coated plates. Medium was changed daily. Cells were passed every 2 days at 1 -4 ratio for the first passage then at a 1 -6 ratio. Additional media used were constituted as follow - serum medium supplemented with either 5-azacytidine (2µM, Sigma) or Hydroxy-Urea (2mM, Sigma). Differentiation of mESCs was done by LIF removal for the first 24h. Then, non-LIF medium was supplemented with retinoic acid (10⁻⁶M,) for 4 days. For cell growth quantification, cells were counted at each passage for at least 3 different experiments.

Vectors and transfections

Cells were harvested using trypsin and one million was plated in a 0.1% gelatin-coated plate and transected with 2.5µg of DNA or 90ng of RNA using the Lipofectamine 2000 reagent (Thermo), following manufacturer's protocol. SiRNAs used are SMARTpools of 4 different siRNAs targeting mRNA of interest (Horizon Discovery). TALE vectors were constructed using previously described methods⁴⁹. A TALE specific DNA binding domain targeting *Major Satellite* repeats was created by the modular assembly of individual TALE repeats inserted into a backbone vector containing TALE-Nrp1-VP64 previously described⁵⁰. The BamHI-NheI fragment containing VP64 was replaced by PCR products encoding the DAXX protein or corresponding DAXX mutants.

Catalytically dead Cas9 was inserted into the pSpCas9(BB)-2A-Puro(pX459) v2.0 vector to generate a SpdCas9-2A-Puro⁴⁶.

Target sequences for the TALE repeat domains and Cas9 associated guides RNA are listed in Supplementary table 1.

RNA extraction for RNAseq or RT-qPCR

Total RNA was extracted using RNeasy extraction kit (Qiagen) according with manufacturer's protocol including DNaseI treatment for 15min at room temperature (Qiagen). Complementary DNA were generated from 1µg of RNA using the Maxima first strand cDNA synthesis kit (Thermo Fisher), with a second round of DNaseI from the Maxima kit for 15min. Real-time qPCR was carried out using a LightCycler 480 instrument (Roche) and the LightCycler 480 SYBR green master mix (Roche). The qRT-PCR primers used in this study are listed in supplementary table. Three independent biological repeats were obtained for each sample. For RNAseq experiment, RNA quality was assessed using the Agilent 2100 bioanalyzer. Libraries were prepared using oligo(dT) beads for mRNA enrichment, then fragmented and reverse transcribed using random hexamers primer. After adaptor ligation, the double-stranded cDNA is completed through size selection of 250-300bp and PCR amplification, then quality of the library is assessed by the Agilent 2100 bioanalyzer. Sequencing was performed in 150bp paired-end reads using an Illumina sequencer platform.

RNA-seq Mapping and Processing

FASTQ files generated by paired end sequencing were aligned to the mouse genome using bowtie2 v2.2.6 (parameters - --local --threads 3; mm9 genome build). Mapped RNA-seq data was processed using tools from the HOMER suite (v4.8). SAM files were converted into tag directories using 'makeTagDirectory' (parameters - -format sam -sspe; Reference – will be uploaded to GEO upon publication). Genomic intervals which extended beyond the end of the chromosomes was removed using 'removeOutOfBoundsReads.pl'. bigWig browser track files were generated using 'makeUCSCfile' (parameters - -fsize 1e20 -strand + -norm 1e8). For gene expression analysis, read depths were quantified for all annotated refseq genes using analyzeRepeats.pl (parameters - rna mm9 -strand both -count exons -rpkm -normMatrix 1e7 -condenseGenes). For repeat analysis, read coverage was quantified for each repeat and then condensed to a single value for each named entry (parameters - repeats mm9 -strand both -rpkm -normMatrix 1e7 -condenseL1). Read depths were then corrected for the number of instances of each repeat prior to expression analysis.

Expression Analysis

Quantified RNA-seq data was processed using the limma package (R/Bioconductor; Reference – will be uploaded to GEO upon publication)⁵¹. Following the addition of an offset value (1 RPKM) to each gene or repeat, data was normalised across all samples using 'normalizeBetweenArrays' with method='quantile'. Fold-changes and p-values for differential

expression of genes and repeats were determined using empirical Bayes statistics. Briefly, data was fit to a linear model using 'lmFit' and specified contrasts were applied using 'makeContrasts' and 'contrasts.fit'. Data was processed using the 'topTable' function with `adjust.method="BH"` (Benjamini-Hochberg multiple-testing correction). Differential expression was defined as \log_2 fold change ≤ -1 or ≥ 1 and an adjusted p-value of ≤ 0.01 . Three biological replicates for each condition represent independently cultured pools of cells.

Data visualization

Heatmaps and boxplots were generated using Prism GraphPad. Histograms were drawn using either Prism GraphPad or Excel. Volcano plots were generated using the plot function of R. Pathway analysis was performed using the EnrichR tool^{52, 53}.

Immunofluorescence

Murine ESCs were harvested with trypsin (Gibco) and plated for 4-6h onto 0.1% gelatin-coated glass cover slips. Cells were fixed with 4% paraformaldehyde for 10min at room temperature, then rinsed three times with PBS. Cells were permeabilized with 0.1X triton for 12min at room temperature, then rinsed three times with PBS. Blocking was done in 3% BSA solution for 30min at room temperature. All incubations with primary antibodies were performed for either 1h at room temperature or overnight at 4°C with the following antibodies for H3K9me3 (Active Motif, 1:1000), DAXX (Santa Cruz, 1:500), γ H2AX (Abcam, 1:1000) and SETDB1 (Proteintech, 1:100). Incubation with secondary antibodies (fluorescently labeled anti-mouse or anti-rabbit, 1:1000) were performed for 1h at room temperature. Mounting was performed using ProLong Diamond with DAPI mounting media (Thermo). Antibodies are listed in supplementary table. For 5mC staining, cells were fixed with 4% PFA for 10 min at room temperature, then permeabilized using 1% BSA, 0.5% triton X-100 for 30 min at room temperature. Cells were washed 3 times in PBS before incubation with RNase A (20mg/mL) for 1h at 37°C. Cells were washed 3 times in PBS, then denatured in 4M HCl for 10 min at 37°C. Slides are neutralized by extensive washes in PBS, then blocked in 1% BSA, 0.1% Triton X-100 for 30 min at room temperature before incubation with 5mC antibody (Diagenode, 1:1000) overnight at 4°C. After 3 washes in PBS, cells were blocked in 1% BSA, 0.1% Triton X-100 for 30 min at room temperature before incubation with secondary antibody for 1h at room temperature. Mounting was performed using ProLong Diamond with DAPI mounting media (Thermo).

Fluorescent *in situ* Hybridization

Murine ESCs were harvested with trypsin (Gibco) and plated for 4-6h onto 0.1% gelatin-coated glass cover slips. Cells were fixed with 4% paraformaldehyde (PFA) for 10min at room temperature, then rinsed three times with PBS. Cells were permeabilized with 0.5X triton for 12min at room temperature, then rinsed three times with PBS. Cells were briefly washed in 2X SSC, then treated with RNaseA (100 μ g/mL, Sigma) for 1h at 37°C. Cells were briefly washed in 2X SSC, then denatured by serial 2min incubation into 70,90 and 100% ethanol. Cover slips

were air dried for 15min. Cover slips are incubated with 200nM of PNA probe, placed for 10min at 95°C for denaturation, then placed for 1h at room temperature in the dark for hybridization. Cover slips were washed twice in 2X SSC 0.1%Tween-20 for 10min at 60°C. Cover slips were immersed at room temperature in 2X SSC 0.1%Tween-20 for 2 min, then in 2X SSC for 2min and 1X SSC for 2min. Mounting is performed using ProLong Diamond with DAPI mounting media (Thermo).

Dot blot experiments

DNA extraction was performed using the Wizard genomic DNA extraction kit (Promega). Genomic DNA (1µg) was then denatured in 0.1M NaOH for 10min at 95°C before neutralization with 1M NH₄OAc on ice for 5min. DNA samples were spotted on a nitrocellulose membrane. Blotted membrane was washed in 2X SSC and dried at 80°C for 5min before UV cross-linking at 120,000µJ/cm². Membrane was then blocked using PBS, 5% milk 0.1% tween for 30min at room temperature. Membrane was incubated with 5mC antibody (Diagenode, 1:1000) for 3h at room temperature. After 3 washes of 10min each in PBS, membrane was blocked again for 30min and then incubated with secondary anti-HRP antibody for 1h at room temperature. Membrane was washed 3 times for 10min in PBS and visualized by chemiluminescence with ECL Plus.

Chromatin accessibility

Chromatin was extracted from desired ES cell lines and digested with MNase (NEB) for different times and stopped before migration onto 1% agarose gel and subsequent Southern blotting with major satellites probe. Southern blot hybridization was performed with DIG-labeled PCR products and DIG wash-and-block kit (Roche) before visualization with CSPD (Roche).

Fluorescent Recovery After Photobleaching

Murine ESCs transfected with GFP-HP1α were harvested with trypsin (Gibco) and plated for 4-6h onto 0.1% gelatin-coated glass live-cell Nunc slides (Thermo). FRAP experiment was carried with an LSM 800 confocal microscope (Zeiss). The 488nm laser was used to bleach and acquire GFP signal. 1 image was taken before a bleach pulse of 5ms. Bleaching area was set to target a single pericentric domain. Images were acquired every second during 35s post-bleach.

Image acquisition and analysis

Images were obtained with an inverted Nikon Ti Eclipse widefield microscope using a 60X immersion objective and LED sources. Z-stacks images were taken and then deconvoluted using a custom ImageJ deconvolution script. Quantifications of images were performed using custom Icy scripts. Number of major satellite foci were counted using a custom Icy script and performed onto the medium focal plane. FRAP analysis was performed using a FRAP analysis

ImageJ Jython script, that generated FRAP curves and the associated half-recovery time and mobile fraction parameters.

GFP-HP1 α variance along time was obtained from ImageJ analysis using z-projection along time. Quantification of heterochromatin barriers were performed using a 2 μ m line across individual non-bleached chromocenter borders, for which the variance intensity along time was measured.

DNA methylation at chromocenters from the Tale-TET1CD experiments were measured using a 2 μ m line across individual DAPI-dense chromocenters. Intensity profiles were obtained and the mean with SEM were calculated for DAPI and 5mC signals for each condition. DNA damage signaling, SETDB1 and H3K9me3-recruitments at chromocenters were counted manually.

Statistical analysis performed are indicated in the text, figures or figure legends and all statistical results are available in Supplementary table 1. Pvalues are represented as follow: * $p < 0.05$; ** $p < 0.01$; *** $p < 0.001$; **** $p < 0.0001$.

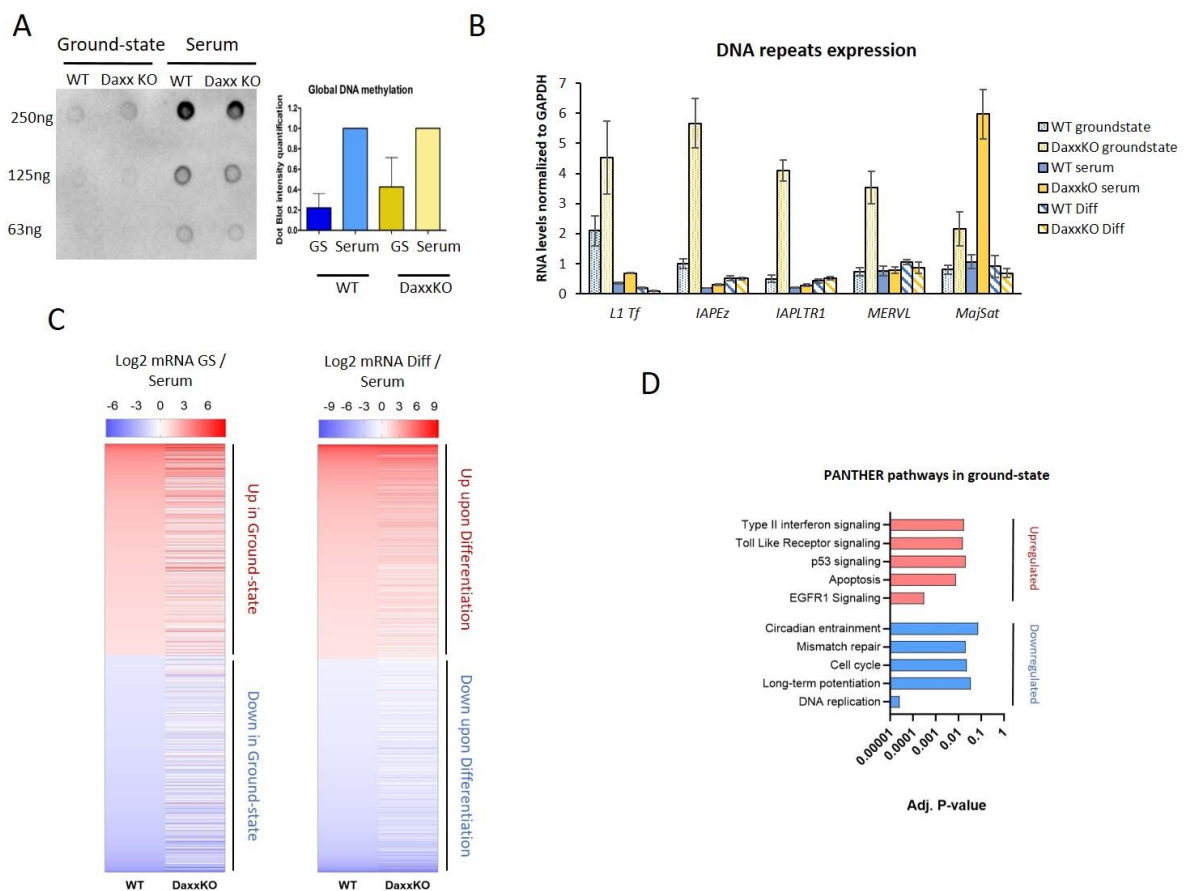
Western blotting

Total protein extracts were prepared in RIPA buffer with protease inhibitor cocktail (Roche). Proteins were separated by electrophoresis in 8-15% poly-acrylamide gels then transferred onto nitrocellulose membranes. Membranes were incubated in ponceau then washed in PBS, 0.1% tween. Membranes were blocked in PBS, 0.1% tween, 5% milk for 30min at room temperature before incubation with primary antibody overnight at 4°C. After 3 washed in PBS, 0.1% tween, membranes were incubated with secondary HRP-conjugated antibody for 1h at room temperature. Membranes were washed 3 times in PBS, 0.1% tween and visualized by chemoluminescence using ECL Plus.

References

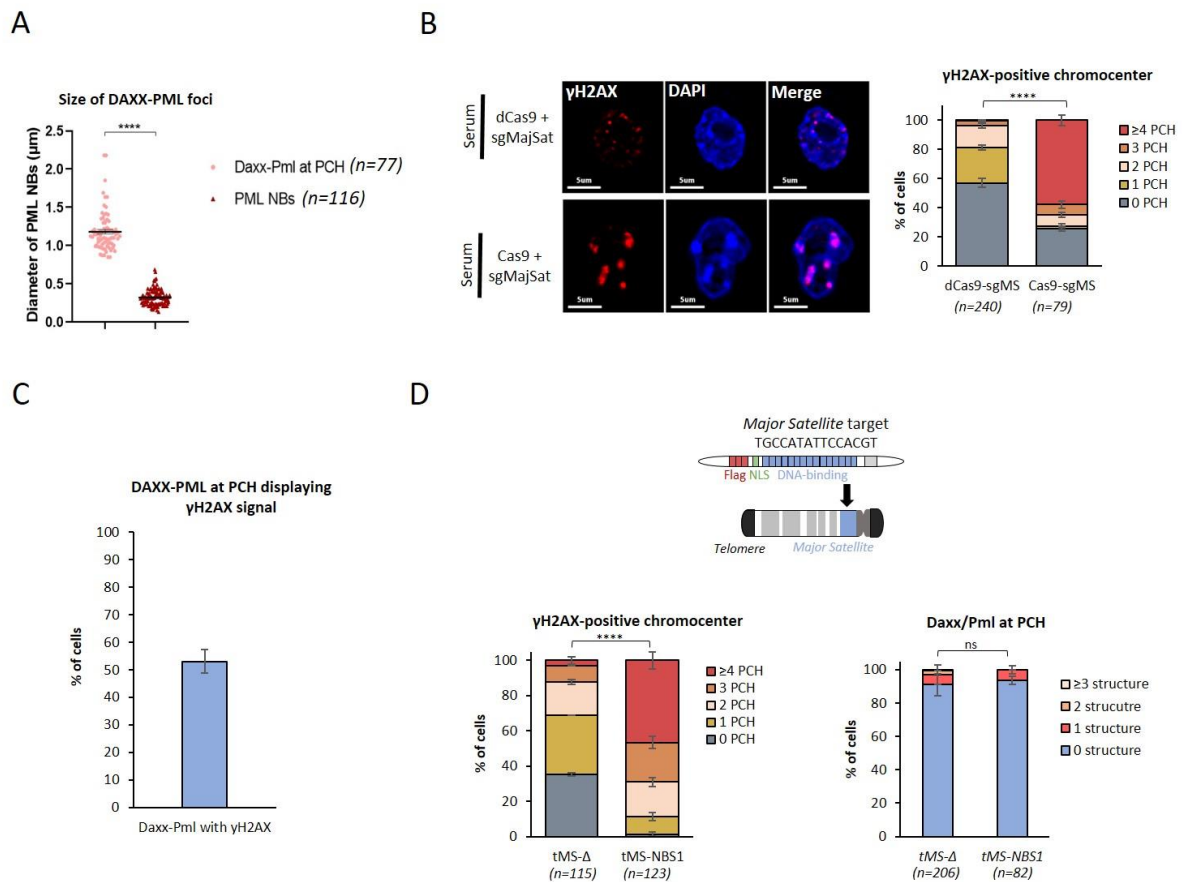
46. Ran, Hsu, Wright *et al.*, *Nature Protocols* (2013)
47. Cho, Kim, Kim *et al.*, *Genome Research* (2014)
48. Lenhertz, Ueda, Derijck *et al.*, *Current Biology* (2003)
49. Zhang, Cong, Lodato *et al.*, *Nature Biotechnology* (2011)
50. Therizols, Illingworth, Courilleau *et al.*, *Science* (2014)
51. R Core Team. *R Foundation for Statistical Computing* (2017)
52. Chen, Tan, Kou *et al.*, *BMC Bioinformatics* (2013)
53. Kuleshov, Jones, Rouillard *et al.*, *Nucleic Acid Research* (2016)

Supplementary figure 1



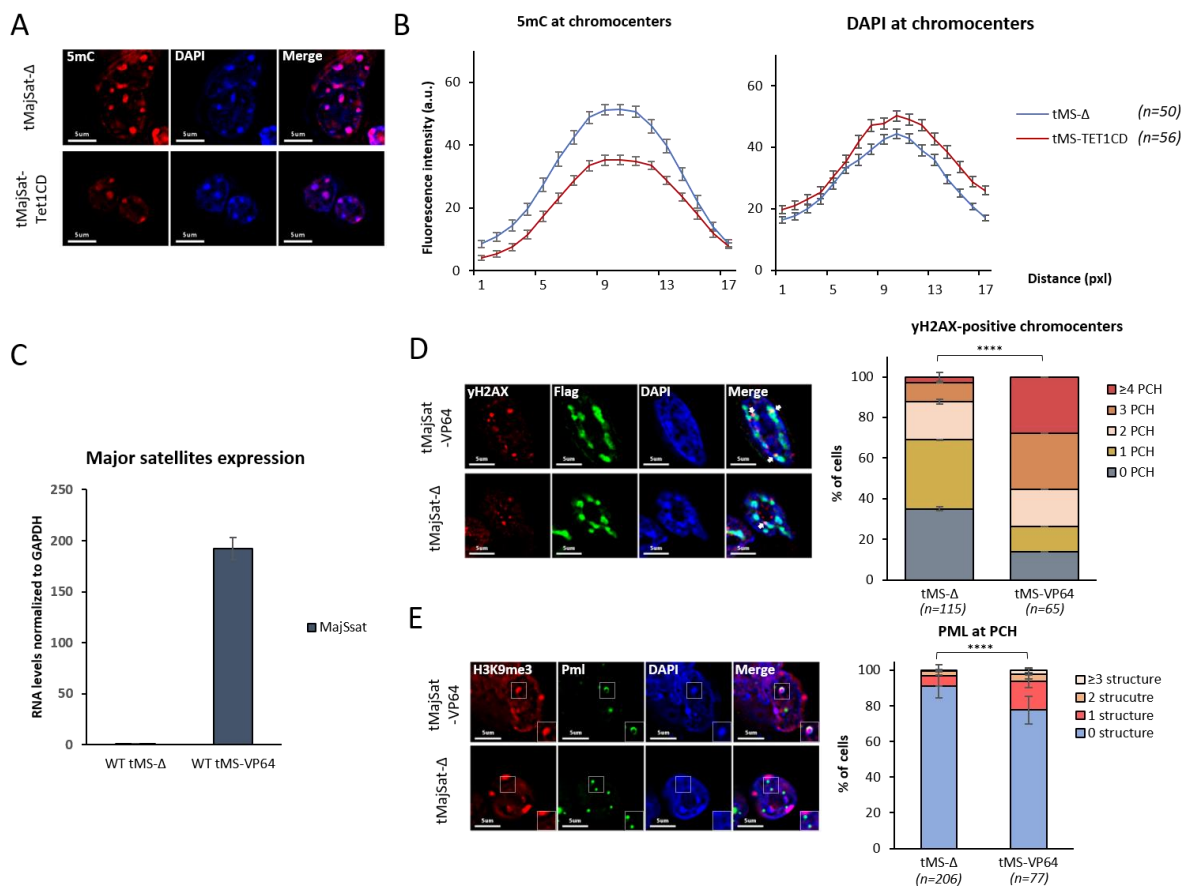
Supplementary figure 1 | DAXX is essential for ES cell survival upon ground-state conversion. **(A)** Dot blot using 5mC antibody to assess global DNA methylation levels upon ground-state conversion. One experiment is shown. Histogram displays mean with SEM from 3 independent replicates. **(B)** RT-qPCR RNA quantification of DNA repeats. Left, *L1Tf*, *IAPEz*, *IAPLTR1*, *MERVL* and major satellites expression in WT and Daxx KO ESCs in serum, and upon differentiation or ground-state conversion. Histogram represents mean with SEM of 3 biological replicates. **(C)** Heatmaps representing genes displaying strongest transcriptional changes upon ground-state conversion on the left or upon differentiation on the right. Same set of genes for the Daxx KO ESCs. Data are from 3 biological replicates of RNA-seq experiments. **(D)** Biological pathways that are statistically enriched in the transcriptomic analysis of WT or Daxx KO ESCs. In red are the pathways present in the up-regulated genes, in blue the pathways from down-regulated genes. Selected genes for PANTHER analysis have adjusted p -value < 0.01.

Supplementary figure 2



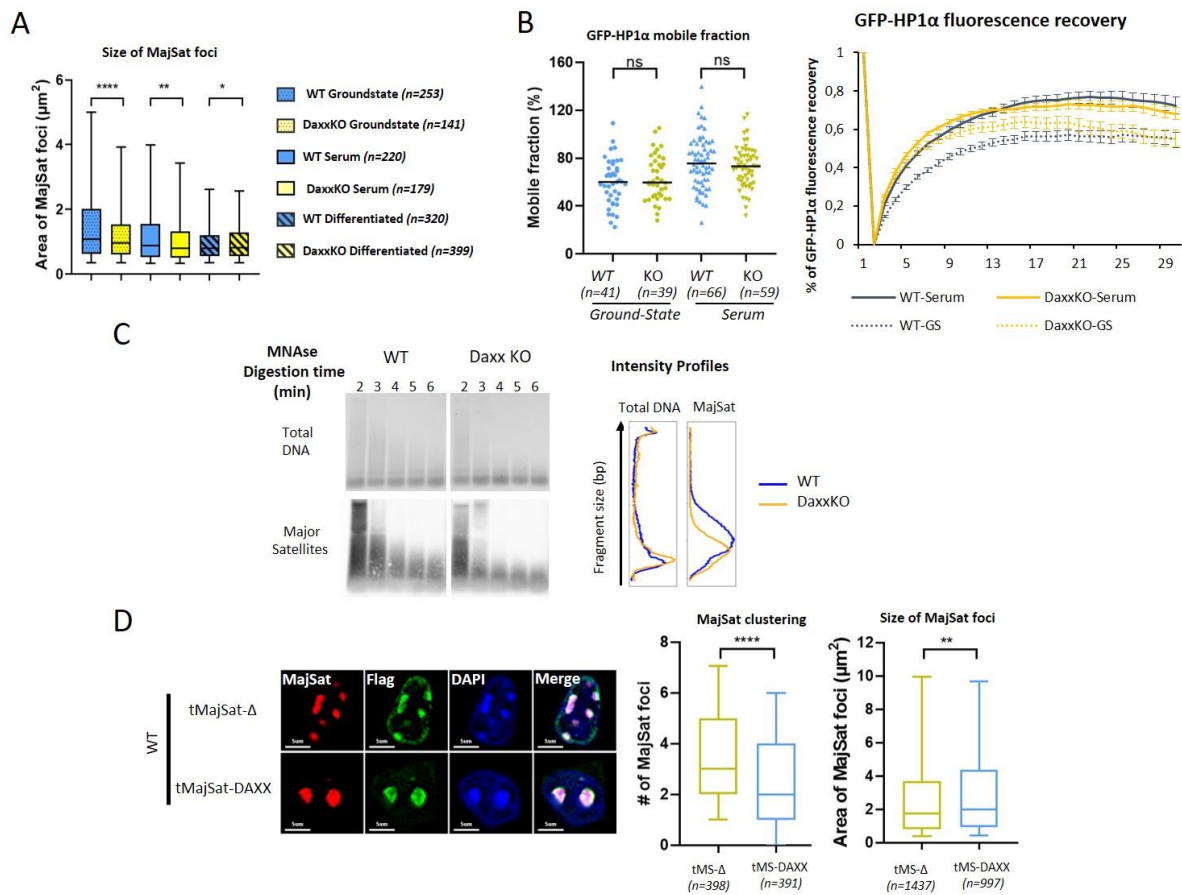
Supplementary figure 2 | DAXX accumulates at PCH upon ground-state conversion and DNA damages but is not part of DDR. (A) Quantification of the sizes of individual ‘classical’ PML NBs or DAXX-PML structures at PCH. n =total number of foci analyzed from 2 biological replicates. **(B)** Left, representative immunofluorescence pictures for γ H2AX of WT serum ESCs transfected with a small guide RNA targeting major satellites and either a dCas9 or a Cas9 enzyme. Right, quantification of the number of nuclei displaying the indicated number of DAPI-dense chromocenter marked with γ H2AX signal. n =total number of nuclei analyzed from 3 biological replicates. **(C)** Measurements of the percentage of WT ESCs in ground-state presenting γ H2AX signal within DAXX-PML structures. n =total number of nuclei analyzed from 2 biological replicates. **(D)** Left, schematic representation of a Tale construct targeting the major satellite repeats. Middle, quantification of WT serum ESCs transfected with Tale- Δ or Tale-NBS1 displaying the indicated number of Flag-DAPI-dense chromocenters with γ H2AX foci. n =total number of nuclei analyzed from 3 biological replicates. Right, quantification of WT serum ESCs transfected with Tale- Δ or Tale-NBS1 displaying the indicated number of DAXX-PML structures at PCH. Two-sided Mann-Whitney test was used for statistical analysis in A. Chi-square tests were used for statistical analysis in C and E.

Supplementary figure 3



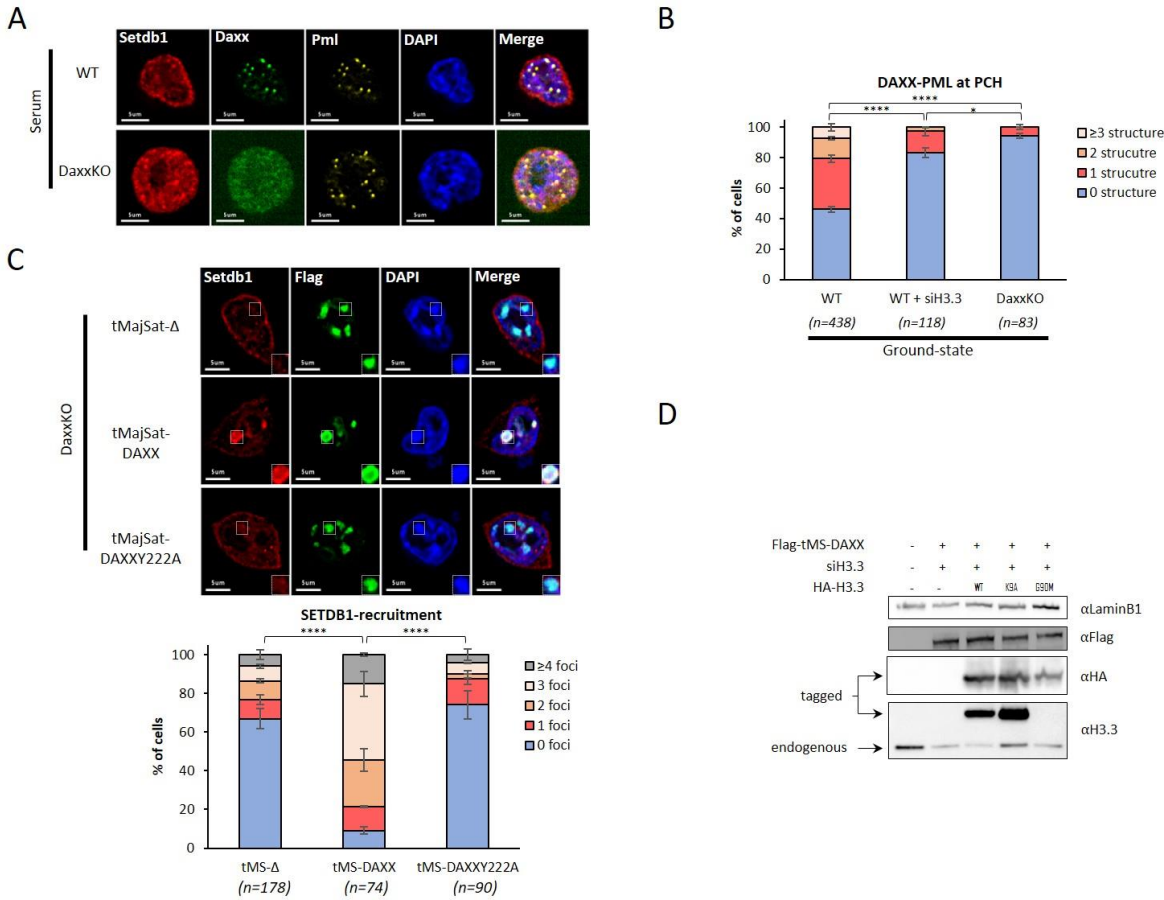
Supplementary figure 3 | DAXX relocates to PCH upon DNA damages induced by active DNA demethylation. (A) Representative immunofluorescence pictures of 5mC staining for WT serum ESCs transfected with Tale-Δ or Tale-TET1CD. (B) Measurements of the intensity profiles of individual DAPI-dense chromocenters for either 5mC (left) or DAPI (right) signals. n=total number of chromocenter analyzed. (C) RT-qPCR quantification of major satellite RNA upon transfection of Tale-Δ or Tale-VP64 in serum. Histogram represent mean with SEM from 2 biological replicates. (D) Left, representative immunofluorescence pictures for γH2AX and Flag in WT serum ESCs transfected with Tale-Δ or Tale-VP64. Right, quantification of the percentage of cells displaying the indicated number of DAPI-dense chromocenters with γH2AX foci. Histogram represents the mean with SEM from 2 biological replicates. n=total number of nuclei analyzed. (E) Left, representative immunofluorescence pictures for H3K9me3 and PML for WT serum ESCs transfected with Tale-Δ or Tale-VP64. Right, quantification of the percentage of cells showing the indicated number of PML structures at PCH. Histogram represents mean with SEM of 2 biological replicates. n=total number of nuclei analyzed. Chi-square tests were used for statistical analysis.

Supplementary figure 4



Supplementary figure 4 | DAXX is necessary and sufficient to maintain heterochromatin organization in pluripotent cells. (A) Quantification of the surface of each major satellite foci from figure 4A. Area was measured for foci detected on the medium focal plane. n =total number of foci analyzed from at least 3 biological replicates. **(B)** Left, mobile fraction of GFP-HP1 α were calculated from data presented in figure 4C. n =total number of cells analyzed from 2 biological replicates. Right, fluorescence recovery curves generated for FRAP experiments in WT or Daxx KO cells in serum or ground-state condition. **(C)** Chromatin accessibility measured by serial digestion of chromatin with MNase from WT and DaxxKO ESCs grown in serum. Left, agarose gel stained with BET showing total digested genomic DNA or membrane hybridized with a major satellite targeting probe. Right, intensity profiles observed at 4 min of digestion for total DNA or major satellites Southern blot. One membrane is shown from 2 biological replicates. **(D)** Left, representative immunofluorescence pictures for major satellites and Flag for WT serum ESCs transfected with Tale- Δ or Tale-DAXX. Right, quantification of the number of major satellite foci detected on focal medium plane and corresponding surface area. n =total number of nuclei for number and foci for sizes analyzed. Two-sided Mann-Whitney tests were used for statistical analysis.

Supplementary figure 5



Supplementary figure 5 | DAXX recruits SETDB1 and mediates chromocenter clustering via H3.3K9me3 modification. (A) Representative immunofluorescence pictures for SETDB1, DAXX and PML in WT or Daxx KO ESCs in serum. **(B)** Quantification of the percentage of cells displaying the indicated number of DAXX-PML structures at PCH. WT data come from figure 2C. Histogram represents mean with SEM from at least 2 biological replicates. n=total number of nuclei analyzed. **(C)** Top, representative immunofluorescence pictures for SETDB1 and Flag from Daxx KO serum ESCs transfected with Tale- Δ , Tale-DAXX or Tale-DAXXY222A. White dashed squares highlight DAPI-dense Flag-positive chromocenters. Bottom, quantification of the percentage of cell displaying the indicated number of DAPI-dense chromocenters with SETDB1 signal. **(D)** Western blot showing the quantity of Tale and H3.3 constructs in Daxx KO serum ESCs transfected with the indicated constructions.

Supplementary table 1

List of primers used for RT-qPCR	
Name	Sequence
exp-GAPDH-F	ATCACCATCTTCCAGGAGCGAG
exp-GAPDH-R	GACCCTTTTGGCTCCACCCTTC
exp-mDAXX-F	GAGGGCGAGAGACAGAAGAG
exp-mDAXX-R	GTCGTCGTCATCATCATCGT
exp-L1Tf-F	CAGCGGTCGCCATCTTG
exp-L1Tf-R	CACCCTCTCACCTGTTCACTAA
exp-IAPLTR1_Mm-F	GCGCTGACAGCTGTGTTCTA
exp-IAPLTR1_Mm-R	GGACGTGTCACTCCCTGATT
exp-IAPEz_int-F	CAGTGCGCAGACTCATTAT
exp-IAPEz_int-R	TATTCTACCGGAGCGTGGAC
exp-Mervl-F	CTCTACCACTTGGACCATATGAC
exp-Mervl-R	GAGGCTCCAAACAGCATCTCTA
exp-MajSat-F	TGGAATATGGCGAGAAAACCTG
exp-MajSat-F	AGGTCCTTCAGTGGGCATTT

Oligo used for CRISPR/Cas9 experiments	
Name	Sequence
Sg-mDaxx	gGACCTCATCCAGCCGGTTCA
sg-MajSat	CCATATCCACGTCCTACAG
Targeting sequence	
Tale	Sequence
Tale-MajSat	TGCCATATCCACGT

Figure 1

C) Number of genes differentially expressed		
RNAseq -1<Log(FC KO/WT)>1; pvalue<0.05		
GS	Up	1345
	down	1250
Serum	Up	497
	down	528
Diff	Up	8
	down	125

Figure 2

C) DAXX at PCH		
Chi-square	pval.	
Serum vs ground-state	4,04122E-08	Serum n=225
		GS n=438
D) yH2AX + foci		
Chi-square	pval.	
WT FCS vs GS	0,000663871	WT FCS n=155

DaxxKO-ServsGS	0,000154933	WT GS n=209
ser-ser	0,522768974	KO FCS n=128
GS-GS	0,012146258	KO GS n=200
E) DAXX at PCH		
Chi-square	pval.	
dcas vs cas9	0,003680042	dcas n=182
dcas vs HU	2,94735E-07	cas9 n=210
cas vs HU	0,077123279	HU n=65

Figure Supp. 2

A) Size of PML NB		
Mann-Whitney	pval.	
classical' vs 'giant'	<0.0001	classical' n=116 giant' n=77
B) γH2AX + foci		
Chi-square	pval.	
dCas9 vs Cas9	1,91581E-85	dcas n=240 cas9 n=79
D) γH2AX + foci		
Chi-square	pval.	
tMS Δ vs nbs1	1,1537E-136	tMS Δ n=115 tMSNBS1 n=123
D) DAXX at PCH		
Chi-square	pval.	
tMS Δ vs nbs1	0,360385276	tMS Δ n=206 tMSNBS1 n=82

Figure 3

B) DAXX at PCH		
Chi-square	pval.	
Serum vs 5aza	8,16745E-24	Serum n=225 5aza n=190
D) γH2AX + foci		
Chi-square	pval.	
tMS Δ vs Tet1CD	3,64197E-37	tMS Δ n=115 tMSTet1CD n=136
E) DAXX at PCH		
Chi-square	pval.	
tMS Δ vs Tet1CD	7,37729E-17	tMS Δ n=206 tMSTet1CD n=108

Figure Supp. 3

D) γH2AX + foci		
Chi-square	pval.	
tMS Δ vs VP64	8,67827E-22	tMS Δ n=115

		tMSVP64 n=65
E) DAXX at PCH		
Chi-square	pval.	
tMSΔ vs VP64	2,80269E-05	tMSΔ n=206
		tMSVP64 n=77

Figure 4

A) # of MajSat foci		
Mann-Whitney	pval.	
WTvsKO-GS	<0.0001	WT FCS n=220
WTvsKO-FCS	<0.0001	KO FCS n=179
WTvsKO-Diff	0.4685	WT GS n=253
		KO GS n=141
		WT Diff n=320
		KO Diff n=399
B) Half-recovery FRAP:		
Mann-Whitney	pval.	
WT GS vs KO GS	0.0005	WT FCS n=66
WT FCS vs KO FCS	<0.0001	KO FCS n=59
		WT GS n=41
		KO GS n=39
D) # foci tMSDAXX in DaxxKO		
Mann-Whitney	pval.	
tMSΔ vs DAXX	<0.0001	tMSΔ n=435
		tMSDAXX n=338
D) Sizes foci tMSDAXX in DaxxKO		
Mann-Whitney	pval.	
tMSΔ vs DAXX	0.0038	tMSΔ n=2064
		tMSDAXX n=1108

Figure Supp. 4

A) Size of MajSat foci		
Mann-Whitney	pval.	
WTvsKO-GS	<0.0001	n=1213vs1044
WTvsKO-FCS	0.0027	n=1121vs1143
WTvsKO-Diff	0.0195	n=4351vs7008
B) Mobile fraction FRAP:		
Mann-Whitney	pval.	
WTGSvsKOGS	0.53	WT-GS n=41
WTFCSvsKOFCS	0.55	KO-GS n=39
		WT-FCS n=66
		KO-FCS n=59
D) # foci tMSDAXX in WT		
Mann-Whitney	pval.	
tMSΔ vs DAXX	<0.0001	tMSΔ n=398

		tMSDAXX n=391
D) Sizes foci tMSDAXX in WT		
Mann-Whitney	pval.	
tMSΔ vs DAXX	0.0016	tMSΔ n=1438
		tMSDAXX n=997

Figure 5

C) H3K9me3-recruitment		
Chi-square	pval.	
tMSΔ vs DAXX	1,8847E-267	tMSΔ n=107
tMSΔ vs DAXXY222A	0.24	tMSDAXX n=73
tMSΔ vs SUV39H1	<0.00001	tMSSUV39H1 n=80
tMSDAXX vs DAXXY222A	2,3102E-102	tMSDAXXY222A n=63
tMSDAXX vs SUV39H1	2,66E-220	tMSSETDB1 n=71
tMSDAXXY222A vs SUV39H1	1.268E-18	
tMSΔ vs SETDB1	<0.00001	
tMSDAXX vs SETDB1	9,8003E-59	
tMSSUV39H1 vs SETDB1	0.30	
D) Flag clustering		
Mann-Whitney	pval.	
tMSΔ vs DAXX	<0.0001	tMSΔ n=107
tMSΔ vs SUV39H1	0.7736	tMSDAXX n=73
tMSΔ vs DAXXY222A	0.9781	tMSSUV39H1 n=80
tMSDAXX vs SUV39H1	<0.0001	tMSDAXXY222A n=63
tMSDAXX vs DAXXY222A	<0.0001	tMSSETDB1 n=71
tMSDAXXY222A vs SUV39H1	0.59	
tMSΔ vs SETDB1	0.91	
tMSDAXX vs SETDB1	<0.0001	
tMSSUV39H1 vs SETDB1	0.73	
E) # foci H3.3 complementation		
Mann-Whitney	pval.	
noH3.3 vs H3.3WT	<0.0001	noH3.3 n=109
H3.3WT vs G90M	<0.0001	H3.3WT n=135
H3.3WT vs H3.3K9A	<0.0001	H3.3G90M n=134
H3.3G90M vs H3.3K9A	0.0829	H3.3K9A n=171

Figure Supp.5

B) DAXX at PCH		
Chi-square	pval.	
WT vs siH3.3	3,59432E-12	WT FCS n=438
WT vs DaxxKO	4,64151E-20	siH3.3 n=118
siH3.3 vs DaxxKO	0.027971171	DaxxKO n=83
C) SETDB1 recruitment		
Chi-square	pval.	
tMSΔ vs DAXX	1,12458E-87	tMSΔ n=178

tMSDAXX vs DAXXY222A	3,022E-99	tMSDAXX n=74
tMSΔ vs DAXXY222A	0,00017048	tMSDAXXY222A n=90

Other results concerning Daxx at PCH

Methods

Cell lines

Feeder-free E14 mESCs were used for most experiment excepts otherwise notified. E14 mESCs were kindly provided by Pablo Navaro (Pasteur Institute). DaxxKO cell line was constructed using CRISPR/cas9 editing in E14 mESCs. Guide-RNA was designed using the online CRISPOR tool (site). Oligos were designed with a BbsI site on 5' to clone them into the pSpCas9(BB)-2A-Puro(pX459) v2.0 vector (Ran *et al.* 2013). Guide was designed carrying two guanines on 5' of the sequence to avoid off-target effects, as previously described (Cho *et al.* 2014).

Culture conditions

Pluripotent cells were cultured either in a serum condition, defined as follow - DMEM (Gibco), supplemented with 10% of ESC-certified FBS (Gibco), 2-mercaptoethanol (0.05mM, Gibco), Glutamax (Gibco), MEM non-essential amino acids (0.1mM, Gibco), Penn-Strep (100units/mL, Gibco) and LIF (1000units/mL,) for serum condition. Serum-cultivated cells were grown on 0.1% gelatin-coated plates or stem cell plates (Stem Cell technology) at 37°C with 5% CO₂. Medium was changed every day and cells were passaged every 2 to 3 days. The other culture condition is the chemically defined serum-free 2i + VitC condition defined as follow - Neurobasal -DMEM/F-12 (50 -50, Gibco) medium, supplemented with N2 and B-27 supplements (Gibco), BSA fraction V (0.05%Gibco), 1-thioglycerol (1.5x10⁻⁴M, Sigma) and ESGRO 2 inhibitors (GSK3i and MEKi) and LIF (Merck). Vitamin C (L-ascorbic acid 2-phosphate, Sigma) was added at a concentration of 100µg/mL (Blaschke *et al.* 2013). Cells were grown on 0.1% gelatin-coated plates. Medium was changed daily. Cells were passed every 2 days at 1 -4 ratio for the first passage then at a 1 -6 ratio. Additional media used were constituted as follow - serum medium supplemented with either 5-azacytidine (2µM, Sigma) or Hydroxy-Urea (2mM, Sigma). Differentiation of mESCs was done by LIF removal for the first 24h. Then, non-LIF medium was supplemented with retinoic acid (10⁻⁶M,) for 4 days. For cell growth quantification, cells were counted at each passage for at least 2 different experiments.

Vectors and transfections

Cells were harvested using trypsin and one million was plated in a 0.1% gelatin-coated plate and transected with 2.5µg of DNA or 90ng of RNA using the Lipofectamine 2000 reagent (Thermo), following manufacturer's protocol. SiRNAs used are SMARTpools of 4 different siRNAs targeting mRNA of interest (Horizon Discovery). TALE vectors were constructed using previously described methods (Zhang *et al.* 2011). A TALE specific DNA binding domain targeting *Major*

Satellite repeats was created by the modular assembly of individual TALE repeats inserted into a backbone vector containing TALE-Nrp1-VP64 previously described (Therizols *et al.* 2014). The BamHI-NheI fragment containing VP64 was replaced by PCR products encoding the DAXX protein or corresponding DAXX mutants. CDS of the different proteins were amplified by PCR from cDNAs obtained after RNA extraction of serum E14 mESCs.

Catalytically dead Cas9 was inserted into the pSpCas9(BB)-2A-Puro(pX459) v2.0 vector to generate a SpdCas9-2A-Puro (Ran *et al.* 2013).

RNA extraction for RNAseq or RT-qPCR

Total RNA was extracted using RNeasy extraction kit (Qiagen) according with manufacturer's protocol including DNaseI treatment for 15min at room temperature (Qiagen). Complementary DNA were generated from 1µg of RNA using the Maxima first strand cDNA synthesis kit (Thermo Fisher), with a second round of DNaseI from the Maxima kit for 15min. Real-time qPCR was carried out using a LightCycler 480 instrument (Roche) and the LightCycler 480 SYBR green master mix (Roche). The qRT-PCR primers used in this study are listed in supplementary table. Three independent biological repeats were obtained for each sample. For RNAseq experiment, RNA quality was assessed using the Agilent 2100 bioanalyzer. Libraries were prepared using oligo(dT) beads for mRNA enrichment, then fragmented and reverse transcribed using random hexamers primer. After adaptor ligation, the double-stranded cDNA is completed through size selection of 250-300bp and PCR amplification, then quality of the library is assessed by the Agilent 2100 bioanalyzer. Sequencing was performed in 150bp paired-end reads using an Illumina sequencer platform.

RNA-seq Mapping and Processing

FASTQ files generated by paired end sequencing were aligned to the mouse genome using bowtie2 v2.2.6 (parameters --local --threads 3; mm9 genome build). Mapped RNA-seq data was processed using tools from the HOMER suite (v4.8). SAM files were converted into tag directories using 'makeTagDirectory' (parameters -format sam -sspe; Reference – will be uploaded to GEO upon publication). Genomic intervals which extended beyond the end of the chromosomes was removed using 'removeOutOfBoundsReads.pl'. bigWig browser track files were generated using 'makeUCSCfile' (parameters -fsize 1e20 -strand + -norm 1e8). For gene expression analysis, read depths were quantified for all annotated refseq genes using analyzeRepeats.pl (parameters -rna mm9 -strand both -count exons -rpkm -normMatrix 1e7 -condenseGenes). For repeat analysis, read coverage was quantified for each repeat and then condensed to a single value for each named entry (parameters -repeats mm9 -strand both -rpkm -normMatrix 1e7 -condenseL1). Read depths were then corrected for the number of instances of each repeat prior to expression analysis.

Expression Analysis

Quantified RNA-seq data was processed using the limma package (R/Bioconductor; Reference – will be uploaded to GEO upon publication)(Team 2017). Following the addition of an offset value (1 RPKM) to each gene or repeat, data was normalised across all samples using 'normalizeBetweenArrays' with method='quantile'. Fold-changes and p-values for differential expression of genes and repeats were determined using empirical Bayes statistics. Briefly, data was fit to a linear model using 'lmFit' and specified contrasts were applied using 'makeContrasts' and 'contrasts.fit'. Data was processed using the 'topTable' function with adjust.method="BH" (Benjamini-Hochberg multiple-testing correction). Differential expression was defined as log₂ fold change ≤ -1 or ≥ 1 and an adjusted p-value of ≤ 0.01 . Three biological replicates for each condition represent independently cultured pools of cells.

Lamina-associated domains-genes analysis

List of LADs from embryonic stem cells were obtained from previously published datasets (Peric-Hupkes *et al.* 2010). Constitutive LADs were defined as ubiquitous lamina-association, and facultative LADs as regions interacting with the nuclear lamina only in embryonic stem cells. Comparison of LAD-genes and interLAD-genes expression was done using the Galaxy platform.

Immunofluorescence

Murine ESCs were harvested with trypsin (Gibco) and plated for 4-6h onto 0.1% gelatin-coated glass cover slips. Cells were fixed with 4% paraformaldehyde for 10min at room temperature, then rinsed three times with PBS. Cells were permeabilized with 0.1X triton for 12min at room temperature, then rinsed three times with PBS. Blocking was done in 3% BSA solution for 30min at room temperature. All incubations with primary antibodies were performed for either 1h at room temperature or overnight at 4°C with the following antibodies for H3K9me3 (Active Motif, 1:1000), DAXX (Santa Cruz, 1 -500), γ H2AX (Abcam, 1:1000), H3K9me2 (Active Motif, 1:1000), LaminB1 (Abcam, 1:1000) and ATRX (Santa Cruz, 1:1000). Incubation with secondary antibodies (fluorescently labeled anti-mouse or anti-rabbit, 1:1000) were performed for 1h at room temperature. Mounting was performed using ProLong Diamond with DAPI mounting media (Thermo). Antibodies are listed in supplementary table.

Fluorescent *in situ* Hybridization

Murine ESCs were harvested with trypsin (Gibco) and plated for 4-6h onto 0.1% gelatin-coated glass cover slips. Cells were fixed with 4% paraformaldehyde for 10min at room temperature, then rinsed three times with PBS. Cells were permeabilized with 0.5X triton for 12min at room temperature, then rinsed three times with PBS. Cells were briefly washed in 2X SSC, then treated with RNaseA (100 μ g/mL, Sigma) for 1h at 37°C. Cells were briefly washed in 2X SSC, then

denatured by serial 2min incubation into 70,90 and 100% ethanol. Cover slips were air dried for 15min. Cover slips are incubated with 200nM of PNA probe, placed for 10min at 95°C for denaturation, then placed for 1h at room temperature in the dark for hybridization. Cover slips were washed twice in 2X SSC 0.1%Tween-20 for 10min at 60°C. Cover slips were immersed at room temperature in 2X SSC 0.1%Tween-20 for 2 min, then in 2X SSC for 2min and 1X SSC for 2min. Mounting is performed using ProLong Diamond with DAPI mounting media (Thermo).

Image acquisition and analysis

Images were obtained with an inverted Nikon Ti Eclipse widefield microscope using a 60X immersion objective and LED sources. Z-stacks images were taken and then deconvoluted using a custom ImageJ deconvolution script. Quantifications of images were performed using custom Icy scripts.

Statistical analysis performed are indicated in the text, figures or figure legends and in Supplementary data. Pvalues are represented as follow: * <0.05; **<0.01; ***<0.001; ****<0.0001.

Western Blotting

Total protein extracts were prepared in RIPA buffer with protease inhibitor cocktail (Roche). Proteins were separated by electrophoresis in 8-15% poly-acrylamide gels then transferred onto nitrocellulose membranes. Membranes were incubated in ponceau then washed in PBS, 0.1% tween. Membranes were blocked in PBS, 0.1% tween, 5% milk for 30min at room temperature before incubation with primary antibody overnight at 4°C. After 3 washed in PBS, 0.1% tween, membranes were incubated with secondary HRP-conjugated antibody for 1h at room temperature. Membranes were washed 3 times in PBS, 0.1% tween and visualized by chemoluminescence using ECL Plus.

RESULTS

Deeper characterization of DAXX function in pluripotent cells

1. Loss of Daxx results in transcriptional 2C-like signature

Transcriptomic analysis of the Daxx KO ESCs in serum-based medium or upon differentiation or ground-state conversions revealed an extensive number of differentially expressed genes especially upon ground-state conversion (**Figure 1D article**). Furthermore, we noticed that the Daxx KO cells displayed an overexpression of the MERVL elements (**Figure 1C article**). MERVL upregulation has notably been reported in a rare subpopulation of ESCs in culture called 2-cell like (2C-like), which transcriptionally resemble the 2-cell state of the embryo. We thus decided to look for 2C-like genes that were either up or down-regulated specifically in 2C-like as previously described, such as *Dppa3*, the *Zscan4* cluster, *Tdpoz4* or the EIF4a1-like genes (*Gm5662* and *Gm2016*) (**Figure 27A**). Remarkably, upon ground-state conversion, Daxx KO ESCs presented a transcriptional profile that resembled to 2C-like cells (**Figure 27B**). Interestingly, this effect is lost in serum-based culture or upon differentiation (**Figure 27B**). Many of the specifically up-regulated genes in 2C-like cells show a strong down-regulation upon differentiation as they correspond to pluripotency-related factors (Rodriguez-Terrones *et al.* 2018). We confirmed the effect on transcription for 3 genes (*Gm5662*, *Spz1* and *Zscan4*) and the MERVL ERV family (**Figure 27C**). These results suggest that DAXX contributes to the repression of the 2C-like transcriptional program. Interestingly, in accordance with our data, DAXX has been found in a large siRNA screen for factors that could enhance the conversion toward a 2C-like state (Rodriguez-Terrones *et al.* 2018). Most of the identified factors repressing 2C-like transcriptional program are chromatin-related factors such as PRC1, EP400-TIP60 histone acetyl-transferase complex or the histone methyl-transferase SETDB1, suggesting a strong importance for heterochromatin regulation in the totipotency to pluripotency transition (Rodriguez-Terrones *et al.* 2018; Wu *et al.* 2020).

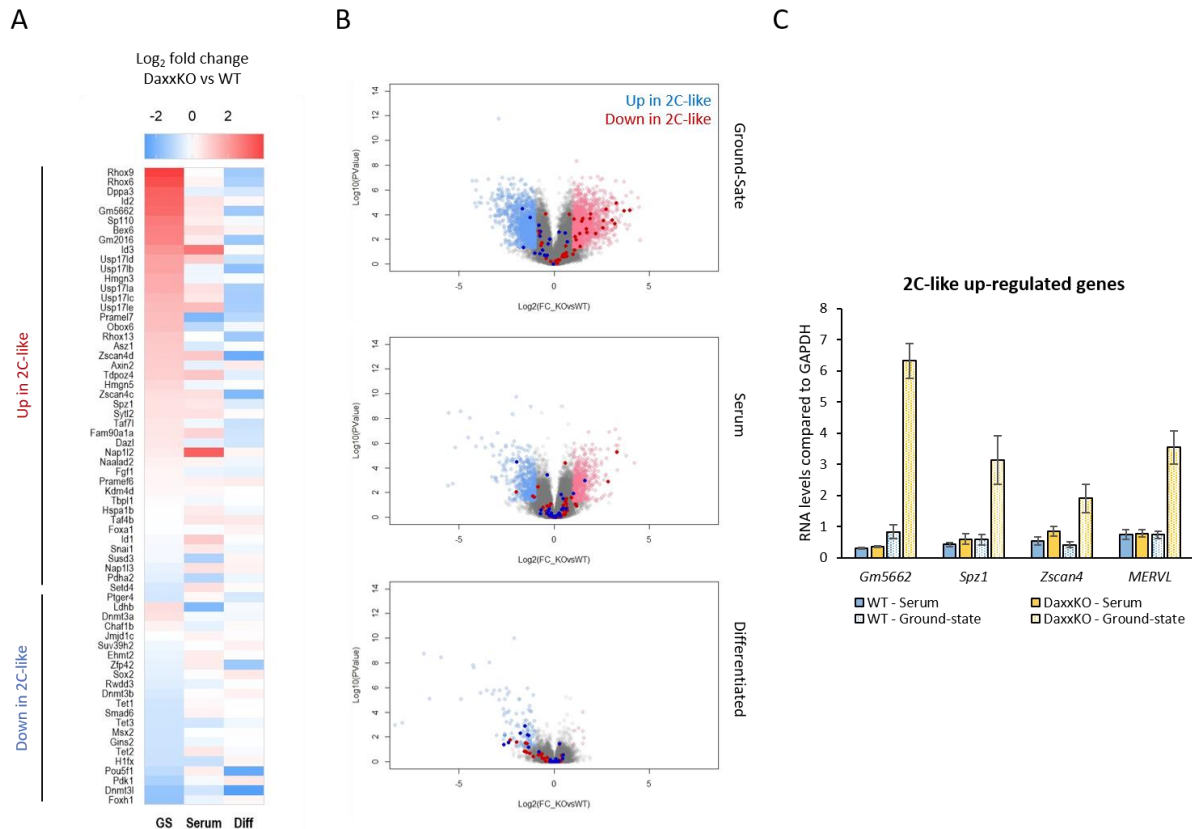


Figure 27 | Absence of Daxx results in 2C-like transcriptional profile. (A) Heatmap displaying Log₂(FoldChange(WT/KO)) in GS, serum or upon differentiation. The list of up- or down-regulated genes comes from Rodriguez-Terrones *et al.*, *Nature Genetics*, 2018 and Wu *et al.*, *Cell Reports*, 2020. 45 up-regulated genes and 21 down-regulated genes are observed. (B) Volcano plot displaying Log₂(FoldChange(KO/WT)) for all genes compared to Log₁₀(pvalue). In light blue or light red are highlighted the differentially expressed genes with Log₂(FoldChange(KO/WT)) <-1 or >1 and pvalue<0.05. In dark blue or dark red are the same genes as in A. (C) RT-qPCR assay for 3 representative genes (*Gm5662*, *Spz1* and *Zscan4*) and 1 repeated element (*MERVL*) up-regulated in 2C-like ESCs. Histogram displays mean and SEM from 3 biological replicates.

2. DAXX contributes to the radial positioning of chromocenters

In embryonic stem cells, chromocenters are randomly distributed throughout the nucleoplasm. However, it has been reported that among the proteins observed at pericentromeric heterochromatin were components of the nuclear lamina (Saksouk *et al.* 2014). Interestingly, cultivating the cells in the 2i/LIF medium can result in a more central positioning of chromocenters than that observed in serum-based medium (Saksouk *et al.* 2014). Saksouk *et al.* proposed that the changes in radial positioning of chromocenters could result from differences in LAMINB binding. We developed an automated approach to quantify the intensity of the major satellite DNA FISH signal at the periphery of the nucleus, such as described previously (Figure 28A) (Saksouk *et al.* 2014). We confirmed this central repositioning in our 2i/LIF with vitamin C medium (Figure 28B, Figure 28C). Interestingly, the longer the conversion toward the ground-state of pluripotency, the more central is the repositioning as we noted from 4 to 10 days in culture. All further experiments

in ground-state were conducted at 4 days of conversion. Thus, ground-state conversion triggers a repositioning of chromocenters away from the nuclear lamina.

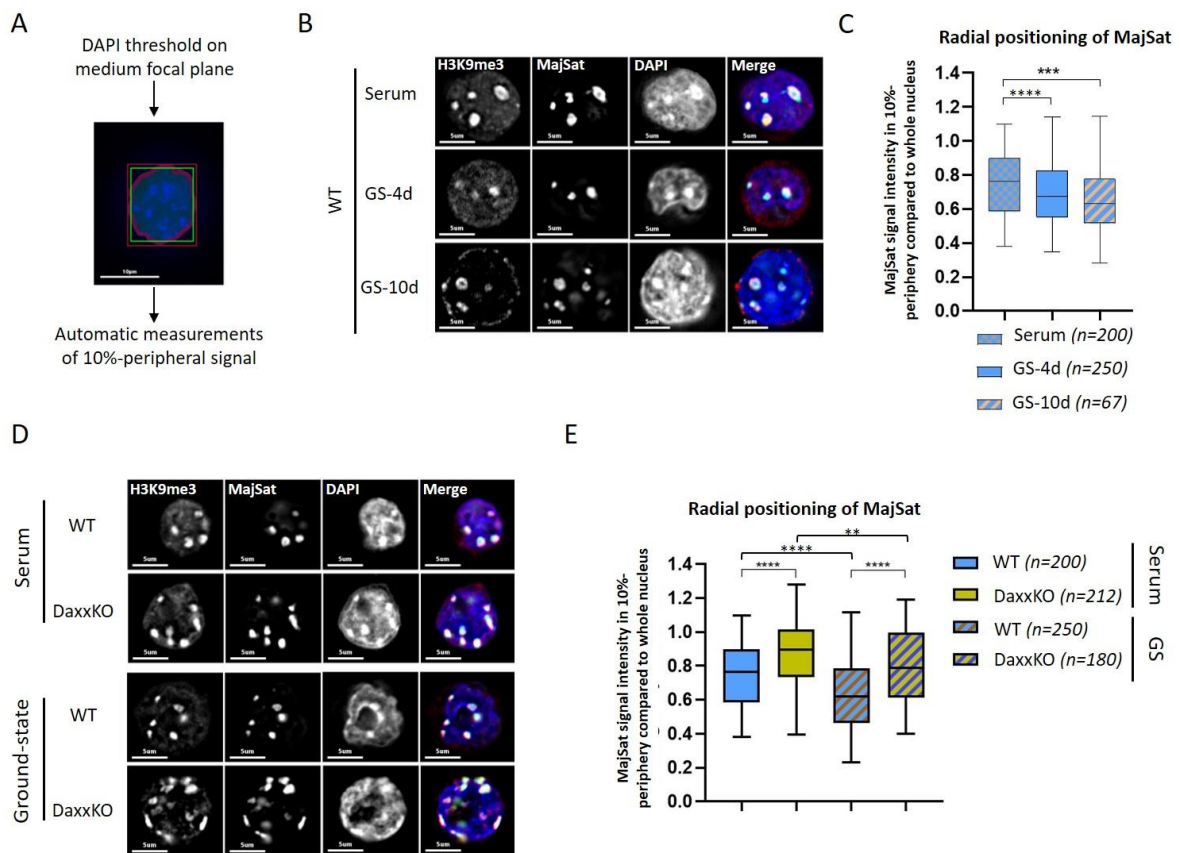


Figure 28 | DAXX contributes to the radial positioning of chromocenters. (A) Representative images of immunoFISH experiments with H3K9me3 staining and DNA FISH of major satellites in the serum-based medium or after 5 or 10 days of ground-state conversion. (B) Scheme of the automatic threshold of DAPI signal and generation of a mask comprising the 10% most peripheral signal. (C) Quantification of the major satellite DNA FISH signal intensity observed within the 10% most peripheral zone compared to the intensity observed within the whole nucleus for the same conditions as in (A). Data from 3 biological replicates except for 10 days in ground-state that comprises 2 biological replicates. n = the total number of cells analyzed (D) Representative images from immunoFISH experiments as in (A) for both WT and Daxx KO ESCs in serum-based medium or 4 days after ground-state conversion. (E) Quantification of the peripheral signal of major satellite DNA FISH signal as in (C). Data from 3 biological replicates except for 10 days in ground-state that comprises 2 biological replicates. n = the total number of cells analyzed. Two-sided Mann-Whitney was used for statistical analysis. GS = ground-state

Because the loss of Daxx impacted the spatial organization of major satellites (Figure 4A article), we wondered whether there were changes in their radial positioning as well. Using our automated approach, we observed that Daxx KO ESCs displayed an altered radial localization of major satellites. Indeed, in both serum and ground-state conditions, the lack of Daxx resulted in a more peripheral positioning of pericentromeric clusters (Figure 28D, Figure 28E). Conversion toward the ground-state of pluripotency induced a slight central relocalization of major satellites foci, although it remained more peripheral compared to WT ESCs. Our results indicate that in addition to the altered organization of major satellites, the loss of Daxx induces a peripheral localization of chromocenters. Interestingly, it has been reported that high levels of H3K9me3 on

a transgene locus was associated with its peripheral localization (Bian *et al.* 2013). Since Daxx KO ESCs presented H3K9me3 signal at PCH as WT cells (**Figure 28D**), our results suggest that subtle differences, perhaps through the loss of tri-methylation of lysine 9 of H3.3, could impact the spatial localization of chromocenters.

3. DAXX contributes to peripheral heterochromatin organization and silencing of LADs

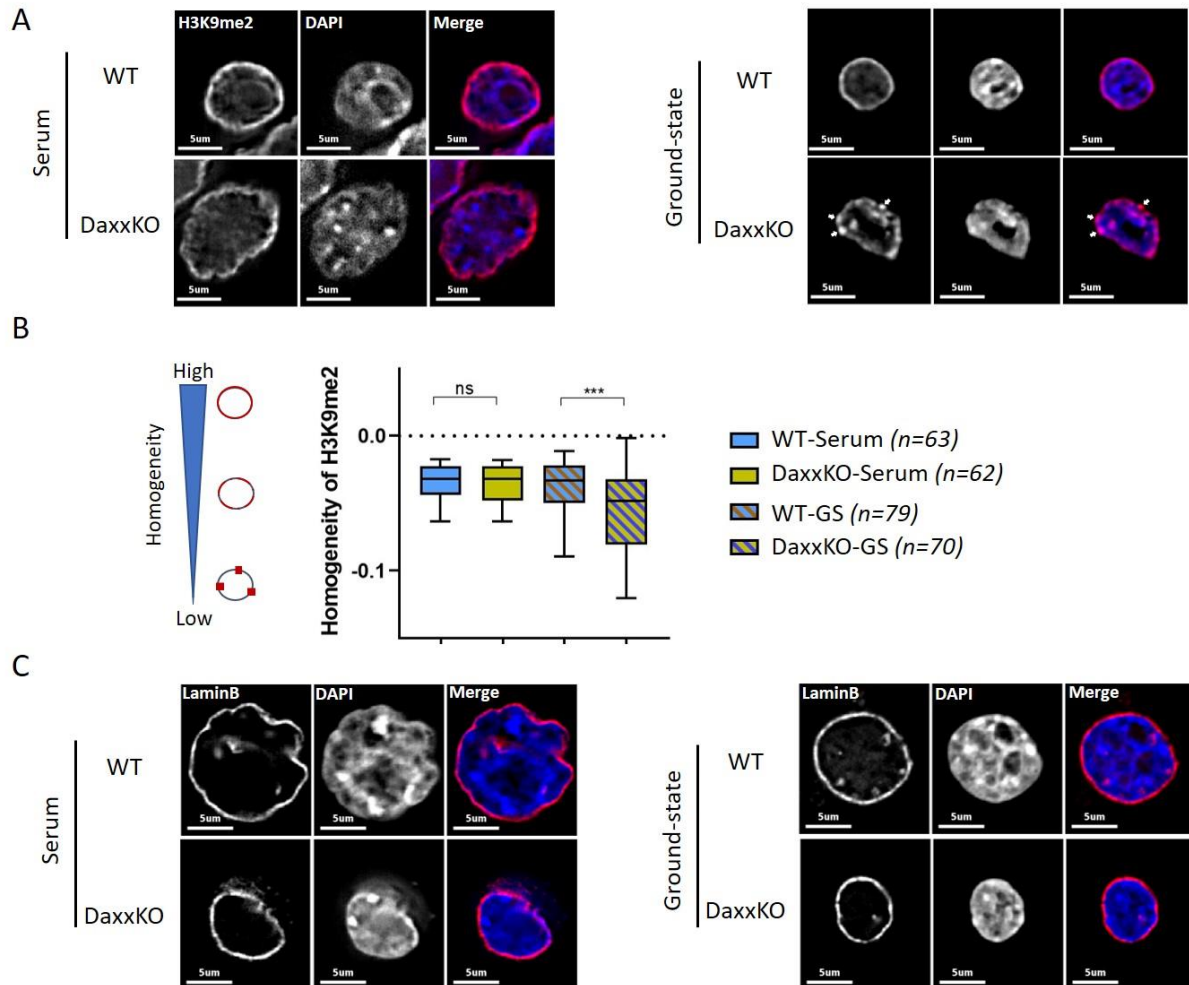


Figure 29 | DAXX contributes to peripheral heterochromatin organization. (A) Representative images of immunofluorescence of H3K9me2 histone modification. On the left are the WT cells in either serum-based or ground-state conditions. On the right are the Daxx KO cells in the two conditions. White arrows indicate the patches of H3K9me2 that are uniquely visible in Daxx KO ESCs converted to ground-state condition. (B) Scheme of the homogeneity score representation where 0 is a perfectly homogenous signal. A line is traced at the nuclear periphery and we calculated the variation of the signal along the line. Boxplot displays the mean of variation for each nucleus. Data from at least 3 biological replicates. n = total number of nuclei analyzed. (C) Representative images of immunofluorescence of LaminB protein, a constituent of the nuclear lamina. On the left are the WT cells in either serum-based or ground-state conditions. On the right are the Daxx KO cells in the two conditions. Two-sided Mann-Whitney was used for statistical analysis. GS = ground-state

As already mentioned, major satellites are enriched in H3K9me3 histone modification, mainly deposited by the SUV39H1/2 enzymes (Peters *et al.* 2001). However, the nuclear periphery and the lamina-associated domains are mainly enriched in H3K9me2 (Kind *et al.* 2013). As major

satellites signal was increased at the nuclear periphery, we next asked how the presence of H3K9me3-rich chromocenters could impact the peripheral heterochromatin compartment (**Figure 28C, Figure 28E**). We detected no differences in H3K9me2 distribution in ground-state compared to serum-based medium in WT ESCs (**Figure 29A**). The loss of Daxx did not impact H3K9me2 peripheral localization in serum-based medium, suggesting that peripheral localization of chromocenters is not challenging for proper establishment of H3K9me2. Intriguingly, conversion of Daxx KO cells toward the ground-state of pluripotency impaired H3K9me2 distribution (**Figure 29A**). Instead of being uniformly distributed along the periphery, H3K9me2 appeared as individual patches. We specifically measured the intensity levels of this histone modification at the nuclear periphery and calculated the standard deviation for the signal intensity of each pixel and quantified the signal heterogeneity in the different conditions. We confirmed the alteration of H3K9me2 signal distribution in ground-state in the absence of Daxx, suggesting a particular feature of ground-state ESCs (**Figure 29B**). It remains to understand if the peripheral localization of chromocenters in ground-state is implicated in the H3K9me2-ring disruptions. Next, we wondered if the altered H3K9me2 distribution could result from defects in the nuclear lamina. We performed immunofluorescence assays of the LAMINB1 constituent of the lamina. We did not observe any changes of LAMINB1 signal in the absence of Daxx in serum-based or ground-state medium (**Figure 29C**). Our results suggest that the absence of Daxx results in impaired distribution of H3K9me2 at the nuclear periphery independently of lamina integrity defects upon ground-state conversion. It would be informative to assess whether additional nuclear lamina proteins such as NET are still present upon ground-state conditions (Czapiewski *et al.* 2016). Furthermore, it remains to assess if there are local or global losses of H3K9me2 onto corresponding chromatin.

The histone modification H3K9me2 is highly enriched in LADs (Kind *et al.* 2013). Because we observed that H3K9me2 signal appeared as patches at the periphery, we decided to assess the transcription of the genes specifically located within LADs. We analyzed the RNA-seq experiment performed in WT and DaxxKO ESCs and classified the genes into LAD or inter-LAD (iLAD) categories based on DamID definitions for mESCs (Peric-Hupkes *et al.* 2010). Association with the nuclear lamina is cell-type dependent for some genes, and these regions are thus defined as facultative LADs (fLADs), whereas the regions always lying at the nuclear periphery are named constitutive LADs (cLADs) (Peric-Hupkes *et al.* 2010). We noted that the distribution of the $\text{Log}_2(\text{FoldChange (DaxxKO/WT)})$ for iLAD-genes presented a high dispersion in ground-state condition compared to serum-based and differentiated cells, which is due to the higher number of differentially transcribed genes in the hypomethylated condition (**Figure 30A**). The distribution of

Log₂(FoldChange (DaxxKO/WT)) for both cLAD and fLAD genes were centered to 0 in both differentiated cells and serum-based ESCs, indicating no preferential bias of transcriptional changes. Statistical difference between iLAD and fLAD in differentiated cells is mainly due to the transcriptional changes of fLAD genes upon differentiation.

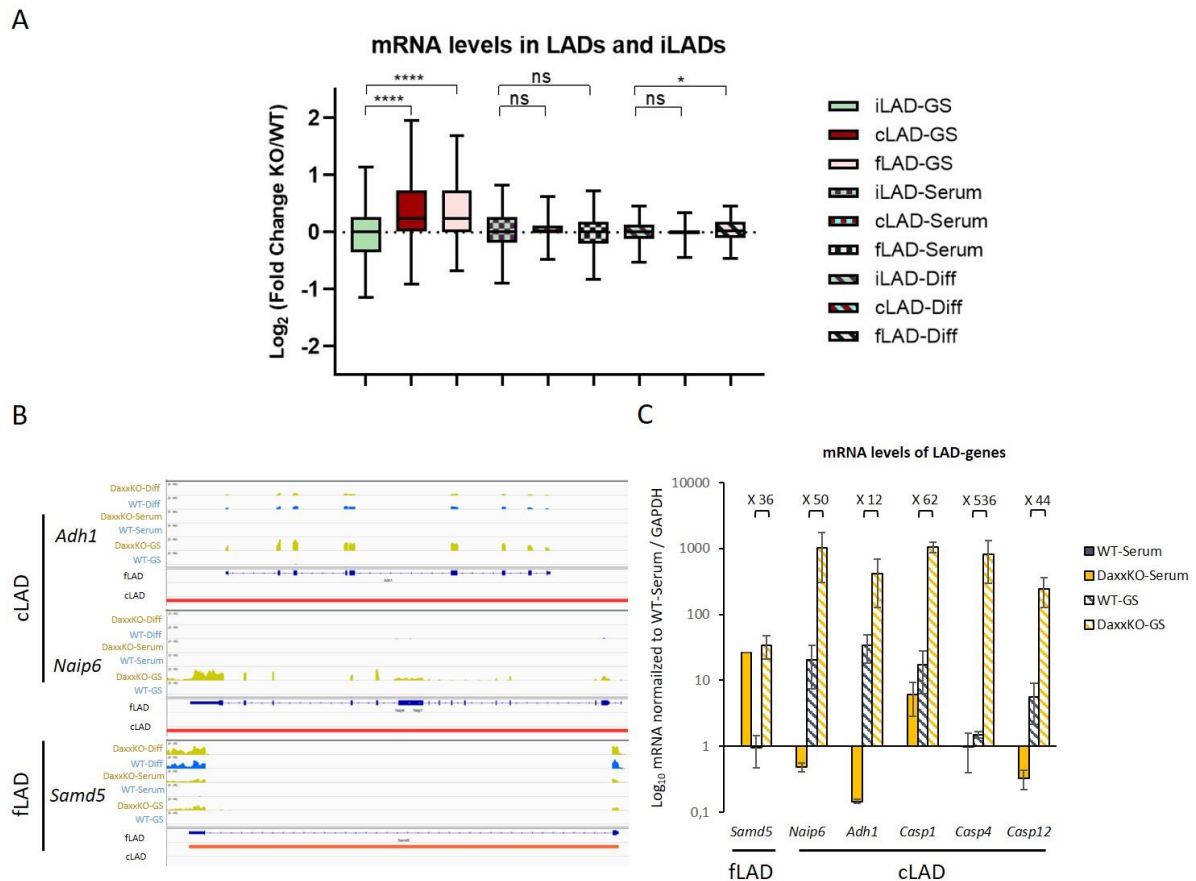


Figure 30 | Loss of Daxx impairs the silencing of genes within LADs. (A) Boxplot of mRNA levels of 904 genes belonging to cLAD, ESC fLAD or ESC iLAD in the different culture conditions. (B) IGV-window example of three genes displaying a strong up-regulation in the absence of Daxx specifically in ground-state. (C) RT-qPCR for 6 genes belonging to either fLAD or cLAD-categories, as indicated. Highlighted is the fold-increased of Daxx KO compared to WT in ground-state. Histogram represents the mean with SEM of three biological replicates. Two-sided unpaired t-tests were used for statistical analysis. GS = ground-state; Diff = Differentiated.

However, in the hypomethylated DNA condition, we observed a strong bias toward the up-regulation of LAD-genes, both constitutive and facultative (Figure 30A). We deeply investigated some of the LAD-genes displaying differential expression and choose 6 genes for which we designed specific qPCR primers (Figure 30B). We selected five genes belonging to the cLAD category (*Adh1*, *Naip6*, *Casp1*, *Casp4* and *Casp12*) and one from the fLAD category (*Samd5*), which is activated upon differentiation. We then confirmed the loss of silencing effect for these 6 LAD-genes by RT-qPCR in ground-state compared to serum conditions (Figure 30C). Intriguingly, we noted that 4 of the 5 constitutive LAD-genes were up-regulated in WT ground-state cells, compared to serum condition, suggesting some changes in peripheral heterochromatin

silencing upon ground-state conversion. We observed a strong upregulation of all the 6 genes from 12 to more than 500-fold. Our results indicate that the absence of Daxx results in the upregulation of LAD-genes upon hypomethylation of pluripotent cells. Interestingly, we noticed an alteration of the H3K9me2 profile (**Figure 29A**). However, these are only correlative data and the causal link between these two observations remains to be confirmed. Furthermore, additional experiments are required to see whether it correlates with delocalization of LAD-genes away from the nuclear lamina. Altogether, our data suggest that the absence of Daxx impairs chromocenter organization in pluripotent cells, whereas peripheral heterochromatin is only altered upon ground-state conversion, suggesting an additional mechanism at play when DNA methylation levels are low.

4. LINE1 elements upregulation contributes to the accumulation of DNA damages in the absence of Daxx

Upon ground-state condition Daxx-deficient ESCs displayed higher rate of γ H2AX foci at chromocenters, we thus decided to assess the total level of DNA damage signaling (**Figure 2D article**). We performed Western blot to quantify the amount of γ H2AX in WT and Daxx KO ESCs in serum or upon ground-state conversion. Remarkably, we detected a strong increase in γ H2AX levels upon ground-state conversion (**Figure 31A**). However, the total amount of γ H2AX in WT cells was similar between serum and ground-state conditions (**Figure 31A**). As the difference between WT and Daxx KO ESCs seemed greater in total γ H2AX signaling compared to the number of chromocenters displaying γ H2AX foci, we reasoned that DNA damage signaling might arise from additional sources.

We demonstrated that activation of major satellites could enhance DNA damage signaling at chromocenters (**Figure S3D article**). As the absence of Daxx resulted in the up-regulation of multiple families of DNA repeats, we asked whether it could be implicated in the increased DNA damage signaling we observed (**Figure 31A**). Among the up-regulated DNA repeats was the LINE1 Tf family, which was increased both in serum and ground-state conditions (**Figure 1C article**). We observed that the absence of Daxx impaired the silencing of LAD genes (**Figure 30A**). Because LINE1 are enriched in LADs, we quantified the number of elements present in constitutive or facultative LADs (Meuleman *et al.* 2013). The LINE1 Tf family (L1Md_T) was enriched in LADs with almost 48% of the elements present in total LADs (**Figure 31B**). As a euchromatic control, SINEB1 appeared largely absent from LADs with only 17% of elements. Loss of silencing of LINE1 elements have often been observed together with increased DNA damages, yet it remains mainly correlative (Belgnaoui *et al.* 2006). To assess whether the elevated

DNA damage signaling was indeed a consequence of heterochromatin derepression, we designed specific sgRNAs targeting the LINE1 Tf family, as this family is already strongly up-regulated in the serum condition. We transfected the cells with a dCas9 fused to the VPR trans-activator to induce the specific upregulation of LINE1 Tf. We detected an up-regulation of the same order of magnitude in the WT and the Daxx KO cells from 2- to 4-fold increase assessed via RT-qPCR (**Figure 31C**). We then assessed the levels of γ H2AX in these conditions by Western-blot and observed that while the dCas9 without a sgRNA did not present any signal, it was strongly increased in LINE1 upregulated conditions (**Figure 31D**). These results show that the up-regulation of DNA repeats, both pericentromeric or dispersed such as LINE1 contributes to γ H2AX signal accumulation. We observed that in ground-state condition active DNA demethylation at PCH could generate DNA damages and DAXX recruitment. Our data suggest that the observed accumulation of γ H2AX might results from the loss of silencing of heterochromatin. It yet remains to understand how the activation of LINE1 elements leads to DNA damages and it will be interesting to assess whether it is the transcription *per se* or the action of LINE1 ORF1 endonuclease.

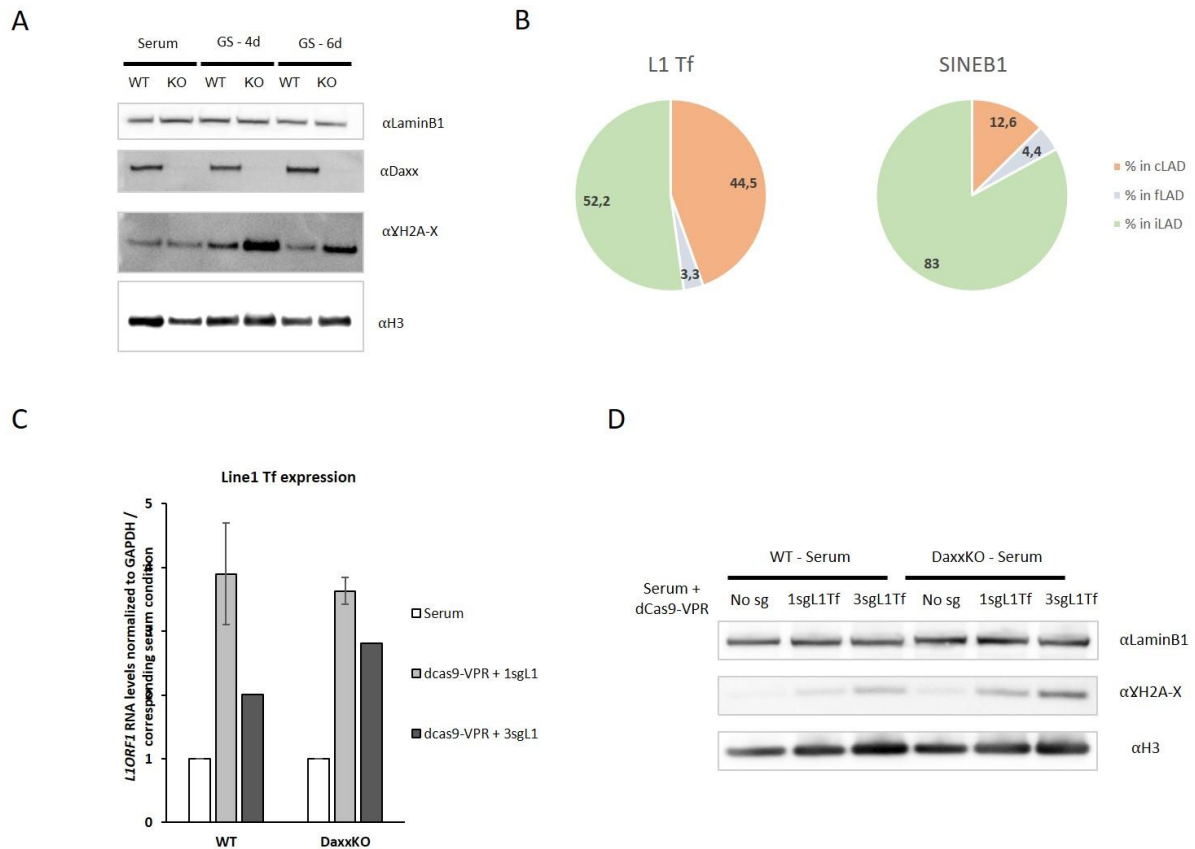


Figure 31 | LINE1 activation contributes to the accumulation of DNA damages in the absence of Daxx. (A) Western blot for γ H2AX signaling in serum and ground-state conditions for WT and Daxx KO ESCs. H3 and LaminB1 serve as loading controls. One experiment is shown, from two independent replicates. (B) Diagram showing the percentage of LINE1 Tf or SINEB1 elements found within cLAD, fLAD or iLAD. Computed from UCSC Repeat Masker data and LAD-status obtained from Peric-Hupkes *et al.*, *Mol. Cell* 2010. (C) Transcriptional activation of LINE1 Tf using a dCas9-VPR in WT or Daxx KO serum ESCs. Cells were either transfected without a LINE1 Tf-targeting sgRNA, with 1 sgRNA or 3 sgRNAs. Mean with SEM are represented. WT data from 2 biological replicates, Daxx KO data from 2 technical replicates (D) Western blot for γ H2AX or two loading controls Lamin B1 or H3 in the different transfections. One experiment is shown from two independent experiments.

Characterization of the role of PML in DAXX-mediated pericentromeric heterochromatin organization

1. PML is essential for pluripotent cell survival upon DNA hypomethylation

DAXX is commonly found at Pml NBs (Lallemand-Breitenbach and de Thé 2010). We confirmed that Daxx localized within Pml NB in serum-based ESCs (Figure 2A article). Upon hypomethylation we noted that Daxx accumulated at pericentromeric regions (Figure 2A article). Daxx signal was embedded within a ‘giant’ Pml NB. Because we observed that the specific targeting of Daxx to major satellite repeats was sufficient to induced Pml relocalization, we wanted to assess the role of Pml. We thus designed a guide RNA targeting the exon 1 of Pml and generated a Pml KO ES cell line (Figure 32A). We confirmed the absence of Pml protein via immunofluorescence

and Western blot of an individual clone that we used following experiments (**Figure 32A**). We have thus generated a Pml-deficient ES cell line.

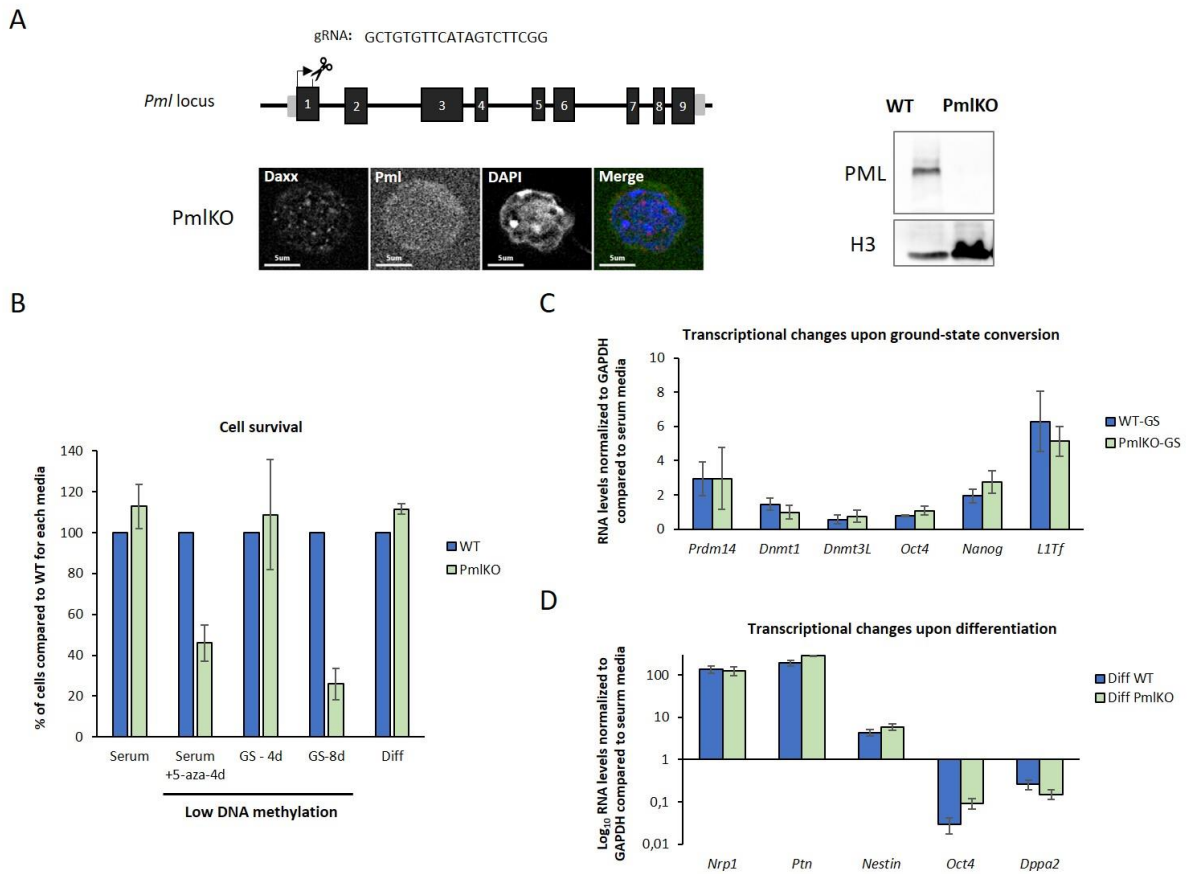


Figure 32 | Generation of Pml KO ESCs. (A) Scheme of the Pml locus located on chromosome . sgRNA was designed to target the exon 1 of the Pml gene. Immunofluorescence of DAXX and PML and Western blot of PML proteins in WT or the selected Pml KO clone. H3 serves as loading control. (B) Quantification of the number of cells compared to WT for each condition. Histogram represents the mean with SEM of 3 biological experiments, except Diff which corresponds to 2 biological replicates. (C) qRT-PCR performed for markers of ground-state conversion. Histogram represents mean with SEM of two biological replicates. (D) qRT-PCR performed for markers of differentiation. Histogram represents mean with SEM of two biological replicates. GS = ground-state; Diff = differentiated

The absence of Pml did not impact the cell survival in serum-based or differentiated cells (**Figure 32B**). However, the loss of Pml prevented cell survival in hypomethylated conditions. Indeed, upon 4 days of 5-azacytidine treatment or 8 days of ground-state conversion resulted in a strong reduction of the number of cells (**Figure 32B**). Thus, the absence of PML resulted in the same reduced cell survival upon DNA hypomethylation than the absence of Daxx (**Figure 1B article**). We confirmed that the impaired cell survival did not result from an alteration of the ground-state conversion and measured the transcription of specific ground-state markers (such as *Prdm14*, *Dnmt3L* and *Nanog*) and detected no difference in Pml KO cells (**Figure 32C**). We detected the same transcriptional up-regulation for DNA repeats such as *LINE1 Tf* (**Figure 32C**). We also confirmed that the absence of Pml did not alter transcriptional response from retinoic acid differentiation and observed the expected activation of *Nrp1*, *Ptn* and *Nestin* and the silencing of

Oct4 and *Dppa2* (**Figure 32D**). Our result points toward an essential role of PML in pluripotent cells upon the loss of DNA methylation.

2. DAXX accumulation at PCH is independent of PML

We observed the relocalization of both DAXX and PML to pericentromeric regions upon DNA hypomethylation and deletion of Pml or Daxx resulted in impaired cell survival in these conditions (**Figure 1B article, 2A article, 3B article, Figure 32B**). To assess the causal link between DAXX and PML, we converted the Pml KO ESCs into the ground-state condition. We demonstrated that the loss of Daxx prevented Pml accumulation at chromocenters (**Figure S5B article**). Moreover, while the loss of Daxx did not prevent the formation of PML NBs, the deletion of Pml dispersed DAXX signaling throughout the nucleoplasm, and only few small foci were detectable (**Figure 33A**). We noted that some of the DAXX signal localized at chromocenters in serum-based medium, although it remained quite rare. Interestingly, upon conversion into ground-

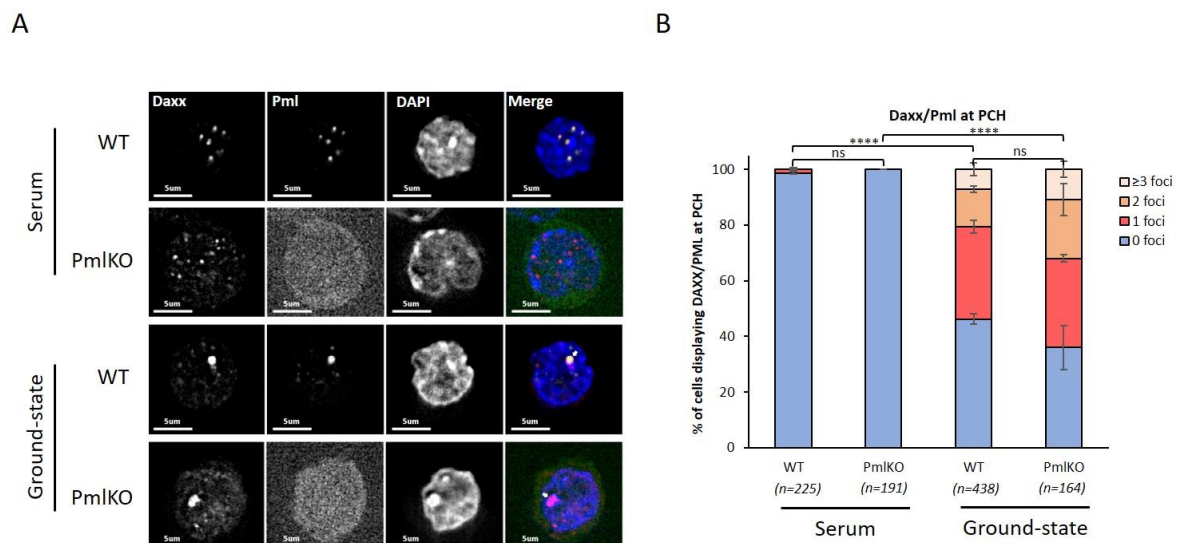


Figure 33 | DAXX accumulation at PCH is independent of PML. (A) Representative immunofluorescence pictures of DAXX and PML in WT and Pml KO ESCs in both serum or ground-state conditions. White arrow highlights DAXX-PML accumulation at PCH. (B) Histogram representing the number of DAXX-PML structures at PCH observed in the different conditions. Mean with SEM is represented. At least 2 biological replicates for each condition. n=total number of nuclei analyzed. Chi-square test were used for statistical analysis.

state, we noted that DAXX still strongly accumulated at PCH regions despite the absence of Pml, indicating that Pml does not recruit nor confine Daxx (**Figure 33A**). We quantified the number of DAXX-accumulation at PCH and observed from 1 to 3 DAXX structures were visible per nucleus, similar to the WT cells (**Figure 33B**). Our data indicate that DAXX is firstly recruited to PCH regions and then recruits PML and that loss of Pml does not impair DAXX accumulation.

3. PML contributes to organization and radial localization of PCH

Although we have shown that PML was recruited by DAXX, we detected the same loss of survival phenotype. DAXX localized within PML NBs and accumulated at chromocenters around DAXX (**Figure 2A article**). Because the absence of Daxx resulted in the alteration of heterochromatin organization in pluripotent cells, we decided to assess the heterochromatin organization in ESCs lacking Pml. We quantified the number of major satellite foci and observed, as for Daxx KO cells, that the number of foci was significantly increased in pluripotent cells (**Figure 34A, Figure 34B**). This effect was abolished upon differentiation of the cells. The increase in the number of major satellite clusters was correlated with a diminution in the sizes of each of these foci (**Figure 34B**). Thus, the loss of Pml in pluripotent cells impairs the clustering of pericentromeric regions, a phenotype that resemble to Daxx-deficient ESCs.

The absence of Pml disturbed the organization of pericentromeric heterochromatin. Because the Daxx KO ESCs displayed the same phenotype together with an altered radial positioning of the chromocenters, we decided to measure the peripheral signal of PCH in the absence of Pml. We observed that Pml KO ESCs displayed an altered radial localization of major satellites. Indeed, in both serum and ground-state conditions, the lack of Pml resulted in a more peripheral positioning of pericentromeric clusters (**Figure 34C**). Conversion toward ground-state induced a central relocalization of major satellites foci, although it remained more peripheral compared to WT ESCs (**Figure 34C**). Our results indicate that in addition to the altered organization of major satellites, the absence of Pml induces a peripheral localization of chromocenters.

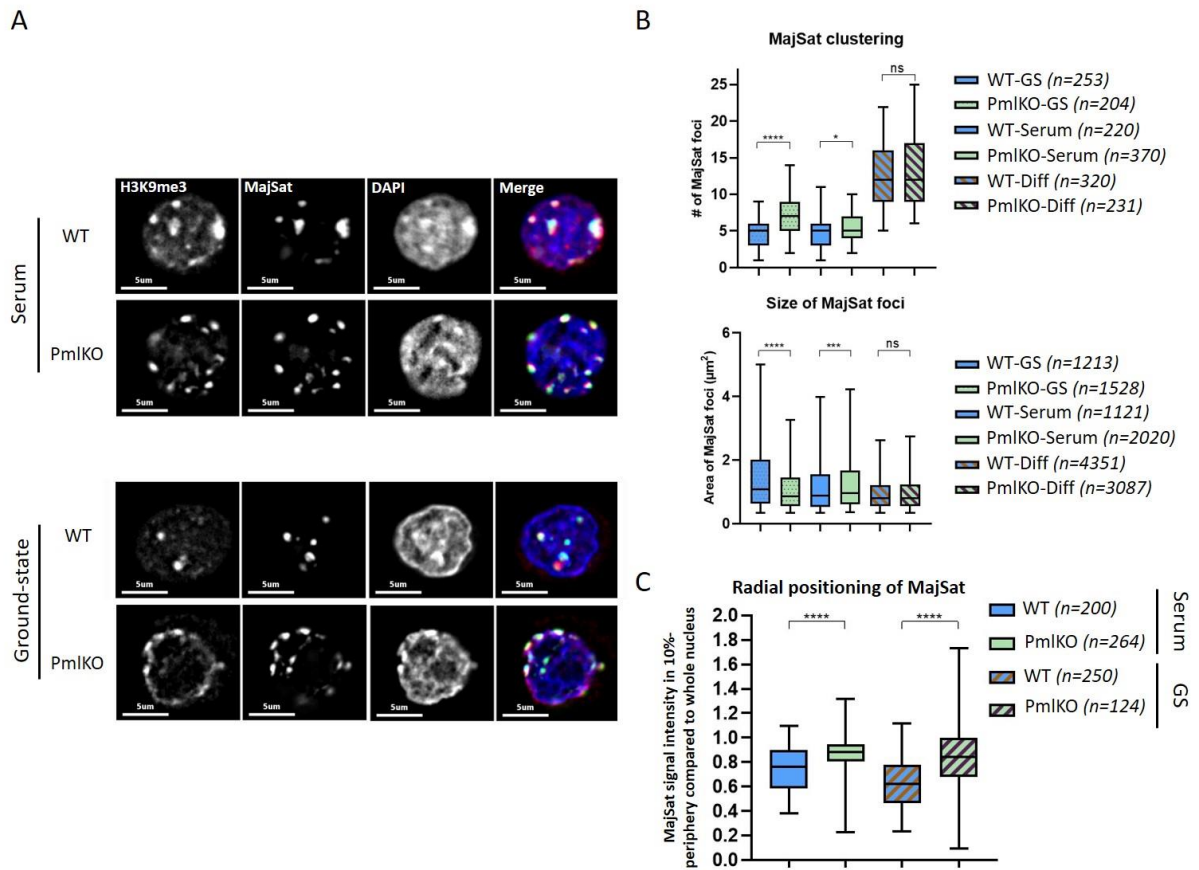


Figure 34| PML contributes to pericentromeric heterochromatin organization. (A) Representative immunofluorescence experiments of H3K9me3 histone modification and major satellite repeats of WT and Pml KO cells in serum-based or ground-state condition. **(B)** Quantification of PCH clustering. Top, number of major satellite foci detected in medium focal plane. Bottom, area of major satellite foci of focal medium plane. Boxplots represents three independent experiments. **(C)** Quantification of radial positioning of major satellite signal in serum or ground-state condition, using automatic threshold as previously described. Boxplot represents 10%-most peripheral compared whole-nucleus major satellite fluorescence intensities of three independent replicates. Two-sided Mann-Whitney tests were used for statistical analysis. GS = ground-state; Diff = Differentiation.

4. Loss of Pml induces alteration of peripheral heterochromatin and loss of LADs silencing upon ground-state conversion

Conversion of Daxx KO ESCs toward the ground-state of pluripotency resulted in defects in pericentromeric heterochromatin spatial organization (**Figure 4A article**). More major satellite clusters were observed, and their radial positioning was closer to the nuclear lamina than those in WT cells (**Figure 28E**). Furthermore, loss of Daxx also impaired the distribution of H3K9me2 histone modification (**Figure 29B**). Because the deletion of Pml resulted in the same disorganization of PCH and peripheral positioning, we reasoned that Pml KO cells might present the same H3K9me2 signal distribution upon ground-state conversion. We thus performed immunofluorescence and observed a peripheral ring of H3K9me2 in serum-grown Pml KO ESCs

(**Figure 35A**). However, upon 2i/VitC conversion, we observed that H3K9me2 signal appeared as patches at the periphery that resembled the signal from Daxx-deficient ESCs (**Figure 35A**). As previously reported, we assessed the fluorescence homogeneity signal. We noted that in Pml-deficient cells, the signal was strongly heterogeneously distributed compared to WT cells (**Figure 35B**). We confirmed the integrity of the nuclear lamina via immunofluorescence of LaminB (**Figure 35C**). Hence, the loss of Pml results in an impaired H3K9me2-signal distribution, which highly resemble to the phenotype observed for Daxx KO cells.

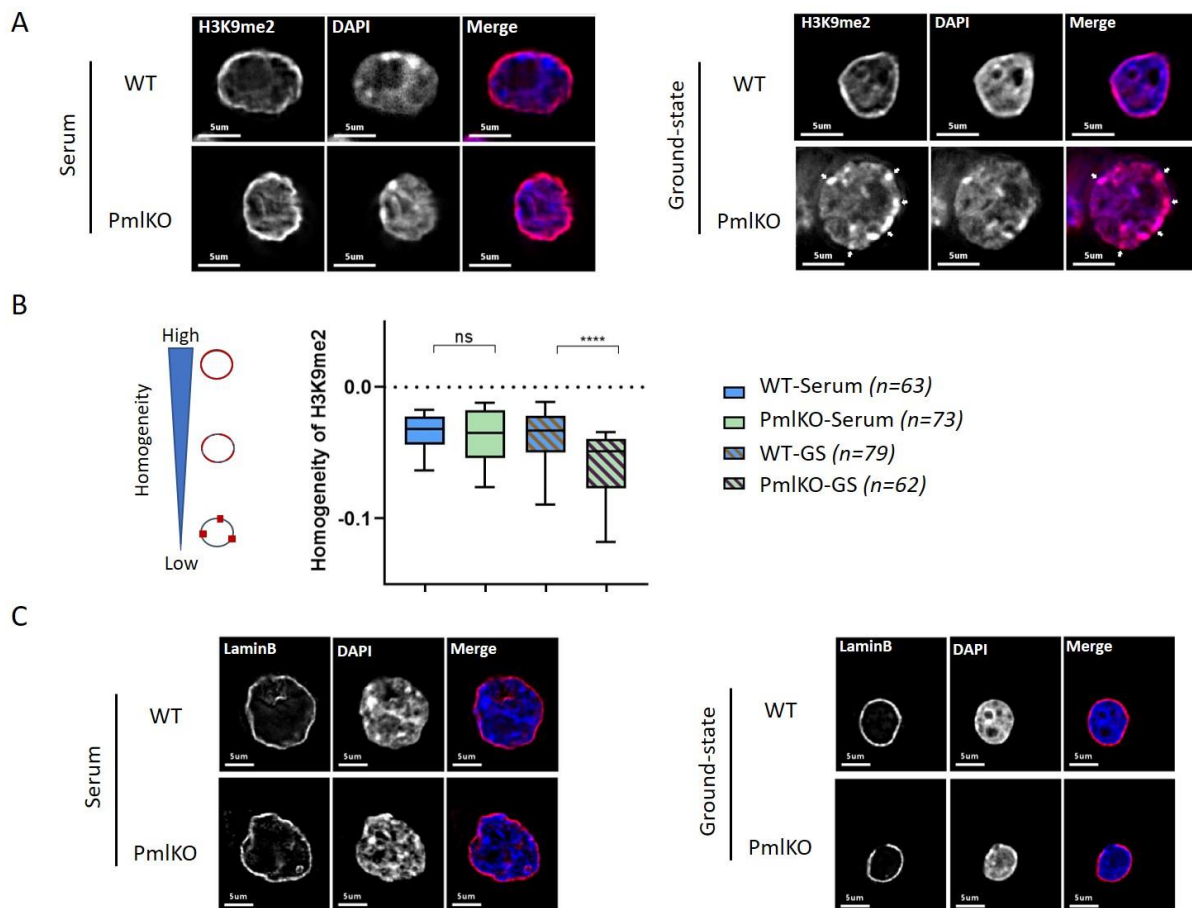


Figure 35 | Loss of Pml induces alteration of H3K9me2 peripheral signal upon ground-state conversion. (A) Representative immunofluorescence pictures of WT or Pml KO cells in serum or ground-state media. White arrows highlight patches of H3K9me2 only visible in Pml KO cells upon ground-state conversion. (B) Quantification of H3K9me2 heterogeneity. A line is traced at the periphery of the nucleus. A homogeneity score is calculated from signal of each pixel from the line representing the variation from the mean. Boxplot displays homogeneity scores measured from at least three biological replicates. n = total number of nuclei analyzed. (C) Representative pictures of LaminB immunofluorescence in WT or Pml KO cells in serum-based or ground-state conditions. GS = ground-state. Two-sided Mann-Whitney tests were used for statistical analysis.

The histone modification H3K9me2 is highly enriched in LADs (Kind *et al.* 2013). Because we observed that H3K9me2 signal appeared as patches at the periphery, a phenotype shared with Daxx KO ESCs, and that the absence of Daxx resulted in the upregulation of LAD-genes, we decided to assess the transcription of some genes specifically located within LADs. We performed qRT-PCR experiments onto ground-state and serum ESCs for six genes belonging to constitutive

(*Naip6*, *Adh1*, *Casp1*, *Casp4*, *Casp12*) or facultative (*Samd5*) LADs categories We observed a slight transcriptional increase for five of the six investigated genes (**Figure 36**). While the loss of Daxx led to strong upregulation of 12 to 500-fold, the absence of Pml resulted in a moderate increase of 2 to 21-fold. Our results indicate that the absence of Pml results in the same tendency of transcriptional up-regulation of LAD-genes upon hypomethylation of pluripotent cells than Daxx-deficient ESCs.

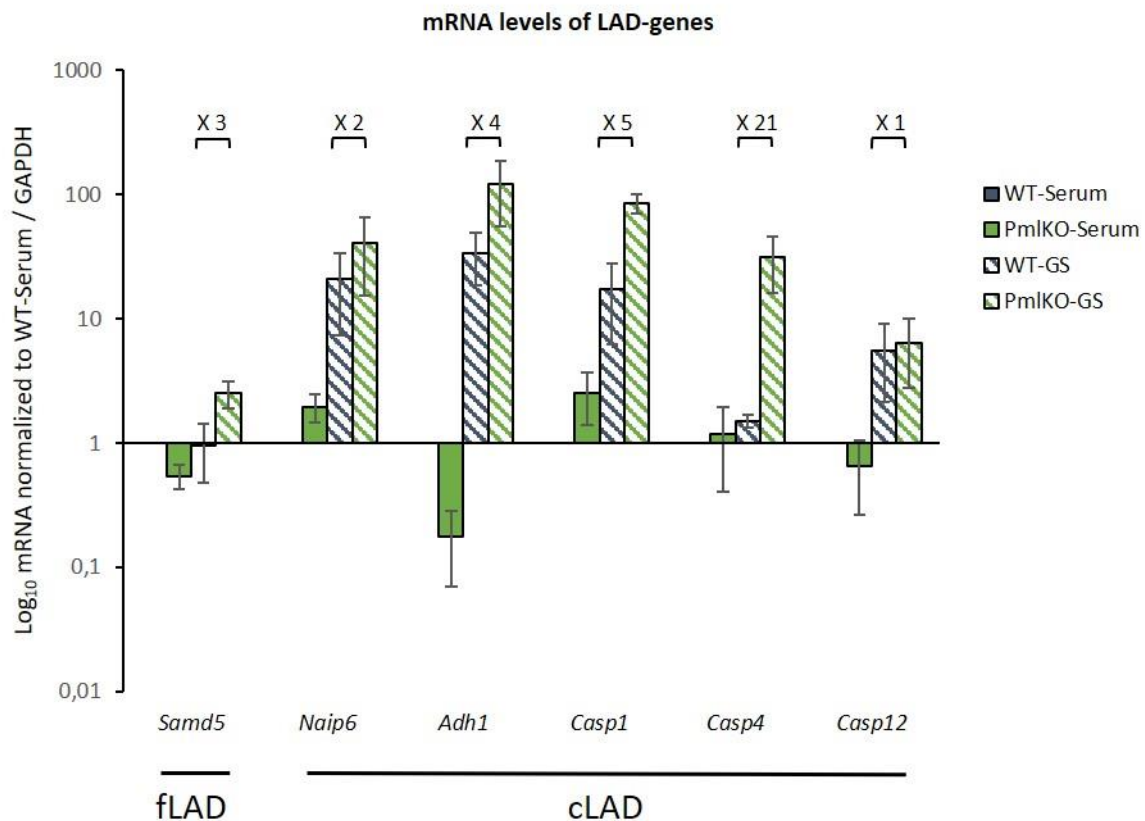


Figure 36 | Absence of Pml induces the loss of LAD-genes upon ground-state conversion. Messenger RNA levels of one fLAD and 5 cLAD-genes in WT or Pml KO in serum or upon ground-state conversion. Histogram represents mean expression with SEM from two biological replicates. Highlighted are the up-regulation measured from Pml KO compared to WT in ground-state. GS = ground-state.

Characterization of DAXX domains necessary for PCH clustering

1. DAXX-mediated PCH clustering is independent of ATRX interaction

We showed that Daxx was necessary for pericentromeric heterochromatin organization in pluripotent cells (**Figure 4A article**). Targeted recruitment of DAXX to major satellites resulted in a strong clustering of PCH regions (**Figure 4D article**). Clustering of PCH depended onto the

binding of H3.3 (**Figure 5D article**). We decided to further characterize PCH-clustering properties of DAXX and investigate which domains of DAXX were necessary.

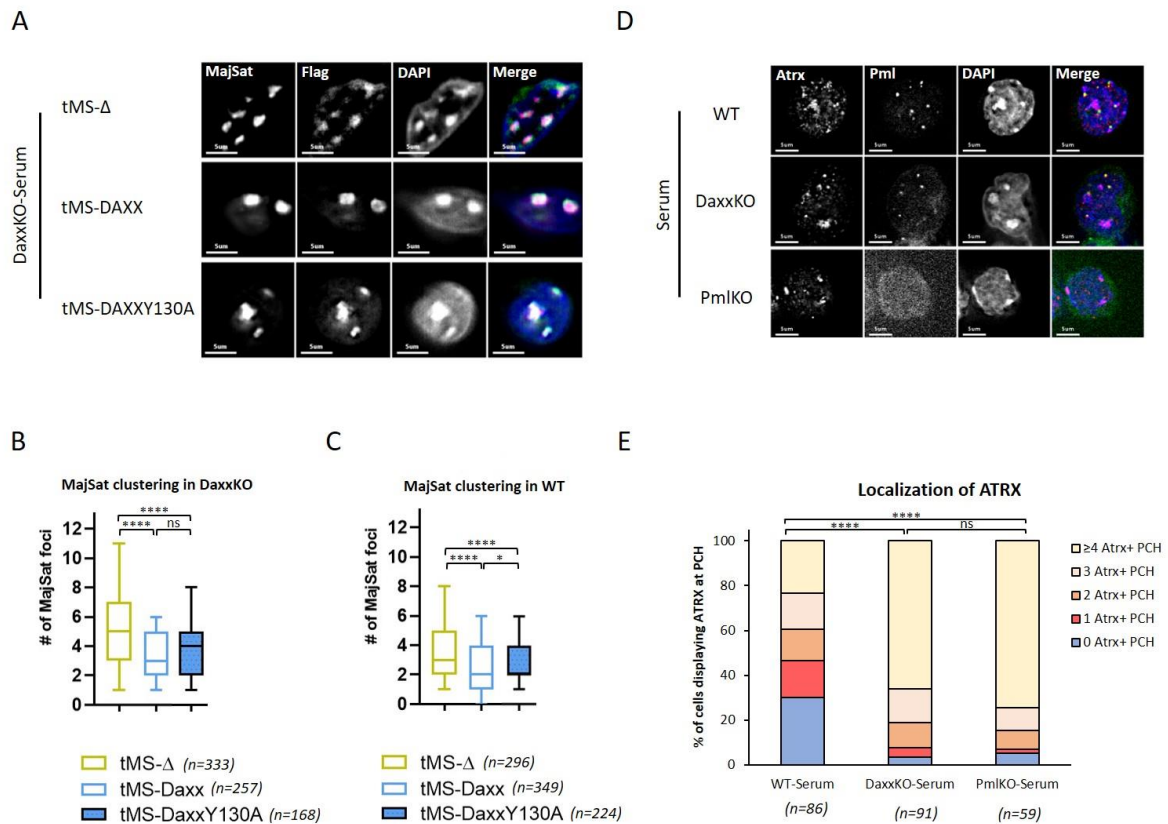


Figure 37 | DAXX-mediated PCH clustering is independent of ATRX interaction. (A) Representative immunofluorescence pictures for Tale-Flag and major satellite repeats in Daxx KO-transfected cells. (B) Quantification of the number of major satellite foci measured in Daxx KO-transfected cells. Boxplot represents data from 3 biological replicates, except for DAXX9KR which is 2 biological replicates. n=total number of nuclei analyzed. (C) Quantification of the number of major satellite foci measured in WT transfected cells. Boxplot represents data from 3 biological replicates, except for DAXXΔSIM which is 2 biological replicates. n=total number of nuclei analyzed. (D) Representative immunofluorescence pictures of ATRX and PML in WT, Daxx or Pml KO ESCs in serum-based condition. (E) Quantification of the number of DAPI-dense chromocenters displaying ATRX signal. Histogram represents one of two independent experiments. Two-sided Mann-Whitney tests were used for statistical analysis in B and C. Chi-square tests were used for statistical analysis in E.

A major partner of DAXX is ATRX. ATRX belongs to the SWI-SNF chromatin remodeler family and is thus able to bind to DNA. ATRX has been shown to be important for H3.3 deposition at telomeres in mESCs (Goldberg *et al.* 2010). Interestingly, ATRX is commonly observed at chromocenters in different cell types, including mESCs (Wong *et al.* 2010; McDowell *et al.* 1999). DAXX-binding to ATRX can be abrogated by a mutation in its Atrx-binding domain at the N-terminal (Hoelper *et al.* 2017). We constructed a Daxx mutated onto the tyrosine 130 (Y130A). We targeted DAXX to major satellites using a Tale-fusion protein as previously described and we performed immunofluorescence to quantify the number of major satellite foci (**Figure 37A**). Intriguingly, the recruitment of DaxxY130A was sufficient to induce a major satellite clustering in Daxx KO ESCs in serum (**Figure 37B**). Targeted recruitment of DAXXY130A was also sufficient

to mediate PCH clustering in WT ESCs (**Figure 37C**). These results are in good agreement with the report that ATRX was implicated chromocenter clustering, yet only in differentiated cells and not in ESCs (Marano *et al.* 2019). Our results indicate that the direct interaction between DAXX and ATRX is not required for DAXX-mediated major satellite clustering.

However, as ATRX was reported to bind to PCH regions, we decided to assess whether the loss of either DAXX or PML would prevent this localization. We thus performed immunofluorescence experiments of ATRX in our cells (**Figure 37D**). In WT cells, ATRX localizes at some or all DAPI-dense chromocenters in 70% of the cells (**Figure 37E**). In WT cells, ATRX often localizes also at PML NBs. Interestingly, the deletion of either *Daxx* or *Pml* results in the same phenotype with more cells displaying ATRX binding at PCH (**Figure 37E**). The absence of *Daxx* did not prevent ATRX localization within PML NBs in our cells, contrarily to previous observations (Delbarre *et al.* 2013). These experiments indicate that the ATRX-recruitment toward PCH is independent of DAXX and PML. We observed that ATRX binding-deficient DAXX was able to induce PCH clustering, however, it remains to assess whether the total absence of *Atrx* is dispensable for DAXX-mediated clustering (**Figure 37B, Figure 37C**).

2. Post-translational regulation of DAXX

We observed that deletion of either *Daxx* or *Pml* resulted in similar phenotypes with alterations of pericentromeric heterochromatin organization (**Figure 4A article, Figure 34B**). Moreover, we demonstrated that specific recruitment of DAXX toward major satellites could drive a strong clustering of chromocenters (**Figure 4D article**). DAXX-mediated PCH clustering is independent of ATRX binding. Interestingly, DAXX localizes within PML NBs and possesses sites of post-translational modifications, we thus decided to further investigate the domains of DAXX necessary for proper pericentromeric clustering in relation with PML. *Daxx* notably possesses two SUMO-interacting motif (SIM) at the N- and C-termini. SIMs are domains that can bind to SUMOylated proteins and can thus participate in protein-protein interactions. It was observed that only the C-terminal SIM was required for recruitment to PML NBs (Escobar-Cabrera *et al.* 2011; Sahin *et al.* 2014; Lin *et al.* 2006). We constructed a DAXX mutant deficient for the C-terminal SIM. We recruited the Tale-MajorSatellite-DAXX Δ SIM and evaluated its clustering capacity by DNA FISH (**Figure 38A**). We noted that the loss of its C-terminal SIM motif did not impair major satellite clustering in both WT and *Daxx* KO ESCs (**Figure 38B, Figure 38C**). However, we noticed that the clustering phenotype was more pronounced in WT cells compared to *Daxx*-deficient cells for which the DAXX Δ SIM-mediated clustering was statistically different from

DAXX clustering, suggesting that the effect in WT cells might be enhanced by the recruitment of endogenous DAXX. Our results suggest that the SIM motif, hence interaction with SUMOylated proteins is not essential for Daxx-mediated clustering, though it may favor this process.

Furthermore, not only DAXX can bind to SUMOylated partners, but it can also be SUMOylated itself onto its lysines. We then constructed a Tale-DAXX mutant for which we replaced the 9 most SUMOylated lysines with arginine (Lin *et al.* 2006). Recruitment of DAXX9KR did not induce the clustering of major satellites in neither the Daxx KO nor the WT cells (**Figure 38D, Figure 38E**). These data indicate that post-translational modifications of DAXX seem important for its ability to mediate PCH-clustering.

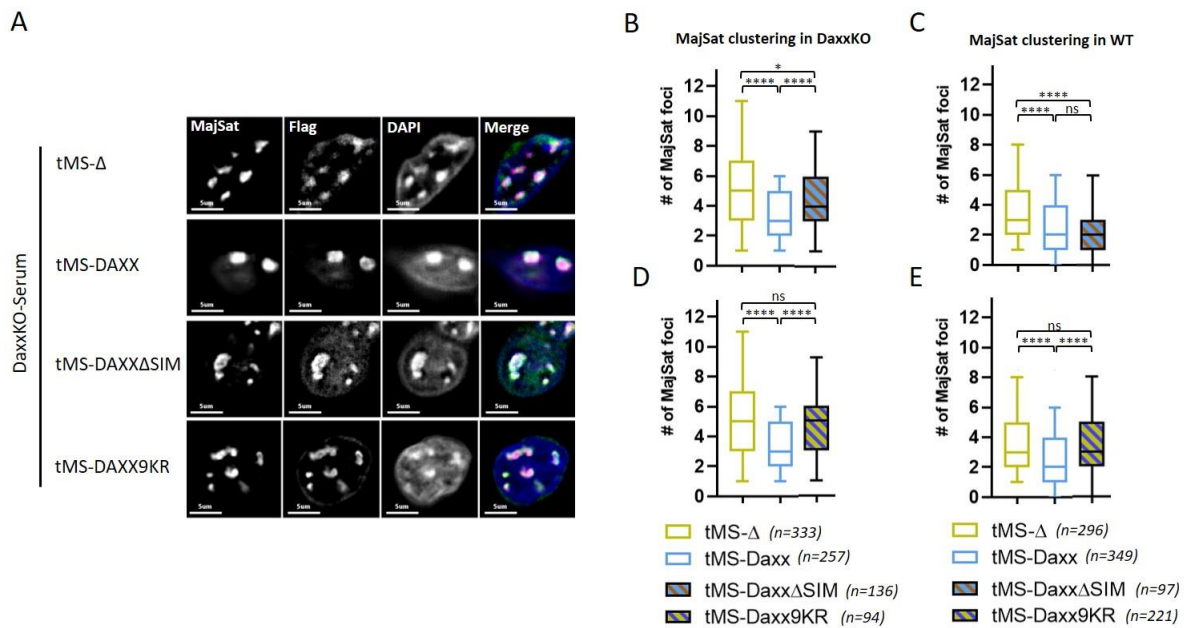


Figure 38 | SUMOylation but not SIM domain of DAXX seem implicated in PCH clustering. (A) Representative immunofluorescence pictures of major satellites and Flag signal in serum Daxx KO ESCs transfected with the indicated Tale constructs. (B, D) Quantification of the number of major satellite foci detected on medium focal plane in Daxx KO ESCs transfected with the indicated Tale constructs. (C, E) Quantification of the number of major satellite foci detected on medium focal plane in Daxx KO ESCs transfected with the indicated Tale constructs. n=total number of nuclei analyzed from 3 biological replicates, except for DAXX9KR which corresponds to 2 biological replicates. Two-sided Mann-Whitney tests were used for statistical analysis.

We next wondered whether our Tale-DAXX constructs were active and could recruit PML or H3.3. We thus performed immunofluorescence assays for PML and H3.3 in the Tale-DAXX, DAXXY222A and DAXXΔSIM conditions (**Figure 39A**). In the Tale-Δ condition, we noted that the H3.3 signal was dispersed throughout the nucleoplasm, with only some small foci sometime visible. Overall, the H3.3 signal was mostly absent from DAPI-rich chromocenters (**Figure 39A**). In the Tale-DAXX condition, H3.3 was strongly recruited to virtually all DAPI-rich PCH, whereas the Tale-DAXXY222A, which cannot bind H3.3, did not recruit H3.3 to PCH as expected (**Figure 39B**). The Tale-Δ did not alter PML localization which only appeared as small and round nuclear bodies (**Figure 39A**). We observed that Daxx recruited PML which formed like ‘giant’ shells

around major satellite foci, similar to what is visible upon ground-state conversion (**Figure 39A**, **Figure 2A article**). However, the number of ‘giant’ PML NBs at PCH was seen in most of the cells (~80%), but not at all PCH with 3 or more PCH foci in ~40% of the cells (**Figure 38B**). Intriguingly, the recruitment of DAXXY222A did not recruit PML, suggesting that the DAXX-H3.3 interaction might be important for the DAXX-PML interaction (**Figure 39A**). The Tale-DAXX Δ SIM that should not bind PML did not recruit PML, however, it still recruited H3.3, which correlates with the clustering phenotype observed with this construct (**Figure 38E**, **Figure 39B**, **Figure 39C**). We thus conclude DAXX tethering to major satellite is sufficient to recruit PML and to induce a visible accumulation of H3.3 and that only H3.3 recruitment correlates with DAXX-mediated clustering, strengthening the role of H3.3 in heterochromatin organization.

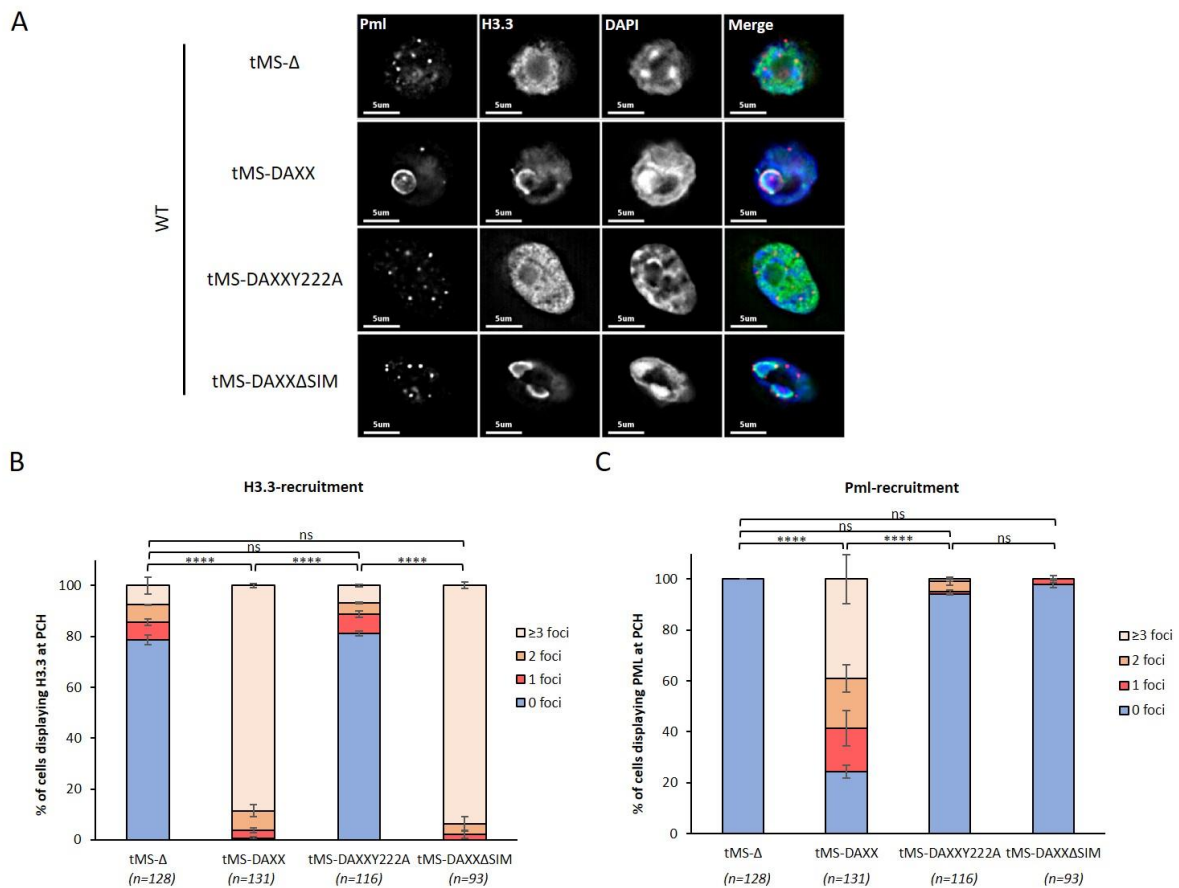


Figure 39 | Recruitment of H3.3 and PML upon DAXX targeting to PCH. (A) Representative immunofluorescence pictures of PML and H3.3 in WT-transfected cells. (B) Quantification of H3.3-recruitment from the different Tale-DAXX constructs. Histogram displays mean with SEM from 2 biological replicates. n=total number of nuclei analyzed. (C) Quantification of PML-recruitment from the different Tale-DAXX constructs. Histogram displays mean with SEM from 2 biological replicates. n=total number of nuclei analyzed. Chi-square tests were used for statistical analysis.

Supplementary data

List of primers used for RT-qPCR	
Name	Sequence
exp-Gm5662-F	GCACAGCCTCCTTACACCAT
exp-Gm5662-R	AAAAACAGGCGCAGAGGTAA
exp-Spz1-F	CTGCAGGAAGCAGATCACTG
exp-Spz1-R	GCTTCTGCTTGGTGGATAGC
exp-Zscan4-F	GAGATTCATGGAGAGTCTGACTGATGAGTG
exp-Zscan4-R	GCTGTTGTTTCAAAGCTTGATGACTTC
exp-MERVL-F	CTCTACCACTTGGACCATATGAC
exp-MERVL-R	GAGGCTCCAAACAGCATCTCTA
exp-Samd5-F	CTGAGCAAACCCCATACTC
exp-Samd5-R	ATACGCCCTTTCCAGTCTT
exp-Naip6-F	CGACATCTTGGACGATGAAA
exp-Naip6-R	GTTGTCCAGGGCTTGAAAGA
exp-Adh1-F	TGTGGCTGACTTCATGGCTA
exp-Adh1-R	AAGTCAGGACGGTACGGATG
exp-Casp1-F	CGTCTTGCCCTCATTATCTGC
exp-Casp1-r	CACCATCTCCAGAGCTGTGA
exp-Casp4-F	TCTCACTGAGGTATGGGGCT
exp-Casp4-R	GTCTGGTGTCTGAGAGTGCA
exp-Cas12-F	CGAACACGTCTGGCTCTCAT
exp-Cas12-R	TGTCTCCATTTCTGAGCTGT
exp-L1Orf1-F	AGAGAACAACAACACTGCAGCC
exp-L1Orf1-R	GCGTTGTTCCCGTTCTTGTA
exp-Prdm14-F	GTTTCCGTGTTCTCTCTGCC
exp-Prdm14-R	GCTTGTTCCAGGCTGGAAGAC
exp-Dnmt1-F	CGGGTCTACTGCAGTTCCAT
exp-Dnmt1-R	GGTACAGGGTCTCGTTCACA
exp-Dnmt3L-F	GCGGCCCTTCTTCTGGATAT
exp-Dnmt3L-R	TAGTCTCTGCCACGGACATC
exp-Oct4-F	CGAGAACAATGAGAACCCTTC
exp-Oct4-R	CCTTCTTAGCCCAAGCTGAT
exp-Nanog-F	AAAGGATGAAGTGCAAGCGG
exp-Nanog-R	CTTCCAGATGCGTTCACCAG
exp-L1Tf-F	CAGCGGTCCGCATCTTG
exp-L1Tf-R	CACCCTCTCACCTGTTCCAGACTAA
exp-Nrp1-F	GGCCGATTCAGGACCATAC
exp-Nrp1-R	ATAGACCACAGGGCTCACCA
exp-Ptn-F	CGAGTGCAAACAGACCATGA
exp-Ptn-R	GGCGGTATTGAGGTCACATT
exp-Nestin-F	GAACTCTCGCTTGCAGACAC
exp-Nestin-R	AGAAGGATGTTGGGCTGAGG
exp-Dppa2-F	CTGCAATTTCTTGCTGGACA
exp-Dppa2-R	TTTTTCTTTGCACGGCTTCT
exp-GAPDH-F	GACCCTTTTGGCTCCACCCTTC

exp-GAPDH-R	ATCACCATCTCCAGGAGCGAG
Oligo used for CRISPR/Cas9 inactivation	
Name	Sequence
sg-mPml	gGGCTGTGTTCATAGTCTTC

Figure 28		
C) Peripheral localization of MajSat signal		
Mann-Whitney	pval.	
WT fcs vs GS	0.0014	WT FCS n=200
WT fcs vs GS 10d	0.0008	WT GS4d n=250
		WT GS10d n=67
E) Radial localization of MajSat signal		
WT fcs vs daxx fcs	<0.0001	WT GS n=250
WT GS vs daxx GS	<0.0001	DaxxKO GS n=180
Figure 29		
B) H3K9me2-signal		
Mann-Whitney	pval.	
WT-Daxx serum	0,8885	WT FCS n=63
WT-daxx GS	0,0006	DaxxKO FCS n=62
		WT GS n=79
		DaxxKO GS n=70
Figure 30		
A) Log2mRNA		
Unpaired t-test, two-tailed	pval.	
iLADsvscLADs-GS	<0.0001	n = 904genes
iLADsvsflADs-GS	<0.0001	n = 904genes
iLADsvscLADs-FCS	0,302	n = 904genes
iLADsvsflADs-FCS	0,3611	n = 904genes
iLADsvscLADs-Diff	0,852	n = 904genes
iLADsvsflADs-Diff	0,0135	n = 904genes
Figure 33		
B) Daxx at PCH		
Chi-square	pval.	
WTvsPmlKO-Serum	0,7215182	WT FCS n=225
WTvsPmlKO-GS	0,06925245	PmlKO FCS n=191
WT-SerumvsGS	8,1674E-24	WT GS n=438
PmlKO-SerumvsGS	2,5516E-38	PmlKO GS n=164
Figure 34		
B) Clustering of MajSat		
Mann-Whitney	pval.	
WT gs vs pml gs	<0.0001	WT GS n=253
WT fcs vs pml fcs	0.0276	PmlKO GS n=204
WT diff vs pml diff	0.4622	WT FCS n=220
		PmlKO FCS n=370

		WT Diff n=320
		PmlKO Diff n=231
B) Area of MajSat foci		
Mann-Whitney	pval.	
WT gs vs pml gs	<0.0001	WT GS n=1213
WT fcs vs pml fcs	0.0008	PmlKO GS n=1528
WT diff vs pml diff	0.5780	WT FCS n=1121
		PmlKO FCS n=2020
		WT Diff n=4351
		PmlKO Diff n=3087
C) Radial positioning of MajSat		
Mann-Whitney	pval.	
WT fcs vs pml fcs	<0.0001	WT FCS n=200
WT GS vs pml GS	<0.0001	DaxxKO FCS n=212
Figure 35		
B) H3K9me2-signal		
Mann-Whitney	pval.	
WT-pml serum	0,8756	WT FCS n=63
WT-pml GS	<0.0001	PmlKO FCS n=73
		WT GS n=79
		PmlKO GS n=62
Figure 37		
B) MajSat clustering in DaxxKO		
Mann-Whitney	pval.	
tMS-Δ vs Daxx	<0,0001	tMS-Δ n=333
tMS-Δ vs DaxxY130A	<0,0001	tMSDaxx n=257
tMS-Daxx vs DaxxY130A	0,0991	tMSDaxx Y130A n=168
C) MajSat clustering in WT		
Mann-Whitney	pval.	
tMS-Δ vs Daxx	<0,0001	tMS-Δ n=296
tMS-Δ vs DaxxY130A	<0,0001	tMSDaxx n=349
tMS-Daxx vs DaxxY130A	0,0264	tMSDaxx Y130A n=224
E) Localization of ATRX		
Chi-square	pval.	
WT vs DaxxKO	1,5867E-59	WT FCS n=
WT vs PmlKO	4,732E-62	DaxxKO FCS n=
DaxxKO vs PmlKO	0,05283488	PmlKO FCS n=
Figure 38		
B & D) MajSat clustering in DaxxKO		
tMS-Δ vs DaxxΔSIM	0,019	tMS-Δ n=333
tMS-Δ vs Daxx9KR	0,5556	tMSDaxx n=257
tMS-Daxx vs DaxxΔSIM	<0,0001	tMSDaxxΔSIM n=136
tMS-Daxx vs Daxx9KR	<0,0001	tMSDaxx9KR n=94
tMS-DaxxΔSIM vs Daxx9KR	0,1704	
C & E) MajSat clustering in WT		
		tMS-Δ n=296
tMS-Δ vs DaxxΔSIM	<0,0001	tMSDaxx n=349

tMS-Δ vs Daxx9KR	0,1143	tMSDaxxΔSIM n=97
tMS-Daxx vs DaxxΔSIM	0,6818	tMSDaxx9KR n=211
tMS-Daxx vs Daxx9KR	<0,0001	
tMS-DaxxΔSIM vs Daxx9KR	0,0018	
Figure 39		
B) Tale-recruitment of H3.3		
Chi-square	pval.	
tMS-Δ vs daxx	1,122E-207	tMS-Δ n=128
tMSDaxx vs DaxxY222A	6,452E-225	tMSDaxx n=131
tMS-Δ vs DaxxY22A	0,73729913	tMSDaxxY222A n=116
tMS-Δ vs DaxxΔSIM	1,971E-233	tMSDaxxΔSIM n=93
tMSDaxx vs DaxxΔSIM	0,39864899	
tMSDaxxY222A vs DaxxΔSIM	9,749E-252	
C) Tale-recruitment of H3.3		
Chi-square	pval.	
tMS-Δ vs daxx	2,88E-67	tMS-Δ n=128
tMSDaxx vs DaxxY222A	4,4013E-57	tMSDaxx n=131
tMS-Δ vs DaxxY22A	0,09394364	tMSDaxxY222A n=116
tMS-Δ vs DaxxΔSIM	0,9977674	tMSDaxxΔSIM n=93
tMSDaxx vs DaxxΔSIM	1,0176E-63	
tMSDaxxY222A vs DaxxΔSIM	0,09258242	

CONCLUSIONS

CONCLUSIONS

In this work, I have studied the role of the H3.3-chaperone DAXX on heterochromatin maintenance in murine embryonic stem cells. The main conclusions from the article are the following (**Figure 40**):

- DAXX is essential for cell survival upon DNA hypomethylated conditions;
- DAXX contributes to the silencing of different heterochromatin regions such as dispersed DNA repeats and pericentromeric satellites;
- Active DNA demethylation of major satellites can generate DNA damage signaling and lead to DAXX accumulation at chromocenters, yet DNA damage signaling alone does not trigger DAXX recruitment;
- At PCH, DAXX recruits SETDB1 in a H3.3-dependent manner and induces H3.3K9 trimethylation;
- DAXX regulates spatial and molecular organization of chromocenters in pluripotent cells.

I deeply investigated the functions of DAXX in the second part of the results and observed that (**Figure 40**):

- DAXX contributes to the maintenance of chromatin state identity and its loss induces a 2C-like transcriptional signature upon ground-state conversion;
- DAXX controls chromocenters radial positioning;
- DAXX contributes to the proper distribution of H3K9me2-peripheral mark and the silencing of genes present within lamina associated domains;
- Loss of Pml results in phenotypes highly similar to the loss of Daxx, suggesting that PML might act as a regulator of DAXX.

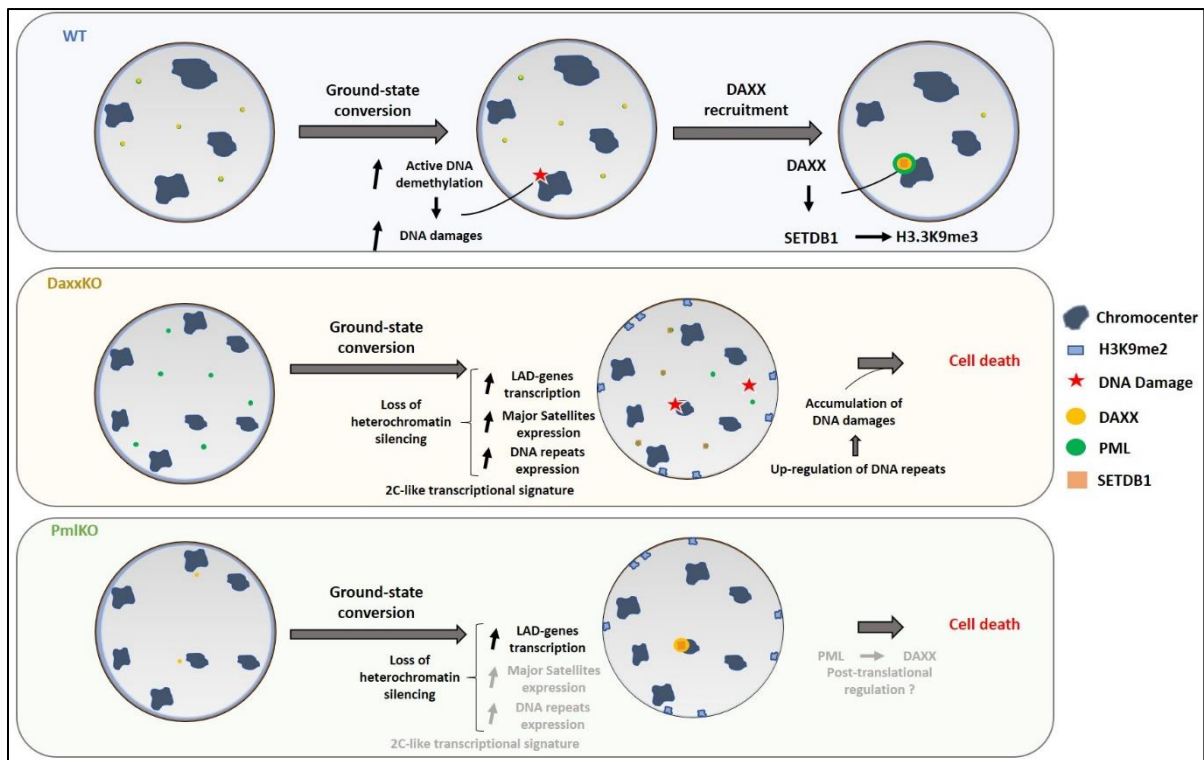


Figure 40 | Model displaying the function of DAXX at pericentromeric heterochromatin and the consequences of its loss. Upon ground-state conversion, active DNA demethylation induced by the TET enzymes can lead to DNA damages at chromocenters. DNA damage response proteins act at the site of the lesion. DAXX accumulates at a limited number of chromocenters and is surrounded by a PML shell. DAXX can then recruit the lysine methyl-transferase SETDB1 to induce H3.3K9 tri-methylation and reform the heterochromatin state. In the absence of Daxx, pericentromeric heterochromatin organization is altered and more chromocenters are visible and major satellites are transcriptionally up-regulated. Upon ground-state conversion, DaxxKO ESCs present a strong increase in DNA repeats expression. Furthermore, genes localized within lamina associated domains are de-repressed and H3K9me2 ring pattern at the nuclear periphery is altered. Many genes are mis-regulated in ground-state condition and a 2C-like transcriptional signature is observed. Finally, prolonged culture in DNA hypomethylated conditions lead to cell death in the absence of Daxx. Depletion of Pml results in phenotypes highly similar to the loss of Daxx such as impaired organization of chromocenters. Ground-state conversion of PmlKO resemble DaxxKO ESCs as an alteration of the H3K9me2 peripheral ring is visible and the concomitant loss of silencing of genes present in LADs. Prolonged culture in DNA hypomethylated conditions results in cell death as well.

DISCUSSION

DISCUSSION

1. DAXX is essential for prolonged culture upon DNA hypomethylation and maintains chromatin identity of pluripotent cells.

We observe that prolonged culture in hypomethylated ESCs requires DAXX (**Figure 1B article**). Our transcriptomic experiments suggest that the loss of Daxx induces an interferon (IFN) response and apoptosis (**Figure S1D article**). It is possible that the IFN response ultimately leads to cell death via induction of apoptosis pathways. It remains to understand the exact molecular events responsible for the observed cell death in Daxx KO ESCs. We demonstrate that the action of DAXX at heterochromatin is to recruit the lysine methyl-transferase SETDB1. Remarkably, SETDB1 has been implicated in repression of LINE and ERV elements in AML (acute myeloid leukemia) cell lines and depletion of Setdb1 resulted in the activation of the IFN pathway (Cuellar *et al.* 2017). Additionally, the loss of Setdb1 in ground-state conditions resulted in the activation of the RIPK3 necroptosis pathways (Wu *et al.* 2020). Henceforth, it would be of interest to look at RIPK3 activation, such as phosphorylation of downstream effectors like RIP1, in the Daxx KO mESCs upon ground-state conversion. In addition, we observe that the loss of Daxx increases the level of DNA damage signaling, as well as P53-transcriptional pathway upon ground-state conversion (**Figure S1D article, Figure 31A**). DNA damage can induce P53-related apoptosis (Roos and Kaina 2006). It would be interesting to assess the function of P53 pathway in cell death in Daxx KO cells.

We observe that in ground-state condition, the loss of Daxx induces transcriptional changes that resemble to the 2C-like ESCs, suggesting that DAXX represses the 2C-like program (**Figure 27B, Figure 27C**). To confirm the role of DAXX in maintaining pluripotent heterochromatin state, it would be relevant to assess the exact conversion rate toward 2C-like state using an MERVL-GFP reporter, as previously published, and at different time of the conversion. Many factors were reported to enhance the conversion of pluripotent ESCs toward totipotent 2C-like ESCs. Such factors include the PRC1 complex, the EP400-TIP60 complex which is implicated in histone modifications and EP400 has been proposed to be an alternative H3.3 chaperone for regulatory region depositions, the methyl-transferase SETDB1 and the E3 SUMO ligase UBC9 (Rodriguez-Terrones *et al.* 2018; Wu *et al.* 2020; Cossec *et al.* 2018; Pradhan *et al.* 2015). These factors are implicated in chromatin regulation, highlighting that chromatin is a crucial feature of cell type identity. Interestingly, Daxx was reported in a 2C-like repressor siRNA screen, which is in good agreement with our RNA-seq results, and points toward a function for DAXX as a regulator of

chromatin state identity (Rodriguez-Terrones *et al.* 2018). Interestingly, DAXX and H3.3 interact with PRC1 and SETDB1 in different contexts (**Figure 5C article, S5D article**) (Liu *et al.* 2020). These results suggest that there might be unidentified functions of H3.3 in regulating the cellular identity of ESCs and that histone variants might contribute to preventing conversion of pluripotent cells toward a more naïve totipotent state during development.

Intriguingly, the E3 SUMO-ligase UBC9 was implicated in the maintenance of pluripotent chromatin state, but also in the maintenance of somatic chromatin states (Cossec *et al.* 2018). It is remarkable that similar mechanisms can be employed by both pluripotent and somatic stem cells. In that direction, it would be interesting to assess the role of DAXX in the reprogramming of induced pluripotent stem cells.

2. Mechanism of DAXX-PML recruitment at PCH upon loss of DNA methylation.

In murine embryonic stem cells, like in most cell types, DAXX localizes within PML NBs which are normally devoid of chromatin. We here show that upon DNA hypomethylated conditions, DAXX is recruited to major satellite repeats and appears as large foci at some chromocenters (**Figure 2A article, 3B article**). Interestingly, it has previously been reported that DAXX could bind to pericentromeric regions during DNA hypomethylated conditions (Baumann *et al.* 2010; Liu *et al.* 2020; Arakawa *et al.* 2015). During the early development, the paternal nucleus displays lower levels of 5mC and correspondingly higher levels of 5hmC. At this stage of development, DAXX is recruited to pericentromeric regions of the paternal nucleus via different proteins. Indeed, the depletion of either Dppa3, Atrx or PRC1 prevented proper localization of DAXX (Baumann *et al.* 2010; Liu *et al.* 2020; Arakawa *et al.* 2015). It would be interesting to assess whether the same proteins are at play in pluripotent cells. Upon the loss of DNA methylation, in both ESCs and the first stages of development, polycomb proteins are recruited to pericentromeric heterochromatin, presumably to protect the heterochromatin state. Polycomb and subsequent H3K27me3 signals are not observed at PCH in basal conditions because of steric hindrance with H3K9me3-modification. PRC1 is recruited to PCH in Dnmt tKO in a BEND3-dependent manner, and then recruits PRC2 to induce H3K27me3-modification in mESCs (Saksouk *et al.* 2014; Cooper *et al.* 2014). Yet, these relocalizations of BEND3, PRCs and H3K27me3 appear at all chromocenters, suggesting a general heterochromatin pathway. Intriguingly, in our conditions, we only detected DAXX at 1 to 3 chromocenters, suggesting that its recruitment might rely on additional signaling than the H3K27me3-based mechanisms. To formally rule this out, it would be interesting to knock-down Bend3, PRC1 factors such as Ring1B and PRC2 factors such as Eed or

Ezh2 in ground-state ESCs to assess if it impedes DAXX-PML relocalizations. We noted that the DAXX-ATRAX interaction did not seem essential for the DAXX-mediated clustering of major satellites (**Figure 37B**). However, because ATRAX is still present at PCH, even in the absence of Daxx, it remains possible that other proteins implicated in PCH clustering might be recruited via ATRAX (**Figure 37E**). As ATRAX is essential in mESCs, it would require a knock-down, or a conditional knock-out strategy to interrogate its role in DAXX-mediated clustering and DAXX recruitment upon hypomethylation.

We detect a strong relocalization of DAXX toward PCH regions upon DNA hypomethylation (**Figure 2A article, 3B article**). However, unmethylated DNA does not necessarily induce DAXX recruitment at PCH. Indeed, in Dnmt tKO ESCs, ChIP-seq experiments reported the increased binding of DAXX at dispersed repeated DNA elements such as ERVs, but not at PCH, suggesting an additional layer of control (He *et al.* 2015). We notice that DAXX recruitment at major satellites could arise from DNA damages, as observed from HU and CRISPR/Cas9 inducible DSBs (**Figure 2E article**). Intriguingly, we notice that upon ground-state conversion or exogenously-induced DNA damages, only 1 to 3 chromocenters displayed DAXX accumulation (**Figure 2C article, 2E article**). Accumulation of DAXX at PCH highly resemble to what is observed in the human ICF syndrome, where only 3 chromosomes present DAXX recruitment toward pericentromeric satellites (Luciani *et al.* 2006). It raises the possibility that DAXX binding might happen at specific chromosomes upon DNA demethylation. Yet, mouse chromosomes, unlike human counterparts, possess highly similar pericentromeric satellites. It would be informative to perform immunoFISH experiments using probes targeting specifically each chromosomes and count whether DAXX accumulation occurs at different rates for every chromosome. The other possibility is that because we are looking in fixed cells, we might only observe a transient binding of DAXX. Investigating the recruitment along time would require the use of live-cell imaging using both a fluorescent marker for chromocenters and for DAXX and see if the assembly-disassembly of DAXX structures can happen at multiple occasions during a single interphase.

We note that SETDB1 is recruited by DAXX at PCH (**Figure 5A article**). Silencing of ERVs in mESCs mostly rely onto the action of KRAB-Zinc finger (ZF) proteins, KAP1, SETDB1 and DAXX (Rowe *et al.* 2010; Wolf *et al.* 2015; Matsui *et al.* 2010; He *et al.* 2015). The DNA binding activity of these proteins is mediated by the zinc finger domains of the KRAB-ZF proteins. Remarkably, murine chromocenters are not only composed of major satellites. In fact, although the majority of the genomic DNA recovered from chromocenters are major satellites, ~30% belongs to LINE1 and ERV families (Ostromyshenskii *et al.* 2018). It would thus be interesting to

test if the reported LTRs from Ostromyshenskii *et al.* also localizes at chromocenters in mESCs and if they carry a role in DAXX-recruitment. In that direction, one could generate Tale-DAXX constructs targeting PCH-LTR sequences and assess if there is a major satellite clustering as well. Moreover, the targeting of Tale-TET1CD toward pericentromeric ERVs could lead to increased DNA damages at chromocenters and DAXX recruitment. Among the proteins acting at ERVs is the repressor KAP1 and physical interaction between DAXX and KAP1 was observed in mESCs (Elsässer *et al.* 2015). However, KAP1 recruitment at PCH is frequent at multiple PCH, even in the absence of DAXX (**data not shown**). It would still be interesting to use some KRAB-ZF-deficient ESCs and to knock-down KAP1, because it is essential in ESCs, to see if it abolishes the accumulation of DAXX at PCH (Walter *et al.* 2016). If this hypothesis is correct, it would then represent a potential new function for ERVs in global genome organization and will require assessing the role of PCH-ERVs and KRAB-ZF in the formation of chromocenters in the early embryo.

We hypothesize that *in vitro* conversion of ESCs and the embryonic development are quite different in term of chromatin modifications. Indeed, while serum-based ESCs display fairly high levels of DNA methylation, the conversion toward ground-state conditions generates a strong active DNA demethylation. Active DNA demethylation occurs at the paternal nucleus during the very early steps of development, while the maternal genome is mostly passively demethylated (Lee *et al.* 2014; Messerschmidt *et al.* 2014). Nevertheless, a second wave of active DNA demethylation takes place during the development of primordial germ cells (PGCs) at ~E9.5 in order to completely reset all epigenetic information (Hackett *et al.* 2013b). Furthermore, deamination of 5mC is implicated in the DNA demethylation process in PGCs (Popp *et al.* 2010). It would thus be interesting to study the role of DAXX in PGCs formation and search for the appearance of DAXX structures at PCH. Overall, it remains to bear in mind that the early embryonic development takes only about 5 days before the implantation and a strong gain in DNA methylation levels. However, ESCs in culture correspond to a somehow artificial environment where the active DNA demethylation takes place for days.

3. DAXX and SETDB1 participate in re-establishment of heterochromatin state following active DNA demethylation-induced DNA damages.

Upon TET1 targeting to chromocenters, using a Tale strategy, we notice that the decrease of 5mC levels at these locations correlates with an increase in γ H2AX foci, demonstrating that active DNA demethylation can induce DNA damages (**Figure S3A article, 3D article**).

Furthermore, recruitment of TET1 at PCH induces DAXX accumulation (**Figure 3E article**). It is in agreement with previously published data that observed a correlation between DNA demethylation and DNA damages (Nakatani *et al.* 2015). Nevertheless, γ H2AX is a broad DNA damage signaling factor and it remains to understand what types of DNA lesions arise from TET1-mediated active DNA demethylation. It has been demonstrated that TET activity hydroxylates 5mC into 5hmC, which can then be removed via the action of TDG and the BER pathway (Cortellino *et al.* 2011; Santos *et al.* 2013). We notice that the number of γ H2AX foci occurring at PCH was increased upon ground-state conversion (**Figure 2D article**). However, to better characterize the active DNA demethylation takes places at PCH, it would be informative to quantify the levels of 5mC and 5hmC in serum-based ESCs and upon ground-state conversion. TDG and BER induce the removal of the 5hmC base, which generates abasic sites (AP-sites). As BER is important for the DNA demethylation process, it would be interesting to evaluate the role of BER proteins such as TDG, XRCC1 or LIG3 onto the accumulation of DAXX at PCH, which would indicate whether AP-sites are driving DAXX recruitment.

Upon TET1CD targeting to major satellites, we detect a homogenous reduction of 5mC signal at chromocenters, while γ H2AX foci appear as discrete dots, suggesting that the visible γ H2AX foci might mark DSB sites (**Figure S3A article, 3D article**). The observation that broad DNA demethylation results in local DNA damage signaling argues against DDR being a mere consequence of BER. Active DNA demethylation can ultimately results in DSBs, although the coordinated action of TET, TDG and BER proteins usually avoid the formation of DSBs (Weber *et al.* 2016). However, since we target genomic regions that are tandemly repeated over Mbs-long distances, it could result in an important number of AP-sites, which can lead to DSBs if unresolved (Kidane *et al.* 2014). Studying the mechanisms of DSB repair at chromocenters, Tsoroula *et al.* observed that somatic NIH3T3 murine cells relocate DSBs to the periphery of chromocenters to perform HR only in G2-phase, whereas in G1-phase, DSBs remain within heterochromatin foci and undergo non-homologous end joining (NHEJ) (Tsouroula *et al.* 2016). Upon ground-state conversion, we observe the presence of discrete γ H2AX foci at chromocenters, which agrees with possible rare DSBs occurring at DNA hypomethylated major satellites (**Figure 2D**). Furthermore, exogenous induction of DSBs via HU-treatment or CRISPR/Cas9 targeting major satellites results in the accumulation of DAXX, indicating that DSBs alone can lead to DAXX recruitment (**Figure 2F**). The accumulation of DAXX, after DSBs or ground-state conversion, often appear at the periphery of chromocenters, which is also compatible with the model proposed by Tsoroula *et al.* (**Figure 2A**). Confirming that active DNA demethylation at PCH could be responsible for DAXX relocalization would require to use the Tale-TET1CD in Dnmt tKO ESCs, which should not lead

to DNA damage signaling. Furthermore, it would be interesting to knock-down TET enzymes in ground-state ESCs and look for the disappearance of DAXX foci. Remarkably, the knock-down of TET enzymes could also rescue the survival of Daxx-deficient cells upon ground-state conversion. Symmetrically, the knock-down of DNMT enzymes or the over-expression of TET enzymes in serum-based medium could increase the number of DAXX foci at PCH.

Intriguingly, the targeted recruitment of NBS1 induce an increase in the number of γ H2AX foci at chromocenters, but does not lead to DAXX accumulation, suggesting that DAXX is not acting within the DDR but rather at later steps during heterochromatin reformation (**Figure 2G article**). Indeed, following DNA lesions, the epigenetic mark of the locus is lost and must be re-established at the end of the DNA repair process (Soria *et al.* 2012). We notice that γ H2AX signaling was only visible in 50% of the DAXX structures at PCH, which agrees with a late DNA repair step when γ H2AX is removed from the chromatin (**Figure S2D article**). We observe the same pattern using CRISPR/Cas9- or TET1-demethylation-induced PCH DNA damages, with γ H2AX foci visible within chromocenters but DAXX mostly localized at the periphery of the DAPI-rich signal (**Figure 2F article, S2C article, 3D article, 3E article**). To confirm that DAXX structures contain chromatin undergoing late DNA repair steps, it would be interesting to perform immunofluorescence of proteins involved at different times of the repair, using inducible DNA damages systems. H3.3-deposition has been implicated in replication fork progression after DNA damages, possibly indicating that DAXX-mediated H3.3 deposition might be important upon ground-state condition to overcome DNA lesions (Frey *et al.* 2014). It has also been reported that Daxx down-regulation prevented H3.3 relocalization at sites of UV lesions and impaired homologous recombination, in good agreement with our observations that loss of Daxx increases DNA damages (Juhász *et al.* 2018). Of particular interest, DAXX and PML are important regulators of SUMOylation, and notably in ESCs (**S. Tessier, V. Lallemand-Breitenbach, submitted article**). Intriguingly, BER proteins necessary upon active DNA demethylation are regulated by SUMOylation. Indeed, SUMOylation of XRCC1 facilitates its interaction with TDG and promotes the assembly of BER complexes at DNA lesions (Steinacher *et al.* 2018). In the same line, it would be interesting to evaluate the impact of DNA damage response-proteins on the recruitment of DAXX in WT cells grown in hypomethylated conditions. Indeed, if DAXX is recruited at late DNA repair stages, it could be interesting to prevent proper DNA repair by knocking-down specific steps such as resection (i.e. SAE2 or EXO1) and see if it abrogates the formation of DAXX structures at PCH and impact cell survival upon ground-state conditions. Finally, to assess the importance of post-repair heterochromatin reformation, it would be informative to measure the

ability of Daxx-deficient cells to perform the different types of DNA repair, which was shown to be dependent on the nuclear positioning (Lemaître *et al.* 2014).

Active DNA demethylation generates AP-sites and can ultimately results in DSBs. However, the observed DNA damages at PCH could arise from indirect sources. Indeed, we observe that HU treatment resulted in DAXX accumulation at PCH (**Figure 2F**). Interestingly, HU generates replication fork collapses and it thus remains to assess if DNA replication stalks are more frequent upon DNA hypomethylation. It is possible that DNA replication fork collapses are more frequent upon active DNA demethylation as it will generates AP-sites which could slow the replication fork, notably at pericentromeric heterochromatin regions, which are highly methylated. Moreover, in the absence of Daxx, pericentromeric satellites are up-regulated, which might increase the level of R-loops (**Figure 1C article**). R-loops formation is increased upon transcription-replication conflicts and can generate DNA breaks, demonstrating that defects in heterochromatin silencing possibly contributes to genome stability (Hamperl *et al.* 2017). Interestingly, in the *C. elegans* worm, it has been observed that the SETDB1 homolog and the BRCA1 homolog are implicated in the silencing of satellite repeats (Padeken *et al.* 2019). Deletion of the SETDB1 homolog induces a loss of satellite repression that ultimately results in DNA damage-mediated recruitment of BRCA1 homolog. Deletion of both SETDB1 and BRCA1 homologs result in enhanced levels of R-loops. It would thus be interesting to gauge the level of R-loops in Daxx-deficient cells and assess whether RNaseH treatment, that specifically degrades DNA-bound RNAs, could both prevent DAXX recruitment at pericentromeric satellites and cell survival of Daxx KO ESCs upon ground-state conversion. Importantly, the specific transcriptional activation of major satellites using a Tale strategy induced γ H2AX foci at PCH, suggesting that strong up-regulation of satellites is sufficient to generate DNA damages (**Figure S3C article**). However, because major satellite transcription decreases upon ground-state conversion, while DNA damages at chromocenters are increased, it seems that DNA damages at PCH can arise from non-transcriptional defects (**Figure 2D article, S1B article**).

We observe a strong recruitment of DAXX at PCH upon DNA hypomethylation (**Figure 2A article, 3B article**). DAXX recruitment at PCH was observed during the first stages of early embryonic development (Arakawa *et al.* 2015; Liu *et al.* 2020). However, the function of DAXX at this stage is primarily thought to deposit H3.3 to participate into the decompaction of heterochromatin regions thus allowing the transcriptional burst of major satellites (Liu *et al.* 2020). Production of major satellite RNAs is necessary for further development of the embryo (Casanova *et al.* 2013). Furthermore, this is in agreement with the reported role for H3.3-specific lysine 27 residue (Santenard *et al.* 2010). Mutation of the lysine 27 of H3.3 impaired localization of H3.3 and

prevented development toward the blastocyst stage. Developmental defects of H3.3K27R could only be overcome with the addition of major satellite dsRNAs. Deletion of zygotic Daxx results in defects to reach the blastocyst stage, with decreased viability from the 4-cell stage, while maternal Daxx is dispensable for proper development, suggesting an additional role for DAXX apart from the transcriptional activation of pericentromeric repeats at the pluripotent stage (Liu *et al.* 2020). Because the loss of Setdb1 also results in early embryonic lethality, before the blastocyst stage, we propose that novel role of DAXX might act through SETDB1. It would be of great interest to assess the *in vivo* relevance of the DAXX-SETDB1—H3.3-H3K9me₃ pathway we uncovered in pluripotent cells.

We observe that DAXX recruits SETDB1 at PCH to perform H3K9 tri-methylation (**Figure 5D article**). Furthermore, we note that the absence of Daxx impairs heterochromatin organization and silencing (**Figure 1C article, 4A article**). We thus propose that DAXX, via SETDB1 and H3.3, participate in the reformation of heterochromatin after DNA damages. As SETDB1-mediated tri-methylation seems important, it suggests that the broken chromatin has lost its H3K9me₃-previous modification. Intriguingly, it was reported that the action of KDM enzymes are essential for the DNA repair pathway choice and repair completion in both *Drosophila* and mammalian cells (Young *et al.* 2013; Janssen *et al.* 2019; Colmenares *et al.* 2017). It would be interesting to assess in mESCs whether the demethylation of H3K9 also takes place prior or during to the DNA repair, and further dissect if preventing the H3K9 demethylation could impact the formation of DAXX structures. Preliminary experiments reveal that KDM4A targeting to chromocenters does not lead to DAXX recruitments, suggesting that loss of H3K9me₃ is not a sufficient information *per se* (**data not shown**). However, it remains to assess KDM functions in the DNA damage response. In the same direction, the Suv39H1/2 dKO mice are viable, but not Setdb1 nor Daxx-deficient mice, suggesting that indeed the role of DAXX is more linked to SETDB1 than to SUV39H1/2 enzymes (Peters *et al.* 2001; Dodge *et al.* 2004; Michaelson *et al.* 1999; Liu *et al.* 2020). Interestingly, H3.3K9R-expressing embryos, that still express endogenous H3.3, can develop to the blastocyst stage, however, it is still unknown whether arginine methylation can arise (Santenard *et al.* 2010).

4. DAXX maintains pericentromeric heterochromatin organization.

In the third part of this discussion, we proposed a model whereby DAXX can accumulate at chromocenters upon DNA damages and then recruit SETDB1 to reform heterochromatin state after DNA repair took place (**Figure 2A article, 2F article, 5A article**). However, we observe that DAXX maintains pericentromeric heterochromatin spatial and molecular organization in both

serum and ground-state conditions (**Figure 4A article, 4B article, 4C article**). These data indicate that we might be observing two distinct mechanisms - the maintenance of chromocenter organization on one hand and the restoration of heterochromatin state following DNA damages on the other hand. Nevertheless, the role of DAXX in serum or ground-state conditions might be similar at PCH, but only visible by immunofluorescence upon ground-state conversion. Indeed, some γ H2AX foci are already visible at chromocenters in serum condition. Thus, it is conceivable that some DNA damages could happen at chromocenters, probably as rare events. In that direction, DAXX can be visible at PCH in serum only after high levels of DNA damages, suggesting that in serum takes place a DNA methylation-related mechanism to avoid such levels of DNA damage or chromatin reformation (**Fig. 2E article**). It remains possible that DAXX and SETDB1 could bind to chromocenters in serum-based medium but in a transient, such as DNA damages, or local, such as pericentromeric ERVs, manners preventing their observation by immunofluorescence. Deeper exploration is required to decipher whether the same triggering mechanisms exist in serum condition such as DAXX and SETDB1 ChIP-seq and live-cell imaging experiments. Depletion of Daxx does not prevent H3K9me3 at chromocenters, likely deposited by SUV39H1/2 (**Figure 28A**). Intriguingly, deletion of only the Suv39H1/2 enzymes does not prevent PCH clustering, but the triple Suv39H1/2 and Setdb1 does, suggesting that SETDB1 and perhaps DAXX carry a function at PCH even in DNA methylated conditions (Peters *et al.* 2001; Pinheiro *et al.* 2012). Moreover, deletion of the H3K9me1 methyl-transferases Prdm3 and Prdm16 in MEFs resulted in altered major satellite clustering, likely via impairment toward further methylation to di or tri-methylated states (Pinheiro *et al.* 2012). Further investigating the role of SETDB1 in PCH organization will give a better understanding of the mechanism at play. Moreover, deletion of the Suv4-20H1/2 enzymes that catalyzes H4K20me3 histone modification results in defects in chromocenter clustering in ESCs and impaired recruitment of cohesins at pericentromeric regions, which enhanced chromosome segregation defects (Hahn *et al.* 2013). It would thus be interesting to assess the levels of other heterochromatin-associated histone modifications in serum-based and ground-state Daxx-deficient ESCs to dissect whether it could explain the observed loss of chromocenter clustering.

We demonstrate that the ability of DAXX to mediate chromocenter clustering depends onto the histone variant H3.3 (**Figure 5D article**). Indeed, recruitment of DAXXY222A that cannot bind H3.3 or the knock-down of H3.3 genes prevents DAXX-mediated PCH clustering (**Figure 5C article, 5E article**). To further characterize the role of DAXX and H3.3 in chromocenter organization, it would be informative to complement Daxx-deficient ESCs with WT DAXX or DAXXY222A and assess major satellites clustering. We demonstrate that DAXX could

recruit SETDB1 to induce H3K9 tri-methylation (**Figure 5C article**). Furthermore, the recruitment of DAXX in ESCs expressing H3.3K9A was not able to induce PCH clustering (**Figure 5D article**). Intriguingly, the recruitment of SUV39H1 does not lead to PCH clustering (**Figure 5C article**) Preliminary data suggests that the targeted recruitment of SETDB1 does not drive PCH clustering neither yet performing H3K9me3 activity (**data not shown**). Since DAXX can recruit H3.3, whereas SUV39H1 and SETDB1 were not reported to be able to bind H3.3, we propose that SETDB1 might tri-methylates DAXX-deposited H3.3K9 and that this specific modification controls PCH clustering. Altogether, we propose a general model where this function of DAXX is strongly visible upon ground-state conversion with important accumulation of DAXX at chromocenters following DNA damages induced by active DNA demethylation. However, the same heterochromatin maintenance might happen in serum condition, but as a more local event. Silencing of ERV requires DAXX-mediated H3.3 (Elsässer *et al.* 2015). In serum condition, there might be DAXX-mediated H3.3 deposition at PCH-specific ERVs. DAXX could then recruit SETDB1 to induce H3.3K9me3 like in ground-state, but as it would happen at a lesser rate to reform heterochromatin and enable transcriptional silencing of PCH-specific ERVs, and as rare or very local binding, it is not visible by immunofluorescence. H3.3 differs from canonical H3 from only 4 to 5 amino acids, among which are residues giving specificities for particular chaperones, but also the Serine 31. Intriguingly, H3.3S31 can be phosphorylated and is observed at pericentromeric regions in somatic cells (Hake *et al.* 2005). We obtained preliminary results suggesting that H3.3S31 might be involved in PCH clustering (**data not shown**). It would be interesting to further investigate the interplay between SETDB1, H3.3S31 and PCH clustering and even additional histone residues undergoing post-translational modifications.

Our model is not exhaustive, and additional players might be involved in this heterochromatin maintenance mechanism. One of the major proteins that binds H3K9me3 is HP1 α . We do not observe striking differences in H3K9me3 and HP1 α presence at chromocenters in Daxx KO ESCs (**Figure 4B article, Figure 28A**). However, when measuring the dynamic of HP1 α using FRAP, we notice that the half-recovery rate was faster in the absence of Daxx (**Figure 4B article**). Furthermore, when we look at the variance of HP1 α signal over time, we detect lower levels of heterochromatin barriers, suggesting that HP1 α is either diffusing more rapidly throughout the nucleoplasm to chromocenters, or that its affinity is reduced in the absence of Daxx (**Figure 4C article**). Intriguingly, we demonstrate that DAXX could recruit SETDB1 at pericentromeric regions to induce H3K9me3, that we propose to take place specifically onto the H3.3 variant (**Figure 5D article**). It raises the possibility that HP1 α , and perhaps other proteins, have different affinities for H3.3K9me3 than for canonical H3K9me3. To gain deeper

understanding of pericentromeric regulation, it would be important to perform biochemistry experiments such as chromatin IP or *in vitro* affinity assays to assess the importance of the histone bearing the tri-methylated lysine 9 for HP1 α binding. As no link has been established so far between DAXX and HP1 α , it is intriguing to observe such differences in HP1 α dynamics (**Figure 4B article**). Furthermore, the absence of Daxx diminishes heterochromatin barrier, possibly via alteration of HP1 α LLPS (**Figure 4C article**). It suggests that additional proteins might be able to modulate the LLPS properties of HP1 α (Strom *et al.* 2017). It would thus be informative to study the LLPS properties of HP1 α in the absence of Daxx using live-cell imaging and treating the cells with the 1,6-hexanediol molecule that abolishes LLPS. Moreover, defects in chromocenter formation might come from additional protein binding to specific DNA sequence or histone modifications. An example is the HMGA1 protein in somatic murine cells that accumulates at chromocenters and is important for major satellite clustering and genome integrity (Jagannathan *et al.* 2018). It would be informative to look at HMGA1 or other HMG proteins in ESCs in serum-based and ground-state conditions in Daxx KO ESCs. Furthermore, to gain a more comprehensive view of pericentromeric heterochromatin protein network and how it is affected upon the loss of Daxx, it could be informative to perform PICH experiments as previously described (Saksouk *et al.* 2014).

An additional layer of control may come from major satellite RNAs. Interestingly, SUV39H1/2 enzymes can bind to RNA and transcription of major satellites has been proposed to help SUV39H1/2 action by retaining the enzymes at the right localization (Johnson *et al.* 2017; Velazquez Camacho *et al.* 2017). We observe that depletion of Daxx in mESCs induces an up-regulation of major satellite transcripts (**Figure 1C article**). Because Daxx KO ESCs display mis-regulation of major satellite transcription, it could impair proper binding of SUV39H1/2 or other RNA-binding proteins. We notice that the specific activation of major satellite transcription using a Tale-VP64 could induce DAXX-recruitment at chromocenters (**Figure S3D article**). Yet, specific activation of PCH generated DNA damages as well, making it difficult to uncouple the functions of the transcription and of the produced RNA from the DNA damages (**Figure S3E article**). It would be interesting to test whether RNA production is important for DAXX recruitment and function at PCH by specifically knocking-down major satellite RNAs or transfecting major satellite dsRNA.

We propose a model of heterochromatin maintenance at pericentromeric heterochromatin. However, this mechanism might extend beyond PCH. Heterochromatin compartments serve as landmarks for heterochromatin regions dispersed throughout the genome, such as the pericentromere-associated domains (PADs) or the lamina-associated domains (LADs) (Canat *et al.*

2020; Wijchers *et al.* 2015; Peric-Hupkes *et al.* 2010). We notice that in the absence of Daxx, chromocenters were scattered within the nucleoplasm (**Figure 4A article**). Because PADs and LADs present a strong overlap of DNA sequences and that we detected a strong upregulation of genes located within LADs in ground-state Daxx KO ESCs, it is likely that PAD-genes could also be mis-regulated (**Figure 30A**). Thus, it would be of interest to choose candidate genes belonging to PADs only or both PADs and LADs and perform DNA FISH. It will be interesting to see whether mis-regulated genes have shifted from heterochromatin to euchromatin regions or if the differences in transcription could happen without any changes in radial positioning. The strong overlap between PADs and LADs results from the high redundancy existing between heterochromatin compartments. It would thus be interesting to describe which genes do move from PADs to LADs and which genes are not relocalized, enabling an uncoupling of transcription and radial positioning.

Lastly, we propose that our heterochromatin maintenance model may not be restricted to mESCs. H3K9me3-establishment at chromocenters was mainly thought to result from the SUV39H1 and 2 enzymes while SETDB1 is mostly associated with telomeric heterochromatin (Martens *et al.* 2005; Peters *et al.* 2001; Gauchier *et al.* 2019; Burton *et al.* 2020). We demonstrate that upon hypomethylation, the other H3K9me3-methylase SETDB1 is recruited by DAXX to PCH and actively generates H3K9me3, even in the absence of Suv39H1/2 (**Figure 5B article**). It agrees with previous observations that Suv39H1/2 dKO ESCs in ground-state presented some H3K9me3 foci onto DAPI-rich chromocenters (Tosolini *et al.* 2018). Our results underlie a previously unexpected redundant action of the different H3K9 tri-methylases at pericentromeric regions. In order to uncouple the action of DAXX from SETDB1, it would be appealing to look at chromocenter organization in Setdb1-deficient cells. It was reported that the loss of Daxx could impact the organization of chromocenters in murine embryonic fibroblasts (Rapkin *et al.* 2015). However, it remains to assess the exact function of DAXX and SETDB1 in pericentromeric heterochromatin regulation in somatic cells. Intriguingly, DAXX can be recruited to PCH in highly methylated cells such as myotubes (Salsman *et al.* 2017). Indeed, in less committed myoblasts, DAXX localizes at PML NBs and upon differentiation into myotubes, there is the disappearance of PML NBs, which correlates with the recruitment of DAXX to chromocenters. Surprisingly, the expression of TET1 and TET2 enzymes is increased upon myotube differentiation, concomitantly with enhanced the level of 5hmC (Zhong *et al.* 2017). It would be interesting to dissect whether the observed DAXX recruitment to PCH also relies onto DNA damages-induced active DNA demethylation.

5. Roles of DAXX-SETDB1 at other genomic regions

As mentioned above, we detect a strong upregulation of LAD-genes in ground-state cells lacking Daxx (**Figure 30A**). Surprisingly, we note that the peripheral ring of H3K9me2 is altered and appears irregular in these cells, a phenotype never described before (**Figure 29A**). We hypothesize that it is a loss of H3K9me2 in LADs that leads to the transcriptional upregulation of LAD-genes. To confirm it, one could perform a ChIP-seq experiments onto H3K9me2 mark and look if there is a global decrease or local decreases at specific loci. Furthermore, because we demonstrated that the function of DAXX at pericentromeres relies on SETDB1, it would also be informative to perform an H3K9me3 ChIP-seq. Indeed, reanalyzing the RNA-seq data from a recent study that studied the conversion toward the ground-state of pluripotency of Setdb1-deficient cells, we detected that an increase of LAD-genes transcriptions, although in both serum-based and ground-state conditions (**data not shown**)(Wu *et al.* 2020). These data suggest that the function of DAXX and SETDB1 extend beyond pericentromeric satellites.

DAXX and SETDB1 have been implicated in the transcriptional regulation of ERVs, notably in hypomethylated ESCs (He *et al.* 2015; Matsui *et al.* 2010; Fukuda *et al.* 2018). We confirm the role of DAXX in regulating diverse families of ERVs upon ground-state conversion (**Figure 1C article**). We report that some LINE1 elements are also controlled by DAXX, even in serum-based medium, which has not been previously reported (**Figure 1C article**). The effect of the transcriptional up-regulation of transposable elements onto nearby genes remains controversial (Elsässer *et al.* 2015; Jachowicz *et al.* 2017). Yet, because of the important number of genes that are up-regulated within LADs, it would be interesting to assess the importance of transposable elements loss of silencing onto LAD-genes. LINE1 Tf elements are mostly enriched in LADs and can be up-regulated using a dCas9-VPR construct (**Figure 31B, Figure 31C**). We notice that Tale-activation was often more efficient than dCas9-activation (**data not shown**). It would thus be informative to up-regulate LINE1 Tf, and perhaps multiple families at once, using a Tale-VP64 approach and perform RNA-seq experiments to assess the transcriptional states of LAD-genes, and genes located near targeted LINE1. Furthermore, because we describe a function of DAXX in heterochromatin reformation after active DNA demethylation-induced DNA damage, it would be interesting to evaluate whether this phenomenon also takes place at retrotransposons using genome-wide mapping of 5hmC, AP-sites and γH2AX signaling. Such ChIP-seq assays could be performed in ESCs transfected with Tale-TET1CD constructs targeting different TE families such as LINE1 Tf and IAPez.

Genome-wide mapping of DAXX binding revealed that about 20% of DAXX peaks appear at gene promoters (He *et al.* 2015). Furthermore, it was recently reported that DAXX physically

interact with PRC1 and might thus regulate polycomb-targeted genes. Indeed, in the zygote, PRC1 can recruit DAXX to major satellites and oocytes and 2-cell embryo lacking Daxx presented an upregulation of genes that were highly marked by H3K27me3 (Liu *et al.* 2020). These results are in good accordance with our transcriptomic as upon preliminary analysis, we noted a good correlation between H3K27me3 presence and up-regulation in the absence of Daxx upon ground-state conversion (**data not shown**). We notice that the absence of Daxx resulted in a 2C-like transcriptional signature upon ground-state conversion, suggesting that DAXX contributes to the repression of 2C-like program (**Figure 27B**). Intriguingly, PRC1 is among the complex implicated in 2C-like repression as its depletion enhanced conversion from pluripotent ESCs toward 2C-like totipotent cells (Rodriguez-Terrones *et al.* 2018). In that direction, it would be interesting to deeper investigate the interplay between DAXX and PRC1 in the control of the 2C-like transcriptional program. PRC1 was demonstrated to participate into the nuclear organization of chromatin in an enzymatic and CTCF-independent manner, suggesting a structural role for PRC1 (Boyle *et al.* 2020; Vieux-rochas *et al.* 2015). One could hypothesize that the structural function of DAXX and possibly H3.3 extend beyond constitutive heterochromatin regions in pluripotent cells via the regulation of polycomb-target genes and it would be interesting to assess the global genome organization and chromatin compaction at polycomb-marked genes in Daxx-deficient cells.

He *et al.* reported that DAXX can recruit SUV39H1 to maintain telomeric heterochromatin notably upon DNA hypomethylation (He *et al.* 2015). Although we notice an increased recruitment of DAXX at telomeres, our data do not support this model (**data not shown**). Indeed, we observe that Suv39H1/2 dKO could grow well even upon ground-state conversion, indicating non-essential functions upon DNA hypomethylation (**Figure 5C article**). We observe that DAXX rather recruit SETDB1 (**Figure 5A article**). DAXX, PML and SETDB1 are observed at telomeres in mESCs and DAXX-deposited H3.3 can be modified into H3.3K9me3 at this location (Udugama *et al.* 2015; Ivanauskiene *et al.* 2014). It would be interesting to assess if the H3.3K9me3-modification is carried specifically by SETDB1. In cancer cells displaying ALT-maintenance of telomeres, deletion of Daxx or Setdb1 results in loss of telomeric heterochromatin, suggesting that the crucial role played by DAXX and SETDB1 is also true in somatic cells (Gauchier *et al.* 2019; Ahvenainen *et al.* 2018). Furthermore, H3.3 have been linked to ALT-mechanism as phosphorylation of H3.3 serine 31 is essential for survival of human ALT-cancer cells (Chang *et al.* 2015). It would be of great interest to deeper investigate the exact role of H3.3 in ALT-cancer, and the possible function H3.3K9. Intriguingly, SETDB1 is the main histone methyl-transferase acting at telomeres, in contrast of the action of SUV39H1/2 at chromocenters. In murine cells, chromosomes are all acrocentric, implying that one telomere is always located close to a

pericentromeric region, hence a chromocenter. As observed in the case of TRF2 protein which has been described as a telomeric protein, which has recently been implicated in the proper replication of pericentromeric satellites, it is conceivable that other telomeric proteins may be involved in chromocenter maintenance primarily via spatial localizations, further strengthening the links between heterochromatin compartments (Mendez-Bermudez *et al.* 2018).

6. Activation of heterochromatin regions can generate DNA damages and IFN signaling

In the second part of the discussion, I proposed a model based on our results that active DNA demethylation at chromocenters could generate DNA damage signaling and recruit DAXX. Interestingly, we notice that Daxx KO ESCs display a strong increase in total γ H2AX levels by Western blot upon ground-state conversion, that is unlikely to be solely explained by major satellite up-regulation (**Figure 31A**). Correlations have often been observed between up-regulation of DNA repeat elements and increased DNA damages, albeit no link has clearly been demonstrated for endogenous elements (Tharp *et al.* 2020; Belgnaoui *et al.* 2006; Gasior *et al.* 2014; Xiang *et al.* 2019). To assess the direct consequences of LINE1 derepression, we targeted a dCas9-VPR protein to specifically activate LINE1 Tf family. We detect a transcriptional up-regulation of the targeted LINE1 family and observe a concomitant increase of γ H2AX signal (**Figure 31B**, **Figure 31C**). Furthermore, the specific activation of major satellite repeats also induce a γ H2AX increase at chromocenters (**Figure S3E article**). These data suggest that the loss of silencing of DNA repeated elements directly contribute to the increase of DNA damages, as it has been described in breast cancer cells where satellite RNAs are sufficient to induce DNA damages (Zhu *et al.* 2018b). To further confirm these results, it would be interesting to assess γ H2AX levels upon specific activation of other DNA repeat families such as IAPEz, which are strongly up-regulated in Daxx KO ESCs (**Figure 1C article**). It then remains to dissect what step of DNA repeats activation drives the accumulation of DNA damages. Indeed, it would be informative to see whether the loss of heterochromatin-associated modifications, such as loss of DNA methylation or H3K9me3 can increase DNA damages, or if it is mainly due to the transcription *per se*. It is also possible that DNA lesions occur at conflicts from DNA replication forks and transcription. It would be informative to see if the activation of LINE1 elements leads to the production of more LINE1 proteins and if this results in enhanced retrotransposition events. As the LINE1 ORF1 encodes for an endonuclease, it would also be informative to assess its role in the elevated DNA damages. Finally, it was demonstrated in cancer cells that the inhibition of DNA repair proteins themselves can induce LINE1 up-regulation, thus creating a vicious circle where inactivation of DNA repair

proteins drives the transcription of LINE1 elements, which generates DSBs that require the action of the DDR (Mita *et al.* 2020).

Transcriptomic analysis of Daxx KO mESCs upon ground-state conversion revealed an important number of mis-regulated genes (1250 down- and 1345 up-regulated) (**Figure 1D article**). We decided to look for transcriptional pathways and observe the activation of type II IFN, P53 and apoptosis responses (**Figure 1E article, S1E article**). Interestingly, it was reported that activation of endogenous retroviruses, LINE elements or pericentromeric repeats could trigger the activation of an IFN response, notably in cancer cells (Cuellar *et al.* 2017; Chiappinelli *et al.* 2015; Cecco *et al.* 2019; Rajshekar *et al.* 2018). We detect higher transcription of multiple families of DNA repeats in Daxx-deficient ground-state ESCs (**Figure 1C article**). It would thus be interesting to dissect if the loss of silencing of heterochromatin regions is responsible for the observed IFN response. In that line, it would be informative to assess IFN and P53 responses upon specific activation of specific families of repeats using Tale-VP64 constructs. Intriguingly, up-regulation of DNA repeat elements is visible in WT cells upon ground-state conversion and there is no induction of IFN nor cell death (**Figure S1B article**). Since the Daxx KO ESCs upon ground-state conversion present the highest transcriptional levels of DNA repeats, it might reach a threshold level triggering an additional response (**Figure S1B article**). Interestingly, high levels of ERV transcription can activate the damage-associated molecular patterns (DAMPs) which is a broad physiological response of the cell in case of non-self-sensing (Roers *et al.* 2016). DAMPs signaling passes through the Toll-like receptors, a signature that we found up-regulated in our transcriptomic analysis, suggesting that a DAMP-signaling might be activated in the absence of Daxx upon ground-state conversion (**Figure S1D article**). To evaluate the role of DAMPs, it would be interesting to measure the amount of DNA or RNA from repeated elements found in the cytoplasm. Furthermore, it would be informative to impede DAMPs signaling pathway such as the Toll-like receptors to test whether it plays a role in the impaired cell survival of Daxx KO ESCs. We performed the RNA-seq experiments at 6 days after initial conversion into 2i/LIF + vitamin C medium, when the cell survival phenotype starts to be visible (**Figure 1B article**). It is thus possible that some of the pathway we identify, such as IFN and apoptosis, might result from the fact that part of the cell population begins to die (**Figure S1E article**). In that direction, it would be interesting to assess transcriptional states of Daxx-deficient cells at different times to better characterize apoptosis and IFN signaling at earlier times after conversion.

7. DAXX interactions and post-translational modifications

We observe that in serum ESCs, DAXX localizes at PML NBs (**Figure 2A article**). However, upon ground-state conversion, DAXX is massively recruited toward chromocenters to form ‘giant’ structures encompassing major satellite repeats (**Figure 2A article, Figure 2B article**). Yet, ‘classical’ small PML NBs are still visible in ground-state condition that contain DAXX as in serum, suggesting that the formation of ‘giant’ structures do not arise merely as a loss of ‘classical’ NBs. We demonstrate that in the absence of Daxx, PML is not recruited to PCH, whereas the lack of Pml do not impair DAXX recruitment to PCH (**Figure S5B article, Figure 33A**). Furthermore, upon Daxx depletion, PML NBs are still visible, but the loss of Pml alters the organization of DAXX into NBs, with only few foci observed that are likely to be telomeres (**Figure S5A article, Figure 33A**). These results indicate that while DAXX localization is impacted by PML, its recruitment toward PCH seems independent of PML. It resembles the observations made during myogenic differentiation where in myoblasts, DAXX localized at PML NBs but upon myotubes differentiation, PML expression was abolished and DAXX relocated toward chromocenters (Salsman *et al.* 2017). However, in myotubes, DAXX was present at all chromocenters, which differs from our observations that DAXX accumulated at 1 to 3 chromocenters (**Figure 2C article**). Intriguingly, SIM domain of DAXX is necessary for its pericentromeric relocalization in myotubes but exogenous expression of PML could not rescue this phenotype and DAXX remained at chromocenters, suggesting that post-translational modifications, and not PML itself, are crucial to control DAXX localization (Salsman *et al.* 2017). We thus propose that PML might contribute to post-translational modifications of DAXX, such as SUMOylation, to regulate its local recruitment at heterochromatin regions. In that direction, it would be informative to better dissect the post-translational modifications of DAXX upon ground-state conversion. Furthermore, confirming the role of the modified residues will require to rescue Daxx KO ESCs with mutant versions of DAXX and assess their capacity to localize at chromocenters. Surprisingly, when prompting DAXX localization in Pml-deficient cells, we noticed that it still accumulates at chromocenters (**Figure 33A**). These data suggest that the loss of Pml does not impact the recruitment of DAXX, but rather its function. It would thus be informative to study the post-translational modifications of DAXX in Pml KO ESCs. We hypothesize that post-translational modifications of DAXX could contribute to increase local concentration of proteins, thus facilitating heterochromatin reformation. In cells lacking Pml, the concentrating role of DAXX might be impaired. In that direction, it will be of great interest to see if DAXX can recruit SETDB1 and H3.3 in Pml-deficient cells upon ground-state conversion.

We notice that deletion of Daxx or Pml result in highly similar phenotypes such as impaired cell survival and defects in heterochromatin organization (**Figure 1B article, Figure 4A article, Figure 34B, Figure 35B**). It could be informative to better characterize Pml KO phenotypes as for Daxx KO such as DNA repeats expression and activation of IFN response upon ground-state conversion. Since PML NBs act as a hub for SUMOylation and that DAXX can be regulated via SUMOylation, it remains to assess whether PML contributes to DAXX regulation. Interestingly, we detected that in the absence of Daxx, ground-state ESCs displayed a 2C-like transcriptional signature (**Figure 27B**). If DAXX is regulated by PML, Pml-deficient cells should display the same transcriptional signature. Indeed, the absence of Pml induces the activation of a 2C-like transcriptional profile, providing evidence that PML might regulate DAXX (**S. Tessier, V. Lallemand-Breitenbach, submitted article**). Interestingly, the only E3 SUMO ligase, UBC9 has been implicated in repression of 2C-like program, indicating a broad SUMOylation network safeguarding chromatin identities (Cossec *et al.* 2018). Furthermore, as mentioned in the second part of the discussion, DAXX is recruited at PCH regions in the early embryo via PRC1 (Liu *et al.* 2020). Interestingly, Liu *et al.* reported that PRC1-mediated recruitment of DAXX is regulated via SUMOylation. Additionally, it was reported that PML could regulate PRC2 activity and that deletion of Pml induced a global redistribution of H3K27me3 histone modification (Amodeo *et al.* 2017; Delbarre *et al.* 2017). Therefore, it would be interesting to assess the role of PML onto polycomb complexes regulation and DAXX-polycomb interaction.

Furthermore, in addition to the impaired spatial organization of chromocenters, we observe differences in HP1 α dynamics in the absence of Daxx, and we propose that DAXX directly or indirectly controls LLPS properties of HP1 α (**Figure 4C article**). It would be interesting to evaluate the impact of Pml loss onto heterochromatin barriers and LLPS properties of HP1 α as well. SUMO-SIM interactions was proposed to mediate LLPS, notably for PML NBs formation (Min *et al.* 2019; Banani *et al.* 2016). HP1 α binding at chromocenters is affected by SUMOylation in MEFs (Maison *et al.* 2011). Indeed, the targeting of the SENP1/2 SUMO proteases at PCH can block HP1 α at chromocenters and thus diminish its dynamical properties (Maison *et al.* 2012; Romeo *et al.* 2015). Because DAXX possesses a SIM motif and binds to SUMOylated proteins such as PML, it would be informative to measure the SUMOylation-deSUMOylation of HP1 α at PCH in the absence of Daxx or Pml. Together, these data suggest the existence of a SUMOylation network that might regulate LLPS properties of different proteins such as PML or HP1 α at PCH.

We demonstrate that targeted recruitment of DAXX to major satellites induces a strong clustering of PCH (**Figure 4D article**). Upon further characterization of the domains of DAXX necessary for PCH clustering, we notice that interaction with H3.3 is essential as neither

DAXXY222A nor expression of H3.3G90M can form big PCH clusters like WT DAXX (**Figure 5C article, 5D article**). Intriguingly, we observe that DAXX could recruit SETDB1 and PML but DAXXY222A could not (**Figure S5C article**). Since the role of DAXX at PCH is to recruit SETDB1, it is possible that SETDB1 regulation might play a role upon ground-state conversion. By immunofluorescence, we detect SETDB1 as homogeneously distributed within the nucleoplasm and the cytoplasm in serum-based ESCs, and rarely as nuclear dots (**Figure S5A article**). However, upon-ground-state conversion, SETDB1 appears as foci colocalizing with PML NBs and ‘giant’ DAXX-PML structures at PCH (**Figure 5A article**). In that direction, the loss of Setdb1 prevents cell survival upon ground-state conversion, strengthening its importance (Wu *et al.* 2020). It yet remains to assess the importance of SETDB1 in H3.3 recruitment. SETDB1 shuttling from the cytoplasm to the nucleoplasm is regulated by ATF7IP, which also localizes at PML NBs (Sasai *et al.* 2013; Tsusaka *et al.* 2019). ATF7IP localization and function can be regulated by post-translational modifications such as SUMOylation and ubiquitylation (Sasai *et al.* 2013). Furthermore, ATF7IP is an important co-factor of SETDB1 and facilitates its enzymatic activity (Wang *et al.* 2003). Hence, it would be interesting to assess if modifications of ATF7IP, induced by PML or DAXX could differentially regulate the function of SETDB1 in pluripotent cells.

Although previous studies reported the control exerted by PML onto DAXX repressive activity, it is the first report that H3.3 binding is implicated in DAXX-PML interaction (Li *et al.* 2000). Furthermore, it was observed that H3.3 could accumulated at PML NBs, in a DAXX-dependent manner (Delbarre *et al.* 2013). In that direction, it would be interesting to evaluate the role of DAXX-H3.3 interaction on PML NB formation. Furthermore, DAXX Δ SIM was able to induce PCH clustering without recruiting PML, strengthening that it is indeed H3.3 that is essential for that phenotype (**Figure 38B**). However, the clustering effect of DAXX Δ SIM was stronger in WT cells than in Daxx KO ESCs, perhaps indicating a recruitment of endogenous DAXX. It would be interesting to assess whether DAXX Δ SIM can interact with WT DAXX and other partners using a mass spectrometry strategy. Remarkably, we could not exclude that it is SETDB1 that recruits PML as SETDB1 localizes at PML NBs and can physically interact with PML (Cho *et al.* 2011). In that direction, it would be useful to specifically recruit SETDB1 at chromocenters using a Tale protein and observe whether it leads to DAXX or PML recruitment. When we recruit the DAXX9KR, we do not observe a strong clustering phenotype, suggesting that SUMOylation of DAXX might be important in its clustering function, and perhaps for H3.3 deposition (**Figure 38D**). It would be informative to assess H3.3 binding for the DAXX9KR mutant to dissect whether SUMOylation of DAXX can control its chaperone activity.

8. Roles of DAXX and pericentromeric regions in pathologies

We describe the presence of DAXX-PML structures at PCH upon hypomethylation (**Figure 2A article**). These DAXX-PML NB are much bigger than the classical PML NBs and could be qualified as ‘giant’ ones (**Figure S2A article**). PML NBs do not usually contain chromatin, yet in a genetic disease, the immunodeficiency, centromeric instability and cranial abnormality (ICF) syndrome, PML NBs appear as ‘giant’ bodies containing the pericentromeric repeats of some chromosomes in lymphocytes of ICF patients (Luciani *et al.* 2006). Interestingly, the ICF syndrome results from defects in the DNA methylation machinery, mostly from a mutated DNMT3B (Xu *et al.* 1999). In the ICF syndrome, hypomethylation occurs notably at pericentromeric repeats of three specific chromosomes 1, 9 and 16 which harbor the particular satellite I and are thus more prone to breakage. Giant PML NBs form around these three peculiar chromosomes and contain DAXX and DNA damage response proteins like BRCA1, TOPII α , BLM and NBS1 (Luciani *et al.* 2006). We demonstrated that the function of DAXX at PCH in pluripotent cells relies onto the action of the SETDB1 enzyme, it would thus be interesting to assess if SETDB1 is also recruited in ICF patients. As we observed that the recruitment of DAXX-SETDB1 might be promoted by DNA damage-induced by TET-mediated active DNA demethylation, it would be interesting to measure the level of DNA damages specifically occurring at PCH of ICF patients. It would further be intriguing to knock-down TET activities in ICF-lymphocytes and ask whether DNA damages and centromeric instabilities might be reduced.

Loss of Daxx impairs pericentromeric heterochromatin organization in pluripotent cells (**Figure 4A article**). Intriguingly, disruption of chromocenters was observed in a murine mouse model for Brca1-deficient breast cancer (Zhu *et al.* 2011). Furthermore, it was demonstrated that the action of BRCA1 at pericentromeric regions was to repress satellite transcription and pericentromeric RNAs could induce the tumorigenesis (Zhu *et al.* 2011, 2018b). Since in ICF syndrome, BRCA1 localizes at DAXX-containing PML NBs, it would be relevant to assess the function of DAXX in BRCA1-mediated heterochromatin maintenance in breast cancers. Furthermore, breast cancers often display hypomethylation of pericentromeric regions, it would thus be interesting to assess the cell survival of these cells upon Daxx depletion (Narayan *et al.* 1998).

Furthermore, we observe that the absence of Daxx results in the loss of silencing of heterochromatin regions, including different classes of transposable elements and pericentromeric satellites (**Figure 1C article**). Over-expression of pericentromeric satellites is observed in different cancer types such as pancreatic cancers (Ting *et al.* 2011). Intriguingly, in lung, kidney, ovary, colon or prostate cancers, up-regulation of satellites correlated with the loss of silencing of LINE1

elements, suggesting broad defects in heterochromatin silencing. Pancreatic cancers notably display higher transcription of LINE1 elements, together with global DNA hypomethylation (Marinoni *et al.* 2017). Pancreatic tumors often bear point mutations in DAXX, which corresponds to high levels of chromosomal instability, suggesting a putative role for DAXX in genome stability in pancreatic cells upon hypomethylation (Marinoni *et al.* 2014; Jiao *et al.* 2011). It would be informative to assess the DNA damages and repair mechanisms in pancreatic tumor cells to dissect the exact function exerted by DAXX. Mutations of H3.3 and DAXX have been reported in pediatric neuroblastoma, and although it mainly seems to affect polycomb-related mechanisms, it remains to understand the exact function of DAXX in these cancers (Schwartzentruber *et al.* 2012; Wu *et al.* 2012; Dyer *et al.* 2017). Finally, as mentioned for breast cancers, other cancer types display DNA hypomethylation, it would be interesting to study the function of DAXX in these diseases (Melanie Ehrlich 2009). It has been reported that SETDB1 was an essential factor for several acute myeloid leukemia cell lines acting on ERV repression and the IFN response (Cuellar *et al.* 2017). Since we observed a role for DAXX in recruiting SETDB1 upon DNA hypomethylation, future studies should explore the potential of DAXX as a clinical target.

**RESUME SUBSTANTIEL DE LA
THESE EN FRANCAIS**

RESUME SUBSTANTIEL DE LA THESE EN FRANCAIS

Introduction

Près de la moitié du génome est composé de séquences répétées correspondant à l'hétérochromatine, et qui doivent être maintenues éteintes transcriptionnellement. Des défauts de maintenance de l'hétérochromatine sont souvent observés dans différentes pathologies et peuvent mener à la tumorigénèse. Les régions hétérochromatiques peuvent être dispersées ou localisées, notamment autour des centromères. Les régions péri-centromériques restent inactives dans les cellules somatiques grâce à l'action combinée de la méthylation de l'ADN et de la modification d'histone H3K9me3, reconnue par différentes protéines dont HP1 α .

Cette organisation particulière émerge au cours du développement embryonnaire précoce. En effet, au stade 2-cellules à lieu une forte activation transcriptionnelle des régions répétées comme les éléments LINE1 qui permettent une décompaction globale du génome. Au même moment se produit une forte transcription des satellites majeurs composant les régions péri-centromériques. Cette activation permet la mise en place dès le stade 4-cellules des chromocentres, régions visibles en DAPI où se regroupent les régions d'hétérochromatine péri-centromériques (PCH) de multiples chromosomes. De manière intéressante, l'activation des régions hétérochromatines correspond à une baisse drastique du niveau de méthylation de l'ADN au stade 2-cellules. Ces régions sont ensuite progressivement réduites et à nouveau fortement réprimées à partir du stade blastocyste quand le niveau de méthylation de l'ADN est rétabli. Ainsi, la transcription de l'hétérochromatine depuis le stade 2-cellules jusqu'au stade blastocyste est contrôlée de manière indépendante de la méthylation de l'ADN (5mC).

Les cellules souches embryonnaires (ESC) présentent des niveaux faibles de méthylation de l'ADN comparés aux cellules différenciées. Les ESC sont dérivées des cellules de la masse interne du blastocyste et représentent un modèle de choix pour étudier le développement embryonnaire. Les ESC présentent les caractéristiques des cellules pluripotentes et peuvent se diviser en tous types cellulaires formant l'organisme. En revanche, lors de la culture des CSE *in vitro*, elles accumulent de plus en plus de méthylation de l'ADN. Un nouveau milieu de culture appelé 2i pour 2 inhibiteurs a été développé par Ying *et al.* En 2008. L'ajout de vitamine C en milieu 2i permet de réduire très substantiellement le niveau de 5mC et les CSE, à l'inverse des cellules différenciées, supportent l'absence de méthylation de l'ADN. Certains facteurs permettant le contrôle de l'hétérochromatine en condition hypométhyliée ont été décrits comme BEND3 et les

protéines des complexes polycomb aux péricentromères et DAXX et SETDB1 aux rétrovirus endogènes dispersés.

De manière intéressante, DAXX localise aux PCH du noyau paternel, fortement déméthylé, dans les tous premiers jours du développement. Cependant, la délétion génétique de Daxx ne perturbe le développement de l'embryon qu'à des stades plus tardifs et empêche la formation du blastocyste, suggérant une forte importance de DAXX pour permettre la transition des cellules embryonnaires vers un état pluripotent, quand les chromocentres se forment.

DAXX est la chaperonne du variant d'histone H3.3 spécifique pour les régions d'hétérochromatine. Un enrichissement de H3.3 est observé à la fois à certaines régions de l'hétérochromatine comme de l'euchromatine, mais sa déposition est alors médiée par le complexe HIRA. De manière intéressante, H3.3 est essentiel pour le développement embryonnaire comme pour la maintenance des ESC en culture. Un défaut de H3.3 entraîne une instabilité chromosomique, suggérant un rôle crucial au niveau de l'hétérochromatine. De plus, H3.3 fournit la modification H3K9me3 aux régions télomériques et aide au maintien de l'état hétérochromatique à certains rétrovirus endogènes (ERV). Cependant, son rôle aux satellites péricentromériques a surtout été envisagé comme facilitant la transcription.

Dans ce travail, j'ai utilisé les cellules souches embryonnaires murines comme un modèle pour étudier le rôle de DAXX dans la maintenance de l'hétérochromatine et obtenir une meilleure compréhension de la régulation des régions péricentromériques dans les cellules pluripotentes.

Résultats

Afin d'étudier le rôle de DAXX, j'ai généré une lignée inactivée pour le gène Daxx grâce à la technologie CRISPR/Cas9. De manière intéressante, j'ai observé que les cellules DaxxKO étaient capable de se différencier. En revanche, en cultivant les cellules dans un milieu 2i et vitamine C afin qu'elles atteignent l'état naïf de pluripotence, j'ai observé qu'après 8 à 10 jours de culture les cellules DaxxKO périssaient. L'analyse transcriptomique dans ces différents milieux a révélé que l'absence de Daxx entraînait une forte activation de nombreuses familles d'ADN répété, notamment certains ERV, certains LINE1 et les satellites majeurs composant les PCH. De plus, un très grand nombre de gènes sont différentiellement exprimés en l'absence de Daxx en condition naïve de pluripotence. Parmi les gènes moins exprimés se trouvent ceux intervenant dans les différentes voies de réparation de l'ADN.

Dans un milieu « classique » contenant du sérum, DAXX localise aux corps nucléaires PML (PML NBs). Après conversion vers l'état naïf de pluripotence, DAXX accumulait à certaines

régions péricentromériques dans la majorité des cellules. PML accumulait également autour de ces structures formées par DAXX. De manière intéressante, la conversion vers l'état naif de pluripotence hausse le nombre de chromocentre présentant des foyers γ H2AX. De plus, l'induction des dommages à l'ADN de manière aléatoire ou ciblée spécifiquement aux régions péricentromériques entraîne la relocalisation de DAXX aux PCH. Néanmoins, le recrutement de NBS1 aux PCH, induisant l'accumulation de γ H2AX ne suffit pas à recruter DAXX.

Traiter les cellules avec du 5-azacytidine, réduisant le niveau de méthylation de l'ADN réduit la survie des cellules DaxxKO de manière similaire à celle observée en milieu 2i et vitamine C. De plus, le traitement avec le 5-azacytidine entraînait également l'accumulation de DAXX aux PCH. Afin de confirmer que la déméthylation de l'ADN était responsable des dommages à l'ADN observés, j'ai recruté une protéine Tale ciblant spécifiquement les satellites majeurs fusionné au domaine catalytique de l'enzyme TET1 (TET1CD). Cette construction Tale-TET1CD permet la déméthylation active spécifique des chromocentres menant à une légère élévation de la transcription des satellites majeurs. De manière remarquable, la déméthylation active entraîne l'apparition de foyers γ H2AX aux chromocentres ainsi que le recrutement de DAXX, démontrant ainsi que la déméthylation active peut mener à des dommages à l'ADN et suffit à entraîner la relocalisation de DAXX.

Bien que DAXX ne soit pas visible aux chromocentres en condition sérum, son absence entraîne une forte désorganisation de l'organisation des séquences satellites majeurs. En effet, j'ai observé que la perte de DAXX augmentait le nombre de foyer de satellites majeurs et ceux-ci sont également plus petits en conditions pluripotentes mais cet effet disparaît après différenciation des cellules. De plus, l'accessibilité de la chromatine, mesurée par digestion à la MNase est plus forte dans les cellules DaxxKO, suggérant une altération de la compaction de l'hétérochromatine. En mesurant par FRAP la récupération de fluorescence de GFP-HP1 α , une protéine reconnaissant la modification H3K9me3 et fortement enrichie aux chromocentres, j'ai montré que l'absence de Daxx augmente la dynamique de HP1 α . Il semble également que cette dynamique accrue corrèle avec une altération de la variance du signal GFP-HP1 α au cours du temps, ce qui suggère que la perte de Daxx puisse influencer sur la capacité de séparation de phase de HP1 α . Enfin, le recrutement de DAXX aux satellites majeurs à l'aide d'une protéine Tale entraîne une forte diminution du nombre de chromocentres visibles, montrant ainsi que DAXX est capable de générer un rassemblement spatial des régions péricentromériques.

La modification H3K9me3 aux chromocentres est mise en place par les enzymes SUV39H1/2. De manière intrigante, la troisième H3K9 tri-méthylase SETDB1 est recrutée aux chromocentres par DAXX. De plus, les enzymes SUV39H1/2 ne sont pas nécessaires à la survie

des ESC en condition naïve de pluripotence, et ces cellules présentes également du signal H3K9me3 aux chromocentres uniquement dans cette condition et pas en sérum. A l'aide de Tales, j'ai observé que l'interaction de DAXX avec H3.3 était nécessaire pour recruter SETDB1 et H3K9ME3, et pour former un rassemblement spatial des séquences péri-centromériques. De plus, le recrutement de l'enzyme SUV39H1, bien que capable d'induire une forte concentration de H3K9me3, ne forme pas de rassemblement spatial des satellites majeurs. Enfin, grâce à des versions mutantes de H3.3, j'ai démontré que la lysine 9 de H3.3 était nécessaire à cette réorganisation spatiale des satellites majeurs.

En outre, l'analyse transcriptionnelle a révélé que l'absence de Daxx entraînait une activation des gènes actifs dans un état ressemblant au stade 2-cellules, suggérant que DAXX participe à la répression de cet état et au maintien de l'identité chromatinienne des cellules pluripotentes.

En plus de la perte d'organisation spatiale des chromocentres, j'ai montré qu'en l'absence de Daxx, les chromocentres étaient plus souvent visibles à la périphérie du noyau. Dans le même temps, la modification d'histone associée à la périphérie nucléaire H3K9me2 est altérée dans le DaxxKO, uniquement en condition naïve de pluripotence et apparaît de manière discontinue. Cette perturbation de la distribution de H3K9me2 en condition naïve de pluripotence corrèle avec l'activation des gènes présents dans les domaines associés à la lamina, même si la relation de cause à effet reste à démontrer.

Lors de la relocalisation de DAXX en conditions hypométhylées, un corps nucléaire géant PML se forme également autour de DAXX. J'ai donc généré une lignée inactivée pour le gène *Pml* et observé que plusieurs phénotypes étaient communs aux Daxx et Pml KO. En effet, l'absence de Pml empêche la survie des cellules en conditions hypométhylées, entraîne une altération de l'organisation des chromocentres, ainsi que l'activation des gènes présent dans les domaines associés à la lamina spécifiquement en condition naïve de pluripotence. Cependant, l'absence de Pml n'impacte pas l'accumulation de DAXX aux chromocentres. De plus, en caractérisant les domaines de DAXX nécessaires au regroupement spatial des satellites majeurs, j'ai observé que seules les lysines de DAXX sujettes à la SUMOylation étaient requises pour cet effet de DAXX. Ces résultats suggèrent que PML pourrait avoir un rôle dans la régulation du mécanisme d'action de DAXX, possiblement par des modifications post-traductionnelles comme la SUMOylation.

Discussion

Ce travail a mis en évidence un nouveau rôle essentiel de DAXX, la chaperonne du variant d'histone H3.3, dans le maintien de l'hétérochromatine péricentromérique des cellules pluripotentes.

J'ai observé que lors de la conversion des ESC vers un milieu diminuant drastiquement le niveau de méthylation de l'ADN, DAXX accumulait fortement aux chromocentres et entraînait la relocalisation de PML autour de ces structures géantes de DAXX. De manière intéressante, une localisation similaire des DAXX aux régions péricentromériques a été décrite au cours des stades précoces du développement embryonnaire. Dans l'embryon, le recrutement de DAXX dépend de plusieurs protéines comme DPPA3 et le complexe PRC1. De plus, la perte de méthylation dans les cellules pluripotentes induit le recrutement de BEND3 et des protéines appartenant au complexe PRC1 aux chromocentres pour induire la modification H3K27me3. Il serait intéressant d'évaluer ces mêmes protéines participant au recrutement de DAXX. Cependant, BEND3 et les protéines du complexe PRC1 sont présents à la plupart des chromocentres, là où le recrutement n'est visible qu'à un nombre très limité de chromocentres lors de la conversion vers la condition naïve de pluripotence. Ces données suggèrent que le recrutement de DAXX pourrait être régulé par des mécanismes différents. Dans les cellules DnmtKO, il a été montré que DAXX se fixait à un certain nombre de d'éléments ERV. Il est intéressant de noter qu'une publication récente par Ostromyshenskii *et al.* rapportait que certains éléments ERV étaient dispersés entre les répétitions de satellites majeurs et étaient donc localisés dans les chromocentres. Il est possible que DAXX puisse être recruté à ces éléments ERV particuliers localisant aux chromocentres (PCH-ERV). Plus d'expériences seront nécessaires pour confirmer cette hypothèse qui ouvrirait de nouvelles perspectives sur un potentiel rôle des éléments ERV dans l'organisation 3D du génome.

Le ciblage de TET1 aux satellites majeurs peut générer l'accumulation de foyers γ H2AX aux chromocentres, démontrant que la déméthylation active de l'ADN peut mener à des dommages à l'ADN. De manière similaire, j'ai observé que la conversion vers l'état naïf de pluripotence entraînait une accumulation de foyers γ H2AX aux chromocentres. De plus, la génération des cassures double brin par CRISPR/Cas9 est suffisante pour induire le recrutement de DAXX aux satellites majeurs, démontrant que DAXX est relocalisé suite à des dommages à l'ADN. Cependant, le ciblage de NBS1, permettant d'induire une forte présence de γ H2AX aux chromocentres ne conduit pas à la relocalisation de DAXX, suggérant ainsi que DAXX ne fasse pas intrinsèquement parti de la voie de réponse aux dommages à l'ADN, mais peut être à un stade plus tardif pour la reformation de l'hétérochromatine.

Les chromocentres montrent une forte présence de la modification H3K9me3, déposée à cet endroit par les enzymes SUV39H1/2. Dans ce travail, j'ai montré que DAXX recrutait l'autre enzyme H3K9 tri-méthylase SETDB1 afin d'exercer son activité aux régions péri-centromériques. Des enzymes KDM permettant l'enlèvement de la modification H3K9me3 ont été impliqués dans le choix et le déroulement de voies de réparations de l'ADN. Cela suggère que la fonction de SETDB1 soit de rétablir la modification d'histone H3K9me3, éventuellement sur le variant H3.3. De futures études sont nécessaires pour mieux appréhender le mécanisme moléculaire permettant le recrutement des KDM puis de DAXX aux sites de cassures. Il est possible qu'un mécanisme similaire dépendant de l'activité de DAXX et de SETDB1 soit effectif dans les ESC en sérum contenant un fort niveau de méthylation. Toutefois, la présence de méthylation de l'ADN pourrait amener à un niveau de cassure plus bas qui générerait un recrutement de DAXX plus transitoire ou plus localisé, comme aux PCH-ERV, empêchant ainsi son observation par nos techniques d'imageries. De plus, une nouvelle compréhension de l'organisation des chromocentres est venue de la réalisation que HP1 α peut s'agréger par séparation de phase. Étonnamment, j'ai observé que l'absence de Daxx altérerait la dynamique et, de manière directe ou non, la capacité de séparation de phase de HP1 α . Comme le rassemblement des régions péri-centromériques induit par DAXX repose sur son lien avec H3.3, cela suggère qu'il puisse y avoir des différences encore inconnues de la fixation de HP1 α sur H3K9me3 et H3.3K9me3.

Enfin, j'ai observé que DAXX était essentiel pour la conversion des ESC vers un milieu diminuant drastiquement le niveau de méthylation de l'ADN. La fonction de DAXX aux chromocentres est de déposer H3.3 et de recruter SETDB1. Il est intéressant de noter que la perte de Setdb1 empêche la survie des cellules pluripotentes et également des cellules somatiques issues de leucémie. Dans cette direction, de futurs travaux devront déterminer si le recrutement essentiel de SETDB1 par DAXX est limité aux cellules pluripotentes, et ainsi étudier un possible rôle vital de DAXX lors de pertes chroniques du niveau de méthylation de l'ADN.

REFERENCES

REFERENCES

- Ablain J, Rice K, Soilihi H, De Reynies A, Minucci S, De Thé H. 2014. Activation of a promyelocytic leukemia-tumor protein 53 axis underlies acute promyelocytic leukemia cure. *Nat Med* **20**: 167–174.
- Adam S, Polo SE, Almouzni G. 2013. Transcription recovery after DNA damage requires chromatin priming by the H3.3 histone chaperone HIRA. *Cell* **155**: 94.
- Agger K, Cloos PAC, Christensen J, Pasini D, Rose S, Rappsilber J, Issaeva I, Canaani E, Salcini AE, Helin K. 2007. UTX and JMJD3 are histone H3K27 demethylases involved in HOX gene regulation and development. *Nature* **449**: 731–734.
- Aguirre-Lavin T, Adenot P, Bonnet-Garnier A, Lehmann G, Fleurot R, Boulesteix C, Debey P, Beaujean N. 2012. 3D-FISH analysis of embryonic nuclei in mouse highlights several abrupt changes of nuclear organization during preimplantation development. *BMC Dev Biol* **12**.
- Ahmad K, Henikoff S. 2002. The Histone Variant H3 . 3 Marks Active Chromatin by Replication-Independent Nucleosome Assembly. **9**: 1191–1200.
- Ahmed S, Brickner DG, Light WH, Cajigas I, McDonough M, Froysheter AB, Volpe T, Brickner JH. 2010. DNA zip codes control an ancient mechanism for gene targeting to the nuclear periphery. *Nat Cell Biol* **12**: 111–118.
- Ahvenainen T V., Mäkinen NM, Von Nandelstadh P, Vahteristo M, Pasanen AM, Bützow RC, Vahteristo P. 2018. Loss of ATRX / DAXX Expression and Alternative Lengthening of Telomeres in Uterine Leiomyomas. *Cancer* 4650–4656.
- Akhtar W, De Jong J, Pindyurin A V., Pagie L, Meuleman W, De Ridder J, Berns A, Wessels LFA, Van Lohuizen M, Van Steensel B. 2013. Chromatin position effects assayed by thousands of reporters integrated in parallel. *Cell* **154**: 914–927.
- Al-Sady B, Madhani HD, Narlikar GJ. 2013. Division of labor between the chromodomains of HP1 and Suv39 methylase enables coordination of heterochromatin spread. *Mol Cell* **51**: 80–91.
<http://dx.doi.org/10.1016/j.molcel.2013.06.013>.
- Alcobia I, Dilao R, Parreira L. 2000. Spatial associations of centromeres in the nuclei of hematopoietic cells: Evidence for cell-type-specific organizational patterns. *Blood* **95**: 1608–1615.
- Allshire RC, Karpen GH. 2008. Epigenetic

- regulation of centromeric chromatin: Old dogs, new tricks? *Nat Rev Genet* **9**: 923–937.
- Allshire RC, Madhani HD. 2017. Ten principles of heterochromatin formation and function. *Nat Rev Mol Cell Biol* **19**: 229–244. <http://dx.doi.org/10.1038/nrm.2017.119>.
- Amendola M, van Steensel B. 2015. Nuclear lamins are not required for lamina-associated domain organization in mouse embryonic stem cells. *EMBO Rep* **16**: 610–7. <http://www.ncbi.nlm.nih.gov/pubmed/25784758> <http://www.pubmedcentral.nih.gov/articlerender.fcgi?artid=PMC4428043>.
- Amir RE, Veyver IB Van Den, Wan M, Tran CQ, Francke U, Zoghbi HY. 1999. Rett syndrome is caused by mutations in X-linked MECP2, encoding methyl-CpG-binding protein 2. *Nat Genet* **23**: 185–188.
- Amodeo V, Deli A, Betts J, Bartesaghi S, Zhang Y, Richard-Londt A, Ellis M, Roshani R, Vouri M, Galavotti S, *et al.* 2017. A PML/Slit Axis Controls Physiological Cell Migration and Cancer Invasion in the CNS. *Cell Rep* **20**: 411–426. <http://dx.doi.org/10.1016/j.celrep.2017.06.047>.
- Amrichová J, Lukášová E, Kozubek S, Kozubek M. 2003. Nuclear and territorial topography of chromosome telomeres in human lymphocytes. *Exp Cell Res* **289**: 11–26.
- Arakawa T, Nakatani T, Oda M, Kimura Y, Sekita Y, Kimura T, Nakamura T, Nakano T. 2015. Stella controls chromocenter formation through regulation of Daxx expression in 2-cell embryos. *Biochem Biophys Res Commun* **466**: 60–65. <http://dx.doi.org/10.1016/j.bbrc.2015.08.106>.
- Arita K, Ariyoshi M, Tochio H, Nakamura Y, Shirakawa M. 2008. Recognition of hemi-methylated DNA by the SRA protein UHRF1 by a base-flipping mechanism. *Nature* **455**: 818–821.
- Armanios M, Chen J, Chang YC, Brodsky RA, Hawkins A, Griffin CA, Eshleman JR, Cohen AR, Chakravarti A, Hamosh A, *et al.* 2005. Haploinsufficiency of telomerase reverse transcriptase leads to anticipation in autosomal dominant dyskeratosis congenita. *Proc Natl Acad Sci* **102**: 1–5.
- Aucott R, Bullwinkel J, Yu Y, Shi W, Billur M, Brown JP, Menzel U, Kioussis D, Wang G, Reisert I, *et al.* 2008. HP1-beta is required for development of the cerebral neocortex and neuromuscular junctions. *J Cell Biol* **183**: 597–606. <http://www.ncbi.nlm.nih.gov/pubmed/19015315> (Accessed January 22, 2019).

- Avilion AA, Nicolis SK, Pevny LH, Perez L, Vivian N, Lovell-badge R. 2003. Multipotent cell lineages in early mouse development depend on SOX2 function. *Genes Dev* **17**: 126–140.
- Avvakumov G V, Walker JR, Xue S, Li Y, Duan S, Bronner C, Arrowsmith CH, Dhe-paganon S. 2008. Structural basis for recognition of hemi-methylated DNA by the SRA domain of human UHRF1. *Nature* **455**: 822–825.
- Azuara V, Perry P, Sauer S, Spivakov M, Jørgensen HF, John RM, Gouti M, Casanova M, Warnes G, Merkenschlager M, *et al.* 2006. Chromatin signatures of pluripotent cell lines. **8**.
- Azzalin CM, Reichenbach P, Khoriauli L, Giulotto E, Lingner J. 2007. Telomeric Repeat-Containing RNA and RNA Surveillance Factors at Mammalian Chromosome Ends. *Science (80-)* **318**: 798–802.
- Bachman KE, Rountree MR, Baylin SB. 2001. Dnmt3a and Dnmt3b Are Transcriptional Repressors That Exhibit Unique Localization Properties to Heterochromatin. *J Biol Chem* **276**: 32282–32287.
- Baldi S. 2019. Nucleosome positioning and spacing: From genome-wide maps to single arrays. *Essays Biochem* **63**: 5–14.
- Banani SF, Lee HO, Hyman AA, Rosen MK. 2017. Biomolecular condensates: Organizers of cellular biochemistry. *Nat Rev Mol Cell Biol* **18**: 285–298. <http://dx.doi.org/10.1038/nrm.2017.7>.
- Banani SF, Rice AM, Peeples WB, Lin Y, Jain S, Parker R, Rosen MK. 2016. Compositional Control of Phase-Separated Cellular Bodies. *Cell* **166**: 651–663. <http://dx.doi.org/10.1016/j.cell.2016.06.010>.
- Banaszynski LAA, Wen D, Dewell S, Whitcomb SJJ, Lin M, Diaz N, Elsässer SJ, Chapgier A, Goldberg ADD, Canaani E, *et al.* 2013. Hira-Dependent Histone H3.3 Deposition Facilitates PRC2 Recruitment at Developmental Loci in ES Cells. *Cell* **155**: 107–120. <http://dx.doi.org/10.1016/j.cell.2013.08.061>.
- Bannister AJ, Schneider R, Myers FA, Thorne AW, Crane-robinson C, Kouzarides T. 2005. Spatial Distribution of Di- and Tri-methyl Lysine 36 of Histone H3 at Active Genes *. *J Biol Chem* **280**: 17732–17736.
- Barau J, Zamudio N, Guillou F. 2016. The DNA methyltransferase DNMT3C protects male germ cells from transposon activity. *Science (80-)* **354**: 909–912.
- Barlow DP, Stöger R, Hermann BG, Saito K, Schweifer N. 1991. The mouse insulin-like growth factor type-2 receptor is imprinted and closely linked to the Tme

- locus. *Nature* **349**: 93–96.
- Barr ML, Bertram EG. 1949. A Morphological Distinction between Neurones of the Male and Female, and the Behaviour of the Nucleolar Satellite during Accelerated Nucleolar Protein Synthesis. *Nature* **163**: 676–677.
- Barthel FP, Wei W, Tang M, Martinez-ledesma E, Hu X, Amin SB, Akdemir KC, Seth S, Song X, Wang Q, *et al.* 2017. Systematic analysis of telomere length and somatic alterations in 31 cancer types. *Nat Genet* **49**: 349–357.
- Bartolomei MS, Zemel S, Tilghman SM. 1991. Parental imprinting of the mouse H19 gene. *Nature* **351**: 153–155.
- Baumann C, Viveiros MM, De La Fuente R. 2010. Loss of maternal ATRX results in centromere instability and aneuploidy in the mammalian oocyte and Pre-implantation embryo. *PLoS Genet* **6**.
- Beck CR, Garcia-perez L, Badge RM, Moran J V. 2011. LINE-1 Elements in Structural Variation and Disease. *Annu Rev Genomics Hum Genet* **12**: 187–215.
- Bejerano G, Lowe CB, Ahituv N, King B, Siepel A, Salama SR, Rubin EM, Kent WJ, Haussler D. 2006. A distal enhancer and an ultraconserved exon are derived from a novel retroposon. *Nature* **441**: 87–90.
- Belgnaoui SM, Gosden RG, Semmes OJ, Haoudi A. 2006. Human LINE-1 retrotransposon induces DNA damage and apoptosis in cancer cells. *Cancer Cell Int* **6**: 1–10.
- Ben-haim N, Lu C, Guzman-ayala M, Pescatore L, Mesnard D, Bischofberger M, Naef F, Robertson EJ, Constam DB, Drive R. 2006. The Nodal Precursor Acting via Activin Receptors Induces Mesoderm by Maintaining a Source of Its Convertases and BMP4. 313–323.
- Benitez JA, Ma J, D’Antonio M, Boyer A, Camargo MF, Zanca C, Kelly S, Khodadadi-Jamayran A, Jameson NM, Andersen M, *et al.* 2017. PTEN regulates glioblastoma oncogenesis through chromatin-associated complexes of DAXX and histone H3.3. *Nat Commun* **8**: 15223. <http://www.nature.com/doi/10.1038/ncomms15223>.
- Benleulmi SS, Matysiak J, Henriquez RR, Vaillant C, Lesbats P, Calmels C, Naughtin M, Leon O, Skalka AM, Ruff M, *et al.* 2015. Intasome architecture and chromatin density modulate retroviral integration into nucleosome. *Retrovirology* **12**: 1–16.
- Berkaeva M, Demakov S, Schwartz YB, Zhimulev I. 2009. Functional analysis of Drosophila polytene chromosomes decompacted unit: The interband. *Chromosom Res* **17**: 745–754.
- Berman B, Weisenberger D, Aman A, Hinoue T, Ramjan Z, Liu Y, Noushmehr H, Lange C, van Dijk C,

- Tollenaar R, *et al.* 2011. Regions of focal DNA hypermethylation and long-range hypomethylation in colorectal cancer coincide with nuclear lamina-associated domains. *Nat Genet* **4**: 40–46.
- Bernstein E, Kim SY, Carmell MA, Murchison EP, Alcorn H, Li MZ, Mills AA, Elledge SJ, Anderson K V., Hannon GJ. 2003. Dicer is essential for mouse development. *Nat Genet* **35**: 215–217.
- Berry J, Weber SC, Vaidya N, Haataja M, Brangwynne CP. 2015. RNA transcription modulates phase transition-driven nuclear body assembly. *Proc Natl Acad Sci* **112**: E5237–E5245.
<http://www.pnas.org/lookup/doi/10.1073/pnas.1509317112>.
- Bertero A, Pawlowski M, Ortmann D, Snijders K, Yiangou L, Brito MC De, Brown S, Bernard WG, Cooper JD, Giacomelli E, *et al.* 2016. Optimized inducible shRNA and CRISPR / Cas9 platforms for in vitro studies of human development using hPSCs. *Development* **143**: 4405–4418.
- Bertrand E, Houser-Scott F, Kendall A, Singer RH, Engelke DR. 1998. Nucleolar localization of early tRNA processing. *Genes Dev* **12**: 2463–2468.
- Bevington SL, Cauchy P, Cockerill PN. 2016. Chromatin priming elements establish immunological memory in T cells without activating transcription. *BioEssays* **39**: 1–12.
- Bian Q, Khanna N, Alvikas J, Belmont AS. 2013. β -Globin cis-elements determine differential nuclear targeting through epigenetic modifications. *J Cell Biol* **203**: 767–783.
- Bickmore WA, van Steensel B. 2013. Genome Architecture: Domain Organization of Interphase Chromosomes. *Cell* **152**: 1270–1284.
<http://linkinghub.elsevier.com/retrieve/pii/S0092867413001463>.
- Bickmore WA, Van Steensel B. 2013. Genome Architecture: Domain Organization of Interphase Chromosomes. *Cell* **152**: 1270–1284.
<http://dx.doi.org/10.1016/j.cell.2013.02.001>.
- Blaschke K, Ebata KT, Karimi MM, Zepeda-Martínez JA, Goyal P, Mahapatra S, Tam A, Laird DJ, Hirst M, Rao A, *et al.* 2013. Vitamin C induces Tet-dependent DNA demethylation and a blastocyst-like state in ES cells. *Nature* **500**: 222–226.
- Bodnar AG, Ouellette M, Frolkis M, Holt SE, Chiu C, Morin GB, Harley CB, Shay JW, Lichtsteiner S, Wright WE. 1998. Extension of Life-Span by Introduction of Telomerase into Normal Human Cells. *Science (80-)* **279**: 349–352.
- Boichuk S, Hu L, Makielski K, Pandolfi PP, Gjoerup O V. 2011. Functional

- Connection between Rad51 and PML in Homology-Directed Repair. *PLoS One* **6**.
- Bolzer A, Craig JM, Cremer T, Speicher MR. 1999. A complete set of repeat-depleted, PCR-amplifiable, human chromosome-specific painting probes. *Cytogenet Cell Genet* **84**: 233–240.
- Bolzer A, Kreth G, Solovei I, Koehler D, Saracoglu K, Fauth C, Mu S, Eils R, Cremer C, Speicher MR, *et al.* 2005. Three-Dimensional Maps of All Chromosomes in Human Male Fibroblast Nuclei and Prometaphase Rosettes. *PLoS Biol* **3**.
- Boroviak T, Loos R, Bertone P, Smith A, Nichols J. 2014. The ability of inner-cell-mass cells to self-renew as embryonic stem cells is acquired following epiblast specification. *Nat Cell Biol* **16**: 513–525.
- Boroviak T, Stirparo GG, Dietmann S, Hernando-herraez I, Mohammed H, Reik W, Smith A, Sasaki E, Nichols J, Bertone P. 2018. Single cell transcriptome analysis of human, marmoset and mouse embryos reveals common and divergent features of preimplantation development.
- Borsos M, Perricone SM, Schauer T, Pontabry J, de Luca KL, de Vries SS, Ruiz-Morales ER, Torres-Padilla ME, Kind J. 2019. Genome–lamina interactions are established de novo in the early mouse embryo. *Nature* **569**: 729–733.
- <http://dx.doi.org/10.1038/s41586-019-1233-0>.
- Bosch-Presegué L, Raurell-Vila H, Thackray JK, González J, Casal C, Kane-Goldsmith N, Vizoso M, Brown JP, Gómez A, Ausió J, *et al.* 2017. Mammalian HP1 Isoforms Have Specific Roles in Heterochromatin Structure and Organization. *Cell Rep* **21**: 2048–2057.
- Bostick M, Kim JK, Estève P-O, Clark A, Pradhan S, Jacobsen SE. 2007. UHRF1 Plays a Role in Maintaining DNA Methylation in Mammalian Cells. *Science (80-)* **317**: 1760–1765.
- Boveri T. 1909. Die Blastomerenkerne von *Ascaris megalocephala* und die Theorie der Chromosomenindividualität. *Arch Zellforsch* **3**: 181–268.
- Boyle S, Flyamer IM, Williamson I, Sengupta D, Bickmore WA, Illingworth RS. 2020. A central role for canonical PRC1 in shaping the 3D nuclear landscape. *Genes Dev* 1–19.
- Boyle S, Gilchrist S, Bridger JM, Mahy NL, Ellis JA, Bickmore WA. 2001. The spatial organization of human chromosomes within the nuclei of normal and emerin-mutant cells. *Hum Mol Genet* **10**: 211–219.
- Bradley A, Evans M, Kaufman MH, Robertson E. 1984. Formation of germ-line chimaeras from embryo-derived

- teratocarcinoma cell lines. *Nature* **309**: 255–256.
- Braunschweig U, Hogan GJ, Pagie L, Steensel B Van. 2009. Histone H1 binding is inhibited by histone variant H3.3. *EMBO J* **28**: 3635–3645. <http://dx.doi.org/10.1038/emboj.2009.301>.
- Briers S, Crawford C, Bickmore WA, Sutherland HG. 2009. KRAB zinc-finger proteins localise to novel KAP1-containing foci that are adjacent to PML nuclear bodies. *J Cell Sci* **122**: 937–946. <http://jcs.biologists.org/cgi/doi/10.1242/jcs.034793>.
- Brocks D, Assenov Y, Minner S, Bogatyrova O, Simon R, Koop C, Oakes C, Zucknick M, Lipka DB, Weischenfeldt J, *et al.* 2014. Intratumor DNA methylation heterogeneity reflects clonal evolution in aggressive prostate cancer. *Cell Rep* **8**: 798–806.
- Brons IGM, Smithers LE, Trotter MWB, Rugg-Gunn P, Sun B, Chuva De Sousa Lopes SM, Howlett SK, Clarkson A, Ahrlund-Richter L, Pedersen RA, *et al.* 2007. Derivation of pluripotent epiblast stem cells from mammalian embryos. *Nature* **448**: 191–195.
- Brown JP, Bullwinkel J, Baron-lühr B, Billur M, Schneider P, Winking H, Singh PB. 2010. HP1 γ function is required for male germ cell survival and spermatogenesis. *Epigenetics Chromatin* **3**: 1–9.
- Brown KE, Amoils S, Horn JM, Buckle VJ, Higgs DR, Merckenschlager M, Fisher AG. 2001. Expression of α - and β -globin genes occurs within different nuclear domains in haemopoietic cells. *Nat Cell Biol* **3**: 602–606.
- Brownell JE, Zhou J, Ranalli T, Kobayashi R, Edmondson DG, Roth SY, Allis CD. 1996. Tetrahymena Histone Acetyltransferase A: A Homolog to Yeast Gcn5p Linking Histone Acetylation to Gene Activation. **84**: 843–851.
- Bruin D De, Zaman Z, Liberatore RA, Ptashne M. 2001. Telomere looping permits gene activation by a downstream UAS in yeast. *Nature* **409**: 109–113.
- Bryan TM, Englezou A, Oalla-pozza L, Ounham MA, Reddel RR. 1997. Evidence for an alternative mechanism for maintaining telomere length in human tumors and tumor-derived cell line. *Nat Med* **3**: 1271–1274.
- Buenrostro JD, Giresi PG, Zaba LC, Chang HY, Greenleaf WJ. 2013. Transposition of native chromatin for fast and sensitive epigenomic profiling of open chromatin, DNA-binding proteins and nucleosome position. *Nat Methods* **10**: 1213–1218.
- Bulut-Karslioglu A, DeLaRosa-Velázquez IA, Ramirez F, Barenboim M, Onishi-

- Seebacher M, Arand J, Galán C, Winter GE, Engist B, Gerle B, *et al.* 2014. Suv39h-Dependent H3K9me3 Marks Intact Retrotransposons and Silences LINE Elements in Mouse Embryonic Stem Cells. *Mol Cell* **55**: 277–290.
- Bulut-Karslioglu A, Perrera V, Scaranaro M, De La Rosa-Velazquez IA, Van De Nobelen S, Shukeir N, Popow J, Gerle B, Opravil S, Pagani M, *et al.* 2012. A transcription factor-based mechanism for mouse heterochromatin formation. *Nat Struct Mol Biol* **19**: 1023–1032.
- Burns KH. 2017. Transposable elements in cancer. *Nat Rev Cancer* **17**: 415–424. <http://dx.doi.org/10.1038/nrc.2017.35>
- Burton A, Brochard V, Galan C, Ruiz-morales ER, Rovira Q, Rodriguez-terrones D, Kruse K, Gras S Le, Udayakumar VS, Chin HG, *et al.* 2020. Heterochromatin establishment during early mammalian development is regulated by pericentromeric RNA and characterized by non-repressive H3K9me3. *Nat Cell Biol.*
- Buschbeck M, Uribealago I, Wibowo I, Rué P, Martin D, Gutierrez A, Morey L, Guigó R, López-schier H, Croce L Di. 2009. The histone variant macroH2A is an epigenetic regulator of key developmental genes. *Nat Struct Mol Biol* **16**: 1074–1079.
- Butler JT, Hall LL, Smith KP, Lawrence JB. 2009. Changing nuclear landscape and unique PML structures during early epigenetic transitions of human embryonic stem cells. *J Cell Biochem* **107**: 609–614.
- Byrd K, Corces VG. 2003. Visualization of chromatin domains created by the gypsy insulator of *Drosophila*. *J Cell Biol* **162**: 565–574.
- Cabianca DS, Muñoz-Jiménez C, Kalck V, Gaidatzis D, Padeken J, Seeber A, Askjaer P, Gasser SM. 2019. Active chromatin marks drive spatial sequestration of heterochromatin in *C. elegans* nuclei. *Nature* **569**: 734–739. <http://dx.doi.org/10.1038/s41586-019-1243-y>.
- Canat A, Veillet A, Bonnet A, Therizols P. 2020. Genome anchoring to nuclear landmarks drives functional compartmentalization of the nuclear space. *Brief Funct Genomics* **00**: 1–10.
- Cao R, Wang L, Wang H, Xia L, Erdjument-Bromage H, Tempst P, Jones RS, Zhang Y. 2002. Role of Histone H3 Lysine 27 Methylation in Polycomb-Group Silencing. *Science (80-)* **298**: 1039–1044.
- Carbone R, Pearson M, Minucci S, Pelicci PG. 2002. PML NBs associate with the hMre11 complex and p53 at sites of irradiation induced DNA damage. *Oncogene* **21**: 1633–1640.
- Carracedo A, Ito K, Pandolfi PP. 2011. The nuclear bodies inside out: PML

- conquers the cytoplasm. *Curr Opin Cell Biol* **23**: 360–366. <http://dx.doi.org/10.1016/j.jceb.2011.03.011>.
- Carvalho C, Pereira HM, Ferreira J, Pina C, Mendonça D, Rosa AC, Carmo-Fonseca M. 2001. Chromosomal G-dark bands determine the spatial organization of centromeric heterochromatin in the nucleus. *Mol Biol Cell* **12**: 3563–3572.
- Casanova M, Pasternak M, ElMarjou F, LeBaccon P, Probst A V., Almouzni G. 2013. Heterochromatin Reorganization during Early Mouse Development Requires a Single-Stranded Noncoding Transcript. *Cell Rep* **4**: 1156–1167.
- Cecco M De, Ito T, Anna P, Elias AE, Skvir NJ, Steven W, Broccoli G, Adney EM, Boeke JD, Le O, *et al.* 2019. L1 drives IFN in senescent cells and promotes age-associated inflammation.
- Celeste A, Petersen S, Romanienko PJ, Fernandez-Capetillo O, Chen HT, Sedelnikova OA, Reina-San-Martin B, Coppola V, Meffre E, Difilippantonio MJ, *et al.* 2002. Genomic instability in mice lacking histone H2AX. *Science (80-)* **296**: 922–927.
- Chambers I, Silva J, Colby D, Nichols J, Nijmeijer B, Robertson M, Vrana J, Jones K, Grotewold L, Smith A. 2007. Nanog safeguards pluripotency and mediates germline development. *Nature* **450**: 3–8.
- Chang FTM, Chan FL, McGhie JDR, Udugama M, Mayne L, Collas P, Mann JR, Wong LH. 2015. CHK1-driven histone H3.3 serine 31 phosphorylation is important for chromatin maintenance and cell survival in human ALT cancer cells. *Nucleic Acids Res* **43**: 2603–2614.
- Chang FTM, McGhie JD, Chan FL, Tang MC, Anderson MA, Mann JR, Andy Choo KH, Wong LH. 2013. PML bodies provide an important platform for the maintenance of telomeric chromatin integrity in embryonic stem cells. *Nucleic Acids Res* **41**: 4447–4458.
- Chang HY, Nishitoh H, Yang X, Ichijo H, Baltimore D. 1998. Activation of Apoptosis Signal – Regulating Kinase 1 (ASK1) by the Adapter Protein Daxx. *Science (80-)* **281**: 1860–1864.
- Chedin F, Lieber MR, Hsieh C. 2002. The DNA methyltransferase-like protein DNMT3L stimulates de novo methylation by Dnmt3a. *Proc Natl Acad Sci*.
- Chen C-K, Blanco M, Jackson C, Aznauryan E, Ollikainen N, Surka C, Chow A, Cerase A, McDonel P, Guttman M. 2016. Xist recruits the X chromosome to the nuclear lamina to enable chromosome-wide silencing. *Science (80-)* **354**: 468–473.
- Chen H, Guo R, Zhang Q, Guo H, Yang M, Wu Z, Gao S, Liu L, Chen L. 2015. Erk

- signaling is indispensable for genomic stability and self-renewal of mouse embryonic stem cells. *Proc Natl Acad Sci U S A* **112**: E5936–E5943.
- Chen P, Zhao J, Wang Y, Wang M, Long H, Liang D, Huang L, Wen Z, Li W, Li X, *et al.* 2013. H3.3 actively marks enhancers and primes gene transcription via opening higher-ordered chromatin. *Genes Dev* **27**: 2109–2124.
- Chen ZH, Zhu M, Yang J, Liang H, He J, He S, Wang P, Kang X, McNutt MA, Yin Y, *et al.* 2014. PTEN Interacts with Histone H1 and controls chromatin condensation. *Cell Rep* **8**: 2003–2014. <http://dx.doi.org/10.1016/j.celrep.2014.08.008>.
- Chiappinelli KB, Strissel PL, Desrichard A, Li H, Henke C, Akman B, Hein A, Rote NS, Cope LM, Snyder A, *et al.* 2015. Inhibiting DNA Methylation Causes an Interferon Response in Cancer via dsRNA Including Endogenous Retroviruses. *Cell* **162**: 974–86. <http://www.ncbi.nlm.nih.gov/pubmed/26317466> (Accessed January 22, 2019).
- Ching RW, Ahmed K, Boutros PC, Penn LZ, Bazett-jones DP. 2013. Identifying gene locus associations with promyelocytic leukemia nuclear bodies using immunotRAP. *J Cell Biol* **201**: 325–335.
- Cho S, Park JS, Kang YK. 2011. Dual functions of histone-lysine N-methyltransferase Setdb1 protein at promyelocytic leukemia-nuclear body (PML-NB): Maintaining PML-NB structure and regulating the expression of its associated genes. *J Biol Chem* **286**: 41115–41124.
- Cho SW, Kim S, Kim Y, Kweon J, Kim HS, Bae S, Kim J. 2014. Analysis of off-target effects of CRISPR Cas-derived RNA-guided endonucleases and nickases sup2. *Genome Res* **24**: 132–141.
- Christensen MO, Krokowski RM, Barthelmes HU, Hock R, Boege F, Mielke C. 2004. Distinct effects of topoisomerase I and RNA polymerase I inhibitors suggest a dual mechanism of nucleolar/nucleoplasmic partitioning of topoisomerase I. *J Biol Chem* **279**: 21873–21882.
- Chuong EB, Elde NC, Feschotte C. 2017. Regulatory activities of transposable elements: from conflicts to benefits. *Nat Rev Genet* **18**: 71–86.
- Clouaire T, Webb S, Skene P, Illingworth R, Kerr A, Andrews R, Lee J, Skalnik D, Bird A. 2012. Cfp1 integrates both CpG content and gene activity for accurate H3K4me3 deposition in embryonic stem cells. *Genes Dev* **26**: 1714–1728.
- Clowney EJ, Legros MA, Mosley CP, Clowney FG, Markenskoff-papadimitriou EC, Myllys M, Barnea G, Larabell CA. 2012. Nuclear Aggregation of Olfactory Receptor Genes Governs Their Monogenic Expression. *Cell* **151**:

- 724–737.
<http://dx.doi.org/10.1016/j.cell.2012.09.043>.
- Clynes D, Jelinska C, Xella B, Ayyub H, Scott C, Mitson M, Taylor S, Higgs DR, Gibbons RJ. 2015. Suppression of the alternative lengthening of telomere pathway by the chromatin remodelling factor ATRX. *Nat Commun* **6**: 7538. <http://www.pubmedcentral.nih.gov/articlerender.fcgi?artid=4501375&tool=pmcentrez&rendertype=abstract>.
- Cobb BS, Morales-Alcelay S, Kleiger G, Brown KE, Fisher AG, Smale ST. 2000. Targeting of Ikaros to pericentromeric heterochromatin by direct DNA binding. *Genes Dev* **14**: 2146–2160.
- Cohen C, Corpet A, Roubille S, Maroui MA, Pocard N, Rousseau A, Kleijwegt C, Binda O, Texier P, Sawtell N, *et al.* 2018. Promyelocytic leukemia (PML) nuclear bodies (NBs) induce latent / quiescent HSV-1 genomes chromatinization through a PML NB / Histone H3 . 3 / H3 . 3 Chaperone Axis. *PLoS Pathog* **1**–39.
- Cohen SB, Graham ME, O. LG, Bache N, Robinson PJ, Reddel RR. 2007. Protein Composition of Catalytically Active Human Telomerase from Immortal Cells. *Science (80-)* **315**: 1850–1854.
- Colmenares SU, Swenson JM, Langley SA, Kennedy C, Costes S V., Karpen GH. 2017. Drosophila Histone Demethylase KDM4A Has Enzymatic and Non-enzymatic Roles in Controlling Heterochromatin Integrity Drosophila Histone Demethylase KDM4A Has Enzymatic and Non-enzymatic Roles in Controlling Heterochromatin Integrity. *Dev Cell* **42**: 156-169.e5. <http://dx.doi.org/10.1016/j.devcel.2017.06.014>.
- Comet I, Rüsing EM, Leblanc B, Helin K. 2016. Maintaining cell identity: PRC2 - mediated regulation of transcription and cancer. *Nat Rev Cancer* **16**: 803–810.
- Comings DE. 1968. The rationale for an ordered arrangement of chromatin in the interphase nucleus. *Am J Hum Genet* **20**: 440–460.
- Condemine W, Takahashi Y, Le Bras M, de Thé H. 2007. A nucleolar targeting signal in PML-I addresses PML to nucleolar caps in stressed or senescent cells. *J Cell Sci* **120**: 3219–3227. <http://jcs.biologists.org/cgi/doi/10.1242/jcs.007492>.
- Condemine W, Takahashi Y, Zhu J, Puvion-dutilleul F, Guegan S, Janin A, de Thé H. 2006. Characterization of Endogenous Human Promyelocytic Leukemia Isoforms. *Cancer Res* **66**: 6192–6199.
- Constantinescu D, Gray HL, Sammak PJ, Schatten G, Csoka AB. 2006. Lamin A/C Expression Is a Marker of Mouse and Human Embryonic Stem Cell

- Differentiation. *Stem Cells* **24**: 177–185.
- Cooper S, Dienstbier M, Hassan R, Schermelleh L, Sharif J, Blackledge NP, DeMarco V, Elderkin S, Koseki H, Klose R, *et al.* 2014. Targeting Polycomb to Pericentric Heterochromatin in Embryonic Stem Cells Reveals a Role for H2AK119u1 in PRC2 Recruitment. *Cell Rep* **7**: 1456–1470. <http://dx.doi.org/10.1016/j.celrep.2014.04.012>.
- Corpet A, Olbrich T, Gwerder M, Fink D, Stucki M. 2014. Dynamics of histone H3.3 deposition in proliferating and senescent cells reveals a DAXX-dependent targeting to PML-NBs important for pericentromeric heterochromatin organization. *Cell Cycle* **13**: 249–267.
- Cortellino S, Xu J, Sannai M, Moore R, Caretti E, Cigliano A, Coz M Le, Devarajan K, Wessels A, Soprano D, *et al.* 2011. Thymine DNA Glycosylase Is Essential for Active DNA Demethylation by Linked Deamination-Base Excision Repair. *Cell* **146**: 67–79. <http://dx.doi.org/10.1016/j.cell.2011.06.020>.
- Cosby RL, Chang NC, Feschotte C. 2019. Host–transposon interactions: Conflict, cooperation, and cooption. *Genes Dev* **33**: 1098–1116.
- Cossec J, Theurillat I, Chica C, Bua Aguin S, Gaume X, Andrieux A, Iturbide A, Jouvion G, Li H, Bossis G, *et al.* 2018. SUMO Safeguards Somatic and Pluripotent Cell Identities by Enforcing Distinct Chromatin States. *Cell Stem Cell* 1–16.
- Costanzi C, Pehrson JR. 1998. Histone macroH2A1 is concentrated in the inactive X chromosome of female mammals. *Nature* **628**: 1997–1999.
- Coura Koné M, Fleurot R, Chebrou M, Debey P, Beaujean N, Bonnet-Garnier A. 2016. Three-Dimensional Distribution of UBF and Nopp140 in Relationship to Ribosomal DNA Transcription During Mouse Preimplantation Development1. *Biol Reprod* **94**: 1–12.
- Cournac A, Koszul R, Mozziconacci J, Curie M. 2016. The 3D folding of metazoan genomes correlates with the association of similar repetitive elements. *Nucleic Acids Res* **44**: 245–255.
- Cowell IG, Sunter NJ, Singh PB, Austin CA, Durkacz BW, Tilby MJ. 2007. γ H2AX Foci Form Preferentially in Euchromatin after. *PLoS One* 1–8.
- Crabbe L, Cesare AJ, Kasuboski JM, Fitzpatrick JAJ, Karlseder J. 2012. Human Telomeres Are Tethered to the Nuclear Envelope during Postmitotic Nuclear Assembly. *Cell Rep* **2**: 1521–1529.
- Croft JA, Bridger JM, Boyle S, Perry P, Teague P, Bickmore WA. 1999.

- Differences in the localization and morphology of chromosomes in the human nucleus. *J Cell Biol* **145**: 1119–1131.
- Cuellar L, Herzner AM, Zhang X, Goyal Y, Watanabe C, Friedman BA, Janakiraman V, Durinck S, Stinson J, Arnott D, *et al.* 2017. Silencing of retrotransposons by SET DB1 inhibits the interferon response in acute myeloid leukemia. *J Cell Biol* **216**: 3535–3549.
- Czapiewski R, Robson MI, Schirmer EC. 2016. Anchoring a Leviathan: How the nuclear membrane tethers the genome. *Front Genet* **7**: 1–13.
- Dan J, Yang J, Liu Y, Xiao A, Liu LIN, Al DANET. 2015. Roles for Histone Acetylation in Regulation of Telomere Elongation and Two-cell State in Mouse ES Cells. *J Cell Physiol.*
- Daniali L, Benetos A, Susser E, Kark JD, Labat C, Kimura M, Desai KK, Granick M, Aviv A. 2013. Telomeres shorten at equivalent rates in somatic tissues of adults. *Nat Commun* **4**: 1–7.
- Daniel MT, Koken M, Romagn O, Barbey S, Bazarbachi A, Stadler M, Guillemin MC, Degos L, Chomienne C, de Thé H. 1993. PML Protein Expression in Hematopoietic and Acute Promyelocytic Leukemia Cells. *Blood* **82**: 1858–1867.
- Daskalos A, Nikolaidis G, Xinarianos G, Savvari P, Cassidy A, Zakopoulou R. 2009. Hypomethylation of retrotransposable elements correlates with genomic instability in non-small cell lung cancer. *Int J Cancer* **87**: 81–87.
- Davidson KC, Mason EA, Pera MF. 2015. The pluripotent state in mouse and human. *Development* 3090–3099.
- Dawlaty MM, Breiling A, Le T, Barrasa MI, Cheng AW, Gao Q, Powell BE, Li Z, Xu M, Faull KF, *et al.* 2013. Combined Deficiency of Tet1 and Tet2 Causes Epigenetic Abnormalities but Is Compatible with Postnatal Development. *Dev Cell* **3**: 310–323.
- De La Fuente R, Baumann C, Viveiros MM. 2015. ATRX contributes to epigenetic asymmetry and silencing of major satellite transcripts in the maternal genome of the mouse embryo. *Development* **142**: 1806–1817. <http://dev.biologists.org/cgi/doi/10.1242/dev.118927>.
- de Lange T. 2018. Shelterin-Mediated Telomere Protection. *Annu Rev Genet* **52**: 223–247.
- Deaton AM, Gómez-Rodríguez M, Mieczkowski J, Tolstorukov MY, Kundu S, Sadreyev RI, Jansen LET, Kingston RE. 2016. Enhancer regions show high histone H3.3 turnover that changes during differentiation. *Elife* **5**: 1–24.
- DeChiara TM, Robertson EJ, Efstratiadis A. 1991. Parental Imprinting of the Mouse

- Insulin-like Growth Factor II Gene. *Cell* **64**: 849–859.
- Deininger P. 2011. Alu elements : know the SINEs. *Genome Biol* **12**: 1–12.
- Déjardin J, Kingston RE. 2009. Purification of Proteins Associated with Specific Genomic Loci. *Cell* **136**: 175–186.
- Delbarre E, Ivanauskienė K, Ku T, Collas P, Küntziger T, Collas P. 2013. DAXX-dependent supply of soluble (H3.3-H4) dimers to PML bodies pending deposition into chromatin. *Genome Res* **23**: 440–451.
- Delbarre E, Ivanauskienė K, Spirkoski J, Shah A, Vekterud K, Oivind Moskaug J, Ove Boe S, Wong LH, Küntziger T, Collas P. 2017. PML protein organizes heterochromatin domains where it regulates histone H3 . 3 loading by ATRX / DAXX. *Genome Res* 1–6.
- Delhommeau F, Dupont S, Della Valle V, James C, Trannoy S, Massé A, Kosmider O, Couedic J Le, Alberdi A, Lécluse Y, *et al.* 2009. Mutation in TET2 in Myeloid Cancers. *New Engl J Med* **360**: 2289–2301.
- Dellaire G, Ching RW, Ahmed K, Jalali F, Tse KCK, Bristow RG, Bazett-jones DP. 2006. Promyelocytic leukemia nuclear bodies behave as DNA damage sensors whose response to DNA double-strand breaks is regulated by NBS1 and the kinases ATM, Chk2, and ATR. *J Cell Biol* **175**: 55–66.
- Deng Q, Ramsköld D, Reinius B, Sandberg R. 2014. Single-Cell RNA-Seq Reveals Dynamic, Random Monoallelic Gene Expression in Mammalian Cells. *Science (80-)* **343**: 193–196.
- Dennis K, Fan T, Geiman T, Yan Q, Muegge K. 2001. Lsh , a member of the SNF2 family , is required for genome-wide methylation. *Genes Dev* **15**: 2940–2944.
- Di Masi A, Cilli D, Berardinelli F, Talarico A, Pallavicini I, Pennisi R, Leone S, Antoccia A, Noguera NI, Lo-Coco F, *et al.* 2016. PML nuclear body disruption impairs DNA double-strand break sensing and repair in APL. *Cell Death Dis* **7**: e2308-13. <http://dx.doi.org/10.1038/cddis.2016.115>.
- Dillinger S, Straub T, Nemeth A. 2017. Nucleolus association of chromosomal domains is largely maintained in cellular senescence despite massive nuclear reorganisation. *PLoS One* **12**: 1–28.
- Dimitrova N, Chen YM, Spector DL, Lange T De. 2008. 53BP1 promotes non-homologous end joining of telomeres by increasing chromatin mobility. *Nature* **456**: 524–528.
- Dixon JR, Selvaraj S, Yue F, Kim A, Li Y, Shen Y, Hu M, Liu JS, Ren B. 2012. Topological domains in mammalian genomes identified by analysis of chromatin interactions. *Nature* **485**: 376–380.

- <http://dx.doi.org/10.1038/nature11082>
- 2%5Cn<http://www.nature.com/doi/finder/10.1038/nature11082>.
- Dodge JE, Kang YK, Beppu H, Lei H, Li E. 2004. Histone H3-K9 methyltransferase ESET is essential for early development. *Mol Cell Biol* **24**: 2478–2486. [file:///C:/Afile:///Documents and Settings/Jianlong Wang/Local Settings/Application Data/Quosa/Data/My Citations/e74notonl22kv3bddo2jpc11lo.qpw%0Ahttp://www.ncbi.nlm.nih.gov/entrez/query.fcgi?cmd=Retrieve&db=pubmed&dopt=Citation&list_uids=14993285%0Ahttp://www.ncbi.nlm.nih.gov/entrez/query.fcgi?cmd=Retrieve&db=pubmed&dopt=Citation&list_uids=14993285](http://www.ncbi.nlm.nih.gov/entrez/query.fcgi?cmd=Retrieve&db=pubmed&dopt=Citation&list_uids=14993285)
- Dodge JE, Okano M, Dick F, Tsujimoto N, Chen T, Wang S, Ueda Y, Dyson N, Li E. 2005. Inactivation of Dnmt3b in Mouse Embryonic Fibroblasts Results in DNA Hypomethylation, Chromosomal Instability, and Spontaneous Immortalization *. *J Biol Chem* **280**: 17986–17991.
- Douet J, Corujo D, Malinverni R, Renaud J, Sansoni V, Posavec Marjanović M, Cantariño N, Valero V, Mongelard F, Bouvet P, *et al.* 2017. MacroH2A histone variants maintain nuclear organization and heterochromatin architecture. *J Cell Sci* **130**: 1570–1582. <http://jcs.biologists.org/lookup/doi/10.1242/jcs.199216>.
- Drané P, Ouararhni K, Depaux A, Shuaib M, Hamiche A. 2010. The death-associated protein DAXX is a novel histone chaperone involved in the replication-independent deposition of H3.3. *Genes Dev* **24**: 1253–1265.
- Draskovic I, Arnoult N, Steiner V, Bacchetti S, Lomonte P, Londono-Vallejo A. 2009. Probing PML body function in ALT cells reveals spatiotemporal requirements for telomere recombination. *Proc Natl Acad Sci* **106**: 15726–15731. <http://www.pnas.org/cgi/doi/10.1073/pnas.0907689106>.
- Du Z, Zheng H, Huang B, Ma R, Wu J, Zhang X, He J, Xiang Y, Wang Q, Li Y, *et al.* 2017. Allelic reprogramming of 3D chromatin architecture during early mammalian development. *Nature* **547**: 232–235. <http://www.nature.com/doi/finder/10.1038/nature23263>.
- Dunleavy EM, Roche D, Tagami H, Lacoste N, Ray-Gallet D, Nakamura Y, Daigo Y, Nakatani Y, Almouzni-Pettinotti G. 2009. HJURP Is a Cell-Cycle-Dependent Maintenance and Deposition Factor of CENP-A at Centromeres. *Cell* **137**: 485–497.
- Duprez E, Saurin AJ, Desterro JM, Lallemand-breitenbach V, Howe K, Boddy MN, Solomon E, Thé H De, Hay RT, Freemont PS. 1999. SUMO-1 modification of the acute promyelocytic

- leukaemia protein PML: implications for nuclear localisation. *J Cell Sci* **393**: 381–393.
- Dutrieux J, Maarifi G, Portilho DM, Arhel NJ, Chelbi-Alix MK, Nisole S. 2015. PML/TRIM19-Dependent Inhibition of Retroviral Reverse-Transcription by Daxx. *PLoS Pathog* **11**: e1005280. <http://dx.plos.org/10.1371/journal.ppat.1005280>.
- Dyck JA, Maul GG, Miller WH, Chen JD, Kakizuka A, Evans RM. 1994. A Novel Macromolecular Structure Is a Target of the Promyelocyte-Retinoic Acid Receptor Oncoprotein. *Cell* **76**: 333–343.
- Dyer KA, Canfield TK, Gartler SM. 1989. Molecular cytological differentiation of active from inactive X domains in interphase: implications for X chromosome inactivation. *Cytogenet Cell Genet* **50**: 116–20. <http://www.ncbi.nlm.nih.gov/pubmed/2776476> (Accessed May 11, 2020).
- Dyer MA, Qadeer ZA, Valle-Garcia D, Bernstein E. 2017. ATRX and DAXX: Mechanisms and mutations. *Cold Spring Harb Perspect Med* **7**.
- Eckersley-maslin MA, Bergmann JH, Lazar Z, Spector DL. 2013. Lamin A / C is expressed in pluripotent mouse embryonic stem cells © 2013 Landes Bioscience . Do not distribute © 2013 Landes Bioscience . Do not distribute. 53–60.
- Eckersley-Maslin MA, Svensson V, Krueger C, Stubbs TM, Giehr P, Krueger F, Miragaia RJ, Kyriakopoulos C, Berrens R V., Milagre I, *et al.* 2016. MERVL/Zscan4 Network Activation Results in Transient Genome-wide DNA Demethylation of mESCs. *Cell Rep* **17**: 179–192.
- Efroni S, Dutttagupta R, Cheng J, Dehghani H, Hoepfner DJ, Dash C, Bazett-jones DP, Grice S Le, Mckay RDG, Buetow KH, *et al.* 2008. Global Transcription in Pluripotent Embryonic Stem Cells. *Cell Stem Cell* **2**: 437–447.
- Elsässer SJ, Huang H, Lewis PW, Chin JW, Allis CD, Patel DJ. 2012. DAXX envelops a histone H3.3-H4 dimer for H3.3-specific recognition. *Nature* **491**: 560–5. <http://www.pubmedcentral.nih.gov/articlerender.fcgi?artid=4056191&tool=pmcentrez&rendertype=abstract>.
- Elsässer SJ, Noh K-M, Diaz N, Allis CD, Banaszynski LA. 2015. Histone H3.3 is required for endogenous retroviral element silencing in embryonic stem cells. *Nature* **522**: 240–4. <http://www.ncbi.nlm.nih.gov/pubmed/25938714>.
- Endoh M, Endo TA, Endoh T, Fujimura Y, Ohara O, Toyoda T, Otte AP, Okano M, Brockdorff N, Vidal M, *et al.* 2008. Polycomb group proteins Ring1A / B

- are functionally linked to the core transcriptional regulatory circuitry to maintain ES cell identity. *Development* **1524**: 1513–1524.
- Entrevan M, Schuettengruber B, Cavalli G. 2016. Regulation of Genome Architecture and Function by Polycomb Proteins. *Trends Cell Biol* **26**: 511–525. <http://dx.doi.org/10.1016/j.tcb.2016.04.009>.
- Erdel F, Rademacher A, Vlijm R, Tünnermann J, Frank L, Weinmann R, Schweigert E, Yserentant K, Hummert J, Bauer C, *et al.* 2020. Mouse Heterochromatin Adopts Digital Compaction States without Showing Hallmarks of HP1-Driven Liquid-Liquid Phase Separation Article Mouse Heterochromatin Adopts Digital Compaction States without Showing Hallmarks of HP1-Driven Liquid-Liquid Phase Separation. *Mol Cell* **78**: 236–249.
- Escobar-Cabrera E, Okon M, Lau DKW, Dart CF, Bonvin AMJJ, McIntos LP. 2011. Characterizing the N- and C-terminal small ubiquitin-like modifier (SUMO)-interacting motifs of the scaffold protein DAXX. *J Biol Chem* **286**: 19816–19829.
- Esnault C, Heidmann O, Delebecque F, Dewannieux M, Ribet D, Hance AJ, Heidmann T, Schwartz O. 2005. APOBEC3G cytidine deaminase inhibits retrotransposition of endogenous retroviruses. *Nature* **433**: 1–4.
- Evans MJ, Kaufman MH. 1981. Establishment in culture of pluripotential cells from mouse embryos. *Nature* **292**: 154–156.
- Fadloun A, Le Gras S, Jost B, Ziegler-Birling C, Takahashi H, Gorab E, Carninci P, Torres-Padilla ME. 2013. Chromatin signatures and retrotransposon profiling in mouse embryos reveal regulation of LINE-1 by RNA. *Nat Struct Mol Biol* **20**: 332–338.
- Falaleeva M, Pages A, Matuszek Z, Hidmi S, Agranat-Tamir L, Korotkov K, Nevo Y, Eyraş E, Sperling R, Stamm S. 2016. Dual function of C/D box small nucleolar RNAs in rRNA modification and alternative pre-mRNA splicing. *Proc Natl Acad Sci U S A* **113**: E1625–E1634.
- Falck J, Coates J, Jackson SP. 2005. Conserved modes of recruitment of ATM, ATR and DNA-PKcs to sites of DNA damage. *Nature* **434**: 605–611.
- Fan Y, Nikitina T, Morin-kensicki EM, Zhao J, Magnuson TR, Woodcock CL, Skoultchi AI. 2003. H1 Linker Histones Are Essential for Mouse Development and Affect Nucleosome Spacing In Vivo. *Mol Cell Biol* **23**: 4559–4572.
- Fang H-T, EL Farran CA, Xing QR, Zhang L-F, Li H, Lim B, Loh Y-H. 2018. Global H3.3 dynamic deposition defines

- its bimodal role in cell fate transition. *Nat Commun* **9**: 1537. <http://www.nature.com/articles/s41467-018-03904-7>.
- Ferguson-smith AC, Cattanaach BM, Barton SC, Beechey C V., Surani AM. 1991. Embryological and molecular investigations of parental imprinting on mouse chromosome 7. *Nature* **351**: 667–670.
- Feric M, Vaidya N, Harmon TS, Mitrea DM, Zhu L, Richardson TM, Kriwacki RW, Pappu R V., Brangwynne CP. 2016. Coexisting Liquid Phases Underlie Nucleolar Subcompartments. *Cell* **165**: 1686–1697.
- Fernandez-Capetillo O, Chen H, Celeste A, Ward I, Romanienko PJ, Morales JC, Naka K, Xia Z, Camerini-otero RD, Motoyama N, *et al.* 2002. DNA damage-induced G2 – M checkpoint activation by histone H2AX and 53BP1. *Nat Cell Biol* **4**: 993–998.
- Feschotte C, Gilbert C. 2012. Endogenous viruses : insights into viral evolution and impact on host biology. *Nat Rev Genet* **13**: 283–296.
- Ficz G, Hore TA, Santos F, Lee HJ, Dean W, Arand J, Krueger F, Oxley D, Paul YL, Walter J, *et al.* 2013. FGF signaling inhibition in ESCs drives rapid genome-wide demethylation to the epigenetic ground state of pluripotency. *Cell Stem Cell* **13**: 351–359.
- Fiebig U, Hartmann MG, Bannert N, Kurth R, Denner J. 2006. Transspecies Transmission of the Endogenous Koala Retrovirus. *J Virol* **80**: 5651–5654.
- Filion GJ, Bommel JG Van, Braunschweig U, Talhout W, Kind J, Ward LD, Castro J De, Kerkhoven RM, Bussemaker HJ, Steensel B Van, *et al.* 2010. Systematic Protein Location Mapping Reveals Five Principal Chromatin Types in Drosophila Cells. *Cell* **143**: 212–224.
- Finch JT, Klug A. 1976. Solenoidal model for superstructure in chromatin. *Proc Natl Acad Sci U S A* **73**: 1897–1901.
- Finlan LE, Sproul D, Thomson I, Boyle S, Kerr E, Perry P, Chubb JR, Bickmore WA. 2008. Recruitment to the Nuclear Periphery Can Alter Expression of Genes in Human Cells. *PLoS Genet* **4**.
- Fisher DZ, Chaudhary N, Blobel G. 1986. cDNA sequencing of nuclear lamins A and C reveals primary and secondary structural homology to intermediate filament proteins. *Proc Natl Acad Sci U S A* **83**: 6450–6454.
- Fogarty NME, Mccarthy A, Snijders KE, Powell BE, Kubikova N, Blakeley P, Lea R, Elder K, Wamaitha SE, Kim D, *et al.* 2017. Genome editing reveals a role for OCT4 in human embryogenesis. *Nature* **550**: 67–73. <http://dx.doi.org/10.1038/nature24033>
- Foltz DR, Jansen LET, Bailey AO, Yates JR,

- Bassett EA, Wood S, Black BE, Cleveland DW. 2009. Centromere-Specific Assembly of CENP-A Nucleosomes Is Mediated by HJURP. *Cell* **137**: 472–484. <http://dx.doi.org/10.1016/j.cell.2009.02.039>.
- Francastel C, Walters MC, Groudine M, Martin DIK. 1999. A functional enhancer suppresses silencing of a transgene and prevents its localization close to centromeric heterochromatin. *Cell* **99**: 259–269.
- Frey A, Listovsky T, Guilbaud G, Sarkies P, Sale JE. 2014. Histone H3.3 is required to maintain replication fork progression after UV damage. *Curr Biol* **24**: 2195–2201. <http://www.ncbi.nlm.nih.gov/pubmed/25201682> (Accessed January 18, 2019).
- Friedli M, Trono D. 2015. The Developmental Control of Transposable Elements and the Evolution of Higher Species. *Annu Rev Cell Dev Biol* **31**: 429–451.
- Fritsch L, Robin P, Mathieu JRR, Souidi M, Hinaux H, Rougeulle C, Harel-Bellan A, Ameyar-Zazoua M, Ait-Si-Ali S. 2010. A Subset of the Histone H3 Lysine 9 Methyltransferases Suv39h1, G9a, GLP, and SETDB1 Participate in a Multimeric Complex. *Mol Cell* **37**: 46–56.
- Frost B, Hemberg M, Lewis J, Feany MB. 2014. Tau promotes neurodegeneration through global chromatin relaxation. *Nat Neurosci* **17**: 357–366. <http://dx.doi.org/10.1038/nn.3639>.
- Fu Y, Lv P, Yan G, Fan H, Cheng L, Zhang F, Dang Y. 2015. MacroH2A1 associates with nuclear lamina and maintains chromatin architecture in mouse liver cells. *Sci Rep* 1–12. <http://dx.doi.org/10.1038/srep17186>.
- Fukuda K, Okuda A, Yusa K, Shinkai Y. 2018. A CRISPR knockout screen identifies SETDB1-target retroelement silencing factors in embryonic stem cells. 1–13.
- Fussner E, Ching RW, Bazett-Jones DP. 2011. Living without 30nm chromatin fibers. *Trends Biochem Sci* **36**: 1–6. <http://dx.doi.org/10.1016/j.tibs.2010.09.002>.
- Gagnon-Kugler T, Langlois F, Stefanovsky V, Lessard F, Moss T. 2009. Loss of Human Ribosomal Gene CpG Methylation Enhances Cryptic RNA Polymerase II Transcription and Disrupts Ribosomal RNA Processing. *Mol Cell* **35**: 414–425.
- Galati A, Magdinier F, Colasanti V, Bauwens S, Pinte S, Ricordy R, Giraud-Panis MJ, Pusch MC, Savino M, Cacchione S, *et al.* 2012. TRF2 Controls Telomeric Nucleosome Organization in a Cell Cycle Phase-Dependent Manner. *PLoS One* **7**: 1–10.

- Gamble MJ, Frizzell KM, Yang C, Krishnakumar R, Kraus WL. 2010. The histone variant macroH2A1 marks repressed autosomal chromatin, but protects a subset of its target genes from silencing. *Genes Dev* **24**: 21–32.
- Gang Wang Z, Delva L, Gaboli M, Rivi R, Giorgio M, Cordon-Cardo C, Grosveld F, Pandolfi P. 1998. Role of PML in Cell Growth and the Retinoic Acid Pathway. *Science (80-)* **279**: 1547–1551. <http://www.sciencemag.org/cgi/doi/10.1126/science.279.5356.1547>.
- García-Cao M, O’Sullivan R, Peters AHFM, Jenuwein T, Blasco MA. 2004. Epigenetic regulation of telomere length in mammalian cells by the Suv39h1 and Suv39h2 histone methyltransferases. *Nat Genet* **36**: 94–99.
- Garrido-Ramos M. 2017. Satellite DNA: An Evolving Topic. *Genes (Basel)* **8**: 230. <http://www.mdpi.com/2073-4425/8/9/230> (Accessed May 6, 2020).
- Gasior SL, Wakeman TP, Xu B, Deininger PL. 2014. The Human LINE-1 Retrotransposon Creates DNA Double-strand Breaks. *J Mol Biol* **357**: 1383–1393.
- Gauchier M, Kan S, Barral A, Sauzet S, Agirre E, Bonnell E, Saksouk N, Barth TK, Ide S, Urbach S, *et al.* 2019. SETDB1-dependent heterochromatin stimulates alternative lengthening of telomeres. *Sci Adv.*
- Gesson K, Rescheneder P, Skoruppa MP, Haeseler A Von, Dechat T, Foisner R, Von Haeseler A, Dechat T, Foisner R. 2016. A-type Lamins bind both hetero- and euchromatin, the latter being regulated by lamina-associated polypeptide 2 alpha. *Genome Res* **26**: 462–473.
- Gibson BA, Doolittle LK, Schneider MWG, Jensen LE, Gamarra N, Henry L, Gerlich DW, Redding S, Rosen MK. 2019. Organization of Chromatin by Intrinsic and Regulated Phase Separation. *Cell* **179**: 470-484.e21. <https://doi.org/10.1016/j.cell.2019.08.037>.
- Giordano M, Infantino L, Biggiogera M, Montecucco A, Biamonti G. 2020. Heat Shock Affects Mitotic Segregation of Human Chromosomes Bound to Stress-Induced Satellite III RNAs. *Int J Mol Sci* **21**: 2812. <https://www.mdpi.com/1422-0067/21/8/2812> (Accessed May 7, 2020).
- Giorgi C, Ito K, Lin H-K, Santangelo C, Wieckowski MR, Lebedzinska M, Bononi A, Bonora M, Duszynski J, Bernardi R, *et al.* 2010. PML Regulates Apoptosis at Endoplasmic Reticulum by Modulating Calcium Release. *Science (80-)* **330**: 1247–1252.
- Giri S, Chakraborty A, Sathyan KM, Prasanth K V, Prasanth SG. 2016. Orc5 induces

- large-scale chromatin decondensation in a GCN5-dependent manner. *J Cell Sci* **117**: 417–429.
- Goldberg AD, Banaszynski LA, Noh K, Lewis PW, Elsaesser SJ, Stadler S, Dewell S, Law M, Guo X, Li X, *et al.* 2010. Distinct Factors Control Histone Variant H3.3 Localization at Specific Genomic Regions. *Cell* **140**: 678–691. <http://linkinghub.elsevier.com/retrieve/pii/S0092867410000048>.
- Goldman RD, Shumaker DK, Erdos MR, Eriksson M, Goldman AE, Gordon LB, Gruenbaum Y, Khuon S, Mendez M, Varga R, *et al.* 2004. Accumulation of mutant lamin A causes progressive changes in nuclear architecture in Hutchinson-Gilford progeria syndrome. *Proc Natl Acad Sci* **101**: 8963–8968. <http://www.pubmedcentral.nih.gov/articlerender.fcgi?artid=428455&tool=pmcentrez&rendertype=abstract>.
- Goll MG, Kirpekar F, Maggert KA, Yoder JA, Hsieh C, Zhang X, Golic KG, Jacobsen SE, Bestor TH. 2006. Methylation of tRNA Asp by the DNA Methyltransferase Homolog Dnmt2. *Science (80-)* **311**: 395–399.
- Gómez-del Arco P, Koipally J, Georgopoulos K. 2005. Ikaros SUMOylation: Switching Out of Repression. *Mol Cell Biol* **25**: 2688–2697.
- González-Aguilera C, Ikegami K, Ayuso C, de Luis A, Íñiguez M, Cabello J, Lieb JD, Askjaer P. 2014. Genome-wide analysis links emerin to neuromuscular junction activity in *Caenorhabditis elegans*. *Genome Biol* **15**: R21. <http://genomebiology.biomedcentral.com/articles/10.1186/gb-2014-15-2-r21> (Accessed May 8, 2020).
- Gonzalez-Sandoval A, Towbin BD, Kalck V, Cabianca DS, Gaidatzis D, Hauer MH, Geng L, Wang L, Yang T, Wang X, *et al.* 2015. Perinuclear Anchoring of H3K9-Methylated Chromatin Stabilizes Induced Cell Fate in *C. elegans* Embryos. *Cell* **163**: 1333–1347. <http://dx.doi.org/10.1016/j.cell.2015.10.066>.
- Gostissa M, Morelli M, Mantovani F, Guida E, Piazza S, Collavin L, Brancolini C, Schneider C, Del Sal G. 2004. The Transcriptional Repressor hDaxx Potentiates p53-dependent Apoptosis *. *J Biol Chem* **279**: 48013–48023.
- Gottschling DE, Aparicio OM, Billington BL, Zakiant VA. 1990. Position Effect at *S. cerevisiae* Telomeres: Reversible Repression of Pol II Transcription. *Cell* **63**: 751–762.
- Goutte-Gattat D, Shuaib M, Ouararhni K, Gautier T, Skoufias DA, Hamiche A, Dimitrov S. 2013. Phosphorylation of the CENP-A amino-terminus in mitotic centromeric chromatin is required for kinetochore function. *Proc Natl Acad Sci U S A* **110**: 8579–8584.

- Govoni M, Farabegoli F, Pession A, Novello F. 1994. Inhibition of Topoisomerase II Activity and its Effect on Nucleolar Structure and Function. *Exp Cell Res* **211**: 36–41.
- Greenberg MVC, Bourc'his D. 2019. The diverse roles of DNA methylation in mammalian development and disease. *Nat Rev Mol Cell Biol* **20**: 590–607. <http://dx.doi.org/10.1038/s41580-019-0159-6>.
- Greider CW, Blackburn EH. 1987. The Telomere Terminal Transferase of Tetrahymena Is a Ribonucleoprotein Enzyme with Two Kinds of Primer Specificity. *Cell* **51**: 887–898.
- Griffith JD, Comeau L, Rosenfield S, Stansel RM, Bianchi A, Moss H, Hill C, Carolina N. 1999. Mammalian Telomeres End in a Large Duplex Loop. *Cell* **97**: 503–514.
- Grimaud C, Bantignies F, Pal-Bhadra M, Ghana P, Bhadra U, Cavalli G. 2006. RNAi Components Are Required for Nuclear Clustering of Polycomb Group Response Elements. *Cell* **124**: 957–971.
- Gu Q, Hao J, Zhao X, Li W, Liu L, Wang L, Liu Z, Zhou Q. 2012. Rapid conversion of human ESCs into mouse ESC-like pluripotent state by optimizing culture conditions. *Protein Cell* **3**: 71–79.
- Gu T, Lin X, Cullen SM, Luo M, Jeong M, Estecio M, Shen J, Hardikar S, Sun D, Su J, *et al.* 2018. DNMT3A and TET1 cooperate to regulate promoter epigenetic landscapes in mouse embryonic stem cells. *Genome Biol* **19**: 88. <https://genomebiology.biomedcentral.com/articles/10.1186/s13059-018-1464-7> (Accessed May 11, 2020).
- Gu TP, Guo F, Yang H, Wu HP, Xu GF, Liu W, Xie ZG, Shi L, He X, Jin SG, *et al.* 2011. The role of Tet3 DNA dioxygenase in epigenetic reprogramming by oocytes. *Nature* **477**: 606–612.
- Guelen L, Pagie L, Brasset E, Meuleman W, Faza MB, Talhout W, Eussen BH, de Klein A, Wessels L, de Laat W, *et al.* 2008. Domain organization of human chromosomes revealed by mapping of nuclear lamina interactions. *Nature* **453**: 948–51. <http://www.ncbi.nlm.nih.gov/pubmed/18463634>.
- Guenatri M, Bailly D, Maison C, Almouzni G. 2004. Mouse centric and pericentric satellite repeats form distinct functional heterochromatin. *J Cell Biol* **166**: 493–505.
- Guenther MG, Frampton GM, Soldner F, Hockemeyer D, Mitalipova M, Jaenisch R, Young RA. 2010. Chromatin Structure and Gene Expression Programs of Human Embryonic and Induced Pluripotent Stem Cells. *Cell Stem Cell* **7**: 249–257. <http://dx.doi.org/10.1016/j.stem.2010.06.015>.

- Guo G, Pinello L, Han X, Lai S, Shen L, Lin TW, Zou K, Yuan GC, Orkin SH. 2016. Serum-Based Culture Conditions Provoke Gene Expression Variability in Mouse Embryonic Stem Cells as Revealed by Single-Cell Analysis. *Cell Rep* **14**: 956–965. <http://dx.doi.org/10.1016/j.celrep.2015.12.089>.
- Guo L, Giasson BI, Glavis-Bloom A, Brewer MD, Shorter J, Gitler AD, Yang X. 2014. A cellular system that degrades misfolded proteins and protects against neurodegeneration. *Mol Cell* **55**: 15–30. <http://dx.doi.org/10.1016/j.molcel.2014.04.030>.
- Ha M, Kraushaar DC, Zhao K. 2014. Genome-wide analysis of H3.3 dissociation reveals high nucleosome turnover at distal regulatory regions of embryonic stem cells. *Epigenetics Chromatin* **7**: 38. <http://www.epigeneticsandchromatin.com/content/7/1/38>.
- Hackett JA, Dietmann S, Murakami K, Down TA, Leitch HG, Surani MA. 2013a. Synergistic mechanisms of DNA demethylation during transition to ground-state pluripotency. *Stem Cell Reports* **1**: 518–531. <http://dx.doi.org/10.1016/j.stemcr.2013.11.010>.
- Hackett JA, Sengupta R, Zyllicz JJ, Murakami K, Lee C, Down TA, Surani MA. 2013b. Germline DNA Demethylation Dynamics and Imprint Erasure Through 5-Hydroxymethylcystosine. *Science (80-)* **9**: 448–453.
- Hadjimichael C, Chanoumidou K, Nikolaou C, Klonizakis A, Theodosi G-I, Makatounakis T, Papamatheakis J, Krestovali A. 2017. Promyelocytic Leukemia Protein Is an Essential Regulator of Stem Cell Pluripotency and Somatic Cell Reprogramming. *Stem Cell Reports* **9**: 1–16.
- Hahn M, Dambacher S, Dulev S, Kuznetsova AY, Sadic D, Schulte M, Mallm J, Eck S, Wo S, Maiser A, *et al.* 2013. Suv4-20h2 mediates chromatin compaction and is important for cohesin recruitment to heterochromatin. *Genes Dev* **1**: 859–872.
- Hake SB, Garcia B a, Kauer M, Baker SP, Shabanowitz J, Hunt DF, Allis CD. 2005. Serine 31 phosphorylation of histone variant H3.3 is specific to regions bordering centromeres in metaphase chromosomes. *Proc Natl Acad Sci U S A* **102**: 6344–6349.
- Hammond JJ. 1949. Recovery and Culture of Tubal Mouse Ova. *Nature* **163**: 28–29.
- Hamperl S, Bocek MJ, Saldivar JC, Swigut T, Cimprich KA. 2017. Transcription-replication conflict orientation modulates R-loop levels and activates distinct DNA damage responses. *Cell* **170**: 774–786.
- Hanasoge S, Ljungman M. 2007. H2AX

- phosphorylation after UV irradiation is triggered by DNA repair intermediates and is mediated by the ATR kinase. *Carcinogenesis* **28**: 2298–2304.
- Harada A, Okada S, Konno D, Odawara J, Yoshimi T, Yoshimura S, Kumamaru H, Saiwai H, Tsubota T, Kurumizaka H, *et al.* 2012. Chd2 interacts with H3.3 to determine myogenic cell fate. *EMBO J* **31**: 2994–3007. <http://dx.doi.org/10.1038/emboj.2012.136><http://www.pubmedcentral.nih.gov/articlerender.fcgi?artid=3395093&tool=pmcentrez&rendertype=abstract>.
- Harhoury K, Navarro C, Depetris D, Mattei M, Nissan X, Cau P, Sandre-giovannoli A De, Lévy N. 2017. MG 132 -induced progerin clearance is mediated by autophagy activation and splicing regulation. *EMBO Mol Med* **9**: 1294–1313.
- Harr JC, Luperchio TR, Wong X, Cohen E, Wheelan SJ, Reddy KL. 2015. Directed targeting of chromatin to the nuclear lamina is mediated by chromatin state and A-type lamins. *J Cell Biol* **208**: 33–52.
- Harr JC, Schmid CD, Muñoz-jiménez C, Romero-bueno R, Kalck V, Gonzalez-sandoval A, Hauer MH, Padeken J, Askjaer P, Mattout A, *et al.* 2020. Loss of an H3K9me anchor rescues laminopathy-linked changes in nuclear organization and muscle function in an Emery-Dreifuss muscular dystrophy model. *Genes Dev* **34**: 560–579.
- Harris RS, Bishop KN, Sheehy AM, Craig HM, Petersen-mahrt SK, Watt IN, Neuberger MS, Malim MH. 2003. DNA Deamination Mediates Innate Immunity to Retroviral Infection. *Cell* **113**: 803–809.
- Hayashi K, Ohta H, Kurimoto K, Aramaki S, Saitou M. 2011. Reconstitution of the mouse germ cell specification pathway in culture by pluripotent stem cells. *Cell* **146**: 519–532. <http://dx.doi.org/10.1016/j.cell.2011.06.052>.
- Hayflick L, Moorhead PS. 1961. The serial cultivation of human diploid cell strains. *Exp Cell Res* **25**: 585–621.
- He Q, Kim H, Huang R, Lu W, Tang M, Shi F, Yang D, Zhang X, Huang J, Liu D, *et al.* 2015. The Daxx/Atrx Complex Protects Tandem Repetitive Elements during DNA Hypomethylation by Promoting H3K9 Trimethylation. *Cell Stem Cell* **17**: 273–286. <http://dx.doi.org/10.1016/j.stem.2015.07.022>.
- Heaphy CM, Wilde RF De, Jiao Y, Klein AP, Edil BH, Shi C, Bettgowda C, Rodriguez FJ, Eberhart CG, Hebbar S, *et al.* 2011. Altered Telomeres in Tumors with ATRX and DAXX mutations. *Science (80-)* **333**: 425.
- Hebbes TR, Clayton AL, Thorne AW, Crane-

- robinson C. 1994. DNase I sensitivity in the chicken β -globin chromosomal domain. *EMBO J* **13**: 1823–1830.
- Heintzman ND, Stuart RK, Hon G, Fu Y, Ching CW, Hawkins RD, Barrera LO, Calcar S Van, Qu C, Ching KA, *et al.* 2007. Distinct and predictive chromatin signatures of transcriptional promoters and enhancers in the human genome. *Nat Genet* **39**: 311–318.
- Hemann MT, Strong MA, Hao L, Greider CW. 2001. The Shortest Telomere , Not Average Telomere Length , Is Critical for Cell Viability and Chromosome Stability. *Cell* **107**: 67–77.
- Henikoff JG, Belsky JA, Krassovsky K, Macalpine DM, Henikoff S. 2011. Epigenome characterization at single base-pair resolution. *Proc Natl Acad Sci* **108**: 18318–18323.
- Herz H, Nakanishi S, Shilatifard A. 2009. The Curious Case of Bivalent Marks. *Dev Cell* **17**: 301–303. <http://dx.doi.org/10.1016/j.devcel.2009.08.014>.
- Heyer W-D, Ehmsen KT, Liu J. 2010. Regulation of homologous recombination in eukaryotes. *Annu Rev Genet* **44**: 113–139. <http://dx.doi.org/10.1016/j.febslet.2010.05.037>.
- Hidalgo I, Herrera-merchan A, Ligos JM, Carramolino L, Nun J, Martinez F, Dominguez O, Torres M, Gonzalez S. 2012. Ezh1 Is Required for Hematopoietic Stem Cell Maintenance and Prevents Senescence-like Cell Cycle Arrest. *Cell Stem Cell* **11**: 649–662.
- Hiratani I, Ryba T, Itoh M, Rathjen J, Kulik M, Papp B, Fussner E, Bazett-jones DP, Plath K, Dalton S, *et al.* 2010. Genome-wide dynamics of replication timing revealed by in vitro models of mouse embryogenesis. *Genome Res* **20**: 155–169.
- Hoeijmakers J, Jackson S, Jiricny J, Kanaar R, Hans Krokan. 2009. DNA Damage Response and Repair Mechanisms. *Integr Proj DNA Damage Response Mech.*
- Hoelper D, Huang H, Jain AY, Patel DJ, Lewis PW. 2017. Structural and mechanistic insights into ATRX-dependent and -independent functions of the histone chaperone DAXX. *Nat Commun* **8**. <http://dx.doi.org/10.1038/s41467-017-01206-y>.
- Holohan B, Wright WE, Shay JW. 2014. Telomeropathies : An emerging spectrum disorder. *J Cell Biol* **205**: 289–299.
- Horowitz RA, Agard DA, Woodcock CL. 1994. The Three-dimensional Architecture of Chromatin In Situ: Electron Tomography Reveals Fibers Composed of a Continuously Variable Zig-Zag Nucleosomal Ribbon. *J Cell Biol* **125**: 1–10.
- Howlett SK, Reik W. 1991. Methylation

- levels of maternal and paternal genomes during preimplantation development. *Development* **127**: 119–127.
- Hozé N, Ruault M, Amoruso C, Taddei A, Holcman D. 2013. Spatial telomere organization and clustering in yeast *Saccharomyces cerevisiae* nucleus is generated by a random dynamics of aggregation-dissociation. *Mol Biol Cell* **24**: 1791–1800.
- Hu L, Lu J, Cheng J, Rao Q, Li Z, Hou H, Lou Z, Zhang L, Li W, Gong W, *et al.* 2015. Structural insight into substrate preference for TET-mediated oxidation. *Nature* **527**: 118–122.
- Huang FW, Hodis E, Xu MJ, Kryukov G V., Chin L, Garraway LA. 2013. Highly Recurrent TERT Promoter Mutations in Human Melanoma. *Science (80-)* **339**: 957–960.
- Huang G, Ye S, Zhou X, Liu D, Ying Q-L. 2015. Molecular basis of embryonic stem cell self-renewal: from signaling pathways to pluripotency network. *Cell Mol Life Sci* **72**: 1741–1757.
- Huang J, Fan T, Yan Q, Zhu H, Fox S, Issaq HJ, Best L, Gangi L, Munroe D, Muegge K. 2004. Lsh , an epigenetic guardian of repetitive elements. *Nucleic Acids Res* **32**: 5019–5028.
- Huang S, Tao X, Yuan S, Zhang Y, Li P, Bellinson HA, Zhang Y, Yu W, Pontarotti P, Escriva H, *et al.* 2016. Discovery of an Active RAG Transposon Illuminates the Origins of V (D) J Recombination Article Discovery of an Active RAG Transposon Illuminates the Origins of V (D) J Recombination. *Cell* **166**: 102–114. <http://dx.doi.org/10.1016/j.cell.2016.05.032>.
- Hug CB, Grimaldi AG, Kruse K, Vaquerizas JM. 2017. Chromatin Architecture Emerges during Zygotic Genome Activation Independent of Transcription. *Cell* **169**: 216-228.e19. <http://dx.doi.org/10.1016/j.cell.2017.03.024>.
- Hughes AL, Jin Y, Rando OJ, Struhl K. 2012. A Functional Evolutionary Approach to Identify Determinants of Nucleosome Positioning: A Unifying Model for Establishing the Genome-wide Pattern. *Mol Cell* **48**: 5–15. <http://dx.doi.org/10.1016/j.molcel.2012.07.003>.
- Huntley S, Baggott DM, Hamilton AT, Trangyamfi M, Yang S, Kim J, Gordon L, Branscomb E, Stubbs L. 2006. A comprehensive catalog of human KRAB-associated zinc finger genes: Insights into the evolutionary history of a large family of transcriptional repressors. *Genome Res* **16**: 669–677.
- Huo X, Ji L, Zhang Y, Lv P, Cao X, Wang Q, Yan Z, Dong S, Du D, Zhang F, *et al.* 2019. The Nuclear Matrix Protein SAFB

- Cooperates with Major Satellite RNAs to Stabilize Heterochromatin Architecture Partially through Phase Separation. *Mol Cell* 1–16. <http://www.ncbi.nlm.nih.gov/pubmed/31677973>.
- Iacovoni JS, Caron P, Lassadi I, Nicolas E, Massip L, Trouche D, Legube G. 2010. High-resolution profiling of c H2AX around DNA double strand breaks in the mammalian genome. *EMBO J* **29**: 1446–1457.
- Ibarra A, Benner C, Tyagi S, Cool J, Hetzer MW. 2016. Nucleoporin-mediated regulation of cell identity genes. *Genes Dev* 2253–2258.
- Ishiuchi T, Enriquez-Gasca R, Mizutani E, Boškovič A, Ziegler-Birling C, Rodriguez-Terrones D, Wakayama T, Vaquerizas JM, Torres-Padilla ME. 2015. Early embryonic-like cells are induced by downregulating replication-dependent chromatin assembly. *Nat Struct Mol Biol* **22**: 662–671. <http://dx.doi.org/10.1038/nsmb.3066>.
- Iskow RC, McCabe MT, Mills RE, Torene S, Pittard WS, Neuwald AF, Meir EG Van, Vertino PM, Devine SE. 2010. Natural Mutagenesis of Human Genomes by Endogenous Retrotransposons. *Cell* **141**: 1253–1261. <http://dx.doi.org/10.1016/j.cell.2010.05.020>.
- Ito S, Alessio ACD, Taranova O V, Hong K, Sowers LC, Zhang Y. 2010. Role of Tet proteins in 5mC to 5hmC conversion, ES-cell self-renewal and inner cell mass specification. *Nature* **466**: 1129–1133. <http://dx.doi.org/10.1038/nature09303>.
- Ito S, Shen L, Dai Q, Wu SC, Collins LB, Swenberg JA, He C, Zhang Y. 2011. Tet Proteins Can Convert 5-Methylcytosine to 5-Formylcytosine and 5-Carboxylcytosine. *Science (80-)* **333**: 1300–1304.
- Ivanauskiene K, Delbarre E, McGhie JD, Küntziger T, Wong LH, Collas P. 2014. The PML-associated protein DEK regulates the balance of H3.3 loading on chromatin and is important for telomere integrity. *Genome Res* **24**: 1584–1594. <http://genome.cshlp.org/lookup/doi/10.1101/gr.173831.114>.
- Jachowicz JW, Bing X, Pontabry J, Bošković A, Rando OJ, Torres-Padilla ME. 2017. LINE-1 activation after fertilization regulates global chromatin accessibility in the early mouse embryo. *Nat Genet* **49**: 1502–1510. <http://dx.doi.org/10.1038/ng.3945>.
- Jachowicz JW, Santenard A, Bender A, Muller J, Torres MEP. 2013. Heterochromatin establishment at pericentromeres depends on nuclear position. *Genes Dev* **27**: 2427–2432.
- Jacinto F V, Benner C, Hetzer MW. 2015. The nucleoporin Nup153 regulates

- embryonic stem cell pluripotency through gene silencing. *Genes Dev* **29**: 1224–1238.
- Jackson-Grusby L, Beard C, Possemato R, Tudor M, Fambrough D, Csankovszki G, Dausman J, Lee P, Wilson C, Lander E, *et al.* 2001. Loss of genomic methylation causes p53- dependent apoptosis and epigenetic. *Nat Genet* **27**: 31–39.
- Jacobs FMJ, Greenberg D, Nguyen N, Haeussler M, Ewing AD, Katzman S, Paten B, Salama SR, Haussler D. 2014. An evolutionary arms race between KRAB zinc-finger genes ZNF91/93 and SVA/L1 retrotransposons. *Nature* **516**: 242–245. <http://dx.doi.org/10.1038/nature13760>.
- Jagannathan M, Cummings R, Yamashita YM. 2018. A conserved function for pericentromeric satellite DNA. *Elife* **7**. <https://elifesciences.org/articles/34122>.
- Jagannathan M, Cummings R, Yamashita YM. 2019. The modular mechanism of chromocenter formation in *Drosophila*. *Elife* **8**.
- Jagannathan M, Yamashita YM. 2017. Function of Junk: Pericentromeric Satellite DNA in Chromosome Maintenance. *Cold Spring Harb Symp Quant Biol* **LXXXII**: 319–327.
- Jain D, Cooper JP. 2010. Telomeric Strategies: Means to an End. *Annu Rev Genet* **44**: 243–169.
- Jambhekar A, Dhall A, Shi Y. 2019. Roles and regulation of histone methylation in animal development. *Nat Rev Mol Cell Biol* **20**. <http://dx.doi.org/10.1038/s41580-019-0151-1>.
- Janer A, Martin E, Muriel M, Latouche M, Fujigasaki H, Ruberg M, Brice A, Trottier Y, Sittler A. 2006. PML clastosomes prevent nuclear accumulation of mutant ataxin-7 and other polyglutamine proteins. *J Cell Biol* **174**: 65–76.
- Jang CW, Shibata Y, Starmer J, Yee D, Magnuson T. 2015. Histone H3 . 3 maintains genome integrity during mammalian development. *Genes Dev* **1**: 1377–1392.
- Jang SM, Kauzlaric A, Quivy J-P, Pontis J, Rauwel B, Coluccio A, Offner S, Duc J, Turelli P, Almouzni G, *et al.* 2018. KAP1 facilitates reinstatement of heterochromatin after DNA replication. *Nucleic Acids Res* **1**–15. <https://academic.oup.com/nar/advance-article/doi/10.1093/nar/gky580/5046100>.
- Janssen A, Colmenares SU, Lee T, Karpen GH. 2019. Timely double-strand break repair and pathway choice in pericentromeric heterochromatin

- depend on the histone demethylase dKDM4A. *Genes Dev* 1–13.
- Jefferson A, Colella S, Moralli D, Wilson N, Yusuf M, Gimelli G, Ragoussis J, Volpi E V. 2010. Altered intra-nuclear organisation of heterochromatin and genes in ICF syndrome. *PLoS One* 5.
- Jenuwein T, Allis CD. 2001. Translating the Histone Code. *Science (80-)* 293: 1074–1081.
- Jiao Y, Shi C, Edil BH, de Wilde RF, Klismtra DS, Maitra A, Schulick RD, Tang LH, Wolfgang CL, Choti MA, *et al.* 2011. DAXX/ATRX, MEN1, and mTOR Pathway Genes Are Frequently Altered in Pancreatic Neuroendocrine Tumors. *Science (80-)* 331: 1199–1203.
- Jin C, Zang C, Wei G, Cui K, Peng W, Zhao K, Felsenfeld G. 2009. H3 . 3 / H2A . Z double variant – containing nucleosomes mark ‘ nucleosome-free regions ’ of active promoters and other regulatory regions. *Nat Genet* 41.
- Johnson BR, Nitta RT, Frock RL, Mounkes L, Barbie DA, Stewart CL, Harlow E, Kennedy BK. 2004. A-type lamins regulate retinoblastoma protein function by promoting subnuclear localization and preventing proteasomal degradation. *Proc Natl Acad Sci U S A* 101: 9677–9682.
- Johnson WL, Yewdell WT, Bell JC, McNulty SM, Duda Z, O’Neill RJ, Sullivan BA, Straight AF. 2017. RNA-dependent stabilization of SUV39H1 at constitutive heterochromatin. *Elife* 6: 4–7.
- Jolly C, Metz A, Govin J, Vigneron M, Turner BM, Khochbin S, Vourc’h C. 2004. Stress-induced transcription of satellite III repeats. *J Cell Biol* 164: 25–33.
- Juhász S, Elbakry A, Mathes A, Löbrich M. 2018. ATRX Promotes DNA Repair Synthesis and Sister Chromatid Exchange during Homologous Article ATRX Promotes DNA Repair Synthesis and Sister Chromatid Exchange during Homologous Recombination. *Mol Cell* 71: 11–24.
- Kahl P, Gullotti L, Heukamp LC, Wolf S, Friedrichs N, Vorreuther R, Solleder G, Bastian PJ, Metzger E, Schu R, *et al.* 2006. Androgen Receptor Coactivators Lysine-Specific Histone Demethylase 1 and Four and a Half LIM Domain Protein 2 Predict Risk of Prostate Cancer Recurrence. *Cancer Res* 11341–11348.
- Kaiser SM, Malik HS, Emerman M. 2007. Restriction of an Extinct Retrovirus by the Human TRIM5 a Antiviral Protein. *Science (80-)*.
- Kanellopoulou C, Muljo SA, Kung AL, Ganesan S, Drapkin R, Jenuwein T, Livingston DM, Rajewsky K. 2005. Dicer-deficient mouse embryonic stem cells are defective in differentiation and centromeric silencing. *Genes Dev* 19:

- 489–501.
- Kapoor A, Goldberg MS, Cumberland LK, Ratnakumar K, Segura MF, Emanuel PO, Menendez S, Vardabasso C, Leroy G, Vidal CI, *et al.* 2010. The histone variant macroH2A suppresses melanoma progression through regulation of CDK8. *Nature* **468**: 1105–1109.
- Karimi MM, Goyal P, Maksakova IA, Bilenky M, Leung D, Tang JX, Shinkai Y, Mager DL, Jones S, Hirst M, *et al.* 2011. Article DNA Methylation and SETDB1 / H3K9me3 Regulate Predominantly Distinct Sets of Genes , Retroelements , and Chimeric Transcripts in mESCs. *Stem Cell* **8**: 676–687. <http://dx.doi.org/10.1016/j.stem.2011.04.004>.
- Karmodiya K, Krebs AR, Oulad-abdelghani M, Kimura H, Tora L. 2012. H3K9 and H3K14 acetylation co-occur at many gene regulatory elements , while H3K14ac marks a subset of inactive inducible promoters in mouse embryonic stem cells. *BMC Genomics* **13**.
- Kasper LH, Lerach S, Wang J, Wu S, Jeevan T, Brindle PK, Cre-treated A. 2010. CBP / p300 double null cells reveal effect of coactivator level and diversity on CREB transactivation. *EMBO J* **29**: 3660–3672. <http://dx.doi.org/10.1038/emboj.2010.235>.
- Kastner P, Perez A, Lutz Y, Rochette-egly C, Gaub M, Durand B, Lanotte M, Berger R, Chambon P. 1992. Structure , localization and transcriptional properties of two classes of retinoic acid receptor fusion proteins in acute promyelocytic leukemia (APL): structural similarities with a new family of oncoproteins. *EMBO J* **11**: 629–642.
- Kellner S, Kikyo N. 2010. Transcriptional regulation of the Oct4 gene, a master gene for pluripotency. *Histol Histopathol* **25**: 405–412.
- Kidane D, Murphy DL, Sweasy JB. 2014. Accumulation of abasic sites induces genomic instability in normal human gastric epithelial cells during Helicobacter pylori infection. *Oncogenesis* **3**.
- Kieffer-Kwon K-R, Nimura K, Rao SSP, Xu J, Jung S, Pekowska A, Dose M, Stevens E, Mathe E, Dong P, *et al.* 2017. Myc Regulates Chromatin Decompaction and Nuclear Architecture during B Cell Activation. *Mol Cell* 1–13. <http://linkinghub.elsevier.com/retrieve/pii/S1097276517305075>.
- Kim J-M, Kim K, Punj V, Liang G, Ulmer TS, Lu W, An W. 2015. Linker histone H1.2 establishes chromatin compaction and gene silencing through recognition of H3K27me3. *Sci Rep* **5**: 16714. <http://www.nature.com/articles/srep16714>.

- Kim Y, Sharov A, McDole K, Cheng M, Hao H, Fan C-M, Gaiano N, Ko M, Zheng Y. 2011. Mouse B-Type Lamins Are Required for Proper Organogenesis But Not by Embryonic Stem Cells. *Science (80-)* **334**: 1706–1711.
- Kind J, Pagie L, De Vries SS, Dekker J, Van Oudenaarden A, Van B, Correspondence S, Eu JKK. 2015a. Genome-wide Maps of Nuclear Lamina Interactions in Single Human Cells. *Cell* **163**: 134–147.
- Kind J, Pagie L, Ortazokoyun H, Boyle S, de Vries SS, Janssen H, Amendola M, Nolen LD, Bickmore WA, van Steensel B. 2013. Single-Cell Dynamics of Genome-Nuclear Lamina Interactions. *Cell* **153**: 178–192. <http://linkinghub.elsevier.com/retrieve/pii/S0092867413002171>.
- Kind J, Pagie L, Vries SS De, Dekker J, Oudenaarden A Van, Kind J, Pagie L, Vries SS De, Nahidiazar L, Dey SS, *et al.* 2015b. Genome-wide Maps of Nuclear Lamina Interactions in Single Human Cells. *Cell* **163**: 134–147. <http://dx.doi.org/10.1016/j.cell.2015.08.040>.
- Kinner A, Wu W, Staudt C, Iliakis G. 2008. Gamma-H2AX in recognition and signaling of DNA double-strand breaks in the context of chromatin. *Nucleic Acids Res* **36**: 5678–5694.
- Kishikawa S, Murata T, Ugai H, Yamazaki T, Yokoyama KK. 2003. Control elements of Dnmt1 gene are regulated in cell-cycle dependent manner. *Nucleic Acids Res Suppl* 307–308.
- Klutstein M, Nejman D, Greenfield R, Cedar H. 2016. DNA methylation in cancer and aging. *Cancer Res* **76**: 3446–3450.
- Kohwi M, Lupton JR, Lai S, Miller MR, Doe CQ. 2013. Developmentally Regulated Subnuclear Genome Reorganization Restricts Neural Progenitor Competence in Drosophila. *Cell* **152**: 97–108. <http://dx.doi.org/10.1016/j.cell.2012.11.049>.
- Kolodziejczyk AA, Kim JK, Tsang JCH, Liu P, Marioni JC, Teichmann SA, Kolodziejczyk AA, Kim JK, Tsang JCH, Ilicic T, *et al.* 2015. Single Cell RNA-Sequencing of Pluripotent States Unlocks Modular Transcriptional Variation Resource Single Cell RNA-Sequencing of Pluripotent States Unlocks Modular Transcriptional Variation. *Cell Stem Cell* 471–485.
- Komissarov AS, GavriloVA E V., Demin SJ, Ishov AM, Podgornaya OI. 2011. Tandemly repeated DNA families in the mouse genome. *BMC Genomics* **12**.
- Kondo Y, Issa J-PJ. 2003. Enrichment for Histone H3 Lysine 9 Methylation at Alu Repeats in Human Cells. *J Biol Chem* **278**: 27658–27662.
- Konev AY, Tribus M, Park SY, Podhraski V,

- Lim CY, Emelyanov A V, Vershilova E, Pirrotta V, Kadonaga JT, Lusser A, *et al.* 2007. CHD1 Motor Protein Is Required for Deposition of Histone Variant H3.3 into Chromatin in Vivo. *Science (80-)* **317**: 1087–1091.
- Kornberg RD. 1974. Chromatin structure: a repeating unit of histones and DNA. *Science (80-)* **184**: 868–871.
- Kornberg RD, Thomas JO. 1974. Chromatin Structure: Oligomers of the Histones. *Science (80-)* **184**: 865–868.
- Kosak ST, Skok JA, Medina KL, Riblet R, Le Beau MM, Fisher AG, Singh H. 2002. Subnuclear Compartmentalization of Immunoglobulin Loci During Lymphocyte Development. *Science (80-)* **296**: 158–162.
- Kraushaar DC, Jin W, Maunakea A, Abraham B, Ha M, Zhao K. 2013. Genome-wide incorporation dynamics reveal distinct categories of turnover for the histone variant H3.3. *Genome Biol* **14**: R121. <http://www.pubmedcentral.nih.gov/articlerender.fcgi?artid=3983652&tool=pmcentrez&rendertype=abstract>.
- Kresoja-rakic J, Santoro R. 2019. Nucleolus and rRNA Gene Chromatin in Early Embryo Development. *Trends Genet* **35**: 868–879. <https://doi.org/10.1016/j.tig.2019.06.005>.
- Krijger Lodewijk PH, Di Stefano B, de Wit E, Limone F, van Oevelen C, de Laat W, Graf T. 2016. Cell-of-Origin-Specific 3D Genome Structure Acquired during Somatic Cell Reprogramming Article Cell-of-Origin-Specific 3D Genome Structure Acquired during Somatic Cell Reprogramming. *Cell Stem Cell* **18**: 597–610. <http://dx.doi.org/10.1016/j.stem.2016.01.007>.
- Krimer DB, Cheng G, Skoultchi A. 1993. Induction of H3 . 3 replacement histone mRNAs during the precommitment period of murine erythroleukemia cell differentiation. **21**: 2873–2879.
- Kubben N, Adriaens M, Meuleman W. 2012. Mapping of lamin A- and progerin-interacting genome regions. *Chromosoma* **447–464**.
- Kumar PP, Bischof O, Purbey PK, Notani D, Urlaub H, Dejean A, Galande S. 2007. Functional interaction between PML and SATB1 regulates chromatin-loop architecture and transcription of the MHC class I locus. *Nat Cell Biol* **9**: 45–56. <http://www.ncbi.nlm.nih.gov/pubmed/17173041>.
- Kumaran RI, Spector DL. 2008. A genetic locus targeted to the nuclear periphery in living cells maintains its transcriptional competence. *J Cell Biol* **180**: 51–65.
- Kundu S, Ji F, Sunwoo H, Jain G, Lee JT, Sadreyev RI, Dekker J, Kingston RE.

2017. Polycomb Repressive Complex 1 Generates Discrete Compacted Domains that Change during Differentiation. *Mol Cell* **65**: 432-446.e5. <http://dx.doi.org/10.1016/j.molcel.2017.01.009>.
- Kuo M, Brownell JE, Sobel RE, Ranalli TA, Cook RG, Edmondson DG, Roth SY, Allis CD. 1996. Transcription-linked acetylation by Gcn5p of histones H3 and H4 at specific lysines. *Nature* **383**: 269–272.
- Kupiec M. 2014. Biology of telomeres: Lessons from budding yeast. *FEMS Microbiol Rev* **38**: 144–171.
- Ladstätter S, Tachibana K. 2018. Genomic insights into chromatin reprogramming to totipotency in embryos. **218**: 70–82.
- Lallemand-Breitenbach V, de Thé H. 2010. PML nuclear bodies. *Cold Spring Harb Perspect Biol* **2**: 1–17.
- Lander ES, Linton LM, Birren B, Nusbaum C, Zody MC, Baldwin J, Devon K, Dewar K, Doyle M, FitzHugh W, *et al.* 2001. Initial sequencing and analysis of the human genome. *Nature* **409**.
- Lane N, Dean W, Erhardt S, Hajkova P, Surani A, Reik W. 2003. Resistance of IAPs to Methylation Reprogramming May Provide a Mechanism for Epigenetic Inheritance in the Mouse. *Genesis* **35**: 88–93.
- Lange UC, Siebert S, Wossidlo M, Weiss T, Ziegler-Birling C, Walter J, Torres-Padilla ME, Daujat S, Schneider R. 2013. Dissecting the role of H3K64me3 in mouse pericentromeric heterochromatin. *Nat Commun* **4**: 1–10.
- Larson AG, Elnatan D, Keenen MM, Trnka MJ, Johnston JB, Burlingame AL, Agard DA, Redding S, Narlikar GJ. 2017. Liquid droplet formation by HP1 α suggests a role for phase separation in heterochromatin. *Nature* **547**: 236–240. <http://dx.doi.org/10.1038/nature22822>.
- Lee DD, Castelo-branco P, Tabori U, Lee DD, Leão R, Komosa M, Gallo M, Zhang CH, Lipman T, Remke M, *et al.* 2019. DNA hypermethylation within TERT promoter upregulates TERT expression in cancer. *J Clin Investig* **129**: 223–229.
- Lee E, Iskow R, Yang L, Gockumen O, Haseley P, Lovelace LJI, Lohr JG, Harris CC, Ding L, Wilson RK, *et al.* 2012. Landscape of Somatic Retrotransposition in Human Cancers. *Science (80-)* **10**: 1–6.
- Lee HJ, Hore TA, Reik W. 2014. Reprogramming the methylome: Erasing memory and creating diversity. *Cell Stem Cell* **14**: 710–719. <http://dx.doi.org/10.1016/j.stem.2014.05.008>.
- Lee MG, Villa R, Trojer P, Norman J, Yan K, Reinberg D, Croce LD, Shiekhattar R. 2007. Demethylation of H3K27

- Regulates Polycomb Recruitment and H2A Ubiquitination. *Science (80-)* **26**: 447–451.
- Lehnertz B, Ueda Y, Derijck AAHA, Braunschweig U, Perez-burgos L, Kubicek S, Chen T, Li E, Jenuwein T, Peters AHFM. 2003. Suv39h -Mediated Histone H3 Lysine 9 Methylation Directs DNA Methylation to Major Satellite Repeats at Pericentric Heterochromatin. *Curr Biol* **13**: 1192–1200.
- Lemaître C, Grabarz A, Tsouroula K, Andronov L, Furst A, Pankotai T, Heyer V, Rogier M, Attwood KM, Kessler P, *et al.* 2014. Nuclear position dictates DNA repair pathway choice. *Genes Dev* **28**: 2450–2463.
- Lenain C, De Graaf CA, Pagie L, Visser NL, De Haas M, De Vries SS, Peric-Hupkes D, Van Steensel B, Peeper DS. 2017. Massive reshaping of genome-nuclear lamina interactions during oncogene-induced senescence. *Genome Res* **27**: 1634–1644.
- Lepack AE, Bagot RC, Peña CJ, Loh YHE, Farrelly LA, Lu Y, Powell SK, Lorsch ZS, Issler O, Cates HM, *et al.* 2016. Aberrant H3.3 dynamics in NAc promote vulnerability to depressive-like behavior. *Proc Natl Acad Sci U S A* **113**: 12562–12567.
- Leung DC, Lorincz MC. 2012. Silencing of endogenous retroviruses: when and why do histone marks predominate? *Trends Biochem Sci* **37**: 127–133. <http://dx.doi.org/10.1016/j.tibs.2011.11.006>.
- Lewis PW, Elsaesser SJ, Noh K, Stadler SC, Allis CD. 2010. DAXX is an H3.3-specific histone chaperone and cooperates with ATRX in replication-independent chromatin assembly at telomeres. *Proc Natl Acad Sci* **107**.
- Li E, Bestor TH, Jaenisch R. 1992. Targeted Mutation of the DNA Methyltransferase Gene Results in Embryonic Lethality. *Cell* **69**: 915–926.
- Li HUI, Leo C, Zhu J, Wu X, Neil JO, Park E, Chen JDON. 2000. Sequestration and Inhibition of Daxx-Mediated Transcriptional Repression by PML. *Mol Cell Biol* **20**: 1784–1796.
- Lin C-J, Conti M, Ramalho-Santos M. 2013. Histone variant H3.3 maintains a decondensed chromatin state essential for mouse preimplantation development. *Development* **140**: 3624–34. <http://www.ncbi.nlm.nih.gov/pubmed/23903189>.
- Lin DY, Huang YS, Jeng JC, Kuo HY, Chang CC, Chao TT, Ho CC, Chen YC, Lin TP, Fang HI, *et al.* 2006. Role of SUMO-Interacting Motif in Daxx SUMO Modification, Subnuclear Localization, and Repression of Sumoylated Transcription Factors. *Mol Cell* **24**: 341–354.

- Lin H, Bergmann S, Pandolfi PP. 2004. Cytoplasmic PML function in TGF- β signalling. *Nature* **431**: 205–211.
- Liu H, Chang L-H, Sun Y, Lu X, Stubbs L. 2014. Deep Vertebrate Roots for Mammalian Zinc Finger Transcription Factor Subfamilies. *Genome Biol Evol* **6**: 510–525.
- Liu L, Liu C, Fotouhi O, Fan Y, Xia C, Shi B, Zhang G, Wang K, Kong F, Larsson C, *et al.* 2017. TERT Promoter Hypermethylation in Gastrointestinal Cancer: A Potential Stool Biomarker. *Oncologist* **22**: 1178–1188.
- Liu Z, Tardat M, Gill ME, Royo H, Thierry R, Ozonov EA, Peters AHFM. 2020. SUMOylated PRC1 controls histone H3.3 deposition and genome integrity of embryonic heterochromatin. *EMBO J* 1–24.
- Lou Z, Wei J, Riethman H, Baur JA, Voglauer R, Shay JW, Wright WE. 2009. Telomere length regulates ISG15 expression in human cells. *Aging (Albany NY)* **1**: 608–621.
- Lowe CB, Haussler D. 2012. 29 Mammalian Genomes Reveal Novel Exaptations of Mobile Elements for Likely Regulatory Functions in the Human Genome. *PLoS One* **7**.
- Loyola A, Bonaldi T, Imhof A, Almouzni G. 2006. PTMs on H3 Variants before Chromatin Assembly Potentiate Their Final Epigenetic State Short Article. *Mol Cell* 309–316.
- Lu J, Gilbert DM. 2007. Proliferation-dependent and cell cycle-regulated transcription of mouse pericentric heterochromatin. *J Cell Biol* **179**: 411–421.
- Luciani JJ, Depetris D, Missirian C, Mignon-Ravix C, Metzler-Guillemain C, Megarbane A, Moncla A, Mattei MG. 2005. Subcellular distribution of HP1 proteins is altered in ICF syndrome. *Eur J Hum Genet* **13**: 41–51.
- Luciani JJ, Depetris D, Usson Y, Metzler-Guillemain C, Mignon-Ravix C, Mitchell MJ, Megarbane A, Sarda P, Sirma H, Moncla A, *et al.* 2006. PML nuclear bodies are highly organised DNA-protein structures with a function in heterochromatin remodelling at the G2 phase. *J Cell Sci* **119**: 2518–2531. <http://jcs.biologists.org/cgi/doi/10.1242/jcs.02965>.
- Luger K, Mäder AW, Richmond RK, Sargent DF, Richmond TJ. 1997. Crystal structure of the nucleosome core particle at 2.8 Å resolution. *Nature* **389**: 251–260.
- Luijsterburg MS, de Krijger I, Wiegant WW, Shah RG, Smeenk G, de Groot AJL, Pines A, Vertegaal ACO, Jacobs JJJ, Shah GM, *et al.* 2016. PARP1 Links CHD2-Mediated Chromatin Expansion and H3.3 Deposition to DNA Repair by Non-homologous End-Joining. *Mol Cell*

- 61:** 547–562.
<http://linkinghub.elsevier.com/retrieve/pii/S1097276516000460>.
- Lyst MJ, Ekiert R, Ebert DH, Merusi C, Nowak J, Selfridge J, Guy J, Kastan NR, Robinson ND, De Lima Alves F, *et al.* 2013. Rett syndrome mutations abolish the interaction of MeCP2 with the NCoR/SMRT co-repressor. *Nat Neurosci* **16**: 898–902.
- Macfarlan TS, Gifford WD, Agarwal S, Driscoll S, Lettieri K, Wang J, Andrews SE, Franco L, Rosenfeld MG, Ren B, *et al.* 2011. Endogenous retroviruses and neighboring genes are coordinately repressed by LSD1 / KDM1A. *Genes Dev* **4**: 594–607.
- Macfarlan TS, Gifford WD, Driscoll S, Lettieri K, Rowe HM, Bonanomi D, Firth A, Singer O, Trono D, Pfaff SL. 2012. Embryonic stem cell potency fluctuates with endogenous retrovirus activity. *Nature* 2–10.
- MacLennan M, García-Cañadas M, Reichmann J, Khazina E, Wagner G, Playfoot CJ, Salvador-Palomeque C, Mann AR, Peressini P, Sanchez L, *et al.* 2017. Mobilization of LINE-1 retrotransposons is restricted by Tex19.1 in mouse embryonic stem cells. *Elife* **6**: 1–32.
- Maison C, Bailly D, Roche D, De Oca RM, Probst A V., Vassias I, Dingli F, Lombard B, Loew D, Quivy JP, *et al.* 2011. SUMOylation promotes de novo targeting of HP1 \pm to pericentric heterochromatin. *Nat Genet* **43**: 220–227. <http://dx.doi.org/10.1038/ng.765>.
- Maison C, Romeo K, Bailly D, Dubarry M, Quivy J-P, Almouzni G. 2012. The SUMO protease SENP7 is a critical component to ensure HP1 enrichment at pericentric heterochromatin. *Nat Struct Mol Biol* **19**: 458–460. <http://www.nature.com/articles/nsmb.2244> (Accessed January 14, 2019).
- Maiti A, Drohat AC. 2011. Thymine DNA Glycosylase Can Rapidly Excise 5-Formylcytosine and 5-Carboxylcytosine. *J Biol Chem* **286**: 35334–35338.
- Makarov VL, Lejnine S, Bedoyan J, Langmore JP. 1993. Nucleosomal Organization of Telomere-Specific Chromatin in Rat. *Cell* **73**: 775–787.
- Maksakova IA, Romanish MT, Gagnier L, Dunn CA, Lagemaat LN Van De, Mager DL. 2006. Retroviral Elements and Their Hosts: Insertional Mutagenesis in the Mouse Germ Line. *PLoS Genet* **2**.
- Malik HS, Henikoff S. 2003. Phylogenomics of the nucleosome. **10**: 882–891.
- Mangeat B, Turelli P, Caron G, Friedli M, Perrin L, Trono D. 2003. Broad antiretroviral defence by human APOBEC3G through lethal editing of nascent reverse transcripts. *Nature* 99–103.

- Mannironi C, Bonner WM, Hatch CL. 1989. H2A.X, a histone isoprotein with a conserved C-terminal sequence, is encoded by a novel mRNA with both DNA replication type and polyA 3' processing signals. *Nucleic Acids Res* **17**: 9113–9126. <https://academic-oup-com.proxy.insermbiblio.inist.fr/nar/article-abstract/17/22/9113/1176602?redirectedFrom=fulltext> (Accessed May 11, 2020).
- Mansuroglu Z, Benhelli-Mokrani H, Marcato V, Sultan A, Violet M, Chauderlier A, Delattre L, Loyens A, Talahari S, Bégard S, *et al.* 2016. Loss of Tau protein affects the structure, transcription and repair of neuronal pericentromeric heterochromatin. *Sci Rep* **6**: 1–16.
- Marano D, Fioriniello S, Fiorillo F, Gibbons RJ, D'Esposito M, Ragione F Della. 2019. ATRX contributes to MECP2-mediated pericentric heterochromatin organization during neural differentiation. *Int J Mol Sci* **20**: 1–28.
- Marchi E, Kanapin A, Magiorkinis G. 2014. Unfixed Endogenous Retroviral Insertions in the Human Population. *J Virol* **88**: 9529–9537.
- Marinoni I, Kurrer AS, Vassella E, Dettmer M, Rudolph T, Banz V, Hunger F, Pasquinelli S, Speel EJ, Perren A. 2014. Loss of DAXX and ATRX Are Associated With Chromosome Instability and Reduced Survival of Patients with Pancreatic Neuroendocrine Tumors. *Gastroenterology* **146**: 453–460.e5. <http://dx.doi.org/10.1053/j.gastro.2013.10.020>.
- Marinoni I, Wiederkeher A, Wiedmer T, Pantasis S, Di Domenico A, Frank R, Vassella E, Schmitt A, Perren A. 2017. Hypo-methylation mediates chromosomal instability in pancreatic NET. *Endocr Relat Cancer* **24**: 137–146.
- Marks H, Kalkan T, Menafrá R, Denissov S, Jones K, Hofemeister H, Nichols J, Kranz A, Francis Stewart A, Smith A, *et al.* 2012. The transcriptional and epigenomic foundations of ground state pluripotency. *Cell* **149**: 590–604.
- Marques Paya SL, de Arruda Cardoso Smith M, Fetteira Bertolucci PH. 1998. Differential Chromosome Sensitivity to 5-Azacytidine in Alzheimer's Disease. *Gerontology* **55**: 267–271.
- Martens JHA, Sullivan RJO, Braunschweig U, Opravil S, Radolf M, Steinlein P, Jenuwein T. 2005. The profile of repeat-associated histone lysine methylation states in the mouse epigenome. *EMBO J* **24**: 800–812.
- Martin GR. 1981. Isolation of a pluripotent cell line from early mouse embryos cultured in medium conditioned by teratocarcinoma stem cells. *Developmental Biology: Proc Natl Acad*

- Sci* **78**: 7634–7638.
- Marzec P, Armenise C, Pérot G, Roumelioti FM, Basyuk E, Gagos S, Chibon F, Déjardin J. 2015. Nuclear-Receptor-Mediated Telomere Insertion Leads to Genome Instability in ALT Cancers. *Cell* **160**: 913–927.
- Marzluff WF, Gongidi P, Woods KR, Jin J, Maltais LJ. 2002. The Human and Mouse Replication-Dependent Histone Genes. *Genomics* **80**: 487–498.
- Masui S, Nakatake Y, Toyooka Y, Shimosato D, Yagi R, Takahashi K, Okochi H, Okuda A, Matoba R, Sharov AA, *et al.* 2007. Pluripotency governed by Sox2 via regulation of Oct3 / 4 expression in mouse embryonic stem cells. *Nat Cell Biol* **9**.
- Matsui T, Leung D, Miyashita H, Maksakova IA, Miyachi H, Kimura H, Tachibana M, Lorincz MC, Shinkai Y. 2010. Proviral silencing in embryonic stem cells requires the histone methyltransferase ESET. *Nature* **464**: 927–931.
- Mattout A, Dechat T, Adam SA, Goldman RD, Gruenbaum Y. 2006. Nuclear lamins, diseases and aging. *Curr Opin Cell Biol* **18**: 335–341.
- Mayer J, Blomberg J, Seal RL. 2011. A revised nomenclature for transcribed human endogenous retroviral loci. *Mob DNA* **2**: 1–8.
- Maze I, Wenderski W, Noh K, Shen L, Molina H, Allis CD, Maze I, Wenderski W, Noh K, Bagot RC, *et al.* 2015. Critical Role of Histone Turnover in Neuronal Transcription and Plasticity. *Neuron* **77**–94.
- McClintock B. 1956. Controlling Elements and the Gene. *Cold Spring Harb Symp Quant Biol* **21**: 197–216.
- McDowell TL, Gibbons RJ, Sutherland H, O'Rourke DM, Bickmore WA, Pombo A, Turley H, Gatter K, Picketts DJ, Buckle VJ, *et al.* 1999. Localization of a putative transcriptional regulator (ATRX) at pericentromeric heterochromatin and the short arms of acrocentric chromosomes. *Proc Natl Acad Sci* **96**: 13983–13988. <http://www.pnas.org/cgi/doi/10.1073/pnas.96.24.13983> (Accessed May 7, 2020).
- Mckeeon FD, Kirschner MW, Caputtt D. 1986. Homologies in both primary and secondary structure between nuclear envelope and intermediate filament proteins. *Nature* **319**: 3–8.
- Meaburn KJ, Gudla PR, Khan S, Lockett SJ, Misteli T. 2009. Disease-specific gene repositioning in breast cancer. *J Cell Biol* **187**: 801–812.
- Meaburn KJ, Misteli T. 2008. Locus-specific and activity-independent gene repositioning during early tumorigenesis. *J Cell Biol* **180**: 39–50.
- Meinecke I, Cinski A, Baier A, Peters MA, Dankbar B, Wille A, Drynda A,

- Mendoza H, Gay RE, Hay RT, *et al.* 2007. Modification of nuclear PML protein by SUMO-1 regulates Fas-induced apoptosis in rheumatoid arthritis synovial fibroblasts. *Proc Natl Acad Sci* **104**: 1–6.
- Meissner A, Mikkelsen TS, Gu H, Wernig M, Hanna J, Sivachenko A, Zhang X, Bernstein BE, Nusbaum C, Jaffe DB, *et al.* 2008. Genome-scale DNA methylation maps of pluripotent and differentiated cells. *Nature* **454**: 766–770.
- Melanie Ehrlich. 2009. DNA hypomethylation in cancer cells. *Epigenomics* **1**: 239–259.
- Mendez-Bermudez A, Lototska L, Bauwens S, Giraud-Panis MJ, Croce O, Jamet K, Irizar A, Mowinckel M, Koundrioukoff S, Nottet N, *et al.* 2018. Genome-wide Control of Heterochromatin Replication by the Telomere Capping Protein TRF2. *Mol Cell* **70**: 449–461.e5.
- Meshorer E, Yellajoshula D, George E, Scambler PJ, Brown DT, Misteli T. 2006. Hyperdynamic plasticity of chromatin proteins in pluripotent embryonic stem cells. *Dev Cell* **10**: 105–116.
- Messerschmidt DM, Knowles BB, Solter D. 2014. DNA methylation dynamics during epigenetic reprogramming in the germline and preimplantation embryos. *Genes Dev* **28**: 812–828.
- Metzger E, Wissmann M, Yin N, Müller JM, Schneider R, Peters AHFM, Günther T, Buettner R, Schüle R. 2005. LSD1 demethylates repressive histone marks to promote androgen-receptor-dependent transcription. *Nature* **437**: 25–28.
- Meuleman W, Peric-hupkes D, Kind J, Beaudry J, Pagie L, Kellis M, Reinders M, Wessels L, Steensel B Van. 2013. Constitutive nuclear lamina – genome interactions are highly conserved and associated with A / T-rich sequence. *Genome Res* 270–280.
- Meyer C, Hofmann J, Burmeister T, Gro D, Park TS, Emerenciano M, Oliveira MP De, Renneville A, Villarese P. 2013. The MLL recombinome of acute leukemias in 2013. *Leukemia* 2165–2176.
- Meyne J, Ratliff RL, Moyzis RK. 1989. Conservation of the human telomere sequence (TTAGGG) among vertebrates. *Proc Natl Acad Sci* **86**: 7049–7053.
- Michaelson JS, Bader D, Kuo F, Kozak C, Leder P. 1999. Loss of Daxx, a promiscuously interacting protein, results in extensive apoptosis in early mouse development. *Genes Dev* 1918–1923.
- Michod D, Bartesaghi S, Khelifi A, Bellodi C, Berliocchi L, Nicotera P, Salomoni P. 2015. Calcium-Dependent Dephosphorylation of the Histone

- Chaperone DAXX Regulates H3.3 Loading and Transcription upon Neuronal Activation. *Neuron* **74**: 122–135.
<http://dx.doi.org/10.1016/j.neuron.2012.02.021>.
- Michod D, Bartesaghi S, Khelifi A, Bellodi C, Berliocchi L, Nicotera P, Salomoni P. 2012. Calcium-Dependent Dephosphorylation of the Histone Chaperone DAXX Regulates H3.3 Loading and Transcription upon Neuronal Activation. *Neuron* **74**: 122–135.
- Miki Y, Nishisho I, Horii A, Miyoshi Y, Utsunomiya J, Kinzler KW, Vogelstein B, Nakamura Y. 1992. Disruption of the APC Gene by a Retrotransposal Insertion of LI Sequence in a. *Cancer Res* **52**: 643–645.
- Mikkelsen TS, Ku M, Jaffe DB, Issac B, Lieberman E, Giannoukos G, Alvarez P, Brockman W, Kim T-K, Koche RP, *et al.* 2007. Genome-wide maps of chromatin state in pluripotent and lineage-committed cells. *Nature* **448**: 553–560.
<http://www.nature.com/doifinder/10.1038/nature06008>.
- Millanes-Romero A, Herranz N, Perrera V, Iturbide A, Loubat-casnovas J, Gil J, Jenuwein T, Garcia de Herreros A, Peiro S. 2013. Regulation of Heterochromatin Transcription during Epithelial-to-Mesenchymal Transition. *Mol Cell* **52**: 746–757.
- Min J, Wright WE, Shay JW. 2019. Clustered telomeres in phase-separated nuclear condensates engage mitotic DNA synthesis through BLM and RAD52. *Genes Dev* 1–14.
- Mita P, Sun X, Fenyö D, Kahler DJ, Li D, Agmon N, Wudzinska A, Keegan S, Bader JS, Yun C, *et al.* 2020. BRCA1 and S phase DNA repair pathways restrict LINE-1 retrotransposition in human cells. *Nat Struct Mol Biol* **27**: 179–191.
<http://dx.doi.org/10.1038/s41594-020-0374-z>.
- Mitchell JR, Wood E, Collins K. 1999. A telomerase component is defective in the human disease dyskeratosis congenita. *Nature* **402**: 551–555.
- Mito Y, Henikoff JG, Henikoff S. 2005. Genome-scale profiling of histone H3.3 replacement patterns. *Nat Genet* **37**: 1090–1097.
- Miyanari Y, Torres-Padilla M-E. 2012. Control of ground-state pluripotency by allelic regulation of Nanog. *Nature* **483**: 470–473.
<http://dx.doi.org/10.1038/nature10807>.
- Morozov VM, Gavrilova E V., Ogryzko V V., Ishov AM. 2012. Dualistic function of Daxx at centromeric and pericentromeric heterochromatin in normal and stress conditions. *Nucl*

- (United States) **3**.
- Moyzis RK, Buckingham JM, Crams LS, Dani M, Larry L, Jones MD, Meyne J, Ratliff RL, Wu J, Rich A. 1988. A highly conserved repetitive DNA sequence, (TTAGGG)_n present at the telomeres of human chromosomes. *Proc Natl Acad Sci* **85**: 6622–6626.
- Müller-Ott K, Erdel F, Matveeva A, Mallm J-P, Rademacher A, Hahn M, Bauer C, Zhang Q, Kaltofen S, Schotta G, *et al.* 2014. Specificity, propagation, and memory of pericentric heterochromatin. *Mol Sys Biol* **10**: 746. <http://www.ncbi.nlm.nih.gov/pubmed/25134515>.
- Müller S, Almouzni G. 2014. A network of players in H3 histone variant deposition and maintenance at centromeres. *Biochim Biophys Acta - Gene Regul Mech* **1839**: 241–250. <http://dx.doi.org/10.1016/j.bbagr.2013.11.008>.
- Müller S, MontesdeOca R, Lacoste N, Dingli F, Loew D, Almouzni G. 2014. Phosphorylation and DNA binding of HJURP determine its centromeric recruitment and function in CenH3CENP-A loading. *Cell Rep* **8**: 190–203.
- Muotri AR, Marchetto MCN, Coufal NG, Oefner R, Yeo G, Nakashima K, Gage FH. 2010. L1 retrotransposition in neurons is modulated by MeCP2. *Nature* **468**: 443–446. <http://dx.doi.org/10.1038/nature09544>.
- Murchison EP, Partridge JF, Tam OH, Cheloufi S, Hannon GJ. 2005. Characterization of Dicer-deficient murine embryonic stem cells. *Proc Natl Acad Sci* **102**: 12135–12140.
- Nagano T, Lubling Y, Stevens TJ, Schoenfelder S, Yaffe E, Dean W, Laue ED, Tanay A, Fraser P. 2013. Single-cell Hi-C reveals cell-to-cell variability in chromosome structure. *Nature* **502**: 59–64.
- Nagata T, Kato T, Morita T, Nozaki M, Kubota H, Yagi H, Matsushiro A. 1991. Polyadenylated and 3' processed mRNAs are transcribed from the mouse histone H2A.X gene. *Nucleic Acids Res* **19**: 2441–2447. <https://academic-oup-com.proxy.insermbiblio.inist.fr/nar/article-abstract/19/9/2441/2387355?redirectedFrom=fulltext> (Accessed May 11, 2020).
- Nagy A, Rossant J, Nagy R, Abramow-Newerly W, Roder JC. 1993. Derivation of completely cell culture-derived mice from early-passage embryonic stem cells. *Proc Natl Acad Sci U S A* **90**: 8424–8428.
- Nakamura T, Arai Y, Umehara H, Masuhara M, Kimura T, Taniguchi H, Sekimoto T, Ikawa M, Yoneda Y, Okabe M. 2007.

- PGC7 / Stella protects against DNA demethylation in early embryogenesis. *Nat Cell Biol* **9**.
- Nakatani T, Yamagata K, Kimura T, Oda M, Nakashima H, Hori M, Sekita Y, Arakawa T, Nakamura T, Nakano T. 2015. Stella preserves maternal chromosome integrity by inhibiting 5 hmC-induced γ H2AX accumulation. *EMBO Rep* **16**: 582–589.
- Napier CE, Huschtscha LI, Harvey A, Bower K, Noble JR, Hendrickson EA, Reddel RR. 2015. ATRX represses alternative lengthening of telomeres. *Oncotarget* **6**: 16543–16558.
<http://www.oncotarget.com/fulltext/3846>.
- Narayan A, Ji W, Zhang XY, Marrogi A, Graff JR, Baylin SB, Ehrlich M. 1998. Hypomethylation of pericentromeric DNA in breast adenocarcinomas. *Int J Cancer* **77**: 833–838.
- Narita M, Nun S, Heard E, Narita M, Lin AW, Hearn SA, Spector DL, Hannon GJ, Lowe SW. 2003. Rb-Mediated Heterochromatin Formation and Silencing of E2F Target Genes during Cellular Senescence. *Cell* **113**: 703–716.
- Nasr R, Guillemain M, Ferhi O, Soilhi H, Peres L, Berthier C, Gourmel B, Rousselot P, Robledo-sarmiento M, Vitoux D, *et al.* 2009. Eradication of acute promyelocytic leukemia-initiating cells through PML-RARA degradation. *Nat Med* **14**.
- Németh A, Conesa A, Santoyo-Lopez J, Medina I, Montaner D, Péterfia B, Solovei I, Cremer T, Dopazo J, Längst G. 2010. Initial genomics of the human nucleolus. *PLoS Genet* **6**.
- Ng RK, Gurdon JB. 2008. Epigenetic memory of an active gene state depends on histone H3.3 incorporation into chromatin in the absence of transcription. *Nat Cell Biol* **10**: 102–109.
- Ng SB, Bigham AW, Buckingham KJ, Hannibal MC, Mcmillin MJ, Gildersleeve HI, Beck AE, Tabor HK, Cooper GM, Mefford HC, *et al.* 2011. Exome sequencing identifies MLL2 mutations as a cause of Kabuki syndrome. *Nat Genet* **42**.
- Nguyen HTD, Tam J, Wu RA, Greber BJ, Toso D, Nogales E, Collins K. 2018. Cryo-EM structure of substrate-bound human telomerase holoenzyme. *Nature* **557**.
- Nichols J, Zevnik B, Anastassiadis K, Niwa H, Klewe-nebenius D, Chambers I, Smith A. 1998. Formation of Pluripotent Stem Cells in the Mammalian Embryo Depends on the POU Transcription Factor Oct4. *Cell* **95**: 379–391.
- Niwa-Kawakita M, Ferhi O, Soilhi H, Le Bras M, Lallemand-Breitenbach V, de Thé H. 2017. PML is a ROS sensor activating p53 upon oxidative stress. *J*

- Exp Med* **214**: 3197–3206.
<http://www.ncbi.nlm.nih.gov/pubmed/28931625>
<http://www.pubmedcentral.nih.gov/articlerender.fcgi?artid=PMC5679165>.
- Nora EP, Lajoie BR, Schulz EG, Giorgetti L, Okamoto I, Servant N, Piolot T, van Berkum NL, Meisig J, Sedat J, *et al.* 2012. Spatial partitioning of the regulatory landscape of the X-inactivation centre. *Nature* **485**: 381–385.
- Novo CL, Tang C, Ahmed K, Djuric U, Fussner E, Mullin NP, Morgan NP, Hayre J, Sienerth AR, Elderkin S, *et al.* 2016. The pluripotency factor Nanog regulates pericentromeric heterochromatin organization in mouse embryonic stem cells. *Genes Dev* **30**: 1101–1115.
- Nye J, Sturgill D, Athwal R, Dalal Y. 2018. HJURP antagonizes CENP-A mislocalization driven by the H3.3 chaperones HIRA and DAXX. *PLoS One* **13**: 1–21.
- Ogino S, Nosho K, Kirkner GJ, Kawasaki T, Chan T, Schernhammer ES, Giovannucci EL, Fuchs CS. 2008. A Cohort Study of Tumoral LINE-1 Hypomethylation and Prognosis in Colon Cancer. *J Natl Cancer Inst* **100**: 1734–1738.
- Oh JH, Gertych A, Tajbakhsh J. 2013. Nuclear DNA Methylation and Chromatin Condensation Phenotypes Are Distinct Between Normally Proliferating / Aging , Rapidly Growing / Immortal , and Senescent Cells
 ABSTRACT : *Oncotarget* **4**: 474–493.
- Ohno S. 1972. So much “junk” DNA in our genome. *Brookhaven Symp Biol* **23**: 366–70.
<http://www.ncbi.nlm.nih.gov/pubmed/5065367> (Accessed May 11, 2020).
- Okano M, Bell DW, Haber DA, Li E. 1999. DNA Methyltransferases Dnmt3a and Dnmt3b Are Essential for De Novo Methylation and Mammalian Development. *Cell* **99**: 247–257.
- Okumura-Nakanishi S, Saito M, Niwa H, Ishikawa F. 2005. Oct-3 / 4 and Sox2 Regulate Oct-3 / 4 Gene in Embryonic Stem Cells. *J Biol Chem* **280**: 5307–5317.
- Olins AL, Olins DE. 1973. Spheroid Chromatin Units (v Bodies). *Science (80-)* **183**: 330–333.
- Olley G, Ansari M, Bengani H, Grimes GR, Rhodes J, Kriegsheim A Von, Blatnik A, Stewart FJ, Wakeling E, Carroll N, *et al.* 2018. BRD4 interacts with NIPBL and BRD4 is mutated in a Cornelia de Lange – like syndrome. *Nat Genet* **50**.
- Osterwald S, Deeg KI, Chung I, Parisotto D, Wörz S, Rohr K, Erfle H, Rippe K. 2015. PML induces compaction, TRF2 depletion and DNA damage signaling at telomeres and promotes their alternative lengthening. *J Cell Sci* 1887–1900.
<http://www.ncbi.nlm.nih.gov/pubmed>

- /25908860.
- Ostromyshenskii DI, Chernyaeva EN, Kuznetsova IS, Podgornaya OI. 2018. Mouse chromocenters DNA content: Sequencing and in silico analysis. *BMC Genomics* **19**: 1–15.
- Padeken J, Zeller P, Towbin B, Katic I, Kalck V, Methot SP, Gasser SM. 2019. Synergistic lethality between BRCA1 and H3K9me2 loss reflects satellite derepression. *Genes Dev* **33**: 436–451.
- Papait R, Pistore C, Negri D, Pecoraro D, Cantarini L, Bonapace IM. 2007. Np95 Is Implicated in Pericentromeric Heterochromatin Replication and in Major Satellite Silencing ed. W. Bickmore. *Mol Biol Cell* **18**: 1098–1106. <http://www.molbiolcell.org/doi/10.1091/mbc.e06-09-0874> (Accessed January 22, 2019).
- Pardue M, Debaryshe PG. 2003. Retrotransposons Provide an Evolutionarily Robust Non-Telomerase Mechanism to Maintain Telomeres. *Annu Rev Genet* **37**: 485–511.
- Park J, Lee H, Han N, Kwak S, Lee H-T, Kim J-H, Kang K, Youn BH, Yang J-H, Jeong H-J, *et al.* 2018. Long non-coding RNA ChRO1 facilitates ATRX/DAXX-dependent H3.3 deposition for transcription-associated heterochromatin reorganization. *Nucleic Acids Res* **46**: 11759–11775. <https://academic.oup.com/nar/article/46/22/11759/5134335> (Accessed March 13, 2019).
- Passarge E. 1979. Emil Heitz and the Concept of Heterochromatin: Longitudinal Chromosome Differentiation was Recognized Fifty Years Ago. *Am J Hum Genet* **31**: 106–115.
- Pederson T. 2011. The Nucleolus. *Cold Spring Harb Perspect Biol* **3**: 1–16.
- Pehrson JR, Fried VA. 1992. MacroH2A, a Core Histone Containing a Large Nonhistone Region. *Science (80-)* **4**–7.
- Peng JC, Karpen GH. 2007. H3K9 methylation and RNA interference regulate nucleolar organization and repeated DNA stability. *Nat Cell Biol* **9**: 25–35.
- Peric-Hupkes D, Meuleman W, Pagie L, Bruggeman SWM, Solovei I, Brugman W, Gräf S, Flicek P, Kerkhoven RM, van Lohuizen M, *et al.* 2010. Molecular Maps of the Reorganization of Genome-Nuclear Lamina Interactions during Differentiation. *Mol Cell* **38**: 603–613.
- Perovanovic J, Dell’Orso S, Gnochi VF, Jaiswal JK, Sartorelli V, Vigouroux C, Mamchaoui K, Mouly V, Bonne G, Hoffman EP. 2016. Laminopathies disrupt epigenomic developmental programs and cell fate. *Sci Transl Med* **8**.
- Pertel T, Hausmann S, Morger D, Züger S, Guerra J, Lascano J, Reinhard C, Pertel

- T, Albert ML, Strambio-de-castillia C, *et al.* 2011. TRIM5 is an innate immune sensor for the retrovirus capsid lattice. *Nature* **472**: 361–365.
- Peters AHFM, O’Carroll D, Scherthan H, Mechtler K, Sauer S, Schöfer C, Weipoltshammer K, Pagani M, Lachner M, Kohlmaier A, *et al.* 2001. Loss of the Suv39h histone methyltransferases impairs mammalian heterochromatin and genome stability. *Cell* **107**: 323–337.
- Phan HM, Xu AW, Coco C, Srajer G, Wyszomierski S, Evrard YA, Eckner R, Dent SYR. 2005. GCN5 and p300 Share Essential Functions During Early Embryogenesis. *Dev Dyn* 1337–1347.
- Piazzesi A, Papic D, Bertan F, Salomoni P, Nicotera P, Bano D. 2016. Controls Animal Lifespan through the Regulation of Pro-longevity Transcriptional Programs. *Cell Rep* 987–996.
- Pickersgill H, Kalverda B, de Wit E, Talhout W, Fornerod M, van Steensel B. 2006. Characterization of the *Drosophila melanogaster* genome at the nuclear lamina. *Nat Genet* **38**: 1005–14. <http://www.ncbi.nlm.nih.gov/pubmed/16878134>.
- Pinheiro I, Margueron R, Shukeir N, Eisold M, Fritsch C, Richter FM, Mittler G, Genoud C, Goyama S, Kurokawa M, *et al.* 2012. Prdm3 and Prdm16 are H3K9me1 methyltransferases required for mammalian heterochromatin integrity. *Cell* **150**: 948–60. <http://www.ncbi.nlm.nih.gov/pubmed/22939622> (Accessed November 18, 2018).
- Plath K, Fang J, Mlynarczyk-evans SK, Cao R, Worringer KA, Wang H, de la Cruz CC, Otte AP, Panning B, Zhang Y. 2003. Role of Histone H3 Lysine 27 Methylation in X Inactivation. *Science (80-)* **300**: 131–136.
- Plusa B, Hadjantonakis AK. 2014. Embryonic stem cell identity grounded in the embryo. *Nat Cell Biol* **16**: 502–504. <http://dx.doi.org/10.1038/ncb2984>.
- Pluta AF, Earnshaw WC, Goldberg IG. 1998. Interphase-specific association of intrinsic centromere protein CENP-C with HDaxx , a death domain-binding protein implicated in Fas-mediated cell death. *J Cell Sci* **2041**: 2029–2041.
- Pogo BYBGT, Allfrey VG, Mirsky AE. 1966. RNA SYNTHESIS AND HISTONE ACETYLATION DURING THE COURSE OF GENE ACTIVATION IN LYMPHOCYTES *. *Proc Natl Acad Sci* 805–812.
- Poleshko A, Mansfield KM, Burlingame CC, Andrade MD, Shah NR, Katz RA. 2013. The Human Protein PRR14 Tethers Heterochromatin to the Nuclear Lamina during Interphase and Mitotic Exit. *CellReports* **5**: 292–301. <http://dx.doi.org/10.1016/j.celrep.2013.09.024>.

- Poleshko A, Shah PP, Gupta M, Smith CL, Epstein JA, Jain R, Poleshko A, Shah PP, Gupta M, Babu A, *et al.* 2017. Genome-Nuclear Lamina Interactions Regulate Cardiac Stem Cell Lineage Restriction Article Genome-Nuclear Lamina Interactions Regulate Cardiac Stem Cell Lineage Restriction. *Cell* 1–15.
- Pope BD, Ryba T, Dileep V, Yue F, Wu W, Vera DL, Wang Y, Hansen RS, Canfield TK, Robert E, *et al.* 2014. Topologically-associating domains are stable units of replication-timing regulation. *Nature* **515**: 402–405.
- Popova EY, Grigoryev SA, Fan Y, Skoultchi AI, Zhang SS, Barnstable CJ. 2013. Developmentally regulated linker histone H1c promotes heterochromatin condensation and mediates structural integrity of rod photoreceptors in mouse retina. *J Biol Chem* **288**: 17895–17907.
- Popp C, Dean W, Feng S, Cokus SJ, Andrews S, Pellegrini M, Jacobsen SE, Reik W. 2010. Genome-wide erasure of DNA methylation in mouse primordial germ cells is affected by AID deficiency. *Nature* **463**: 1101–1105. <http://dx.doi.org/10.1038/nature08829>.
- Prada D, González R, Sánchez L, Castro C, Fabián E, Herrera LA. 2012. Satellite 2 demethylation induced by 5-azacytidine is associated with missegregation of chromosomes 1 and 16 in human somatic cells. *Mutat Res - Fundam Mol Mech Mutagen* **729**: 100–105. <http://dx.doi.org/10.1016/j.mrfmmm.2011.10.007>.
- Pradhan SK, Su T, Yen L, Jacquet K, Huang C, Côté J, Kurdistani SK, Carey MF. 2016. EP400 Deposits H3.3 into Promoters and Enhancers during Gene Activation. *Mol Cell* **61**: 27–38. <http://linkinghub.elsevier.com/retrieve/pii/S1097276515008308>.
- Pradhan SK, Su T, Yen L, Jacquet K, Huang C, Côté J, Kurdistani SK, Carey MF. 2015. EP400 Deposits H3.3 into Promoters and Enhancers during Gene Activation. *Mol Cell*.
- Probst A V., Okamoto I, Casanova M, El Marjou F, Le Baccon P, Almouzni G. 2010. A Strand-specific burst in transcription of pericentric satellites is required for chromocenter formation and early mouse development. *Dev Cell* **19**: 625–638.
- Prudencio M, Gonzales PK, Cook CN, Gendron TF, Daugherty LM, Song Y, Ebbert MTW, van Blitterswijk M, Zhang YJ, Jansen-West K, *et al.* 2017. Repetitive element transcripts are elevated in the brain of C9orf72 ALS/FTLD patients. *Hum Mol Genet* **26**: 3421–3431.
- Rafique S, Thomas JS, Sproul D, Bickmore WA. 2015. Estrogen-induced chromatin

- decondensation and nuclear re-organization linked to regional epigenetic regulation in breast cancer. *Genome Biol* **16**: 1–19.
- Rajshekar S, Yao J, Arnold PK, Payne SG, Zhang Y, Bowman T V, Schmitz RJ, Edwards JR, Goll M. 2018. Pericentromeric hypomethylation elicits an interferon response in an animal model of ICF syndrome. *Elife* **7**: 1–21. <https://elifesciences.org/articles/39658>.
- Ramamoorthy M, Smith S. 2015. Loss of ATRX Suppresses Resolution of Telomere Cohesion to Control Recombination in ALT Cancer Article Loss of ATRX Suppresses Resolution of Telomere Cohesion to Control Recombination in ALT Cancer Cells. *Cancer Cell* **28**: 357–369. <http://dx.doi.org/10.1016/j.ccell.2015.08.003>.
- Ran FA, Hsu PD, Wright J, Agarwala V, Scott DA, Zhang F. 2013. Genome engineering using the CRISPR-Cas9 system. *Nat Protoc* **8**: 2281–2308. <http://dx.doi.org/10.1038/nprot.2013.143> <http://www.nature.com/nprot/journal/v8/n11/abs/nprot.2013.143.html#supplementary-information>.
- Rapkin LM, Ahmed K, Dulev S, Li R, Kimura H, Ishov AM, Bazett-Jones DP. 2015. The histone chaperone DAXX maintains the structural organization of heterochromatin domains. *Epigenetics Chromatin* **8**: 44. <http://www.epigeneticsandchromatin.com/content/8/1/44>.
- Ratnakumar K, Duarte LF, Leroy G, Hasson D, Smeets D, Vardabasso C, Zeng T, Xiang B, Zhang DY, Li H, *et al.* 2012. ATRX-mediated chromatin association of histone variant macroH2A1 regulates a -globin expression. *Genes Dev* **26**: 433–438.
- Ray-gallet D, Quivy J, Scamps C, Martini EM, Lipinski M, Cedex V. 2002. HIRA Is Critical for a Nucleosome Assembly Pathway Independent of DNA Synthesis. *Mol Cell* **9**: 1091–1100.
- Rea S, Eisenhaber F, O’Carroll D, Strahl BD, Sun Z-W, Schmid M, Opravil S, Mechtler K, Ponting CP, Allis CD, *et al.* 2000. Regulation of chromatin structure by site-specific histone H3 methyltransferases. *Nature* **406**: 593–599.
- Regad T, Bellodi C, Nicotera P, Salomoni P. 2009. The tumor suppressor Pml regulates cell fate in the developing neocortex. *Nat Neurosci* **12**: 132–140.
- Ribet D, Harper F, Dupressoir A, Dewannieux M, Pierron G, Heidmann T. 2008. An infectious progenitor for the murine IAP retrotransposon: Emergence of an intracellular genetic parasite from an ancient retrovirus.

- Genome Res* **18**: 597–609.
- Ricci MA, Manzo C, Garcia-Parajo MF, Lakadamyali M, Cosma MP. 2015. Chromatin fibers are formed by heterogeneous groups of nucleosomes in vivo. *Cell* **160**: 1145–1158.
- Ricketts MD, Frederick B, Hoff H, Tang Y, Schultz DC, Rai TS, Vizioli MG, Adams PD, Marmorstein R. 2015. Ubinuclein-1 confers histone H3.3-specific-binding by the HIRA histone chaperone complex. *Nat Commun* 1–11.
- Ridsdale AJ, Hendzel MJ, Delcuve GP, Davie JR. 1990. Histone Acetylation Alters the Capacity of the H1 Histones to Condense Transcriptionally Active / Competent Chromatin *. *J Biol Chem* **265**: 5150–5156.
- Rivron NC, Frias-Aldeguer J, Vrij EJ, Boisset JC, Korving J, Vivié J, Truckenmüller RK, Van Oudenaarden A, Van Blitterswijk CA, Geijsen N. 2018. Blastocyst-like structures generated solely from stem cells. *Nature* **557**: 106–111.
- Röber R, Weber K, Osborn M. 1989. Differential timing of nuclear lamin A / C expression in the various organs of the mouse embryo and the young animal: a developmental study. *Development* **378**: 365–378.
- Robin JD, Ludlow AT, Batten K, Magdinier F, Stadler G, Wagner KR, Shay JW, Wright WE. 2014. Telomere position effect: Regulation of gene expression with progressive telomere shortening over long distances. *Genes Dev* **28**: 2464–2476.
- Robson MI, de las Heras JI, Czapiewski R, Lê Thành P, Booth DG, Kelly DA, Webb S, Kerr ARW, Schirmer EC. 2016. Tissue-Specific Gene Repositioning by Muscle Nuclear Membrane Proteins Enhances Repression of Critical Developmental Genes during Myogenesis. *Mol Cell* 834–847.
<http://linkinghub.elsevier.com/retrieve/pii/S109727651630137X>.
- Rodriguez-Terrones D, Gaume X, Ishiuchi T, Weiss A, Kopp A, Kruse K, Penning A, Vaquerizas JM, Brino L, Torres-Padilla ME. 2018. A molecular roadmap for the emergence of early-embryonic-like cells in culture. *Nat Genet* **50**: 106–119.
<http://dx.doi.org/10.1038/s41588-017-0016-5>.
- Roers A, Hiller B, Hornung V. 2016. Recognition of Endogenous Nucleic Acids by the Innate Immune System. *Immunity* **44**: 739–754.
- Rogakou EP, Boon C, Redon C, Bonner WM. 1999. Megabase chromatin domains involved in DNA double-strand breaks in vivo. *J Cell Biol* **146**: 905–915.
- Romeo K, Louault Y, Cantaloube S, Loiodice

- I, Almouzni G, Quivy J-P. 2015. The SENP7 SUMO-Protease Presents a Module of Two HP1 Interaction Motifs that Locks HP1 Protein at Pericentric Heterochromatin. *Cell Rep* **10**: 771–782. <https://www.sciencedirect.com/science/article/pii/S2211124715000054> (Accessed November 18, 2018).
- Roos WP, Kaina B. 2006. DNA damage-induced cell death by apoptosis. *Trends Mol Med* **12**.
- Rothbart SB, Krajewski K, Nady N, Tempel W, Xue S, Badeaux AI, Barsyte-lovejoy D, Martinez JY, Bedford MT, Fuchs SM, *et al.* 2012. Association of UHRF1 with methylated H3K9 directs the maintenance of DNA methylation. *Nat Struct Mol Biol* **19**.
- Roulland Y, Ouararhni K, Naidenov M, Ramos L, Shuaib M, Syed SH, Nizar Lone I, Boopathi R, Fontaine E, Papai G, *et al.* 2016. The Flexible Ends of CENP-A Nucleosome Are Required for Mitotic Fidelity Article The Flexible Ends of CENP-A Nucleosome Are Required for Mitotic Fidelity. *Mol Cell* **63**: 674–685. <http://dx.doi.org/10.1016/j.molcel.2016.06.023>.
- Rowe HM, Jakobsson J, Mesnard D, Rougemont J, Reynard S, Aktas T, Maillard P V., Layard-Liesching H, Verp S, Marquis J, *et al.* 2010. KAP1 controls endogenous retroviruses in embryonic stem cells. *Nature* **463**: 237–240.
- Ryu T, Spatola B, Delabaere L, Bowlin K, Hopp H, Karpen GH, Chiolo I. 2015. Heterochromatic breaks move to the nuclear periphery to continue recombinational repair. *Nat Cell Biol* **17**: 1401–1411.
- Sadic D, Schmidt K, Groh S, Kondofersky I, Ellwart J, Fuchs C, Theis FJ, Schotta G. 2015. Atrx promotes heterochromatin formation at retrotransposons. *EMBO Rep* **16**.
- Sahin U, Ferhi O, Jeanne M, Benhenda S, Berthier C, Jollivet F, Niwa-Kawakita M, Faklaris O, Setterblad N, Thé H de, *et al.* 2014. Oxidative stress–induced assembly of PML nuclear bodies controls sumoylation of partner proteins. *J Cell Biol* **204**: 931–945. <http://jcb.rupress.org/content/204/6/931.short> (Accessed January 28, 2019).
- Saito K, Kawakami K, Matsumoto I, Oda M. 2010. Long Interspersed Nuclear Element 1 Hypomethylation Is a Marker of Poor Prognosis in Stage IA Non – Small Cell Lung Cancer. *Clin Cancer Res* **16**: 2418–2427.
- Saiz N, Plusa B. 2013. Early cell fate decisions in the mouse embryo. *Reproduction* 1470–1626.
- Saksouk N, Barth TK, Ziegler-Birling C, Olova N, Nowak A, Rey E, Mateos-Langerak J, Urbach S, Reik W, Torres-Padilla ME, *et al.* 2014. Redundant

- Mechanisms to Form Silent Chromatin at Pericentromeric Regions Rely on BEND3 and DNA Methylation. *Mol Cell* **56**: 580–594.
- Salsman J, Rapkin LM, Margam NN, Duncan R, Bazett-Jones DP, Dellaire G. 2017. Myogenic differentiation triggers PML nuclear body loss and DAXX relocalization to chromocentres. *Cell Death Dis* **8**: e2724. <http://www.nature.com/doifinder/10.1038/cddis.2017.151>.
- Samstein RM, Josefowicz SZ, Arvey A, Treuting PM, Rudensky AY. 2012. Extrathymic Generation of Regulatory T Cells in Placental Mammals Mitigates Maternal-Fetal Conflict. *Cell* **150**: 29–38. <http://dx.doi.org/10.1016/j.cell.2012.05.031>.
- Saniy E, Poortinga G, Sharkey K, Hung S, Holloway TP, Quin J, Robb E, Wong LH, Thomas WG, Stefanovsky V, *et al.* 2008. UBF levels determine the number of active ribosomal RNA genes in mammals. *J Cell Biol* **183**: 1259–1274.
- Santenard A, Ziegler-birling C, Koch M, Tora L, Andrew J. 2013. Heterochromatin formation in the mouse embryo requires critical residues of the histone variant H3 . 3. *Nat Cell Biol* **12**: 853–862.
- Santenard A, Ziegler-Birling C, Koch M, Tora L, Bannister AJ, Torres-Padilla ME. 2010. Heterochromatin formation in the mouse embryo requires critical residues of the histone variant H3.3. *Nat Cell Biol* **12**: 853–862. <http://dx.doi.org/10.1038/ncb2089>.
- Santos F, Peat J, Burgess H, Rada C, Reik W, Dean W. 2013. Active demethylation in mouse zygotes involves cytosine deamination and base excision repair. *Epigenetics and Chromatin* **6**: 1–12.
- Sanulli S, Trnka MJ, Dharmarajan V, Tibble RW, Pascal BD, Burlingame AL, Griffin PR, Gross JD, Narlikar GJ. 2019. HP1 reshapes nucleosome core to promote phase separation of heterochromatin. *Nature* **575**: 390–394. <http://dx.doi.org/10.1038/s41586-019-1669-2>.
- Sasai N, Saitoh N, Saitoh H, Nakao M. 2013. The Transcriptional Cofactor MCAF1/ATF7IP Is Involved in Histone Gene Expression and Cellular Senescence. *PLoS One* **8**: 1–9.
- Saurin AJ, Freemont PS, Shiels C, Williamson J, Sheer D, Satijn DPE, Otte AP, Sheer D, Freemont PS. 1998. The human polycomb group complex associates with pericentromeric heterochromatin to form a novel nuclear domain. *J Cell Biol* **142**: 887–898.
- Savić N, Bär D, Leone S, Frommel SC, Weber FA, Vollenweider E, Ferrari E, Ziegler U, Kaeck A, Shakhova O, *et al.* 2014. lncRNA Maturation to Initiate Heterochromatin Formation in the Nucleolus Is Required for Exit from

- Pluripotency in ESCs. *Cell Stem Cell* **15**: 720–734.
<https://www.sciencedirect.com/science/article/pii/S1934590914004561>
 (Accessed November 18, 2018).
- Sawatsubashi S, Murata T, Lim J, Fujiki R, Ito S, Suzuki E, Tanabe M, Zhao Y, Kimura S, Fujiyama S, *et al.* 2010. A histone chaperone, DEK, transcriptionally coactivates a nuclear receptor. *Genes Dev* **24**: 159–170.
- Schirmer EC, Florens L, Guan T, Iii JRY, Gerace L. 2003. Nuclear Membrane Proteins with Subtractive Proteomics. *301*: 1380–1383.
- Schlesinger S, Meshorer E, Goff SP. 2014. Asynchronous transcriptional silencing of individual retroviral genomes in embryonic cells. *Retrovirology* **11**: 1–11.
- Schlesinger S, Selig S, Bergman Y, Cedar H. 2009. Allelic inactivation of rDNA loci. *Genes Dev* **23**: 2437–2447.
- Schmidt D, Schwalie PC, Wilson MD, Ballester B, Brown GD, Marshall A, Flicek P, Odom DT. 2012. Waves of Retrotransposon Expansion Remodel Genome Organization and CTCF Binding in Multiple Mammalian Lineages. *Cell* **148**: 335–348.
- Schmutz I, Timashev L, Xie W, Patel DJ, De Lange T. 2017. TRF2 binds branched DNA to safeguard telomere integrity. *Nat Struct Mol Biol* **24**: 734–742.
- Schneiderman JI, Orsi GA, Hughes KT, Loppin B, Ahmad K. 2012. Nucleosome-depleted chromatin gaps recruit assembly factors for the H3.3 histone variant. *Proc Natl Acad Sci U S A* **109**: 19721–6.
<http://www.pubmedcentral.nih.gov/articlerender.fcgi?artid=3511725&tool=pmcentrez&rendertype=abstract>.
- Schnerch A, Cerdan C, Bhatia M. 2010. Distinguishing Between Mouse and Human Pluripotent Stem Cell Regulation: The Best Laid Plans of Mice and Men. *Stem Cells* **28**: 419–430.
- Schotta G, Lachner M, Sarma K, Ebert A, Sengupta R, Reuter G, Reinberg D, Jenuwein T. 2004. A silencing pathway to induce H3-K9 and H4-K20 trimethylation at constitutive heterochromatin. *Genes Dev* **1**: 1251–1262.
- Schuettengruber B, Bourbon H, Croce L Di, Cavalli G. 2017. Genome Regulation by Polycomb and Trithorax: 70 Years and Counting. *Cell* **171**: 34–57.
<http://dx.doi.org/10.1016/j.cell.2017.08.002>.
- Schultz DC, Friedman JR, Rauscher III FJ. 2001. Targeting histone deacetylase complexes via KRAB-zinc finger proteins: the PHD and bromodomains of KAP-1 form a cooperative unit that recruits a novel isoform of the Mi-2 α subunit of NuRD. *Genes Dev* **15**: 428–443.

- Schwartzentruber J, Korshunov A, Liu X-Y, Jones DTW, Pfaff E, Jacob K, Sturm D, Fontebasso AM, Quang D-AK, Tönjes M, *et al.* 2012. Driver mutations in histone H3.3 and chromatin remodelling genes in paediatric glioblastoma. *Nature* **484**: 130–130.
- Scott EC, Gardner EJ, Masood A, Chuang NT, Vertino PM, Devine SE. 2016. A hot L1 retrotransposon evades somatic repression and initiates human colorectal cancer. *Genome Res* **26**: 745–755.
- Sexton T, Yaffe E, Kenigsberg E, Bantignies F, Leblanc B, Hoichman M, Parrinello H, Tanay A, Cavalli G. 2012. Three-Dimensional Folding and Functional Organization Principles of the Drosophila Genome. *Cell* **148**: 458–472.
- Shachar S, Voss TC, Pegoraro G, Sciascia N, Misteli T. 2015. Identification of Gene Positioning Factors Using High-Throughput Imaging Mapping. *Cell* **162**: 911–923.
<http://www.sciencedirect.com/science/article/pii/S0092867415009125>.
- Shahbazi MN, Zernicka-goetz M. 2018. Deconstructing and reconstructing the mouse and human early embryo. *Nat Cell Biol* **20**.
<http://dx.doi.org/10.1038/s41556-018-0144-x>.
- Shahbazian MD, Grunstein M. 2007. Functions of Site-Specific Histone Acetylation and Deacetylation. *Annu Rev Biochem* **76**: 75–100.
- Sharif J, Muto M, Takebayashi S, Suetake I, Iwamatsu A, Endo TA, Shinga J, Mizutani-koseki Y, Toyoda T, Okamura K, *et al.* 2007. The SRA protein Np95 mediates epigenetic inheritance by recruiting Dnmt1 to methylated DNA. *Nature* **450**: 908–912.
- Shay JW, Wright WE. 2005. Senescence and immortalization: Role of telomeres and telomerase. *Carcinogenesis* **26**: 867–874.
- Shay JW, Wright WE. 2019. Telomeres and telomerase: three decades of progress. *Nat Rev Genet* **20**: 299–309.
<http://dx.doi.org/10.1038/s41576-019-0099-1>.
- Shen TH, Lin H, Scaglioni PP, Yung TM, Pandolfi PP. 2006. The Mechanisms of PML-Nuclear Body Formation. *Mol Cell* **1**: 331–339.
- Shevelyov YY, Lavrov SA, Mikhaylova LM, Nurminsky ID, Kulathinal RJ, Egorova KS, Rozovsky YM. 2009. The B-type lamin is required for somatic repression of testis-specific gene clusters.
- Shi Y, Lan F, Matson C, Mulligan P, Whetstine JR, Cole PA, Casero RA, Shi Y. 2004. Histone Demethylation Mediated by the Nuclear Amine Oxidase Homolog LSD1. *Cell* **119**: 941–953.
- Shiels C, Islam SA, Vatcheva R, Sasieni P, Sternberg MJE, Freemont PS, Sheer D.

2001. PML bodies associate specifically with the MHC gene cluster in interphase nuclei. *J Cell Sci* **114**: 3705–3716.
- Shin Y, Chang YC, Lee DSW, Berry J, Sanders DW, Ronceray P, Wingreen NS, Haataja M, Brangwynne CP. 2018. Liquid Nuclear Condensates Mechanically Sense and Restructure the Genome. *Cell* **175**: 1481-1491.e13. <https://doi.org/10.1016/j.cell.2018.10.057>.
- Shirai A, Kawaguchi T, Shimojo H, Muramatsu D, Ishida-Yonetani M, Nishimura Y, Kimura H, Nakayama JI, Shinkai Y. 2017. Impact of nucleic acid and methylated H3K9 binding activities of Suv39h1 on its heterochromatin assembly. *Elife* **6**.
- Shogren-Knaak M, Ishii H, Sun J-M, Pazin MJ, Davie JR, Peterson CL. 2006. Histone H4-K16 Acetylation Controls Chromatin Structure and Protein Interactions. *Science (80-)* **16**: 844–848.
- Siggins L, Cordeddu L, Rönnerblad M, Lennartsson A, Ekwall K. 2015. Transcription-coupled recruitment of human CHD1 and CHD2 influences chromatin accessibility and histone H3 and H3.3 occupancy at active chromatin regions. *Epigenetics Chromatin* **8**: 4. <http://www.ncbi.nlm.nih.gov/pubmed/25621013>.
- Sim YJ, Kim MS, Nayfeh A, Yun YJ, Kim SJ, Park KT, Kim CH, Kim KS. 2017. 2i Maintains a Naive Ground State in ESCs through Two Distinct Epigenetic Mechanisms. *Stem Cell Reports* **8**: 1312–1328. <http://dx.doi.org/10.1016/j.stemcr.2017.04.001>.
- Skene PJ, Illingworth RS, Webb S, Kerr ARW, James KD, Turner DJ, Andrews R, Bird AP. 2010. Neuronal MeCP2 Is Expressed at Near Histone-Octamer Levels and Globally Alters the Chromatin State. *Mol Cell* **37**: 457–468. <http://dx.doi.org/10.1016/j.molcel.2010.01.030>.
- Smit AFA, Riggs AD. 1996. Tiggers and other DNA transposon fossils in the human genome. *Proc Natl Acad Sci* **93**: 1443–1448.
- Smith ZD, Meissner A. 2013. DNA methylation: roles in mammalian development. *Nat Rev Genet* **14**: 204–220.
- Sobecki M, Souaid C, Boulay J, Guerineau V, Noordermeer D, Crabbe L. 2018. MadID, a Versatile Approach to Map Protein-DNA Interactions, Highlights Telomere-Nuclear Envelope Contact Sites in Human Cells. *Cell Rep* **25**: 2891-2903.e5. <https://doi.org/10.1016/j.celrep.2018.11.027>.
- Sobel RE, Cook RG, Perry CA, Annunziato AT, Allis CD. 1995. Conservation of deposition-related acetylation sites in

- newly synthesized histones H3 and H4. *Proc Natl Acad Sci* **92**: 1237–1241.
- Solovei I, Grandi N, Knoth R, Volk B, Cremer T. 2004. Positional changes of pericentromeric heterochromatin and nucleoli in postmitotic Purkinje cells during murine cerebellum development. *Cytogenet Genome Res* **105**: 302–310.
- Solovei I, Kreysing M, Lancto C, Kösem S, Peichl L, Cremer T, Guck J, Joffe B. 2009. Nuclear Architecture of Rod Photoreceptor Cells Adapts to Vision in Mammalian Evolution. *Cell* 356–368.
- Solovei I, Wang AS, Thanisch K, Schmidt CS, Krebs S, Zwerger M, Cohen T V, Devys D, Foisner R, Peichl L, *et al.* 2011. LBR and Lamin A / C Sequentially Tether Peripheral Heterochromatin and Inversely Regulate Differentiation. *Cell* **152**: 584–598. <http://dx.doi.org/10.1016/j.cell.2013.01.009>.
- Solovei I, Wang AS, Thanisch K, Schmidt CS, Krebs S, Zwerger M, Cohen T V, Devys D, Foisner R, Peichl L, *et al.* 2013. LBR and Lamin A / C Sequentially Tether Peripheral Heterochromatin and Inversely Regulate Differentiation. *Cell* **152**: 584–598. <http://dx.doi.org/10.1016/j.cell.2013.01.009>.
- Song MS, Salmena L, Carracedo A, Egia A, Lo-coco F, Teruya-feldstein J, Pandolfi PP. 2008. The deubiquitylation and localization of PTEN are regulated by a HAUSP – PML network. *Nature* **455**: 813–818.
- Soria G, Polo SE, Attikum V. 2012. Prime , Repair , Restore : The Active Role of Chromatin in the DNA Damage Response. *Mol Cell* **46**: 722–734.
- Spirkoski J, Shah A, Reiner AH, Collas P, Delbarre E. 2019. PML modulates H3.3 targeting to telomeric and centromeric repeats in mouse fibroblasts. *Biochem Biophys Res Commun* **511**: 882–888. <https://doi.org/10.1016/j.bbrc.2019.02.087>.
- Sripathy SP, Stevens J, Schultz DC. 2006. The KAP1 Corepressor Functions To Coordinate the Assembly of De Novo HP1-Demarcated Microenvironments of Heterochromatin Required for KRAB Zinc Finger Protein-Mediated Transcriptional Repression. *Mol Cell Biol* **26**: 8623–8638. <http://mcb.asm.org/cgi/doi/10.1128/MCB.00487-06>.
- Stadler MB, Murr R, Burger L, Ivanek R, Lienert F, Schöler A, van Nimwegen E, Wirbelauer C, Oakeley EJ, Gaidatzis D, *et al.* 2012. DNA-binding factors shape the mouse methylome at distal regulatory regions. *Nature* **480**: 490–495.
- Steinacher R, Barekati Z, Botev P, Kuśnierczyk A, Slupphaug G, Schär P. 2018. SUMOylation coordinates BERosome assembly in active DNA

- demethylation during cell differentiation. *EMBO J* **e99242**. <http://emboj.embopress.org/lookup/doi/10.15252/emj.201899242>.
- Stetson DB, Ko JS, Heidmann T, Medzhitov R. 2008. Trex1 Prevents Cell-Intrinsic Initiation of Autoimmunity. *Cell* **134**: 587–598.
- Stixova L, Matula P, Kozubek S, Gombitov A, Cmarko D, Raška I, Břetov E. 2012. Trajectories and nuclear arrangement of PML bodies are influenced by A-type lamin deficiency. *Biol Cell* **104**: 418–432.
- Strahl BD, Allis CD. 2000. The language of covalent histone modifications. *Nature* **403**: 41–45.
- Strom AR, Emelyanov A V., Mir M, Fyodorov D V., Darzacq X, Karpen GH. 2017. Phase separation drives heterochromatin domain formation. *Nature* **547**: 241–245. <http://www.nature.com/doi/10.1038/nature22989>.
- Stults DM, Killen MW, Williamson EP, Hourigan JS, Vargas HD, Arnold SM, Moscow JA, Pierce AJ. 2009. Human rRNA gene clusters are recombinational hotspots in cancer. *Cancer Res* **69**: 9096–9104.
- Sun X, Clermont PL, Jiao W, Helgason CD, Gout PW, Wang Y, Qu S. 2016. Elevated expression of the centromere protein-A(CENP-A)-encoding gene as a prognostic and predictive biomarker in human cancers. *Int J Cancer* **139**: 899–907.
- Sun Y, Durrin LK, Krontiris TG. 2003. Specific interaction of PML bodies with the TP53 locus in Jurkat interphase nuclei. *Genomics* **82**: 250–252.
- Szenker E, Ray-Gallet D, Almouzni G. 2011. The double face of the histone variant H3.3. *Cell Res* **21**: 421–434. <http://www.ncbi.nlm.nih.gov/pmc/articles/PMC3193428/pdf/cr201114a.pdf>.
- Tachibana M, Sugimoto K, Nozaki M, Ueda J, Ohta T, Ohki M, Fukuda M, Takeda N, Niida H, Kato H, *et al.* 2002. G9a histone methyltransferase plays a dominant role in euchromatic histone H3 lysine 9 methylation and is essential for early embryogenesis. *Genes Dev* **3**: 1779–1791.
- Tachibana M, Ueda J, Fukuda M, Takeda N, Ohta T, Iwanari H, Sakihama T, Kodama T, Hamakubo T, Shinkai Y. 2005. Histone methyltransferases G9a and GLP form heteromeric complexes and are both crucial for methylation of euchromatin at H3-K9. *Genes Dev* **9**: 815–826.
- Tachiwana H, Kagawa W, Shiga T, Osakabe A, Miya Y, Saito K, Hayashi-Takanaka Y, Oda T, Sato M, Park SY, *et al.* 2011. Crystal structure of the human centromeric nucleosome containing

- CENP-A. *Nature* **476**: 232–235.
- Taddei A, Maison C, Roche D, Almouzni G. 2001. Reversible disruption of pericentric heterochromatin and centromere function by inhibiting deacetylases. *Nat Cell Biol* **3**: 114–120.
- Tahiliani M, Koh KP, Shen Y, Pastor WA, Bandukwala H, Brudno Y, Agarwal S, Iyer LM, Liu DR, Aravind L, *et al.* 2009. Conversion of 5-Methylcytosine to 5-Hydroxymethylcytosine in Mammalian DNA by MLL Partner TET1. *Science (80-)* **324**: 930–936.
- Takahashi K, Tanabe K, Ohnuki M, Narita M, Ichisaka T, Tomoda K, Yamanaka S. 2007. Induction of Pluripotent Stem Cells from Adult Human Fibroblasts by Defined Factors. *Cell* **131**: 861–872.
- Takahashi K, Yamanaka S. 2006. Induction of Pluripotent Stem Cells from Mouse Embryonic and Adult Fibroblast Cultures by Defined Factors. *Cell* **126**: 663–676.
- Takayama S, Dhahbi J, Roberts A, Mao G, Heo S, Pachter L, Martin DIK, Boffelli D. 2014. Genome methylation in *D. melanogaster* is found at specific short motifs and is independent of DNMT2 activity. *Genome Res* 821–830.
- Taleahmad S, Mirzaei M, Parker LM, Hassani SN, Mollamohammadi S, Sharifi-Zarchi A, Haynes PA, Baharvand H, Salekdeh GH. 2015. Proteome Analysis of Ground State Pluripotency. *Sci Rep* **5**: 1–10. <http://dx.doi.org/10.1038/srep17985>.
- Tamura T, Smith M, Kanno T, Dasenbrock H, Nishiyama A, Ozato K. 2009. Inducible Deposition of the Histone Variant H3 . 3 in Interferon-stimulated Genes. *J Biol Chem* **284**: 12217–12225.
- Tanabe H, Müller S, Neusser M, Von Hase J, Calcagno E, Cremer M, Solovei I, Cremer C, Cremer T. 2002. Evolutionary conservation of chromosome territory arrangements in cell nuclei from higher primates. *Proc Natl Acad Sci U S A* **99**: 4424–4429.
- Tanaka S, Kunath T, Hadjantonakis AK, Nagy A, Rossant J. 1998. Promotion to trophoblast stem cell proliferation by FGF4. *Science (80-)* **282**: 2072–2075.
- Tang J, Qu LK, Zhang J, Wang W, Michaelson JS, Degenhardt YY, El-Deiry WS, Yang X. 2006. Critical role for Daxx in regulating Mdm2. *Nat Cell Biol* **8**: 855–862.
- Tang MCW, Jacobs SA, Mattiske DM, Soh YM, Graham AN, Tran A, Lim SL, Hudson DF, Kalitsis P, O'Byrne MK, *et al.* 2015. Contribution of the Two Genes Encoding Histone Variant H3.3 to Viability and Fertility in Mice. *PLoS Genet* **11**: 1–23.
- Tao H, Simmons BN, Singireddy S, Jakkidi M, Short KM, Cox TC, Massiah MA. 2008. Structure of the MID1 Tandem B-Boxes Reveals an Interaction

- Reminiscent of. *Biochemistry* **47**: 2450–2457.
- Tarlinton RE, Meers J, Young PR. 2006. Retroviral invasion of the koala genome. *Nature* **442**: 79–81.
- Taunton J, Hassig CA, Schreiber SL. 1996. A Mammalian Histone Deacetylase Related to the Yeast Transcriptional Regulator Rpd3p. *Science (80-)* **272**: 408–412.
- Team RC. 2017. R: A language and environment for statistical computing. *R Found Stat Comput*. <https://www.r-project.org/>.
- Teich NM, Weiss RA, Martin GR, Lowy DR. 1977. Virus Infection of Murine Teratocarcinoma Stem Cell Lines. *Cell* **12**: 973–982.
- Teresa Teixeira M, Arneric M, Sperisen P, Lingner J. 2004. Telomere Length Homeostasis Is Achieved via a Switch between Telomerase- Extendible and - Nonextendible States. *Cell* **117**: 323–335.
- Terranova R, Yokobayashi S, Stadler MB, Otte AP, Lohuizen M Van, Orkin SH, Peters AHFM. 2008. Polycomb Group Proteins Ezh2 and Rnf2 Direct Genomic Contraction and Imprinted Repression in Early Mouse Embryos. *Dev Cell* 668–679.
- Terris B, Dubois S, Degott C, Hénis D, Dejean A. 1995. PML Nuclear Bodies Are General Targets for Inflammation and Cell Proliferation¹. *Cancer Res* **55**: 1590–1597.
- Tesar PJ, Chenoweth JG, Brook FA, Davies TJ, Evans EP, Mack DL, Gardner RL, McKay RDG. 2007. New cell lines from mouse epiblast share defining features with human embryonic stem cells. *Nature* **448**: 196–199.
- Tharp ME, Malki S, Bortvin A. 2020. Maximizing the ovarian reserve in mice by evading LINE-1 genotoxicity. *Nat Commun* 1–13.
- Therizols P, Illingworth RS, Courilleau C, Boyle S, Wood AJ, Bickmore W a. 2014. Chromatin decondensation is sufficient to alter nuclear organization in embryonic stem cells. *Science (80-)* **346**: 1238–42. <http://www.ncbi.nlm.nih.gov/pubmed/25477464>.
- Thienpont B, Steinbacher J, Zhao H, Anna FD, Kuchnio A, Ploumakis A, Ghesquière B, Dyck L Van, Boeckx B, Schoonjans L, *et al.* 2016. Tumour hypoxia causes DNA hypermethylation by reducing TET activity. *Nature* **537**: 63–68.
- Thijssen PE, Ito Y, Grillo G, Wang J, Velasco G, Nitta H, Unoki M, Yoshihara M, Suyama M, Sun Y, *et al.* 2015. Mutations in CDCA7 and HELLS cause immunodeficiency-centromeric instability-facial anomalies syndrome. *Nat Commun* **6**: 1–8.
- Thomas JH, Schneider S. 2011. Coevolution

- of retroelements and tandem zinc finger genes. *Genome Res* **21**: 1800–1812.
- Thompson PJ, Macfarlan TS, Lorincz MC. 2016. Long Terminal Repeats: From Parasitic Elements to Building Blocks of the Transcriptional Regulatory Repertoire. *Mol Cell* **62**: 766–776. <http://dx.doi.org/10.1016/j.molcel.2016.03.029>.
- Thomson JP, Skene PJ, Selfridge J, Clouaire T, Guy J, Webb S, Kerr ARW, Deaton AM, Andrews R, James KD, *et al.* 2010. CpG islands influence chromatin structure via the CpG-binding protein Cfp1. *Nature* **464**: 1082–1086.
- Thomson M, Liu SJ, Zou L, Smith Z, Meissner A, Ramanathan S. 2011. Pluripotency Factors in Embryonic Stem Cells Regulate Differentiation into Germ Layers. *Cell* **145**: 875–889. <http://dx.doi.org/10.1016/j.cell.2011.05.017>.
- Tiku V, Antebi A. 2018. Nucleolar Function in Lifespan Regulation. *Trends Cell Biol* **28**: 662–672. <http://dx.doi.org/10.1016/j.tcb.2018.03.007>.
- Tillotson R, Bird A. 2020. The Molecular Basis of MeCP2 Function in the Brain. *J Mol Biol* **432**: 1602–1623. <https://doi.org/10.1016/j.jmb.2019.10.004>.
- Ting C-N, Rosenber MP, Snow CM, Samuelson LC, Meisler MH. 1992. Endogenous retroviral sequences are required for tissue-specific expression of a human salivary amylase gene. *Genes Dev* **6**: 1457–1465.
- Ting DT, Lipson D, Paul S, Brannigan BW, Akhavanfard S, Coffman EJ, Contino G, Deshpande V, Iafrate AJ, Letovsky S, *et al.* 2011. Aberrant Overexpression of Satellite Repeats in Pancreatic and Other Epithelial Cancers. *Science (80-)* **331**: 593–597.
- Tosolini M, Brochard V, Adenot P, Chebrou M, Grillo G, Navia V, Beaujean N, Francastel C, Bonnet-Garnier A, Jouneau A. 2018. Contrasting epigenetic states of heterochromatin in the different types of mouse pluripotent stem cells. *Sci Rep* **8**: 1–14.
- Towbin BD, González-Aguilera C, Sack R, Gaidatzis D, Kalck V, Meister P, Askjaer P, Gasser SM. 2012. Step-wise methylation of histone H3K9 positions heterochromatin at the nuclear periphery. *Cell* **150**: 934–947.
- Towbin BD, Meister P, Pike BL, Gasser SM. 2010. Repetitive transgenes in *C. elegans* accumulate heterochromatic marks and are sequestered at the nuclear envelope in a copy-number and lamin-dependent manner. *Cold Spring Harb Symp Quant Biol* **75**: 555–565.
- Toyooka Y, Shimosato D, Murakami K, Takahashi K, Niwa H. 2008. Identification and characterization of

- subpopulations in undifferentiated ES cell culture. *918*: 909–918.
- Tsouroula K, Furst A, Rogier M, Heyer V, Maglott-Roth A, Ferrand A, Reina-San-Martin B, Soutoglou E. 2016. Temporal and Spatial Uncoupling of DNA Double Strand Break Repair Pathways within Mammalian Heterochromatin. *Mol Cell* **63**: 293–305. <http://dx.doi.org/10.1016/j.molcel.2016.06.002>.
- Tsumura A, Hayakawa T, Kumaki Y, Takebayashi SI, Sakaue M, Matsuoka C, Shimotohno K, Ishikawa F, Li E, Ueda HR, *et al.* 2006. Maintenance of self-renewal ability of mouse embryonic stem cells in the absence of DNA methyltransferases Dnmt1, Dnmt3a and Dnmt3b. *Genes to Cells* **11**: 805–814.
- Tsusaka T, Shimura C, Shinkai Y. 2019. ATF7IP regulates SETDB1 nuclear localization and increases its ubiquitination. *EMBO Rep* **20**: 1–12.
- Tu X, Batta P, Innocent N, Prisco M, Casaburi I, Belletti B, Baserga R. 2002. Nuclear translocation of insulin receptor substrate-1 by oncogenes and Igf-I: Effect on ribosomal RNA synthesis. *J Biol Chem* **277**: 44357–44365.
- Turelli P, Castro-diaz N, Marzetta F, Kapopoulou A, Duc J, Tieng V, Quenneville S, Trono D. 2014. Interplay of TRIM28 and DNA methylation in controlling human endogenous retroelements. *Genome Res* **24**: 1260–1270.
- Tvardovskiy A, Schwämmle V, Kempf SJ, Rogowska-Wrzesinska A, Jensen ON. 2017. Accumulation of histone variant H3.3 with age is associated with profound changes in the histone methylation landscape. *Nucleic Acids Res* **45**: 9272–9289.
- Udugama M, Chang FTM, Chan FL, Tang MC, Pickett HA, McGhie JDR, Mayne L, Collas P, Mann JR, Wong LH. 2015. Histone variant H3.3 provides the heterochromatic H3 lysine 9 trimethylation mark at telomeres. *Nucleic Acids Res* **43**: 10227–10237.
- Udugama M, Sanij E, Voon HPJ, Son J, Hii L, Henson JD, Lyn Chan F, Chang FTM, Liu Y, Pearson RB, *et al.* 2018. Ribosomal DNA copy loss and repeat instability in ATRX-mutated cancers. *Proc Natl Acad Sci U S A* **115**: 4737–4742.
- Ueda Y, Okano M, Williams C, Chen T, Georgopoulos K, Li E. 2006. Roles for Dnmt3b in mammalian development: a mouse model for the ICF syndrome. *Development* **133**: 1183–1192. <http://dev.biologists.org/cgi/doi/10.1242/dev.02293>.
- Valgardsdottir R, Chiodi I, Giordano M, Rossi A, Bazzini S, Ghigna C, Riva S, Biamonti G. 2008. Transcription of Satellite III non-coding RNAs is a general stress response in human cells.

- Nucleic Acids Res* **36**: 423–434.
- Vallot C, Herault A, Boyle S, Bickmore WA, Radvanyi F. 2015. PRC2-independent chromatin compaction and transcriptional repression in cancer. *Oncogene* 741–751.
- van Hoesel AQ, van de Velde CJH, Kuppen PJK, Liefers GJ, Putter H, Sato Y, Elashoff DA, Turner RR, Shamonki JM, de Kruijf EM, *et al.* 2012. Hypomethylation of LINE-1 in primary tumor has poor prognosis in young breast cancer patients: a retrospective cohort study. *Breast Cancer Res Treat* **134**: 1103–1114.
- van Steensel B, Belmont AS. 2017. Lamina-Associated Domains: Links with Chromosome Architecture, Heterochromatin, and Gene Repression. *Cell* **169**: 780–791. <http://linkinghub.elsevier.com/retrieve/pii/S0092867417304737>.
- van Steensel B, de Lange T. 1997. Control of telomere length by the human telomeric protein TRF1. *Nature* **385**: 740–743.
- Van Steensel B, Henikoff S. 2000. Identification of in vivo DNA targets of chromatin proteins using tethered Dam methyltransferase. *Nat Biotechnol* **18**: 424–428. https://www-nature-com.proxy.insermbiblio.inist.fr/articles/nbt0400_424 (Accessed June 21, 2020).
- Vastenhouw NL, Zhang Y, Woods IG, Imam F, Regev A, Liu XS, Rinn J, Schier AF. 2010. Chromatin signature of embryonic pluripotency is established during genome activation. *Nature* **464**.
- Veland N, Lu Y, Hardikar S, Gaddis S, Zeng Y, Liu B, Estecio MR, Takata Y, Lin K, Tomida MW, *et al.* 2018. DNMT3L facilitates DNA methylation partly by maintaining DNMT3A stability in mouse embryonic stem cells. *Nucleic Acids Res* **47**: 152–167.
- Velasco G, Grillo G, Touleimat N, Ferry L, Ivkovic I, Ribierre F, Deleuze JF, Chantalat S, Picard C, Francastel C. 2018. Comparative methylome analysis of ICF patients identifies heterochromatin loci that require ZBTB24, CDCA7 and HELLS for their methylated state. *Hum Mol Genet* **27**: 2409–2424.
- Velazquez Camacho O, Galan C, Swist-Rosowska K, Ching R, Gamalinda M, Karabiber F, De La Rosa-Velazquez I, Engist B, Koschorz B, Shukeir N, *et al.* 2017. Major satellite repeat RNA stabilize heterochromatin retention of Suv39h enzymes by RNA-nucleosome association and RNA:DNA hybrid formation. *Elife* **6**. <https://elifesciences.org/articles/25293>.
- Versteeg R, Schaik BDC Van, Batenburg MF Van, Roos M, Monajemi R, Caron H, Bussemaker HJ, Kampen AHC Van.

2004. The Human Transcriptome Map Reveals Extremes in Gene Density , Intron Length , GC Content , and Repeat Pattern for Domains of Highly and Weakly Expressed Genes. *Genome Res* **13**: 1998–2004.
- Vertii A, Ou J, Yu J, Yan A, Pagès H, Liu H, Zhu LJ, Kaufman PD. 2019. Two contrasting classes of nucleolus-associated domains in mouse fibroblast heterochromatin. *Genome Res* gr.247072.118.
- Vieux-rochas M, Fabre PJ, Leleu M, Duboule D, Noordermeer D. 2015. Clustering of mammalian Hox genes with other H3K27me3 targets within an active nuclear domain. *Proc Natl Acad Sci* **112**: 2–7.
- Villarreal G, Zhang Y, Larman HB, Gracia-Sancho J, Koo A, García-Cardena G. 2010. Defining the regulation of KLF4 expression and its downstream transcriptional targets in vascular endothelial cells. *Biochem Biophys Res Commun* **391**: 984–989. <http://dx.doi.org/10.1016/j.bbrc.2009.12.002>.
- Vissel B, Choo KH. 1989. Mouse major (γ) satellite DNA is highly conserved and organized into extremely long tandem arrays: Implications for recombination between nonhomologous chromosomes. *Genomics* **5**: 407–414.
- Voisset E, Moravcsik E, Stratford EW, Jaye A, Palgrave CJ, Hills RK, Salomoni P, Kogan SC, Solomon E, Grimwade D. 2018. PML nuclear body disruption cooperates in APL pathogenesis and impairs DNA damage repair pathways in mice. *Blood* **131**: 636–648.
- Voon HPJ, Collas P, Wong LH. 2016. Compromised telomeric heterochromatin promotes ALTERNative lengthening of telomeres. *Trends in Cancer* **2**: 114–116. <http://dx.doi.org/10.1016/j.trecan.2016.02.003>.
- Voong LN, Xi L, Sebeson AC, Xiong B, Wang J, Wang X. 2016. Insights into Nucleosome Organization in Mouse Embryonic Stem Cells through Chemical Mapping. *Cell* 1555–1570.
- Walter M, Teissandier A, Pérez-Palacios R, Bourc'his D. 2016. An epigenetic switch ensures transposon repression upon dynamic loss of DNA methylation in embryonic stem cells. *Elife* **53**: 1689–1699.
- Wang A, Kurdistani SK, Grunstein M. 2002. Requirement of Hos2 Histone Deacetylase for Gene Activity in Yeast. *Science (80-)* **298**: 1412–1415.
- Wang H, An W, Cao R, Xia L, Erdjument-bromage H, Chatton B, Tempst P, Roeder RG, Zhang Y. 2003. mAM Facilitates Conversion by ESET of Dimethyl to Trimethyl Lysine 9 of Histone H3 to Cause Transcriptional

- Repression. *Mol Cell* **12**: 475–487.
- Wang J, Shiels C, Sasieni P, Wu PJ, Islam SA, Freemont PS, Sheer D. 2001. Promyelocytic leukemia nuclear bodies associate with transcriptionally active genomic regions. *J Cell Biol* **164**: 515–526.
- Wang J, Xie LY, Allan S, Beach D, Hannon GJ. 1998a. Myc activates telomerase. *Genes Dev* **12**: 1769–1774.
- Wang M, Wang L, Qian M, Tang X, Liu Z, Lai Y, Ao Y, Huang Y, Meng Y, Shi L, *et al.* 2020. PML2-mediated thread-like nuclear bodies mark late senescence in Hutchinson – Gilford progeria syndrome. *Aging Cell* 1–14.
- Wang Z, Ruggiero D, Ronchetti S, Zhong S, Gaboli M, Rivi R, Pandolfi PP. 1998b. Pml is essential for multiple apoptotic pathways. *Nat Genet* **20**: 266–272.
- Wang Z, Zang C, Cui K, Schones DE, Barski A, Peng W, Zhao K. 2009. Genome-wide Mapping of HATs and HDACs Reveals Distinct Functions in Active and Inactive Genes. *Cell* **138**: 1019–1031.
<http://dx.doi.org/10.1016/j.cell.2009.06.049>.
- Wang Z, Zang C, Rosenfeld JA, Schones DE, Barski A, Cuddapah S, Cui K, Roh T, Peng W, Zhang MQ, *et al.* 2008. Combinatorial patterns of histone acetylations and methylations in the human genome. *Nat Genet* **40**: 897–903.
- Ward IM, Chen J. 2001. Histone H2AX Is Phosphorylated in an ATR-dependent Manner in Response to Replicational Stress *. *J Biol Chem* **276**: 47759–47762.
- Ward JR, Vasu K, Deutschman E, Halawani D, Larson A, Zhang D, Willard B, Fox PL, Moran J V, Longworth S. 2017. Condensin II and GAIT complexes cooperate to restrict LINE-1 retrotransposition in epithelial cells. *PLoS Genet* **1**: 1–31.
- Watson JD. 1972. Origin of concatemeric T7 DNA. *Nat New Biol* **239**: 197–201.
<https://www.nature.com/articles/newbio239197a0> (Accessed June 21, 2020).
- Watson JD, Crick FHC. 1953. Molecular structure of nucleic acids. *Nature* **171**: 737–738.
- Weber AR, Krawczyk C, Robertson AB, Kusnierczyk A, Vagbo CB, Schuermann D, Klungland A, Schär P. 2016. Biochemical reconstitution of TET1-TDG-BER-dependent active DNA demethylation reveals a highly coordinated mechanism. *Nat Commun* **7**.
- Weber K, Plessmann U, Traub P. 1990. Protein chemical analysis of purified murine lamin B identifies two distinct polypeptides B1 and B2. *FEBS Lett* **261**: 361–364.
[http://doi.wiley.com/10.1016/0014-5793\(90\)2980592-7](http://doi.wiley.com/10.1016/0014-5793(90)2980592-7) (Accessed May 6, 2020).
- Weis K, Lavau C, Jansen J, Carvalho T,

- Carmo-fonseca M, Lamond A, Dejean A. 1994. Retinoic Acid Regulates Aberrant Nuclear Localization of PML-RARa in Acute Promyelocytic Leukemia Cells. *Cell* **76**: 345–356.
- Wen B, Wu H, Shinkai Y, Irizarry RA, Feinberg AP. 2009. Large histone H3 lysine 9 dimethylated chromatin blocks distinguish differentiated from embryonic stem cells. *Nat Genet* **41**: 246–250.
<http://www.nature.com/doifinder/10.1038/ng.297>.
- Whitten WK. 1956. Culture of Tubal Mouse Ova. *Nature* **177**: 0–1.
- Wijchers PJ, Geeven G, Eyres M, Bergsma AJ, Janssen M, Versteegen M, Zhu Y, Schell Y, Vermeulen C, de Wit E, *et al.* 2015. Characterization and dynamics of pericentromere-associated domains in mice. *Genome Res* **25**: 958–69.
<http://www.ncbi.nlm.nih.gov/pubmed/25883320>
<http://www.pubmedcentral.nih.gov/articlerender.fcgi?artid=PMC4484393>.
- Wijchers PJ, Krijger PHL, Geeven G, Aninkgroenen LCM, Verschure PJ, Laat W De, Wijchers PJ, Krijger PHL, Geeven G, Zhu Y, *et al.* 2016. Cause and Consequence of Tethering a SubTAD to Different Nuclear Compartments. *Mol Cell* **61**: 1–13.
<http://dx.doi.org/10.1016/j.molcel.2016.01.001>.
- Williams RL, Hilton DJ, Pease S, Willson TA, Stewart CL, Gearing DP, Wagner EF, Metcalf D, Nicola NA, Gough NM. 1988. Myeloid leukaemia inhibitory factor maintains the developmental potential of embryonic stem cells. *Nature* **336**: 684–687.
- Williams RRE, Azuara V, Perry P, Sauer S, Dvorkina M, Jørgensen H, Roix J, McQueen P, Misteli T, Merckenschlager M, *et al.* 2006. Neural induction promotes large-scale chromatin reorganisation of the Mash1 locus. *J Cell Sci* **119**: 132–140.
<http://jcs.biologists.org/content/119/1/132.long>.
- Willis ND, Cox TR, Rahman-Casañs SF, Smits K, Przyborski SA, van den Brandt P, van Engeland M, Weijnenberg M, Wilson RG, de Bruïne A, *et al.* 2008. Lamin A/C Is a Risk Biomarker in Colorectal Cancer ed. K.G. Hardwick. *PLoS One* **3**: e2988.
<https://dx.plos.org/10.1371/journal.pone.0002988> (Accessed May 9, 2020).
- Winters AC, Bernt KM. 2017. MLL-Rearranged Leukemias — An Update on Science and Clinical Approaches. *Front Pediatr* **5**: 11–13.
- Wolf D, Cammas F, Losson R, Goff SP. 2008. Primer Binding Site-Dependent Restriction of Murine Leukemia Virus Requires HP1 Binding by TRIM28. *J Virol* **82**: 4675–4679.

- Wolf D, Goff SP. 2007. TRIM28 Mediates Primer Binding Site-Targeted Silencing of Murine Leukemia Virus in Embryonic Cells. *Cell* **131**: 46–57.
- Wolf G, Yang P, Füchtbauer AC, Silva AM, Park C, Wu W, Nielsen AL, Pedersen FS, Macfarlan TS. 2015. The KRAB zinc finger protein ZFP809 is required to initiate epigenetic silencing of endogenous retroviruses. *Genes Dev* **29**: 538–554.
- Wong JMY, Kusdra L, Collins K. 2002. Subnuclear shuttling of human telomerase induced by transformation and DNA damage. *Nat Cell Biol* **4**: 731–736.
- Wong LH, McGhie JD, Sim M, Anderson MA, Ahn S, Hannan RD, George AJ, Morgan KA, Mann JR, Choo KHA. 2010. ATRX interacts with H3.3 in maintaining telomere structural integrity in pluripotent embryonic stem cells. *Genome Res* **20**: 351–360.
- Wong X, Luperchio TR, Reddy KL. 2014. NET gains and losses: The role of changing nuclear envelope proteomes in genome regulation. *Curr Opin Cell Biol* **28**: 105–120. <http://dx.doi.org/10.1016/j.ceb.2014.04.005>.
- Wood AM, Danielsen JMR, Lucas CA, Rice EL, Scalzo D, Shimi T, Goldman RD, Smith ED, Beau MM Le, Kosak ST. 2014. TRF2 and lamin A/C interact to facilitate the functional organization of chromosome ends. *Nat Commun* **5**: 1–9. <http://dx.doi.org/10.1038/ncomms6467>.
- Wood KH, Johnson BS, Welsh SA, Lee JY, Cui Y, Brodtkin ES, Blendy JA, Robinson MB, Bartolomei MS, Zhou Z. 2016. Tagging methyl-CpG-binding domain proteins reveals different spatiotemporal expression and supports distinct functions. *Epigenomics* **8**: 455–473.
- Wu G, Broniscer A, Mceachron TA, Lu C, Paugh BS, Becksfors J, Qu C, Ding L, Huether R, Parker M, *et al.* 2012. Somatic histone H3 alterations in pediatric diffuse intrinsic pontine. *Nat Genet* **44**: 2011–2013.
- Wu H, Alessio ACD, Ito S, Xia K, Wang Z, Cui K, Zhao K, Sun YE, Zhang Y. 2011. Dual functions of Tet1 in transcriptional regulation in mouse embryonic stem cells. *Nature* **473**: 389–393.
- Wu K, Liu H, Wang Y, He J, Xu S, Chen Y, Kuang J, Liu J, Guo L, Li D, *et al.* 2020. SETDB1-Mediated Cell Fate Transition between 2C-Like and Pluripotent States. *Cell Rep* **30**: 25–36.e6. <https://doi.org/10.1016/j.celrep.2019.12.010>.
- Xiang Y, Yan K, Zheng Q, Ke H, Cheng J, Xiong W, Shi X, Wei L, Zhao M, Yang F, *et al.* 2019. Histone Demethylase KDM4B Promotes DNA Damage by

- Activating Long Interspersed Nuclear Element-1. *Cancer Res* **9**: 86–99.
- Xu G-L, Bestor TH, Bourc'his D, Hsieh C-L, Tommerup N, Bugge M, Hulten M, Qu X, Russo JJ, Viegas-Péquignot E. 1999. Chromosome instability and immunodeficiency syndrome caused by mutations in a DNA methyltransferase gene . PubMed Commons. *Nature* **402**: 187–191.
- Xu J, Carter AC, Gendrel A-V, Attia M, Loftus J, Greenleaf WJ, Tibshirani R, Heard E, Chang HY. 2017. Landscape of monoallelic DNA accessibility in mouse embryonic stem cells and neural progenitor cells. *Nat Genet* **49**: 377–386. <http://www.nature.com/doifinder/10.1038/ng.3769>.
- Xue Z, Huang K, Cai C, Cai L, Jiang C, Feng Y, Liu Z, Zeng Q. 2013. Genetic programs in human and mouse early embryos revealed by single-cell RNA sequencing. *Nature* **500**: 593–597. <http://dx.doi.org/10.1038/nature12364>.
- Yan Q, Cho E, Lockett S, Muegge K. 2003. Association of Lsh, a Regulator of DNA Methylation, with Pericentromeric Heterochromatin Is Dependent on Intact Heterochromatin. *Mol Cell Biol* **23**: 8416–8428.
- Yang P, Wang Y, Macfarlan TS. 2017. The Role of KRAB-ZFPs in Transposable Element Repression and Mammalian Evolution. *Trends Genet* **33**: 871–881. <http://dx.doi.org/10.1016/j.tig.2017.08.006>.
- Yang X, Khosravi-far R, Chang HY, Baltimore D. 1997. Daxx , a Novel Fas-Binding Protein That Activates JNK and Apoptosis. *Cell* **89**: 1067–1076.
- Yao R-W, Xu G, Wang Y, Xing Y, Yang L, Chen L, Yao R, Xu G, Wang Y, Shan L, *et al.* 2019. Nascent Pre-rRNA Sorting via Phase Separation Drives the Assembly of Dense Fibrillar Components in the Human Nucleolus Article Nascent Pre-rRNA Sorting via Phase Separation Drives the Assembly of Dense Fibrillar Components in the Human Nucleolus. *Mol Cell* **76**: 767-783.e11. <https://doi.org/10.1016/j.molcel.2019.08.014>.
- Yeo JC, Jiang J, Tan ZY, Yim GR, Ng JH, Göke J, Kraus P, Liang H, Gonzales KAU, Chong HC, *et al.* 2014. Klf2 is an essential factor that sustains ground state pluripotency. *Cell Stem Cell* **14**: 864–872.
- Yeung PL, Denissova NG, Nasello C, Hakhverdyan Z, Chen JD, Brenneman MA. 2012. Promyelocytic Leukemia Nuclear Bodies Support a Late Step in DNA Double-Strand Break Repair by Homologous Recombination. *J Cell Biochem* **1799**: 1787–1799.
- Ying QL, Wray J, Nichols J, Battle-Morera L,

- Doble B, Woodgett J, Cohen P, Smith A. 2008. The ground state of embryonic stem cell self-renewal. *Nature* **453**: 519–523.
- You SH, Lim HW, Sun Z, Broache M, Won KJ, Lazar MA. 2013. Nuclear receptor co-repressors are required for the histone-deacetylase activity of HDAC3 in vivo. *Nat Struct Mol Biol* **20**: 182–187.
- Young LC, McDonald DW, Hendzel MJ. 2013. Kdm4b Histone Demethylase Is a DNA Damage Response. *J Biol Chem* **288**: 21376–21388.
- Yu W, McIntosh C, Lister R, Zhu I, Han Y, Ren J, Landsman D, Lee E, Briones V, Terashima M, *et al.* 2014. Genome-wide DNA methylation patterns in LSH mutant reveals de-repression of repeat elements and redundant epigenetic silencing pathways. *Genome Res* **24**: 1613–1623.
- Yukawa M, Akiyama T, Franke V, Mise N, Isagawa T, Suzuki Y, Suzuki MG, Vlahovicek K, Abe K, Aburatani H, *et al.* 2014. Genome-wide analysis of the chromatin composition of histone H2A and H3 variants in mouse embryonic stem cells. *PLoS One* **9**.
- Zasadzińska E, Huang J, Bailey AO, Guo LY, Lee NS, Srivastava S, Wong KA, French BT, Black BE, Foltz DR. 2018. Inheritance of CENP-A Nucleosomes during DNA Replication Requires HJURP. *Dev Cell* **47**: 348–362.e7.
- Zha S, Sekiguchi J, Brush JW, Bassing CH, Alt FW. 2008. Complementary functions of ATM and H2AX in development and suppression of genomic instability. *Proc Natl Acad Sci* **2008**: 2–6.
- Zhang F, Cong L, Lodato S, Kosuri S, Church GM, Arlotta P. 2011. Efficient construction of sequence-specific TAL effectors for modulating mammalian transcription. *Nat Biotechnol* **29**: 149–154.
- Zhang H, Gan H, Wang Z, Wold MS, Zhang H, Gan H, Wang Z, Lee J, Zhou H, Ordog T, *et al.* 2017. RPA Interacts with HIRA and Regulates H3 . 3 Deposition at Gene Regulatory Elements in Mammalian Cells. *Mol Cell* **65**: 272–284. <http://dx.doi.org/10.1016/j.molcel.2016.11.030>.
- Zhang LF, Huynh KD, Lee JT. 2007. Perinucleolar Targeting of the Inactive X during S Phase: Evidence for a Role in the Maintenance of Silencing. *Cell* **129**: 693–706.
- Zhang R, Poustovoitov M V, Ye X, Santos HA, Chen W, Daganzo SM, Erzberger JP, Serebriiskii IG, Canutescu AA, Dunbrack RL, *et al.* 2005. Formation of MacroH2A-Containing Senescence-Associated Heterochromatin Foci and Senescence Driven by ASF1a and HIRA. *Dev Cell* **8**: 19–30.
- Zhang Y, Cheng TC, Huang G, Lu Q, Surleac MD, Mandell JD, Pontarotti P, Petrescu

- AJ, Xu A, Xiong Y, *et al.* 2019a. Transposon molecular domestication and the evolution of the RAG recombinase. *Nature* **569**: 79–84. <http://dx.doi.org/10.1038/s41586-019-1093-7>.
- Zhang YJ, Guo L, Gonzales PK, Gendron TF, Wu Y, Jansen-West K, O’Raw AD, Pickles SR, Prudencio M, Carlomagno Y, *et al.* 2019b. Heterochromatin anomalies and double-stranded RNA accumulation underlie C9orf72 poly(PR) toxicity. *Science (80-)* **363**.
- Zhao LY, Liu J, Sidhu GS, Niu Y, Liu Y, Wang R, Liao D. 2004. Negative Regulation of p53 Functions by Daxx and the Involvement of MDM2 *. *J Biol Chem* **279**: 50566–50579.
- Zhong X, Wang QQ, Li JW, Zhang YM, An XR, Hou J. 2017. Ten-eleven translocation-2 (Tet2) is involved in myogenic differentiation of skeletal myoblast cells in vitro. *Sci Rep* **7**: 1–11. <http://dx.doi.org/10.1038/srep43539>.
- Zhu F, Farnung L, Kaasinen E, Sahu B, Yin Y, Wei B, Dodonova SO, Nitta KR, Morgunova E, Taipale M, *et al.* 2018a. The interaction landscape between transcription factors and the nucleosome. *Nature* **562**: 76–81.
- Zhu Q, Hoong N, Aslanian A, Hara T, Benner C, Heinz S, Miga KH, Ke E, Verma S, Soroczynski J, *et al.* 2018b. Heterochromatin-Encoded Satellite RNAs Induce Article Heterochromatin-Encoded Satellite RNAs Induce Breast Cancer. *Mol Cell* **70**: 842–853.e7. <https://doi.org/10.1016/j.molcel.2018.04.023>.
- Zhu Q, Pao GM, Huynh AM, Suh H, Tonnu N, Nederlof PM, Gage FH, Verma IM. 2011. BRCA1 tumour suppression occurs via heterochromatin-mediated silencing. *Nature* **477**: 179–184. <http://dx.doi.org/10.1038/nature10371>.
- Ziegler-birling C, Helmrich A, Tora L, Torres-Padilla M-E. 2009. phosphorylated H2A . X during mouse preimplantation development in the absence of DNA damage. *Int J Dev Biol* **1011**: 1003–1011.
- Zullo JM, Demarco IA, Piqu??-Regi R, Gaffney DJ, Epstein CB, Spooner CJ, Luperchio TR, Bernstein BE, Pritchard JK, Reddy KL, *et al.* 2012. DNA sequence-dependent compartmentalization and silencing of chromatin at the nuclear lamina. *Cell* **149**: 1474–1487.
- Zwart R, Sleutels F, Wutz A, Schinkel AH, Barlow DP. 2001. Bidirectional action of the Igf2r imprint control element on upstream and downstream imprinted genes. *Genes Dev* **15**: 2361–2366.

RESUME

RESUME

English

Most of mammalian genomes are composed of DNA repeated elements. Pericentromeric heterochromatin (PCH) regions are formed of large arrays of major satellite repeats. DNA repeats are often silenced via similar mechanisms such as DNA methylation, H3K9me3 modification and HP1. Loss of heterochromatin silencing is commonly observed in different cancers and can lead to genomic instability. PCH of different chromosome can assemble into large DAPI-dense foci called chromocenters. Formation of chromocenter arise during the early embryogenesis when the level of DNA methylation is low. Such reorganization is essential for further development of the embryo, yet, the molecular mechanisms regulating its maintenance in the early pluripotent cells remain unknown. This work focuses on the role of the histone variant H3.3 and its chaperone DAXX in heterochromatin organization in embryonic stem cells (ESCs). Firstly, I observed that the loss of Daxx alters the organization of chromocenters in pluripotent cells. ESCs can be converted toward the ground-state of pluripotency which displays a dramatic loss of DNA methylation. I uncovered that DAXX is essential for proper growth of ESC upon ground-state conversion. Furthermore, I observed that active loss of DNA demethylation can generate DNA damages at PCH, which induces a strong accumulation of DAXX. Dissecting the function of DAXX, I discovered that the DAXX-H3.3 interaction was implicated in the recruitment of SETDB1 at chromocenters to reform the heterochromatin state. Finally, I noticed that the function of DAXX extend beyond pericentromeric heterochromatin. Indeed, the absence of Daxx impairs the proper silencing of different heterochromatin regions including the lamina-associated domains. Altogether, this work provides evidence that DAXX is a regulator of heterochromatin maintenance in pluripotent cells.

Keywords: heterochromatin; histone variants; H3.3; DAXX; embryonic stem cells; DNA methylation.

Français

Les génomes des mammifères sont largement composés de séquences ADN répétées. Les régions d'hétérochromatine péricentromérique (PCH) sont formées de nombreuses répétitions de satellites majeurs. Les régions d'ADN répétés sont souvent réprimées par des mécanismes similaires comme la méthylation de l'ADN, la modification H3K9me3 et HP1. Des défauts de l'hétérochromatine sont observés dans différents cancers et contribuent à l'instabilité génomique. Les PCH des différents chromosomes se rassemblent et forment de larges chromocentres. La formation des chromocentres a lieu au cours de l'embryogénèse précoce, un moment où le niveau de méthylation de l'ADN est faible. Cette réorganisation est essentielle pour la poursuite du développement, et pourtant les mécanismes moléculaires la régulant dans les cellules pluripotentes précoces restent inconnus. Ce travail se concentre sur le rôle du variant d'histone H3.3, et de sa chaperonne DAXX, sur l'organisation de l'hétérochromatine dans les cellules souches embryonnaires (ESC). Premièrement, nous avons observé que la perte de Daxx altérait l'organisation des chromocentres dans les cellules pluripotentes. Les ESC peuvent être converti vers un état naïf de pluripotence, qui présentent une très forte diminution de leur niveau de méthylation de l'ADN. Nous avons découvert que DAXX était essentiel pour la survie des ESC lors de la conversion vers l'état naïf de pluripotence. De plus, nous avons observé que la perte active de la méthylation de l'ADN pouvait générer des dommages à l'ADN aux PCH, ce qui induit une forte accumulation de DAXX. En disséquant le rôle de DAXX, nous avons découvert que l'interaction DAXX-H3.3 était impliquée dans le recrutement de SETDB1 aux chromocentres pour reformer l'hétérochromatine. Enfin, nous avons montré que le rôle de DAXX s'étendait à d'autres régions de l'hétérochromatine tels que les domaines associés à la lamina. Dans l'ensemble, ce travail met en évidence un nouveau rôle DAXX dans le maintien de l'hétérochromatine des cellules pluripotentes.

Mots-clés : hétérochromatine ; variants d'histone ; H3.3 ; DAXX ; cellules souches embryonnaires ; méthylation de l'ADN.